8-12-2013 12:00 AM

Neurodevelopmental Consequences of Prenatal Alcohol Exposure: Behavioural and Transcriptomic Alterations in a Mouse Model

Katarzyna Mantha
The University of Western Ontario

Supervisor
Dr. Shiva Singh
The University of Western Ontario

Graduate Program in Biology
A thesis submitted in partial fulfillment of the requirements for the degree in Doctor of Philosophy

NEURODEVELOPMENTAL CONSEQUENCES OF PRENATAL ALCOHOL EXPOSURE: BEHAVIOURAL AND TRANSCRIPTOMIC ALTERATIONS IN A MOUSE MODEL

(Thesis format: Monograph)

By

Katarzyna Mantha

Graduate Program in Biology

A thesis submitted in partial fulfillment
of the requirements for the degree of
Doctor of Philosophy

The School of Graduate and Postdoctoral Studies
The University of Western Ontario
London, Ontario, Canada

ABSTRACT

Fetal Alcohol Spectrum Disorder (FASD) is an umbrella term referring to a range of physical, behavioural, and cognitive deficits resulting from prenatal alcohol exposure. The resulting abnormalities are heterogeneous and often attributed to timing and dosage of alcohol exposure. However, the specific effects of developmental timing are not well-known.

This research used C57BL/6J (B6) as an animal model for early (human trimester one) and mid-gestation (human trimester two) alcohol exposure. Pregnant B6 mice were injected with 2.5 g/kg ethanol on gestational day (GD) 8 and 11 (trimester one equivalent), or on GD 14 and 16 (trimester two equivalent). Resulting pups were followed from birth to adulthood using FASD-relevant behavioural tests. At postnatal day (PD) 70, whole brain tissues were extracted. A third group of dams were injected on GD 16 (short-term). Two hours post injection, fetal brains were removed. Brains were used for genome-wide expression analysis, including microRNAs. Downstream analyses were completed using software packages and online databases.

All ethanol-treated pups showed motor skill delays, increased activity, and spatial learning deficits. Gene expression analysis resulted in altered expression of 48 short-term genes between ethanol and control mice treated during the second trimester. Fifty-five and 68 genes were differentially-expressed in the long-term analyses of mice treated during trimester one and two, respectively. Genes involved in immune system response were disrupted across all treatments. Disrupted short-term processes included cytoskeleton development and immunological functions. Processes altered in long-term exposures included stress signaling, DNA stability, and cellular proliferation. MicroRNA analyses returned eight and 20 differentially-expressed miRNAs in trimesters one and two, respectively. Target filtering of trimester one microRNAs

and mRNAs resulted in inverse relationships between miR-532-5p and *Atf1*, *Itpripl2*, and *Stxbp6*. Trimester two target filtering resulted in miR-302c targeting *Ccdc6*.

Gene expression and microRNA results demonstrate the stage-specific genes and processes altered during neurodevelopment upon ethanol exposure. Certain cellular processes are disrupted no matter the timing of ethanol exposure. Given that microRNAs are fine-tuners of gene expression, they may play an important role in the maintenance of FASD. Furthermore, transcriptomic changes in the brain may explain the observed behavioural effects of prenatal ethanol exposure.

Keywords

Fetal Alcohol Spectrum Disorder (FASD), Ethanol, C57BL/6J, Neurodevelopment, Behaviour, Brain, Gene Expression, Microarray, MicroRNA, Transcriptome.

Co-Authorship Statement

This thesis includes work from papers co-authored by myself, and others:

1. Mantha, K., Kleiber, M.L., and Singh, S.M. Neurodevelopmental timing of ethanol exposure may contribute to observed heterogeneity of behavioural deficits in a mouse model of Fetal Alcohol Spectrum Disorder (FASD). *J Beh Brain Sci*, 2013, 3, 85-99.

   My contribution for this paper included: behavioural experiments for trimester one and two, data collection, data analysis, and writing of the manuscript. MLK performed all experiments for trimester three including: behavioural testing, data collection, and data analysis. All authors contributed to editing the manuscript. The project was developed by myself, MLK, and SMS.

2. Kleiber, M.L., Mantha, K., Stringer, R.L., and Singh, S.M. Neurodevelopmental alcohol exposure elicits long-term changes to gene expression that alter distinct molecular pathways dependent on timing of exposure. *J Neurodev Disord*, 2013, 5:6, 1-19.

   My contribution to this paper included: mouse injections, tissue isolation, RNA extraction, and microarray preparation for trimester one and two samples. RLS helped to perform RNA extractions for trimester one. Gene confirmations were performed by MLK (trimester three), RLS (trimester one) and myself (trimesters one and two). Manuscript was written by MLK. Contributions to manuscript editing were done by myself and SMS. The project was developed by myself, MLK, and SMS.

3. Laufer, B.I., Mantha, K., Kleiber, M.L., Diehl, E.J. Addison, S.M., and Singh, S.M. Long lasting alterations to DNA methylation and ncRNAs may underlie the effects of fetal alcohol exposure. *Dis Model Mech*, 2013, 6, 1-16.

My contribution to this paper included: mouse injections, tissue isolation, RNA extraction, microarray preparation, and microRNA preparation for trimesters one and two. MLK performed all work for trimester three. Mice from the CPD model were raised by EJD. BIL performed bioinformatics analyses and wrote the manuscript. SMA, BIL, and EJD designed and performed all qRT-PCR experiments for the CPD model. The manuscript was written by BIL, MLK, and SMS, with contributions from myself, EJD, and SMA.

4. Mantha, K., Laufer, B.I., and Singh, S.M. Molecular changes during development following prenatal ethanol exposure in a mouse model of FASD: Studies on second-trimester exposure. *Submitted* to the *Journal of Neuroscience*.

   My contribution to this paper included: all mouse work, array preparation, gene expression array analyses, and qRT-PCR confirmation for trimester two short-term and long-term data sets (gene expression and microRNA). BIL performed target filtering analysis of microRNA arrays. The manuscript was written by myself, with contributions from BIL and SMS.

5. Mantha, K., Laufer, B.I., and Singh, S.M. Binge-like alcohol exposure during the first trimester equivalent in C57BL/6J mice leads to alterations to the transcriptome including miR-532-5p. *In preparation*.

   My contribution to this paper included: all mouse work, array preparation, gene expression array analyses, and qRT-PCR confirmation for trimester one gene expression and microRNA data sets. BIL performed target filtering analysis of microRNA arrays. The manuscript was written by myself, with contributions from BIL and SMS.

Acknowledgments

It would not have been possible to complete this doctoral thesis without the help and support of the kind people around me, to only some of whom it is possible to give particular mention here.

First of all, I would like to thank my supervisor, Dr. Shiva Singh, for his outstanding support throughout the past four years. I cannot thank him enough for the opportunities he has given me. His good advice, guidance, and patience have been invaluable on both an academic and a personal level, for which I am extremely grateful. I would also like to acknowledge Dr. Kathleen Hill and Dr. Sashko Damjanovski for their contributions to my research as advisory committee members. In particular, thank you to Dr. Hill for her thorough proofreading, and to Dr. Damjanovski for his constructive insights. Thank you also to all other professors who have examined my progress throughout my graduate milestones.

These past couple of years I have been lucky to work with wonderful colleagues, both past and present. I would especially like to thank those who have been part of the FASD project in our lab for the past few years: Morgan Kleiber, Randa Stringer, Ben Laufer, Eric Diehl, Aniruddho Chokroborty-Hoque, and Bonnie Alberry. Thank you also to all of the undergraduate students who have volunteered their time and effort to this project. I would also like to thank countless colleagues from mine and other labs for their thoughtful inputs and suggestions. Thank you to David Carter at the London Regional Genomics Center for his technical expertise.

Finally, I would like to thank all of my family members for supporting me during my academic endeavors. In particular, my husband and my parents have provided me with invaluable support throughout my educational career.

Table of Contents

LIST OF TABLES

LIST OF FIGURES

Figure **Title** **Page**

LIST OF APPENDICES

Title **Page**

LIST OF ABBREVIATIONS

ADHD	Attention Deficit Hyperactive Disorder
ANOVA	analysis of variance
AR	air righting
ARND	Alcohol-Related Neurodevelopmental Disorder
ARBD	Alcohol-Related Birth Defects
AS	auditory startle
B6	C57BL/6J mouse
BAC	blood alcohol concentration
BDNF	Brain-derived neurotropic factor
BLAST	Basic Local Alignment Search Tool
BP	biological process
CA	cliff aversion
CA1	cornu ammonis area 1
cDNA	complementary DNA
CC	cellular component
CNS	central nervous system
cRNA	complementary RNA
DAVID	Database for Annotation, Visualization and Integrated Discovery
DEG	differentially-expressed gene
DNA	deoxyribonucleic acid
DNase	deoxyribonuclease
ET	ear twitch
EO	eye opening
EPM	Elevated Plus Maze
ER	endoplasmic reticulum
FAE	fetal alcohol effects
FAEE	fatty acid ethyl ester
FAM	6-carboxyfluorescein
FAS	fetal alcohol syndrome
FASD	fetal alcohol spectrum disorders
FDR	false discovery rate
FG	forelimb grasp
FST	forced swim test
GC-RMA	GeneChip-Robust Multiarray Averaging
GD	gestational day
GE	Gene Enrichment
GO	Gene Ontology
HPA	hypothalamic-pituitary-adrenal-gonadal
HTLV-I	Human T-lymphotropic virus Type I
ICD	International Classification of Disease
ip	*intraperitoneal*
IPA	Ingenuity Pathway Analysis
IR	infrared
KEGG	Kyoto Encyclopedia of Genes and Genomes

LDB	Light/Dark Box
LRGC	London Regional Genomics Center
MAS	Microarray Suite software
MDD	Major Depressive Disorder
MF	molecular function
miRNA	microRNA
mRNA	messenger RNA
MS	Multiple Sclerosis
NCBI	National Centre for Biotechnology Information
NG	negative geotaxis
OFT	open field traversal
PBS	phosphate buffered saline
PCR	polymerase chain reaction
PD	postnatal day
PE	Pathway Enrichment
PFAS	partial FAS
PFC	prefrontal cortex
PD	postnatal days
qRT-PCT	quantitative reverse transcription PCR
RNA	ribonucleic acid
RNAseq	RNA sequencing
RMA	Robust Multiarray Averaging
RM-ANOVA	repeated measures ANOVA
ROS	reactive oxygen species
sc	*subcutaneous*
SEM	standard error of the mean
SLE	Systemic Lupus Erythematosus
SMART	Simple Modular Architecture Research Tool
SP-PIR	Swiss-Prot and Protein Information Resource
SPSS	Statistical Package for the Social Sciences
SR	surface righting
sscDNA	single-stranded complementary DNA
ST	sense transcript
SYBR green	Synergy Brands, Inc. (cyanine dye)
T1-L	trimester one treatment, long-term exposure
T2-L	trimester two treatment, long-term exposure
T2-S	trimester two treatment, short-term exposure
TBE	tris-borate-ethylenediaminetetraacetic acid
TEMED	tetramethylethylenediamine
TF	transcription factor
TRIzol	total RNA isolation
tRNA	transfer RNA
UPR	unfolded protein response
UTR	untranslated region

LIST OF GENES/PROTEINS

5-HT	5-hydroxytryptophan
Actb	*Actin, beta*
ADH	alcohol dehydrogenase
ADH2*2	mutated aldehyde dehydrogenase
AhR	aryl hydrocarbon receptor
ALDH	aldehyde dehydrogenase
APP	Amyloid beta (A4) precursor protein
Atf1	*Activating transcription factor 1*
BDNF	brain-derived neurotropic factor
Camk1g	*Calcium/calmodulin-dependent protein kinase 1G*
Cbfa2t3	*Core-binding factor, runt domain, alpha subunit 2; translocated to, 3*
Ccdc6	*Coiled-coil domain containing 6*
Ccl3	*Chemokine (C-C motif) ligand 3*
Ccnt1	*Cyclin T1*
Cdkn1a	*Cyclin-dependent kinase inhibitor 1a*
Ceacam1	*Carcinoembryonic antigen-related cell adhesion molecular 1 (biliary glycoprotein)*
Cisd1	*CDGSH iron sulfur domain 1*
Clp1	*Cleavage and polyadenylation factor I subunit 1*
Crem	*cAMP responsive element modulator*
Cspp1	*Centrosome and spindle pole associated protein 1*
Dnahc3	*Dynein, axonemal, heavy chain 3*
Dnajb11	*DnaJ (Hsp40) homolog, subfamily B, member 11*
DNMT	DNA methyltransferase
DSPc	dual specificity phosphatase, catalytic domain
Dusp19	*Dual specificity phosphatase 19*
E2f	*E2 transcription factor*
Egr3	*Early growth response 3*
Eomes	*Eomesodermin (Xenopus laevis) homolog*
ERBB2	v-erb-b2 erythroblastic leukemia viral oncogene homolog 2, neruo/glioblastoma derived oncogene homolog (avian)
ERK	Extracellular signal-regulated kinase
Fkbp2	*FK506 binding protein 2, 12kDa*
FOS	FBJ murine osteosarcoma viral oncogene homolog
GABA	γ-aminobutyric acid
$GABA_A$	γ-aminobutyric acid type A
$GABA_AR$	γ-aminobutyric acid type A receptor
Galnt7	*UDP-N-acetyl-alpha-D-galactosamine:polypeptide N-acetylgalactosaminyltransferase 7 (GaINAc-T7)*
Galnt9	*UDP-N-acetyl-alpha-D-galactosamine:polypeptide N-acetylgalactosaminyltransferase 9 (GaINAc-T9)*
Gapdh	*Glyceraldehyde-3-phosphate dehydrogenase*
Gpr50	*G protein-coupled receptor 50*
H2-T23	Major histocompatibility complex, class I, E

HLA-E	human leukocyte antigen, E
Hmgcs2	*3-hydroxy-3-methylglutaryl-CoA synthase 2 (mitochondrial)*
Homer1	*Homer homolog 1 (Drosophila)*
Hpca	*Hippocalcin*
Hsp90aa1	*Heat shock protein 90kDa alpha (cytosolic), class A member 1*
Hspa5	*Heat shock 70kDa protein 5 (glucose-regulated protein, 78kDa)*
Htr5a	*5-hydroxytryptamine (serotonin) receptor 5A, G-protein coupled*
HTT	huntingtin
IFNG	interferon-gamma
Ighg	*Immunoglobulin heavy chain (gamma polypeptide)*
IL4	interleukin 4
IL5	interleukin 5
IRE1α	inositol-requiring transmembrane kinase/endonuclease-1
Itga4	*Integrin, alpha 4 (antigen CD49D, alpha 4 subunit of VLA-4 receptor)*
Itpripl2	*Inositol 1,4,5-triphosphate receptor interacting protein-like 2*
JNK	c-Jun NH(2)-terminal kinases
Lair1	*Leukocyte-associated immunoglobulin-like receptor 1*
Manf	*Mesencephalic astrocyte-derived neurotrophic factor*
Map3k1	*Mitogen-activated protein kinase kinase kinase, E3 ubiquitin protein ligase*
MAPK	mitogen-activated protein kinase
Mbd4	*Methyl-CpG binding domain protein 4*
Mup5	*Major urinary protein 5*
nAChRs	nicotinic acetylcholine receptors
Nat1	*N-acetyltransferase 1*
NFkB	nuclear factor-kappaB
NMDA	N-methyl-$_{D}$-asparate
P4HA1	Prolyl 4-hydroxylase, alpha polypeptide I
Pcna	*Proliferating cell nuclear antigen*
Pdia4	*Protein disulfide isomerase family A, member 4*
Pdia6	*Protein disulfide isomerase family A, member 6*
Pip5k1b	*Phosphatidylinositol-4-phosphate 5-kinase, type I, beta*
Pkc	*Polyketide synthase*
Plrg1	*Pleiotropic regulator 1*
PPARα	peroxisome proliferator-activated receptor alpha
PPARγ	peroxisome proliferator-activated receptor gamma
Ptpn22	*Protein tyrosine phosphatase, non-receptor type 22 (lymphoid)*
Prdx1	*Peroxiredoxin 1*
Rasa2	*RAS p21 protein activator 2*
RUNX	runt-related transcription factor
Rybp	*RING1 and YY1 binding protein*
Sdf2l1	*Stromal cell-derived factor 2-like-1*
Setd2	*SET domain containing 2*
Slitrk2	*SLIT and NTRK-like family, member 2*
Smarca5	*SWI/SNF related, matrix associated, actin dependent regulator of chromatin, subfamily A, member 5*

$SMARCB_1$	SWI/SNF related, matrix associated, actin dependent regulator of chromatin, subfamily B, member 1
Spred2	*Sprouty-related, EVH1 domain containing 2*
SPRR2A	Small proline-rich protein 2A
Ssh2	*Slingshot homolog 2 (Drosophila)*
Stxbp6	*Syntaxin binding protein 6 (amisyn)*
Synpr	*Synaptoporin*
Tbxa2r	*Thromboxane A2 receptor*
Tdg	*Thymine-DNA glycosylase*
TGF-β	tansforming growth factor beta
TNF	tumor necrosis factor
Tnfrsf19	*Tumor necrosis factor receptor superfamily, member 19*
TP53	Tumor protein 53
Trdn	*Triadin*
Vpreb1	*pre-B lymphocyte 1*
Xbp1	*X-box binding protein 1*

Introduction

1.1 Fetal alcohol spectrum disorders (FASD)

1.1.1 Clinical background on FASD

The maternal consumption of alcohol during pregnancy may lead to neurodevelopmental abnormalities in exposed children[1,2]. Children exposed to ethanol prenatally may acquire a continuum of permanent birth defects known as Fetal Alcohol Spectrum Disorders (FASD)[3,4]. FASD affects approximately one in 100 live births[5]. FASD-related abnormalities may include physical, behavioural, and cognitive dysfunctions of varying degrees[2,6–9]. Growth deficiency, low birth weight, spatial learning delays, neuromuscular coordination deficits, central nervous system damage, and craniofacial malformations are key features of FASD[9–15]. Children and adults who have been exposed to alcohol *in utero* may experience problems in attention span, judgment, communication, executive functioning, memory, and social adaptation[16–18]. Once affected by alcohol, a child is affected for life, and there is no cure. Even with behavioural interventions, individuals with FASD may live with lifelong learning disabilities and poor social skills[9].

The spectrum of disabilities resulting from prenatal alcohol exposure ranges from mild defects, defined as Fetal Alcohol Effects (FAE), to more severe and diagnosable cases of Fetal Alcohol Syndrome (FAS). FAE are characterized by the occurrence of minimal abnormalities; meanwhile, FAS is the most severe form on the FASD spectrum[19,20]. FAS is characterized by all, or a combination of the following: severe mental illness, craniofacial abnormalities, intrauterine growth retardation, depression or psychosis, and antisocial behaviour[6,19,21]. Unlike any other forms of FASD, FAS is an official International Classification of Diseases (ICD) diagnosis[22]. Other conditions resulting from *in utero* alcohol exposure include Alcohol-Related

Neurodevelopmental Disorder (ARND) and Alcohol-Related Birth Defects (ARBD)[7]. Hyperactivity, anxiety, emotional problems, and learning disabilities are common across the FASD spectrum[7,14,19]. Due to the behavioural heterogeneity in individuals with FASD, it is difficult to diagnose children with different types of FASD. To overcome this limitation, a quantitative behaviour checklist is used to categorize abnormalities observed in children who have been exposed to alcohol prenatally[19]. In this way, cases can be distinguished based on child-specific behavioural manifestations of FASD disabilities. Specific classifications across the FASD spectrum allow for more thorough insight into how an individual was developmentally influenced by alcohol, both physically and mentally.

1.1.2 FASD is a wide-spread and costly disorder

The prevalence of FASD in Canada and the United States is approximately 9.1 in 1000 live births, as reported by the Public Health Agency of Canada[5]. In the late 1980's, this number was 1.9 per 1000 live births[3]. The number of individuals affected with FASD has been steadily increasing. One possibility for the increasing rate of FASD is an increasing rate of disregard for proper lifestyle habits during pregnancy. Also, pregnant women may be unaware of their pregnancies and may continue to consume alcohol throughout early pregnancy. Other possibilities for the increasing numbers of FASD could be due to increased awareness and self-reporting, resulting in more diagnoses. FASD is the most common, preventable cause of mental retardation in Canada and the United States[23]. In Canada, the annual cost of FASD amounts to 5.3 billion dollars[5].

1.1.3 Current treatments for FASD exclude biological mechanisms

There is no treatment or cure for physical defects and central nervous system (CNS) damage resulting from fetal alcohol exposure. However, the severity of learning disabilities can be diminished. Parents and teachers can help children who have been characterized with FASD. A multi-disciplinary approach is needed to characterize deficits in children with FASD[7,18,24]. In the same way, a multi-disciplinary approach is also needed to help a child with FASD reach his or her full potential. Other than parents and teachers, individuals who may be involved include psychologists, social workers, and health counsellors. Techniques used by clinicians to evaluate children with FASD may involve measuring a child's growth rate and examining his or her facial features[25]. Psychologists, speech-language pathologists, and occupational therapists may assess CNS damage to help characterize the severity of defects resulting from prenatal alcohol exposure[26]. Across a population, children with FASD have highly variable IQ scores[27–29]. Individual learning profiles of each child must be developed and implemented. However, many children with FASD are ineligible for special services because their intellectual abilities often fall within the average range of intelligence[30]. These children — who were exposed to alcohol prenatally, but still have average intelligences — benefit from IQ and achievement measurements[30]. Functional classroom assessments, family information, and school assessment processes allow educators and counsellors to work together to assess the impact of environmental conditions on a child's abilities. This helps to evaluate which conditions may disrupt effective functioning and learning. The efficacy of Child Friendship Training has been reported upon; this type of training improves knowledge of appropriate social behaviour in children with FASD[31]. Another method, Cognitive Control Therapy, is often used to teach

progressive skill-building that focusses on the child's ability to understand his or her own learning style and challenges[30].

1.1.4 Difficulty in diagnosing FASD based on phenotypes

Prenatal alcohol exposure is the most common preventable cause of cognitive disabilities in the western world[23]. However, FASD is difficult to properly diagnose, particularly because it shares traits with other complex disorders such as Attention Deficit Hyperactive Disorder (ADHD)[32]. ADHD is diagnosed in up to 94% of individuals who have experienced heavy *in utero* alcohol exposure[32]. Often, children with FASD have co-morbid ADHD, and can be diagnosed improperly. FASD-affected children may receive incorrect or insufficient treatment. Rasmussen and colleagues analyzed 52 children with FASD, and found that 63% received a co-morbid diagnosis of ADHD[33]. The authors also found that children with FASD and ADHD performed worse than children with FASD but without ADHD on sensory/motor, cognitive, communication, memory, executive functioning, attention, and adaptive behaviour tasks[33]. Another study found that out of 2,231 FASD-affected youth, 41% were diagnosed with ADHD, 17% were diagnosed with learning disorders, and 16% were diagnosed with oppositional-defiant/conduct disorder[11]. Although researchers make efforts to identify behavioural characteristics differentiating children with FASD and ADHD, the psychological services are not always available[11,34]. Maternal self-reported drinking as a means of predicting behavioural dysfunctions in "at-risk" children can be misconstrued[35]. Other difficulties in the characterization of FASD include absence of craniofacial malformations in children who have undergone *in utero* alcohol exposure, coupled with the unavailability of maternal drinking data[34]. Also, an increase in binge drinking among women of child-bearing age, coupled with the unawareness of

pregnancy early in the first trimester, could contribute to the pervasiveness and eventual mischaracterization of FASD[36–38].

A further complication resulting in difficulty in characterization of FASD includes the inconsistency of symptoms due to dosage-specific effects of alcohol. Since the 1960's, researchers have reported on the relevance of a multitude of factors in determining the severity of FASD abnormalities; factors include: quantity, frequency, and timing of alcohol[39]. For instance, facial dysmophology is caused by alcohol exposure during early gestation (gastrulation)[40]. Heavy drinking increases the likelihood of FASD in offspring; children prenatally exposed to high amounts of alcohol perform worse on measures important for reading and arithmetic skills than children exposed to low amounts of alcohol[41]. Dosage- and timing-specificity may be attributable to disruption of specific neurodevelopmental patterns that occur during fetal development. Though the timing- and dosage-specificity underlying FASD is not well-established, women have been advised that no amount of alcohol is safe to consume during pregnancy[38]. Researchers suggest that, in addition to genetic background, the timing and dosage of prenatal alcohol exposure is an important factor in determining the variation in behavioural manifestations related to FASD[3,5,42].

1.2 Ethanol exposure can lead to adverse effects in the fetus

1.2.1 Ethanol's mechanism of action

Prenatal alcohol exposure leads to alterations in fetal brain structures that give rise to developmental and behavioural abnormalities in children[19]. The metabolism of alcohol in the maternal liver involves the oxidation of ethanol into acetaldehyde by an enzyme called alcohol dehydrogenase (ADH); ADH is further oxidized into acetate by another enzyme, acetaldehyde

dehydrogenase (ALDH)[43]. The intermediary compound, acetaldehyde, is harmful to the fetus[43]. Acetaldehyde leads to increased accumulation of oxygen radicals, which have harsh implications on the developing brain. For instance, DNA replication and DNA repair enzymes can be impaired[44,45]. Tissue damage may be a direct result of the accumulation of reactive oxygen species (ROS) through the process of ethanol oxidation. Accumulation of acetaldehyde can result from ADH conversion; the ADH complex is used to convert ethanol to acetaldehyde 90% of the time[43]. Acetaldehyde can result in protein adducts, which lead to cellular damage, and subsequent oxidative stress.

1.2.2 Ethanol toxicity in the developing fetus

In a developing fetus, morphological changes occur in multiple areas of the brain due to ethanol toxicity. It is well-established that prenatal alcohol exposure can alter brain development, leading to neurodegeneration in humans[46–49], and in mice[21,50–55]. Ethanol can lead to reductions in cerebellar volume and surface area, reductions in basal ganglia, decreases in dendritic complexity, abnormalities in grey and white matter distribution and density, and apoptosis in sensitive brain regions[2,52,55]. The affected brain areas are necessary for hormone regulation, sensory information processing, learning, and memory. Ethanol (or its metabolites) can pass through the blood-brain barrier and disturb the developing fetal brain. The basis for the observed behavioural heterogeneity in FASD is unknown. Certain time points during pregnancy are critical stages of neurodevelopment, and are particularly sensitive to environmental toxins (eg. alcohol)[2]. Alcohol exposure at critical stages during pregnancy may lead to the spectrum of abnormalities observed in children with FASD.

1.3 Binge drinking and its adverse effects on offspring

Binge drinking is defined as a pattern of alcohol consumption that raises blood alcohol concentration (BAC) to 0.08 gram percent or above, which is equivalent to the consumption of five or more drinks within a couple of hours of each drink[56]. This definition has been revised to three or more drinks per occasion; this level of drinking highly correlates with child dysmorphology and behavioural alterations[57]. Binge drinking has been identified as the most damaging form of alcohol consumption because it produces a high BAC in the mother, which can have adverse effects on the developing fetus[58,59]. Peak BACs are higher in binge models of alcohol exposure than more moderate, continuous-drinking paradigms; these data correlate with increased atherosclerotic plaque development in binge versus continuous models of FASD in mice[60]. Alcohol-induced neuronal loss in developing rats leads to increased brain damage following maternal binge drinking[61]. Binge drinking is particularly harmful to the developing fetus because alcohol takes longer to metabolize at higher BACs, particularly in women[62]. Also, the specific gestational time of binge drinking may correlate with key stages of brain development, which may lead to more severe deficits in offspring. On another note, there is a strong association between binge drinking and unplanned pregnancy[63]. In cases of unplanned pregnancy, women may consume alcohol without knowledge of pregnancy. These women may continue to drink heavily into their pregnancies, having exposed their fetuses to the teratogenic effects of alcohol.

1.4 Timing and dose-dependent effects of alcohol on neurodevelopment

The neurodevelopmental effects of alcohol are specific to the timing of exposure and the developmental processes that occur during specific times. One of the critical points during

neurodevelopment occurs during the embryonic stage of gestation (first trimester)[2]. Exposure to alcohol during gastrulation negatively impacts formation of germ layers and reduces neural progenitors[64]. These reductions lead to long-term effects on the forebrain and brainstem[65,66]. Maternal binge drinking during the early stage of embryogenesis is also associated with a high incidence of craniofacial malformations and mental disabilities[67,68]. Another critical stage during fetal development occurs in humans from 7-20 weeks of gestation (second trimester). At this stage, the fetal brain undergoes neuroepithelial cell proliferation and migration[69]. Most of the areas of the nervous system (except cerebellum) begin to differentiate[2,64,70]. Prenatal ethanol exposure can alter neuronal migration and lead to reductions in the numbers of neurons and glial cells in the neocortex, hippocampus, and sensory nucleus in the fetal brain[64,70]. Such disturbances to brain development can lead to long-term abnormalities in brain size and likely contribute to cognitive deficits in individuals with FASD[48].

Dosage is also an important factor that influences the severity of neurodevelopmental deficits associated with prenatal alcohol exposure. Alcohol may affect the developing fetus in a dose-dependent manner. Binge alcohol consumption produces more severe deficits in offspring development and behaviour than daily moderate consumption[59,60]. Exposure to heavy drinking (> 48-60 grams ethanol/day) may cause FAS, whereas moderate drinking (between 24-48 grams ethanol/day) can result in "alcohol effects"[71]. Binge drinking, with intakes of 4-5 drinks of ethanol per sitting (> 90 grams ethanol/day), can result in greater peak BACs than other forms of alcohol consumption[72]. It is difficult to define and characterize developmental risks associated with binge drinking in human subjects due to inconsistencies in dosage and timing.

1.5 Using mouse models to study FASD

1.5.1 The impact of the C57BL/6J mouse in FASD research

FASD, specifically when studied in the C57BL/6J (B6) mouse, has been examined by various methods. The B6 mouse is the most widely used inbred strain and was the first to have its genome sequenced[73]. The B6 mouse is commonly used in alcohol-related research. Years ago, alcohol's causative role in FAS was examined through administration of ethanol injections in pregnant mice[74]. B6 mice were often used in ethanol preference tests to study defects in locomotor activity and passive avoidance behaviour[1]. Using B6 mice in ethanol preference models was beneficial since B6 mice prefer to drink ethanol to water ~70% of the time[75]. Therefore, these mice are useful for studies on FASD. Once the genetics of alcohol metabolism were elucidated, more researchers used mice for molecular studies of ethanol exposure. The results of this research led to identification of polymorphisms in the ADH genes, which are associated with the conversion of ethanol to acetate; ADH genes were detected in human subjects, and could be subsequently used for knockout studies in mice[76]. Throughout the years, studies have continued using B6 mouse models to identify FASD-related phenotypes through various means. Some of the studies included proteomics screenings of amniotic fluid[77], behavioural testing[78], placental biomarker identification[79], dendrite sectioning[55], candidate gene selection[80,81], and more recently, genome-wide studies[82–84].

1.5.2 Advantages of a mouse model for complex disorders

Although studies use a variety of model organisms, there are many advantages to using a mouse model:

1. Mouse genomes and human genomes both contain the same approximate number of genes (~30,000), of which 95-99% are homologous[85].
2. Genetic determinants of diseases in humans are highly conserved in mice[86–88].
3. The B6 strain has been used successfully in replicating a variety of FASD-related phenotypes with well-defined experimental tools[1,78,89–91].
4. The effects of prenatal ethanol exposure on neurodevelopment are well-studied in B6 mice[21,51,92–95].
5. The B6 mouse has been used to examine transcriptomic alterations in the brain using high-density, mouse-specific arrays[80,81,96–98].
6. Using the B6 mouse allows for precise control of ethanol timing and dosage[21].
7. Many behavioural tests used for mice are well-established and representative of human behaviours[89,91,99–101].

1.5.3 Differences in dosage of ethanol in producing FASD-relevant phenotypes

Various ethanol dosages, resulting in varying BACs, have been examined in mice. BACs must remain above a toxic threshold of neurodegeneration, in the range of 180-200 mg/dl, to produce FASD-relevant behavioural deficits in mice[21]. This toxic threshold was proposed by Ikonomidou and colleagues, who found that ~200 mg/dl was the minimum condition for triggering neurodegeneration[21]. With a dose of 2.5 g/kg of ethanol, given once, BAC barely crosses the toxic threshold for neurodegeneration. When 2.5 g/kg ethanol is given twice, spaced two hours apart, BAC rises to ~500 mg/dl and remains above 200 mg/dl for ~14 hours. This double injection paradigm allows for enough ethanol to raise the BAC above 200 mg/dl. Also, this paradigm gives a second boost of alcohol, allowing the BAC to remain > 200 mg/dl for several hours. The maintenance of increased BAC occurs because the degenerative response

becomes progressively more severe. This effect results in long-lasting behavioural deficits, neurodevelopmental abnormalities, and gene expression changes in the offspring[91,102]. In addition to dose, the method of ethanol delivery is important. Researchers have consistently used injections to administer ethanol to pregnant females[21,103,104]. The most widely used routes of injection in mice include *subcutaneous* (*sc*) and *intraperitoneal* (*ip*) injections[105]. However, because *ip* injections can result in direct ethanol injection into the womb and severe discomfort for the female, *sc* injections provide a safer route of administration[105].

1.5.4 A variety of mouse-specific behaviour tests to model FASD

It is well-known that individuals with FASD have a range of behavioural deficits, depending on the timing and dosage of prenatal alcohol exposure. In order to characterize these disabilities, a variety of mouse-specific behaviour tests can be used. Behavioural traits that can be measured include: developmental milestones, activity, anxiety-related behaviours, and learning and memory. Activity and anxiety-related behaviours can be measured using an Actitrack apparatus (PanLab Harvard Apparatus, Holliston, MA). An Elevated Plus Maze (EPM) and a Light/Dark Box (LDB) and can also be used to measure anxiety-related behaviours[99,100]. Spatial learning and memory can be assessed in mice using a Barnes Maze[89].

Developmental milestone assessment on neonatal and postnatal mice will be completed following a protocol outlined by Hill and colleagues[101]. The milestones outlined in this protocol are: surface righting, negative geotaxis, cliff aversion, forelimb grasp, air righting, open field traversal, eye opening, and ear twitching. The milestones are assessed from postnatal day (PD) 2-21. Each of the tasks represents an examination of FASD-relevant milestones that are delayed in children exposed to alcohol prenatally. Some of the delays represent deficits in strength, reflex,

motor coordination, and balance[44,106–108]. The usefulness of these tasks has been demonstrated in previous studies of complex disorders, including FASD[91,109,110].

As juveniles, mice can be assessed at PD 25-30 for exploratory behaviour to examine general activity and anxiety-related traits in a novel, open-field, environment using the locomotor apparatus[91]. PD 25-30 corresponds to the prepubescent period in mice[111]. The prepubescent stage is a common time for diagnosing ADHD in children[112,113]. At PD 25-30, anxiety can assessed concurrently using the locomotor apparatus. Anxiety disorders manifest in childhood, but rise into adolescence[114]. Examining anxiety-related traits in mice between PD 30-35 will allow for assessment at adolescence. In this case, the EPM and LDB, which are popular tools to assess anxiety-related traits in rodents, are used beginning PD 30[99,100]. The locomotor apparatus, EPM, and LDB rely on the rodent's innate aversion to brightly illuminated or open areas; these tests also rely on the spontaneous exploratory behaviour of the animals[100]. Anxiety-relevant results from each of these tests should be complementary. Due to the complexity and multidimensionality associated with anxiety-related traits, it is beneficial to use more than one tool to generate data regarding anxiety-related behaviours in mice[115].

Spatial learning and memory are assessed using a Barnes Maze, beginning PD 45-50[89]. The timing corresponds to early adulthood in mice, and allows for the comparison of these behaviours to adult humans[36]. Although learning disabilities are observable in children with FASD, the reasoning behind testing at young adulthood is to examine whether disabilities persists from birth to adulthood. In the Barnes Maze, mice rely on spatial orientation to learn the location of a target hole[89]. Given that mice have dichromatic vision, four spatial reference points — coloured black, orange, or blue — are used to visually create shade/shape-differences across

walls. An overhead light and white noise are generated to motivate mice to learn the spatial orientation of a target hole in order to escape the open field area.

1.6 Evidence for ethanol's effect on gene expression

Along with behavioural abnormalities, molecular pathways are differentially affected by prenatal alcohol exposure[43,82]. Cellular death, resulting from prenatal ethanol exposure, is dependent on the ability to transcribe and translate genes[116]. Strongly-supported ethanol targets include enzymes that bind alcohol (i.e. ADH)[43], and postsynaptic receptors such as *N*-methyl-$_D$-asparate (NMDA)-type glutamate receptors and γ-aminobutyric acid type A ($GABA_A$) receptors[117,118]. Treatment of animals with ethanol alters the expression and function of genes and proteins[87,119,120]. Even with the accumulation of knowledge surrounding ethanol's effects on genes, it is not well-understood which genes are affected by ethanol. Also, specific gene knockouts do not necessarily implicate any of the resulting proteins as direct targets of ethanol action[120,121]. A protein's particular role may be downstream from the initial binding sites for alcohol. Candidate gene studies are not sufficient to explain complex mechanisms of ethanol's neurotoxic effects. Complex disorders, such as FASD, are multifactorial, with multiple gene interactions underlying its phenotypes[122]. A polymorphism or misregulation of a single gene is not enough to explain the wide spectrum of FASD phenotypes. Also, a candidate gene approach to conducting genetic studies focuses on associations between genetic variation within pre-defined genes-of-interest and phenotypes or disease states. This approach fails to elucidate the molecular underpinnings of complex disorders for various reasons. Spectrum disorders, like FASD, typically vary in severity of symptoms, which results in difficulty in defining an appropriate phenotype. Also, these disorders vary in their aetiological mechanisms, which may involve various biological pathways. Finally, complex diseases are likely caused by

dysregulation of several, and even numerous, genes, each with a small overall contribution and relative risk[123]. To combat these issues, genome-wide approaches have been undertaken. However, previous genome-wide studies lack consistent and comprehensive dosage regimens. In particular, reports are not consistent when comparing behaviours and transcriptomes in ethanol and control subjects between different time points. With the increase in knowledge from gene chip analysis (microarray) studies, the gene expression changes resulting from prenatal ethanol exposure can be better understood. Once ethanol-responsive genes and pathways are identified, insight into causes, therapies, and treatments may be possible.

1.7 Microarrays to study global gene expression patterns

1.7.1 Microarrays as a means of studying complex disorders

Microarrays, commonly known as DNA chips, are defined as a collection of microscopic DNA spots attached to a solid surface. They are used to measure the expression levels of large numbers of genes simultaneously. Each of the DNA spots contains picomoles of a specific DNA sequence known as a probe. A probe is a short section of a gene, or other DNA element, that is used to hybridize a complementary DNA (cDNA) or complementary RNA (cRNA) sample under high stringency conditions. Detection of hybridization is usually through a fluorophore-labeled target, which is used to determine relative abundance of nucleic acid sequences in the target. Microarrays have been used extensively for humans and mice, in the search for gene expression changes associated with complex disorders such as: aging, cancer, obesity, schizophrenia, Alzheimer's Disease, autism, alcoholism and, more recently, FASD[124–131]. As a disclaimer in this thesis, when referring to gene expression, I specifically mean mRNA levels (i.e. the transcriptome). The application of microarrays to mice, particularly the B6 mouse, is well-

documented; mouse microarrays are useful for examining the underlying biological mechanisms governing complex phenotypes, which include abnormalities resulting from prenatal alcohol exposure[91,132–134]. Complementary DNA microarrays allow for the quantification of large numbers of messenger RNA transcripts for the purpose of large-scale insight into cellular processes involved in the regulation of gene expression[135].

1.7.2 Overview on functional, pathway, and network analysis of microarray data

Following the identification of differentially-expressed genes (DEGs) using microarrays, various software programs can be used to determine the importance of specific pathways and networks in relation to behavioural phenotypes. For functional characterization of DEGs, the following databases are applicable: The Database for Annotation, Visualization and Integrated Discovery (DAVID)[136], Gene Ontology Enrichment (GE) (Partek Inc., St. Louis, MO, USA), and Ingenuity Pathway Analysis (IPA) (Ingenuity® Systems, Redwood, CA). The freely available DAVID program relies on functional annotation clustering, which uses a *p*-value to examine the significance of gene-term enrichment using a modified Fisher's exact test[136,137]. A $p < 0.05$ suggests that an input gene is significantly more enriched than by random chance. The Partek Genomics Suite software version 6.6 (Partek Inc., St. Louis, MO) tool, GE, returns a list of functions based on the DEGs. The higher the enrichment score, the more overrepresented a functional group is in the gene list. This score is calculated using a chi-squared test, which compares the proportion of the gene list in a group to the proportion of the background in the group[138]. An enrichment score > 1 indicates that the functional category is over expressed, while a score of 3 corresponds to significant over expression ($p < 0.05$). IPA, a commercially available tool, is regarded as a high-quality functional analysis and knowledge discovery program. In IPA, a *p*-value is associated with a function, and is calculated using a right-tailed Fisher's exact test[139].

The *p*-value is calculated by considering the number of focus genes that participate in a process, versus the total number of genes that are known to be associated with that process. The *p*-value identifies significant over-representation of focus genes in a given process. Over-represented functional processes are those that have more focus genes than expected by chance (right-tailed)[139].

To identify genes in already-established pathways, Pathway Express (Intelligent Systems and Bioinformatics Laboratory, Michigan, USA), Pathway Enrichment (PE), and IPA will be used. The freely available Pathway Express database is considered as a high-throughput pathway visualization tool that focuses on pathways alone (no functional characterization). By default, Pathway Express uses hypergeometric distribution for *p*-value calculation[140]. The impact factor associated with a pathway is a probabilistic term that takes into consideration the proportion of DEGs in the pathway. Essentially, Pathway Express quantifies the influence of DEGs on a given pathway. The quantification of DEGs, in addition to the *p*-value, is used to distinguish between pathways that have the same proportion of DEGs[141]. Pathway Enrichment is a new feature incorporated in Partek software. PE generates an enrichment score, in addition to a *p*-value, for each pathway. This score is the negative natural log of the enriched *p*-value (Fisher's exact test)[142]. Both PE and Pathway Express rely on information from the Kyoto Encyclopedia of Genes and Genomes (KEGG) database (Kanehisa Laboratories, Tokyo, Japan); therefore, the results should be similar between the programs. Canonical pathway assessment using IPA results in a list of significant pathways that are altered based on the input genes. Canonical pathways are determined based on two parameters: a ratio of the number of genes from the data set that map to the pathway, divided by the total number of genes that map to the canonical pathway, and a *p*-

value calculated using Fisher's exact test that determines the probability that the association between the genes in the data set and canonical pathway is due to chance alone[143].

Two tools, GeneMANIA (Donnelly Centre for Cellular and Biomolecular Research, Toronto, Ontario) and IPA, can be used for network analysis of inputted genes that have shown to interact with other molecules. GeneMANIA incorporates a linear-regression algorithm. This algorithm is used to calculate a functional association network of inputted genes with other genes that are known to interact with the input genes; GeneMANIA uses this algorithm to predict gene function[144]. To complement GeneMANIA results, IPA can be used to further identify interacting networks. IPA has been successfully used by various researchers to examine networks of interacting genes that may play a role in a variety of diseases and disorders including FASD[94,145–148]. IPA links genes and molecules by interactions, which are based on current knowledge from records maintained in the Ingenuity Pathways Knowledge Base. Highly-interconnected networks are likely to represent significant biological function[149,150]. In IPA, each network is limited to ~35 genes, by the algorithm. A *p*-score, which is derived from a *p*-value, is calculated using Fisher's exact test. This score is assigned to each network, and is simply a measure of the number of focus genes in a network (user-specified genes)[151]. Another way to define the score is, the likelihood that the focus gene within the network was found by random chance[152]. A high number of focus genes leads to a higher network score. The network score is equal to the negative exponent of the respective *p*-value such that a score of 3 corresponds to a *p*-value of 10E-3[153]. Therefore, a network is considered significant with a *p*-score > 2. The combination of results from the DEG list, along with the functional, pathway, and network analyses, will give insight into FASD-relevant genes.

For a gene to be determined relevant to FASD-related phenotypes, it must be differentially-expressed on the microarray. Also, the gene must be implicated in neurodevelopment or behaviour, implicated in a top pathway or network, or involved in an inverse relationship with a differentially-expressed microRNA (miRNA). If the gene is classified as a central "hub" molecule in one of the top three networks, it may also be worthy of investigation. For the purpose of this study, a "hub" is defined as a molecule that appears in a top IPA network with strong intramodule connectivity to all other genes in the same module (analogous to the definition of a "hub" node in protein-protein interaction networks); a hub does not necessarily need to be altered, itself[154]. Previous studies have defined "hubs" as nodes with connectivity greater than five molecules[155–157]. In my thesis, a hub is restricted to a minimum of 10 interactions in order to provide a stringent analysis. A hub molecule is linked to dysregulated gene(s), which suggests that there are common mechanisms associated with neurodevelopmental ethanol exposure. The hub genes identified in this thesis are based on the number of interactions in the network[158].

1.8 Examining microRNAs (miRNAs) in the maintenance of FASD

1.8.1 MiRNAs and their role in the brain

In an attempt to explain the maintenance of gene expression changes in the adult brain following prenatal ethanol exposure, I will assess the importance of miRNAs in this role. MiRNAs are short (~17-25 nucleotides) endogenous noncoding RNAs that post-transcriptionally repress expression of protein-coding genes by base-pairing with the 3' untranslated region (UTR) of the target messenger RNA (mRNA)[159,160]. The ability of one miRNA to target multiple mRNAs suggests that miRNA are exceptionally important regulators of various cell processes.

MiRNAs can suppress gene expression through multiple mechanisms such as translational inhibition and mRNA degradation[161]. This degree of coverage implicates miRNAs in a vast regulator RNA network that enables flexible control of mRNA expression, especially in the brain. The brain is composed of 100-200 billion neurons, and each is connected to 5000-200,000 neurons[162–164]. Local control of gene expression upon synaptic activation and/or inhibition, coupled with gene expression, may be influenced by miRNAs. MiRNA genes are encoded within the genome, suggesting that their transcription may be tightly coordinated with their transcription of other genes (i.e. targets).

MiRNAs have been referred to as "master regulators of gene expression", thus it may be useful to examine their roles in complex disorders. MiRNAs appear to be responsible for fine regulation of gene expression, thereby "tuning" the cellular phenotype during delicate cellular processes such as development and differentiation[165]. Given that many miRNAs are conserved in sequence between distantly-related organisms, they may participate in essential processes[166,167]. During neurodevelopment, miRNAs are expressed in neurons and show distinct expression patterns within the developing CNS[168,169]. MiRNA expression in the CNS demonstrates their relevance to brain development and function. Researchers have implicated various miRNAs and their target genes — particularly GABA and NMDA-related genes — in psychopathology including: Tourette's syndrome[170], schizophrenia[171], bipolar disorder[171], autism[172] and Rett Syndrome[173] .

1.8.2 MiRNAs are ethanol-responsive

One of the first pieces of evidence that miRNAs mediate ethanol's teratogenic effects came from Sathyan and colleagues, who screened ~200 mouse miRNAs for ethanol sensitivity in

fetal neural stem cells[174]. Following this discovery, it was demonstrated that, between the latter half of the first trimester to the middle half of the second trimester period in mice, ethanol altered approximately 3% of the assessed mature miRNAs in whole brain RNA samples[175]. More recently, reseachers showed that differentiated neurons exposed to "chronic intermittent ethanol" resulted in significant alterations in ~11% of detected miRNAs[176]. Although only a small subset of miRNAs is known to be regulated by ethanol, these studies provide evidence for the dysregulation of miRNAs in FASD. The number of ethanol-sensitive miRNAs increases with developmental stage, which may reflect increasing complexity and diversity of miRNAs during neuronal maturation[176]. MiRNAs exhibit development stage-specific sensitivity to ethanol[175,176]. Some miRNAs are ethanol-sensitive over multiple developmental stages[174,176]. There is evidence for regional specificity of dysregulated miRNAs in the brains of ethanol individuals[177]. However, a global analysis of miRNA regulation in the whole brain will strive to complement and compare the results to global gene expression results.

MiRNAs may play an important role in the maintenance of FASD. Some miRNAs play important roles in early neural tube patterning, telencephalic neurogenesis, and early differentiation, which occur during fetal development[178,179]. MiRNA knockouts in mice result in FAS-like phenotypes such as fetal growth retardation and microcephaly[180]. Studies suggest that $GABA_A$ receptors ($GABA_AR$) and nicotinic acetylcholine receptors (nAChRs) mediate ethanol effects on miRNA expression[174,181]. Several ethanol-sensitive miRNAs are localized within chromosomal regions that are susceptible to epigenetic modification. Therefore, ligand-gated ion channel receptors, such as $GABA_A$Rs and nAChRs, and epigenetic modifications, are potential mediators of ethanol's effects on fetal miRNA[182].

1.8.3 Detecting globally disrupted miRNAs in the brain using arrays

There are several miRNA:mRNA target strategies that could be employed to examine the relationship between genes and miRNAs. There are various bioinformatic miRNA target prediction programs that produce lists of predicted targets for a given miRNA. For instance, TargetScan uses the Ensembl database to define 3' UTRs in order to identify genuine miRNA targets[183]. Prediction program rates of false positives range between 24-70%[184]. Experimental data are necessary to identify genuine miRNA targets. One experimental strategy to identify miRNA targets includes gene-specific experimental confirmation with well-established techniques such as quantitative reverse transcription PCR (qRT-PCR) to assess individual miRNA:mRNA interactions[185]. However, this strategy would not give a global picture of all possible miRNA:mRNA interactions in a specific state. Additionally, demonstrating individual miRNA:mRNA interactions misses the capacity to regulate complex genetic networks. Uncovering such networks requires large-scale and unbiased methods of miRNA target identification, followed by downstream gene expression analysis (microarray and qRT-PCR). Quantitative RT-PCR may be useful in the downstream confirmation of specific miRNAs.

Only in the past decade have miRNA chips been used to study global changes in response to ethanol exposure[174,185]. When coupled, miRNA and gene expression arrays are useful for detecting inverse relationships between genes and miRNAs[188]. Launched in 2011, the Affymetrix GeneChip miRNA 2.0 Array (Affymetrix, Santa Clara, CA) offers the broadest coverage of known miRNA, encompassing 131 organisms on one array, and allowing for downstream, independent interrogation of mouse-specific miRNA expression[189]. An overall analysis of mouse-specific miRNA alterations in response to prenatal ethanol exposure will be useful in determining molecular changes associated with FASD. MiRNAs that are found to be

differentially-expressed — using the same fold change and *p*-value criteria as those used in gene expression analysis — can be submitted to IPA Target Filtering. Target Filtering is used to predict miRNA:mRNA inverse relationships.

1.9 Background on FASD summarized

FASD represents a major health concern in the developing world. FASD is the leading cause of preventable birth defects in North America, affecting approximately one in 100 individuals, and costing Canada 5.3 billion dollars annually[5]. Given the rise in binge-drinking among women of child-bearing age[190,191], FASD remains a major health concern. The correlation between binge-drinking and risky behaviour, including unplanned pregnancy, further increases the chances of birthing a child with FASD[192]. Difficulties arise in the study of FASD in human populations. The biological mechanisms governing this disorder are not well-elucidated, and require the use of a model organism. Given these issues, researchers should focus on the developmental understanding of prenatal ethanol exposure, including its effects on behaviour and the brain transcriptome. A more-comprehensive understanding of FASD needs to be generated, with a focus on timing, mechanism, and potential molecular targets for corrective measures.

1.10 Hypothesis and objectives

1.10.1 Hypothesis

Prenatal alcohol exposure (binge) during the first and second term of gestation causes FASD-related behavioural abnormalities, and involves immediate and lifelong changes in brain gene expression affecting specific molecular pathways and networks.

1.10.2 Specific objectives

1. To establish if

   a) binge-like prenatal ethanol exposure alters developmental milestones, and

   b) leads to behavioural abnormalities associated with FASD in C57BL/6J mice.

1. To establish if binge-like prenatal ethanol exposure leads to immediate (fetal) and long-term (adult) alterations in genome-wide gene expression in the brain, including miRNAs.
2. To establish if the changes observed in 2. are specific to molecular pathways and networks related to behaviour and/or neurodevelopment.
3. To establish if changes in 3. may account for changes in behaviours observed in 1.a and 1.b.
4. To establish any role for miRNAs in altered gene expression in response to binge-like prenatal ethanol exposure.

2. Materials and Methods

2.1 Animals

2.1.1 Animal care and use

This research uses C57BL/6J mice. All animal protocols were approved by the Animal Use Subcommittee at the University of Western Ontario (Appendix A) and complied with the ethical standards outlined by the Canadian Council on Animal Care. Mice were originally obtained from Jackson Laboratories (The Jackson Laboratory, Bar Harbor, ME) and subsequently bred at the Health Sciences Animal Care Facility at the University of Western Ontario (SOP #2007-059-10). Males and females were housed in separate (same-sex) cages. Food and water were provided *ad libitum*. Eight-week-old B6 females were time-mated overnight with 8-12-week-old B6 males. The following morning, gestational day (GD) 0, males were removed from cages and females remained alone for the duration of their pregnancies. Cages were standardized between animals and included only nestlets and bedding. Mice were kept on a 14/10 hour light/dark cycle at a temperature of 21-24°C with 40-60% humidity.

2.1.2 Experimental design

Pregnant dams were randomly divided into three groups. These included: 1) trimester two treatment, short-term exposure (T2-S), 2) trimester one treatment, long-term exposure (T1-L), and 3) trimester two treatment, long-term exposure (T2-L). Each experimental group consisted of two randomly assigned subgroups of dams: ethanol-exposed (ethanol) and saline-exposed (control). The experimental design is shown in **Figure 1** and includes subjects, treatments, groups, experimental tests, and criteria for FASD-relevant candidate genes and miRNAs.

To assess the immediate effects of ethanol exposure on the developing brain, a group of pregnant dams (T2-S) was randomly assigned to two subgroups: ethanol and control. Dams were *subcutaneously* injected at GD 16 with 2.5 g/kg of ethanol in 0.15 M saline at 0 h and 2 h. Matched control dams were injected with 2.5 g/kg saline at 0 h and 2 h on GD 16. Two hours following the second injection, dams from both subgroups were euthanized by CO_2 asphyxiation and cervical dislocation. Fetal brains from the two groups of dams were extracted and used for gene expression arrays (**Figure 1**).

To model acute, binge-like ethanol exposure during the first trimester equivalent (T1-L) dams were *subcutaneously* injected at GD 8 and 11 with 2.5 g/kg of ethanol in 0.15 M saline at 0 h and 2 h[21,193–195]. Matched control dams were injected with 2.5 g/kg saline on GD 8 and 11 at 0 h and 2 h. Mothers were allowed to give birth, and T1-L offspring were followed from birth (PD 2) until early adulthood (PD 70) using a battery of behavioural tests. At PD 70, animals were euthanized by CO_2 asphyxiation, followed by cervical dislocation. Whole brains were used for transcriptome analysis, which included gene expression arrays and miRNA arrays (**Figure 1**).

To model binge-like ethanol exposure during the second trimester equivalent (T2-L), dams were injected with 2.5 g/kg of ethanol in 0.15 M saline at 0 h and 2 h on GD 14 and 16[21,158]. Matched controls were injected with 2.5 g/kg saline at 0 h and 2 h on GD 14 and 16. Once again, mothers were allowed to give birth, and T2-L offspring were followed from PD 2-70 using a battery of behavioural tests. At PD 70, mice were euthanized by CO_2 asphyxiation and cervical dislocation. Whole brains were dissected for gene expression and miRNA analysis (**Figure 1**).

Short-term	Long-term		CRITERIA
	T1-L	T2-L	
T2-S	**Behaviour** n = 20 control n = 26 ethanol	**Behaviour** n = 26 control n = 28 ethanol	Behavioural abnormalities (activity, anxiety, learning and memory)
Mouse Gene 1.0 ST Array n = 6 control n = 6 ethanol	**Mouse Gene 1.0 ST Array** n = 6 control n = 6 ethanol	**Mouse Gene 1.0 ST Array** n = 6 control n = 6 ethanol	Differentially-expressed ± 1.2 fold change $p < 0.05$
	GeneChip miRNA 2.0 Array n = 6 control n = 6 ethanol	**GeneChip miRNA 2.0 Array** n = 6 control n = 6 ethanol	Differentially-expressed ± 1.2 fold change $p < 0.05$
Gene Function	**Gene Function**	**Gene Function**	Neurodevelopment OR behaviour
Gene Pathway/ Network	**Gene Pathway/ Network**	**Gene Pathway/ Network**	Top pathway/network (hub) OR Inverse miRNA:mRNA
qRT-PCR n = 6 control n = 6 ethanol	**qRT-PCR** n = 6 control n = 6 ethanol	**qRT-PCR** n = 6 control n = 5 ethanol	Differentially-expressed $p < 0.05$

Figure 1. **Experimental layout showing short-term (T2-S) and long-term (T1-L and T2-L) groups, behavioural and transcriptomic experiments, and criteria for relavant transcriptomic changes following prenatal ethanol exposure.** The number of mice (n) used for behavioural experiments are shown. The number (n) of individual mice (biological replicates) is shown for each molecular experiment. For array experiments, six individuals were segregated onto two arrays with three pooled mice on each array. T2-S = trimester two, short-term effect (pink). T1-L = trimester one, long-term effect (blue). T2-L = trimester two, long-term effect (green). miRNA = microRNA. mRNA = messenger RNA. qRT-PCR = quantitative reverse transcription PCR. Gene expression and qRT-PCR were completed on T2-S samples. Behaviour, gene expression, miRNA analysis, and qRT-PCR (genes and miRNAs) were completeted on T1-L and T2-L. Genes and miRNAs were considered candidates for Fetal Alcohol Spectrum Disorder (FASD) if they were: implicated in neurodevelopment or behaviour and/or if they were found in a top pathway/network or had an inverse miRNA:mRNA relationship.

2.2 Behaviour testing

2.2.1 Developmental milestone assessment

T1-L and T2-L ethanol and control mice were followed from PD 2-21 for the achievement of developmental milestones[101]. Achievement was based on the ability of a pup to display a positive response for two consecutive days. For each milestone, the number of days to reach the milestone was recorded. The second consecutive day was recorded as the day of acquisition of the milestone. Testing commenced at 10:00 am each day, with the dam placed in a separate cage throughout the testing procedure.

a) Surface righting

Beginning on PD 2, the pup's ability to right itself on a plastic surface was evaluated. Pups were placed on their backs with all four limbs held to the top and, once released, the time (seconds) taken to roll over and place all four paws on the surface was measured. This test measures the development of the vestibular reflex and motor coordination. Positive responses were noted when pups were able to complete the task for two consecutive days in < 1 second.

b) Negative geotaxis

On PD 2, the pup's ability to rotate its body 180° while on a sloped platform was measured. Pups were placed on a mesh wire platform, angled at 45° from the horizontal, with their nose pointed towards the ground. The latency to rotate the body until the nose pointed upward was recorded. Latency to rotate the body is considered a measurement of vestibular and postural reflexes. Positive responses were noted once pups were able to complete the task for two consecutive days in < 30 seconds.

c) Cliff aversion

Beginning on PD 2, the pup's ability to avert a cliff was assessed. Pups were placed on the end of a 2-inch-high platform with their noses and fore-digits suspended over the edge of the simulated cliff. The latency to back away from the edge of the cliff, turn, and crawl away was measured. This test is considered an evaluation of sensory and motor coordination development. Positive responses were noted when pups completed the task < 30 seconds for two consecutive days.

d) Forelimb grasp

On PD 4, the pup's ability to grasp a wire rod and suspend its own bodyweight was evaluated. Pups were placed with their forepaws on a rod held 10 cm above a 5-cm-deep pile of woodchip bedding. Once released, the time the pup remained grasping onto the rod was recorded. A minimum of 1 second indicated a positive response. This task assesses balance, coordination, and motoric strength.

e) Auditory startle

Beginning on PD 7, pups were tested for an auditory reflex in response to a loud noise. An auditory reflex was assessed in the form of a rapid involuntary jump or "startle" in response to a clapping noise. One clap was performed 10 cm from the pup, and a positive response (startle) was recorded for two consecutive days.

f) Ear twitch

On PD 7, pups were tested for the presence of a tactile reflex of the ear. The edge of a fine filament was gently rubbed against the pup's ear three times. A positive response was recorded when the ear twitched rapidly in response to the brushing motion, for two consecutive days.

g) Open field taversal

On PD 8, the pup's locomotion and ability to extinguish pivoting behaviour was assessed. Pups were placed in the center of a 13-cm circle, and the latency to exit the circle was measured. All four paws must be outside the perimeter of the circle to consider the milestone reached. A positive response was noted once the pup exits the circle in < 30 seconds for two consecutive days.

h) Air righting

Beginning PD 8, pups were tested for the achievement of vestibular reflex function and motor coordination using the air righting task. Pups were held upside down, 10 cm above a 5-cm-deep pile of woodchip bedding, and released. A positive response was noted when a pup could right its body in the air such that it landed on the bedding on all four paws.

i) Eye opening

Beginning PD 10, pups were examined daily for eye opening. The first day in which both eyes were opened was considered achievement of this milestone.

2.2.2 Open-field activity

The daytime and overnight activity of each mouse was assessed using a Panlab Infrared (IR) Actimeter (Harvard Panlab, Holliston, MA) from PD 28-35. The open-field apparatus consisted of a 450 (*W*) mm x 450 (*D*) mm square arena with 450 (*H*) mm x 350 (*W*) mm acrylic walls mounted to the base. Thirty-two IR beam sensors were located around the perimeter of the apparatus to provide sensitive movement detection. Movement was recorded using Actitrack Tracking Software (PanLab, Holliston, MA, USA).

a) Daytime novel activity

Daytime activity levels were assessed from PD 28-30. The Actimeter was used to measure a mouse's locomotor response to a novel environment. Locomotor response was represented by recording breaks in the IR beams (beam breaks) within the recording frame of the apparatus (**Figure 2**). Total locomotor activity, as measured by the total number of beam breaks, was recorded using Actitrack software. Testing commenced at 10:00 am, and lasted for 15 minutes for each individual. The arena and Plexiglas walls of the apparatus were wiped with 30% isopropanol following each test in order to remove olfactory cues and excrement. Solutions of 10-30% isopropanol are sufficient for removal of olfactory cues[91,196].

b) Overnight home cage activity

At PD 30-35, mice were introduced into a simulated home cage 24 hours prior to overnight activity testing. The simulated home cage included standard woodchip bedding, food pellets, and water. Following acclimation, the home cage was placed in the Actimeter for 12 hours overnight. The period of recording consisted of a 2-hr light period (6:00 pm -8:00 pm) and a 10-hr dark period (8:00 pm – 6:00 am), spanning the overnight phase. The IR beams detected locomotor patterns of a mouse's nocturnal activity while encaged. A measurement of total locomotor activity (total number of beam breaks) was recorded using the Actitrack software. Data from the analysis software were analyzed as a whole (one 12-hr period) and in blocks (twelver 1-hr periods).

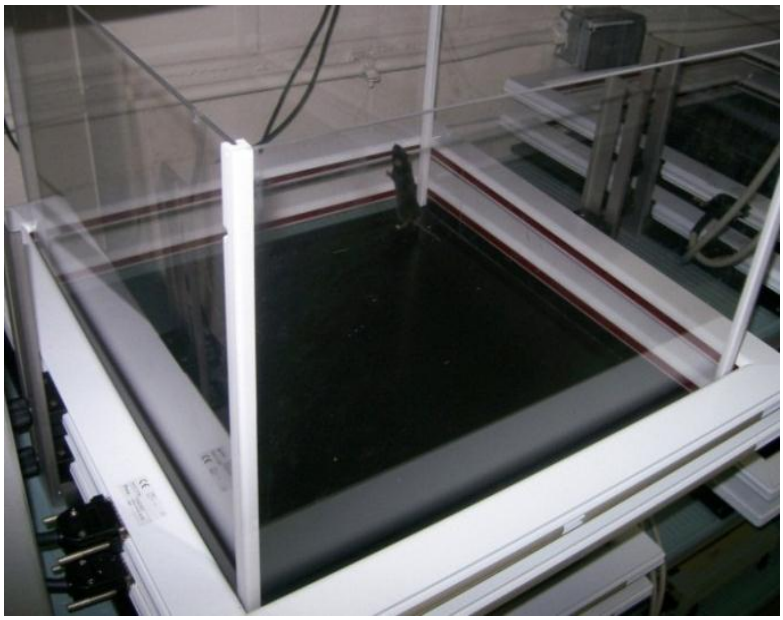

Figure 2. **A photograph of the Panlab Infrared (IR) Actimeter apparatus used to measure novel, open-field activity in mice**. The total number of IR beam breaks was recorded for each 15-minute period. A C57BL/6J mouse is depicted at the top corner of the arena. The Panlab Actimeter was acquired from Harvard Panlab, Holliston, MA.

2.2.3 Anxiety-related traits

a) Panlab infrared actimeter

The IR Actimeter was used to assess thigmotaxis in mice at PD 28-30. The amount of time spent in the center versus the periphery of the locomotor apparatus in the 15 minute period was recorded (**Figure 2**). This measurement relied on the rodent's natural tendency to stay in the periphery of an open field arena and not venture into the middle of the open field.

b) Elevated plus maze

An EPM was used as a measure of anxiety-related behaviour in mice at PD 35-40 (**Figure 3**). The maze comprised of 4 adjoining, cardboard arms (2 open, 2 enclosed) that stood 50 cm above the ground. Closed arms were 50 cm (*L*) x 10 cm (*W*) x 40 cm (*H*). Open arms were 50 cm (*L*) x 10 am (*W*). The arms were connected in a plus-formation such that the mice were able to cross between arms. The EPM relies on the rodent's natural tendency to seek dark, sheltered areas, and avoid bright (200 lx), exposed, and high-altitude areas[197]. At the beginning of the trial, a mouse was placed facing an open arm at the intersection of the apparatus. The mouse's movement was recorded by AnyMAZE Video Tracking software (San Diego Instruments, San Diego, CA). Testing was conducted for a single, 5-minute period for each mouse. A 5-minute interval is considered capable of revealing differences in anxiety-related traits across mice[197]. In between trials, the Plexiglas cover on the maze was wiped with 30% isopropanol.

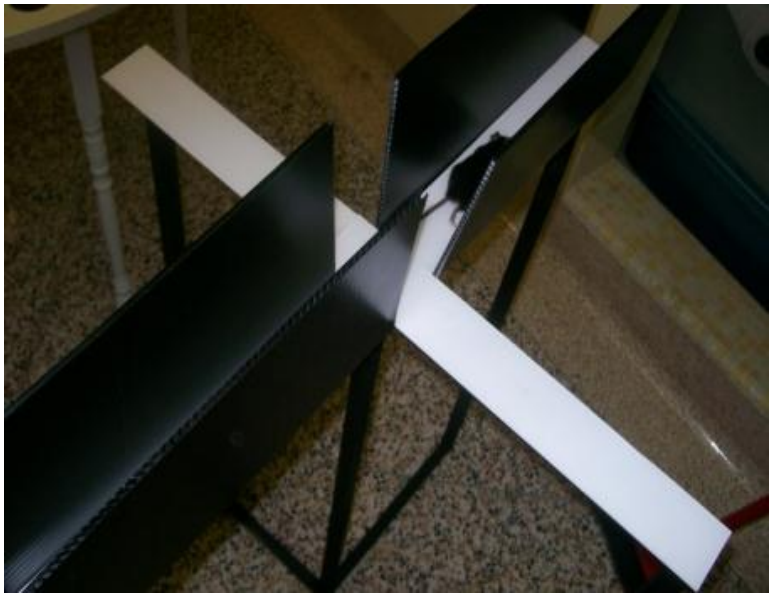

Figure 3. A photograph of the Elevated Plus Maze (EPM) apparatus used to assess anxiety-related traits in mice. The time spent in the closed arms versus the open arms in a 5-minute period was recorded. A C57BL/6J mouse is depicted in the top closed arm of the EPM. Plexiglas, in a plus-formation, covers the white arms of the maze.

c) Light/dark box

At PD 35-40, the LDB was used as a measure of exploratory behaviour and anxiety-related behaviour in a novel, illuminated environment (**Figure 4**). The apparatus was constructed following a design by Bourin and Hascoet, which included two compartments consisting of a 27 cm (*L*) x 27 cm (*W*) x 27 cm (*H*) light arena (plastic), and a 18 cm (*L*) x 27 cm (*W*) x 27 cm (*H*) dark arena (cardboard)[100]. A 7.5 cm x 7.5 cm opening was created between the light and dark regions. At the beginning of each trial, the mouse was placed in the light area facing the opening. The mouse was allowed to freely explore both areas for 5 minutes, with an overhead light at 200 lx. Movement was recorded by AnyMAZE Video Tracking software. In between trials, the plastic arena was wiped with 30% isopropanol

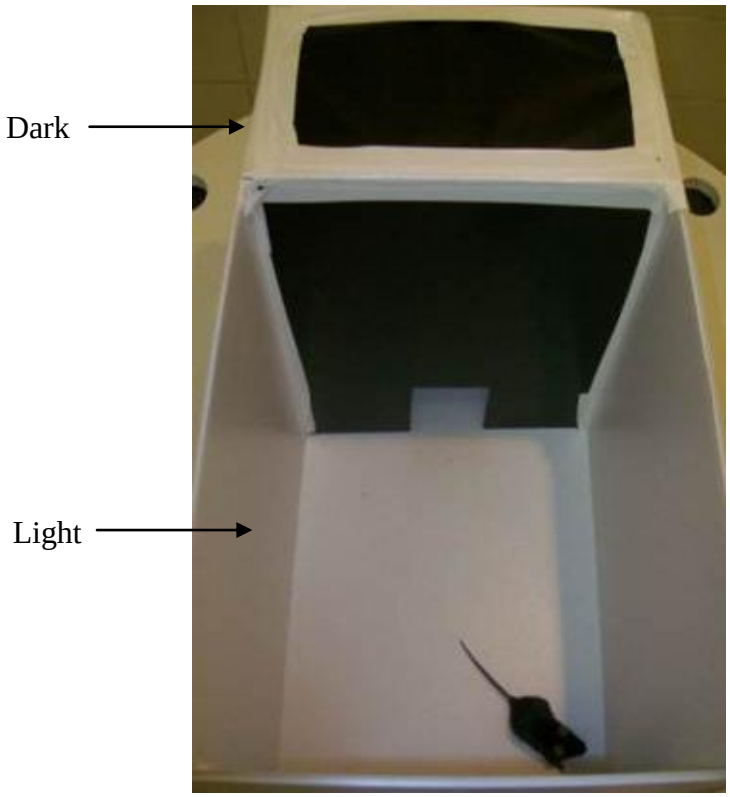

Figure 4. A photograph of the Light/Dark Box (LDB) used to assess anxiety-related traits in mice. The time spent in the closed area (black cardboard box) versus the open area (white plastic box) in a 5-minute period was recorded. A C57BL/6J mouse is depicted in bottom right corner of the LDB. Arrows point to the dark and light areas of the LDB.

2.2.4 Spatial learning and memory

From PD 45-70, the Barnes Maze was used as a test of spatial learning, short-term recall, and long-term recall. The maze was constructed by Ph.D. candidate, Morgan Kleiber, according to Sunyer and colleagues[89] (**Figure 5**). The apparatus was comprised of a circular wood platform with a 92-cm-diameter, punctuated with 20 equally-spaced holes (each 5 cm in diameter) along the periphery of the platform (7.5 cm between holes). The platform stood 105 cm above the ground. One of the holes along the perimeter was a target hole, through which mice were able to enter an escape box. Black cardboard sheets were placed underneath the other 19 holes. The escape box was painted black to remain visually indistinguishable from other holes. Experimenter-prepared visual cues were constructed and placed around the testing room to provide spatial details regarding the location of the target hole. Aversive stimuli were added to the test, in the form of a 150 W bright light. An 85 dB white noise was generated using AnyMAZE software. AnyMAZE was also used to track the mouse's movements during each trial. Upon the mouse's entry into the escape box, the light and white noise were turned off for a period of 1 minute to allow the mouse to acclimatize to the box. The platform and escape box were wiped with 30% isopropanol between trials.

a) Learning

Mice were given four trials over four acquisition days (learning days) to learn the location of the target hole. At the beginning of each trial, a mouse was placed in the center of the maze inside a cylindrical start-chamber for 10 seconds. Once the start-chamber was removed, the mouse was allotted 3 minutes to explore the maze and locate the target hole. If the mouse entered the target hole within the 3 minute period, the overhead light and white noise were terminated. The mouse was allotted 1 minute in the escape box following its entry. If the mouse did not

locate the target hole within the 3 minute period, the mouse was guided to the escape box following the trial and allowed to remain inside the box for 1 minute. Each mouse was trained on the Barnes Maze for four consecutive days, with each training day consisting of four 3-minute trials. There was a 15 minute interval between trials. After each trial, the mouse was returned to its home cage. The latency (seconds) to enter the escape box was measured using AnyMAZE software.

b) Memory

The fifth (short-term recall) and twelfth (long-term recall) days of Barnes Maze testing are referred to as "probe" trials. Good memory on probe trials in the Barnes Maze is defined as selective search for the former location of the target, compared with equivalent locations in other zones[198]. On probe days 5 and 12, the escape box was removed, and the target hole was covered with black cardboard. Each mouse was given one 1-minute trial on each day to explore the maze (**Figure 5**). The number of explorations to each hole was recorded.

2.2.5 Statistical analysis of behavioural data

For each behavioural test, data were analyzed using appropriate analysis of variance (ANOVA) methods depending on the number of independent variables (sex, treatment, repeated day of testing). Where data were analyzed across days, repeated measures ANOVA (RM-ANOVA) with "treatment" as the between-subjects factor. "Day" (Barnes maze) or "hour" (Overnight home-cage activity) was used as the within-subjects factor was used. All data were reported as mean ± standard error of the mean (SEM). For the Barnes Maze probe trials, a Bonferroni correction was applied to correct for multiple testing. Effects of litter were analyzed using "litter" as a covariate in the ANOVA; however, no litter effects were observed for any of

the behavioural measures. Data were stratified by sex only if sexually dimorphic effects were observed. All statistical analyses were performed using Statistical Package for the Social Sciences (SPSS) version 16 (SPSS Inc., Chicago, IL).

Figure 5. A photograph of the Barnes Maze used to assess spatial and learning memory in mice. Spatial cues, consisting of various shapes and colours, are displayed around the testing room. All holes, except the target hole, are covered with black cardboard cut-outs. The target hole leads to a black escape box, positioned underneath the platform. Arrow points to the location of the target hole.

2.3 Gene expression analysis

2.3.1 Tissue extraction and RNA isolation

Whole brains (T2-S, T1-L, and T2-L) were harvested, snap-frozen in liquid nitrogen, and stored at -80°C. Total RNA was extracted using Trizol® according to the manufacturer's instructions (Invitrogen, Carlsbad, CA). To check the quality of RNA, 2 µl of each sample was quantified using the ND-1000 Spectrophotometer (Thermo Fisher Scientific Inc., Wilmington, DE) and Agilent 2100 Bioanalyzer (Agilent Technologies, Inc., Palo Alto, CA) at the London Regional Genomics Center (LRGC) (University of Western Ontario, London, Ontario). An automated gel image was generated based on the results of the electropherogram, in order to visualize the quality of the RNA sample as if it were electrophoresed through on a standard 1% agarose gel. RNA was shown to be of good quality by A260/A280 ratio in the range of 1.8-2.1, which is indicative of pure RNA[199]. Also, only those samples with concentrations > 100 ng/µl, ratios of A260/A230 between 2.0-2.2, and RNA Integrity Numbers within the range of 8-9.5 were used for analysis. If a sample with A260/A280 < 1.8 was identified following microarray analysis, it was discarded in qRT-PCR confirmation experiments.

2.3.2 Microarray preparation

Whole brain RNA from B6 mice was sent to LRGC for hybridization to Affymetrix Mouse Gene 1.0 ST arrays, which are high-density oligonucleotide arrays. Each chip contained three pooled samples (three different mice) of RNA. Pooling samples allowed for reduction of litter effects between mice. For each experiment, one control and one experimental array were analysed, along with a biological replicate of each. For T2-S mice, 4 gene chips were used (2 control, 2 ethanol), with a total of 12 RNA samples (different mice). For T1-L and T2-L, 8 arrays

were used (2 control, 2 ethanol per group), with a total of 24 RNA samples (different mice). A biological replicate was preferred to a technical replicate because biological diversity is controlled by using different samples (ie. mice) of the same treatment. For the entire experiment, a total of 12 microarrays and 36 RNA samples were used. In order to pool samples for each array, 2 µl of RNA was diluted to 100 ng/µl. The concentrations of the diluted samples were double checked. If inaccurate, the original RNA was diluted again using the correct concentration. Samples were then pooled (~100 ng/µl).

Microarray cDNA synthesis, *in vitro* transcription, cRNA fragmentation, and hybridization reactions were carried out at LRGC. Using 200 ng of total RNA, the RNA was first reverse transcribed to single-stranded complementary DNA (sscDNA) using the Ambion WT Expression Kit for Affymetrix GeneChip Whole Transcript WT Expression Arrays (Applied Biosystems, Carlsbad, CA) and the Affymetrix GeneChip WT Terminal Labeling kit and hybridization manual (Affymetrix, Santa Clara, CA). First-cycle cDNA was transcribed *in vitro* to cRNA, and used to synthesize 5.5 µg of sscDNA that was subsequently end-labeled (biotin) and hybridized for 16 hours at 45°C to Affymetrix Mouse Gene 1.0 ST arrays. Liquid-handling steps were performed by a GeneChip Station 450. The arrays were stained using Streptavidin-Phycoerythrin, which binds to the biotin molecules and emits a fluorescence when run through the GeneChip Scanner 3000 7G using Command Console version 1.1 (Affymetrix In., Santa Clara, CA, USA). The scanner output the raw intensity values and images for each probe into a probe level (.CEL) file, which allowed visualization of the fluorescence.

2.3.3 Microarray data analysis

Probe-level (.CEL) data were generated using Affymetrix Command Console version 1.1 and probes were summarized to gene-level data using Partek Genomics Suite software version 6.6 (Partek Inc., St. Louis, MO). Array analysis for each of the experiments (T2-S, T1-L, and T2-L) was completed. Data were background corrected, quantile-normalized, summarized, and $\log_2$-transformed. Subsequent statistical analyses were performed using Partek software to determine gene-level ANOVA *p*-values and fold changes. Because prenatal ethanol exposure has been shown to produce subtle changes in gene expression[94,158], a ± 1.2 fold change and $p < 0.05$ were used as criteria for building gene lists for functional, pathway, and network analyses. Un-annotated genes and standards were removed from the gene lists. All data files from the array experiments have been deposited in the National Center for Biotechnology Information Gene Expression Omnibus, under the accessions: GSE34469 (T1-L and T2-L) and GSE43324 (T2-S). Complete lists of DEGs identified for T2-S, T1-L, and T2-L are given in Appendices B, C, and D, respectively.

2.3.4 Statistical analysis of microarray data

Statistical analysis of microarray data is necessary to make inferences about a phenomenon based on empirically measured data. Microarrays measure the mRNA levels of thousands of genes, and are then analyzed to identify genes that are correlated to a phenotype of interest. Here, gene-level summarization was performed using an ANOVA to compare ethanol and control data. The ANOVA condensed the dataset into a manageable set of DEGs based on certain criteria: a fold-change and an alpha level of significance (based on the ANOVA). The inputted data from the arrays (.CEL file extension) were normalized using an internal algorithm.

The using the GeneChip-Robust Multiarray Averaging algorithm, with GC-content background correction (GC-RMA) — which accounts for probe GC-content[200] — was used since it has been shown to perform well by other researchers[201,202]. GC-RMA incorporates probe sequence composition into background adjustment based on the assumption that probe affinity is dependent on its base composition and the position of each base along the probe; herein, this suggests that the probe sequence can significantly affect the intensity of the signal generated from that probe, independent of the level of quantity of its target[203]. Researchers have reported on the use of GC-RMA and its outstanding performance in detecting low-intensity, DEGs, and its consistency with qRT-PCR[202,204].

Partek is an exploratory data tool used for the identification of DEGs using ANOVA[205]. The ANOVA is a powerful method of data analysis that is motivated by consideration of the experimental design[206]. The challenge with an ANOVA is to detect as many real differences as possible while maintaining control over the rate of false detection. The most popular approach to rectify this is to apply a false discovery rate (FDR) correction; an FDR correction generates a list of DEGs such that the expected proportion of false detections on the list is bounded at a user-defined level[207]. In Partek analysis, the ANOVA was performed on all genes. A table was created that allowed the investigator to browse and create gene lists from the results based on *p*-value and fold change.

2.3.5 Functional, pathway, and network analysis of differentially-expressed genes (DEGs)

Once identified by Partek, DEGs were analyzed using three functional characterization tools. The functional annotation and clustering tool, DAVID[137,208], was used. DAVID uses a modified version of Fisher's exact test to identify statistically significant Gene Ontology (GO) terms including biological process (BP), cellular component (CC), and molecular function (MF)[209]. Other annotations used to group genes in DAVID include: BioCarta pathways (BioCarta LLC, San Diego, California, USA), KEGG pathways, Protein Sequence Analysis and Classification (InterPro) (Wellcome Trust Genome Campus, Cambridgeshire, United Kingdom), Simple Modular Architecture Research Tool (SMART)[210,211], and Swiss-Prot and Protein Information Resource (SP PIR) (Georgetown University Medical Center, Washington, DC, USA). Using the Gene Enrichment tool, Partek was used to identify over-represented GO terms associated with genes showing altered expression. Finally, IPA was used to cluster genes based on biological functions. Upregulated and downregulated gene lists (± 1.2 fold change, $p < 0.05$) were assessed concurrently for each analysis.

To characterize sets of functionally related DEGs, three sets of pathway analysis programs were used. Pathway Express was used. Gene sets (± 1.2 fold change and $p < 0.05$) were inputted into the Pathway Express tool to translate these lists into functional profiles (using GO terms) in order to characterize the impact of prenatal ethanol exposure. For each GO category, statistical significance values were calculated using a Fisher's exact test[140]. The results from Pathway Express were complemented using the Pathway Enrichment tool in Partek. PE also relies on the KEGG database to assign enriched pathways for each of the DEG lists. Lastly, canonical pathways were assessed using IPA. The goal of using three pathway tools was to

compare the results, and to generate biologically meaningful and comprehensive data from each of the gene lists.

Network analysis of the DEGs was completed using two programs. The publically available pathway tool, GeneMANIA, was used to find genes (using a linear regression-based algorithm) that were related to the input genes; such an analysis gives input on specific genetic interactions, pathways, co-expression, co-localization, and protein domain similarity in mice[212]. The gene lists were further inputted into IPA to identify networks in which genes and proteins have been reported to interact with each other, whether directly or indirectly. By employing various functional, pathway, and network analyses on the lists of DEGs, this method gave comprehensive insight into the biological mechanisms underlying FASD.

2.3.6 Confirmation of gene expression by quantitative RT-PCR (qRT-PCR)

Excess RNA extracts that were used for array hybridization were also used to confirm the expression of selected genes by qRT-PCR. Complementary DNA was synthesized using 2 µg of total whole brain RNA using a High-Capacity cDNA Reverse Transcription kit (Applied Biosystems, Foster City, CA) according to the manufacturer's protocol. Gene-specific TaqMan® Assay Reagents and TaqMan Gene Expression Assay products were used on a StepOne™ Real Time PCR System (Applied Biosystems, Foster City, CA). Primers and 6-carboxyfluorescein (FAM)-labeled probes for specific genes (**Table 1**) were obtained from Applied Biosystems Inventoried Assays and used as per the manufacturer's instructions. Reactions were multiplexed with *Glyceraldehyde-3-phosphate dehydrogenase* (*Gapdh*) or *Actin, beta* (*Actb*) using gene-specific primers and VIC-labeled probes. Reactions were performed using a standard ramp speed protocol using 10 µl volumes. PCR cycling consisted of a 10 minute initiation at 95°C, followed

by 40 cycles consisting of a 15 second denaturation at 95°C and an anneal and extension at 60°C for 60 seconds. Experiments included six biological replicates per treatment (only five biological replicates were available for T2-L ethanol samples) and three technical replicates per sample. Relative expression was calculated according to the comparative C_T method[213] using StepOne™ version 2.0 software from Applied Biosystems. All PCR data are reported as mean ± SEM relative expression values. Significant differences were assessed using a student's *t*-test in SPSS.

Table 1. Candidate genes for FASD selected for confirmation by quantitative RT-PCR.

Group[a]	Gene Symbol[b]	Gene Name	Reference Gene[c]
T2-S	*Ccl3*	*Chemokine (C-C motif) ligand 3*	*Actb*
	Ccnt1	*Cyclin T1*	*Gapdh*
	Gpr50	*G protein-coupled receptor 50*	*Gapdh*
	Lair1	*Leukocyte-associated immunoglobulin-like receptor 1*	*Gapdh*
	Pip5k1b	*Phosphatidylinositol-4-phosphate 5-kinase, type I, beta*	*Actb*
	Rybp	*RING1 and YY1 binding protein*	*Gapdh*
	Slitrk2	*SLIT and NTRK-like family, member 2*	*Gapdh*
	Trdn	*Triadin*	*Actb*
T1-L	*Atf1*	*Activating transcription factor 1*	*Actb*
	Ceacam1	*Carcinoembryonic antigen-related cell adhesion molecular 1 (biliary glycoprotein)*	*Actb*
	Eomes	*Eomesodermin (Xenopus laevis) homolog*	*Gapdh*
	Htr5a	*5-hydroxytryptamine (serotonin) receptor 5A, G-protein coupled*	*Gapdh*
	Map3k1	*Mitogen-activated protein kinase kinase kinase, E3 ubiquitin protein ligase*	*Actb*
	Stxbp6	*Syntaxin binding protein 6 (amisyn)*	*Actb*
	Synpr	*Synaptoporin*	*Gapdh*
	Tnfrsf19	*Tumor necrosis factor receptor superfamily, member 19*	*Gapdh*
T2-L	*Camk1g*	*Calcium/calmodulin-dependent protein kinase 1G*	*Gapdh*
	Ccdc6	*Coiled-coil domain containing 6*	*Actb*
	Cdkn1a	*Cyclin-dependent kinase inhibitor 1a*	*Gapdh*
	Egr3	*Early growth response 3*	*Gapdh*
	Homer1	*Homer homolog 1 (Drosophila)*	*Gapdh*
	Hsp90aa1	*Heat shock protein 90kDa alpha (cytosolic), class A member 1*	*Actb*
	Hspa5	*Heat shock 70kDa protein 5 (glucose-regulated protein, 78kDa)*	*Actb*
	Manf	*Mesencephalic astrocyte-derived neurotrophic factor*	*Gapdh*
	Tbxa2r	*Thromboxane A2 receptor*	*Actb*
	Xbp1	*X-box binding protein 1*	*Actb*

[a]Groups: T2-S = trimester two, short-term effect. T1-L = trimester one, long-term effect. T2-L = trimester two, long-term effect.
[b]Genes are listed in alphabetical order for each group.
[c]Reference gene was either *Actin, beta* (*Actb*) or *Glyceraldehyde-3-phosphate dehydrogenase* (*Gapdh*).

2.4 MicroRNA analysis

2.4.1 Experimental design and miRNA arrays

The RNA samples used for long-term gene expression analyses (T1-L and T2-L) were also used for global miRNA analysis using miRNA arrays. For each long-term group, each array contained three pooled samples of RNA, corresponding to the animals used in gene expression experiments. For each group, two biological replicates of a control and ethanol array were performed (n = 4 arrays per group; total n = 8 arrays). All sample labeling, hybridization, and processing were performed at LRGC. One microgram of total RNA was labeled using the Flash Tag Biotin HSR kit (Genisphere, Hatfield, PA, USA) and hybridized to Affymetrix MiRNA 2.0 arrays for 16 hours at 45°C. Probe level (.CEL file) data were generated using Affymetrix Command Console version 1.1 (Affymetrix In., Santa Clara, CA). Probes were summarized to gene-level data in Partek using the Robust Multiarray Averaging (RMA) algorithm[200]. Partek software was used to determine differences between ethanol and control samples using one-way ANOVA and corresponding *p*-values and fold changes. For each group, the miRNAs on the array were filtered using stringency criteria including a $p < 0.05$ and ± 1.2 fold change. The miRNA expression array results for both groups (T1-L and T2-L) were deposited within the NCBI GEO database under accession number GSE34413.

2.4.2 MiRNA target filtering and selection criteria

Data generated using T1-L and T2-L miRNA arrays were analyzed using IPA. Concurrently, T1-L and T2-L gene lists from gene expression analyses (± 1.2 fold change, $p < 0.05$) were combined with their corresponding miRNA list in IPA's Target Filter analysis. Target filtering was performed to generate a list of interactions between genes and miRNAs in each

group. Results were filtered based on a moderate or high confidence of interaction and an inverse miRNA to target mRNA expression relationship[214].

2.4.3 Confirmation of miRNAs using quantitative RT-PCR

Excess RNA extracts that were used for miRNA array hybridization were also used to confirm the expression of selected miRNAs by qRT-PCR. Complementary DNA was synthesized using 2 µg of total whole brain RNA using the Applied Biosystems TaqMan Reverse Transcription Kit (Applied Biosystems, Foster City, CA, USA) and sequence-specific step-loop reverse transcription primers from TaqMan MicroRNA Assays (Applied Biosystems, Foster City, CA, USA) according to the manufacturer's protocol. All qRT-PCR primers and miRNA-specific TaqMan probes were selected using the Applied Biosystems (Carlsbad, CA, USA) search engine to identify previously characterized TaqMan MicroRNA Assays. FAM-labeled probes for miRNA 1192 (miR-1192, T1-L), miRNA 532-5p (miR-532-5p, T1-L), and miRNA 302c (miR-302c, T2-L) were obtained from Applied Biosystems Inventory Assays and used as per the manufacturer's instructions. Small nucleolar RNA 202 (snoRNA 202) was chosen as an endogenous control[95,215]. The target and control reactions were performed in separate tubes on the same plate for each sample as per the manufacturer's protocol. Three technical replicates were used for both the endogenous control and gene of interest for each sample. As with qRT-PCR for genes, six biological samples were used for each treatment (except for T2-L ethanol samples, where only five experimental samples were used). Quantitative PCR reactions were performed on the StepOne Real-Time PCR System according to the manufacturer's protocol. Reactions were run following a standard ramp speed protocol using 20 µl volumes. Fold change was calculated using the $\Delta\Delta C_T$ method[216]. Data were analysed using Applied Biosystems DataAssist™ Software version 3.0. Statistical significance was assessed using a two-tailed *t*-test.

3. Results

3.1 Overview on presentation of results

This chapter includes results on behaviours and brain gene expression, including miRNAs, using B6 mice, following *in vivo* binge-like ethanol treatment at two stages of neurodevelopment. The timings include, GD 8 and 11 (representing human trimester one), and GD 14 and 16 (representing human trimester two). All behavioural testing was performed on resulting trimester one and two progeny. Behavioural testing began at early development (PD 2) until maturity (PD 70), at which time mice were euthanized for brain transcriptome analysis. A separate experiment assessed gene expression patterns 2 hrs following ethanol treatment on GD 16 to represent short-term effects of ethanol exposure. The results are now published in the Journal of Neurodevelopmental Disorders[158], Journal of Behavioural and Brain Science[217], and Disease Models and Mechanisms[95]. I have obtained permission for using copyright images from the editor of the Journal of Behavioural and Brain Science for inclusion in this thesis (Appendix E). This copyright includes the adaptation of any images from the article. A copyright approval was not required from other journal editors since I have not included images from these articles. For specifics on authorship, please refer to co-authorship statement (p. ix).

3.2 FASD-relevant behaviours are altered in mice following gestational ethanol exposure

3.2.1 Developmental milestone achievement is delayed following prenatal ethanol exposure

All pups from trimesters one and two were evaluated from PD 2-21 for the ability to reach critical developmental milestones. The day each specific milestone was achieved (second consecutive day), for each group, is shown in **Table 2**[217]. Ethanol exposure during the first

trimester equivalent significantly delays the abilities of pups to right themselves when placed on their backs ($F_{1,46}$ = 29.90, p < 0.001), grasp a rod with their forelimbs ($F_{1,46}$ = 15.50, p < 0.001), extinguish pivoting behaviour by transversing out of a 15-cm-diameter circle ($F_{1,46}$ = 15.10, p < 0.001), and right themselves in the air when dropped from upside down from 5 cm ($F_{1,46}$ = 23.71, p < 0.001). A significant interaction between sex and treatment was observed for the ability of the pup to right itself in the air when dropped ($F_{1,46}$ = 7.60, p = 0.008), with control males taking longer to right themselves than control females; however, ethanol females took longer to right themselves than ethanol males. Ethanol pups from trimester two were significantly increased, compared to control pups, in the time it took to surface right ($F_{1,54}$ = 4.93, p = 0.03), turn 180°C upward when placed downward on a 45° screen ($F_{1,54}$ = 34.88, p < 0.001), crawl away from the edge of a cliff ($F_{1,54}$ = 25.10, p < 0.001), grasp the rod ($F_{1,54}$ = 6.65, p = 0.01), transverse out of the circle ($F_{1,54}$ = 17.02, p < 0.001), right themselves in the air ($F_{1,54}$ = 10.06, p = 0.003) and open their eyes for the first time ($F_{1,54}$ = 6.21, p = 0.02). Post-hoc testing using all four groups (trimester one control and ethanol; trimester two control and ethanol) revealed that the only developmental milestone in which trimester one and two ethanol mice were significantly different was forelimb grasp ($F_{3,100}$ = 19.66, p < 0.001).

Table 2. Developmental milestone achievement of postnatal day ethanol and control pups.

Treatment	**Control**				**Ethanol**			
Sex	**Male**		**Female**		**Male**		**Female**	
	T1 (n=11)	T2 (n=18)	T1 (n=12)	T2 (n=10)	T1 (n=13)	T2 (n=11)	T1 (n=14)	T2 (n=20)
Milestone[a]								
Surface righting	6.5±0.4	8.7±0.3	6.4±0.4	8.4±0.3	***9.1±0.4	*8.9±0.3	***8.7±0.5	*9.7±0.3
Negative geotaxis[#]	7.0±0.4	6.2±0.4	7.5±0.4	7.4±0.3	6.6±0.5	***9.5±0.7	6.6±0.4	***9.4±0.3
Cliff aversion	9.0±0.4	7.9±0.5	9.7±0.4	6.4±0.9	9.1±0.5	***9.7±0.4	8.7±0.3	***10.4±0.4
Forelimb grasp	9.6±0.6	10.0±0.7	9.3±0.4	9.4±0.8	***11.5±0.7	11.1±0.5	***11.9±0.5	11.6±0.3
Auditory startle	14.7±0.2	13.9±0.4	13.8±0.5	14.0±0.3	13.1±0.5	13.4±0.8	13.8±0.6	14.2±0.4
Ear twitch	9.8±0.3	9.3±0.3	9.5±0.3	10.4±0.5	9.3±0.4	10.4±0.3	9.9±0.5	10.4±0.3
Open field traversal	10.6±0.6	10.9±0.4	11.4±0.4	10.0±0.4	***12.5±0.3	***12.4±0.6	***12.8±0.4	***12.5±0.4
Eye opening	14.7±0.1	13.8±0.2	14.3±0.1	14.2±0.3	14.5±0.1	*14.6±0.2	14.6±0.2	*14.4±0.2
Air righting	12.9±0.7	12.1±0.6	11.0±0.6	12.4±0.5	***14.1±0.5	**14.0±0.7	***15.2±0.4	**14.2±0.4

[a]Mean (± SEM) number of days to complete each task was compared across males and females from trimester one (T1) and trimester two (T2) ethanol and control pups. *$p < 0.05$; **$p < 0.01$; ***$p < 0.001$. Number (n) of mice used for each test are shown.
[#]Negative geotaxis is the only developmental milestone in which T1 and T2 ethanol mice were significantly different ($p < 0.001$).

3.2.2 Locomotor activity is altered in mice following gestational ethanol exposure

a) Daytime novel activity is increased in ethanol-treated mice

Spontaneous activity of control and ethanol juveniles (PD 28-30) from trimesters one and two was assessed over a 15 minute period in a novel, open-field environment. Two-way ANOVA did not result in a significant effect of sex or an interaction between sex and treatment. Therefore, the groups were collapsed and a one-way ANOVA with "treatment" as the main factor was applied. One-way ANOVA showed a significant effect of treatment in trimester one ($F_{1,46} = 6.48$, $p = 0.01$) and trimester two ($F_{1,54} = 69.89$, $p < 0.001$), where the number of beam breaks was increased in ethanol mice (T1-L: 2835.58 ± 136.81; T2-L: 3429.13 ± 93.81 beam breaks) versus control mice (T1-L: 2332.12 ± 142.89; T2-L: 2291.54 ± 98.57 beam breaks). There were no significant differences between T1-L and T2-L control mice. A significant difference was found between trimester one and two ethanol mice ($F_{3,100} = 25.22$, $p = 0.001$), with trimester two ethanol mice displaying increased activity compared to trimester one treated mice (**Figure 6**)[217].

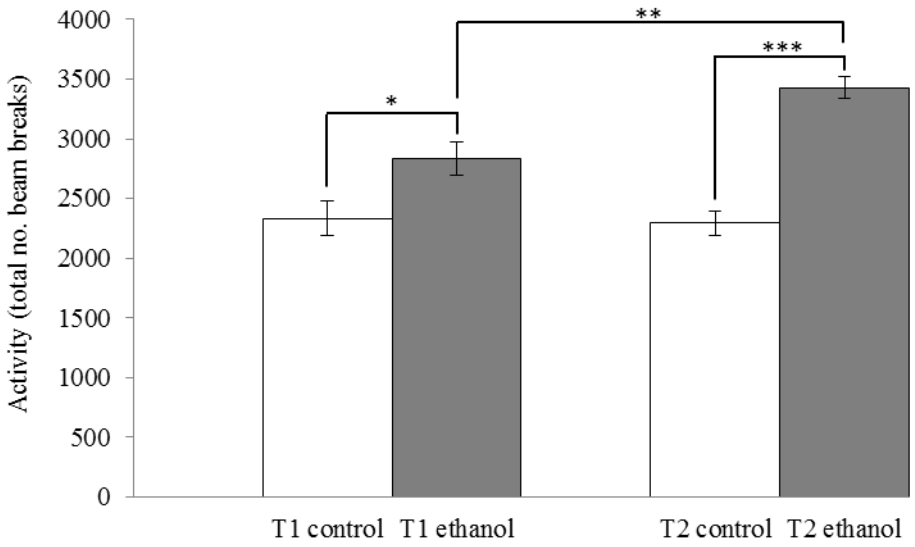

Figure 6. Bar graph of locomotor activity in a novel, open-field encironment in ethanol and control mice. Mean (± SEM) infrared beam breaks (total no. beam breaks) of ethanol and control mice from trimester one (T1) and trimester two (T2) over a 15 min period (n = 20-28 mice per group). *$p < 0.05$; **$p < 0.01$; ***$p < 0.001$.

b) Overnight home cage activity is disrupted in ethanol-treated mice

Locomotor activity in a familiar environment (home cage) was assessed in ethanol and control mice at PD 30-35. For both groups, a two-way ANOVA for total 12-hour activity did not identify any significant effects of treatment, sex, or an interaction between treatment and sex. The data were further analyzed in twelve 1-hour measurements. Two-way RM-ANOVA with "hour" as the within-subjects factor, and "sex" and "treatment" as between-subjects factors detected significant main effects of hour and treatment. A significant main effect of treatment in trimester one was found ($F_{1,46}$ = 12.09, p = 0.001), with ethanol mice demonstrating increased activity (4160.01 ± 192.89 beam breaks) throughout the nocturnal phase, versus control mice (3190.38 ± 201.47 beam breaks) (**Figure 7**)[217]. The pattern in trimester two mice resulted in a nominally significant increase in activity levels ($F_{1,54}$ = 3.311, p = 0.074) in ethanol mice (4762.62 ± 258.37 beam breaks) compared to control mice (4080.70 ± 271.47 beam breaks) (**Figure 8**)[217]. For overnight activity levels, a comparison between trimester one and two ethanol mice was not carried out due to observed discrepancies between males and females, and statistical differences between control mice.

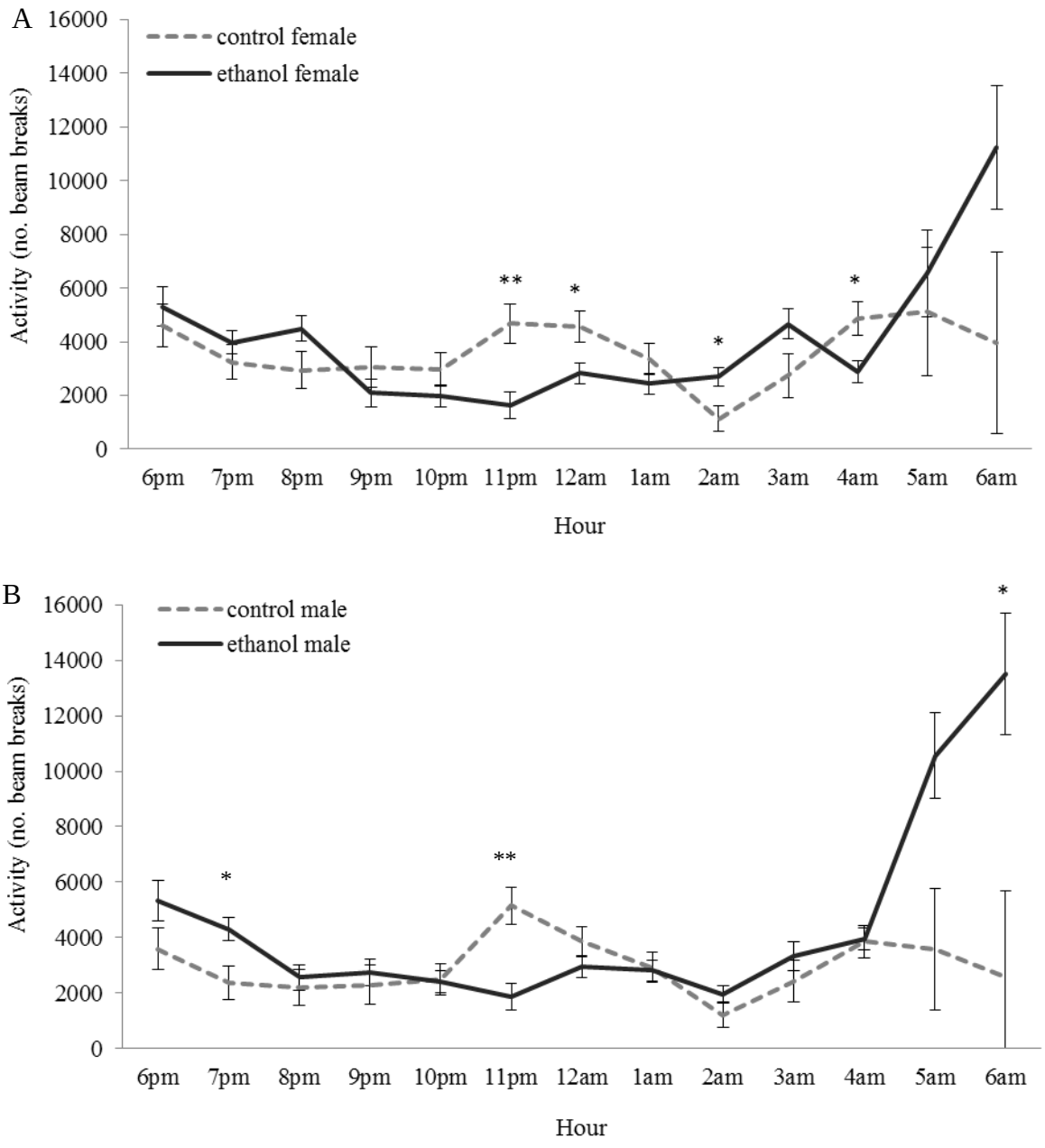

Figure 7. Line graph of locomotor activity in a familiar home-cage environment in trimester one ethanol and control mice. Mean (± SEM) infrared beam breaks (no. beam breaks) by ethanol and control mice from trimester one (A) females (n = 26) and (B) males (n = 20). *$p < 0.05$; **$p < 0.01$. Lights were off between 8:00 pm - 6:00 am.

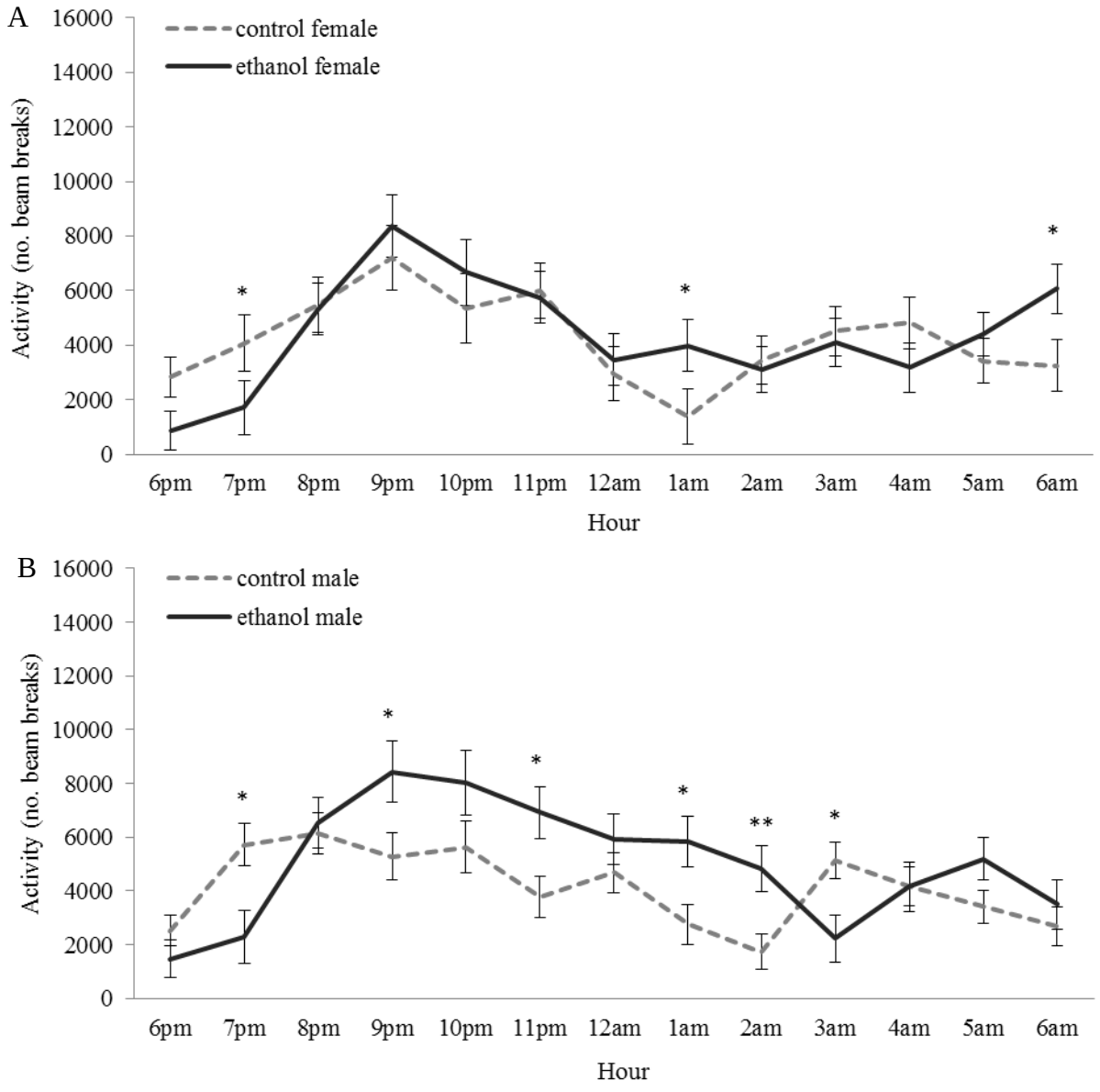

Figure 8. Line graph of locomotor activity in a familiar home cage environment in trimester two ethanol and control mice. Mean (± SEM) infrared beam breaks (no. beam breaks) by ethanol and control mice from trimester two (A) females (n = 28) and (B) males (n = 26). *$p < 0.05$; **$p < 0.01$. Lights were off between 8:00 pm - 6:00 am.

3.2.3 Anxiety-related behaviours are dependent upon timing of ethanol exposure

a) Open field testing

To evaluate the effects of novelty-induced, anxiety-related traits in the open field task, thigmotaxis was examined during open-field testing. No statistically significant effect of treatment was observed between ethanol (214.46 ± 23.60 s) and control (185.88 ± 19.50 s) mice in trimester one ($F_{1,46} = 0.92$, $p = 0.34$). A significant main effect of treatment was observed in trimester two ($F_{1,54} = 59.65$, $p < 0.001$), with ethanol offspring spending significantly more time (477.31 ± 26.94 s) in the center zone than control mice (175.52 ± 28.30 s). Trimester two ethanol mice also spent significantly more time in the center zone ($F_{3,100} = 34.34$, $p < 0.001$) than ethanol and control trimester one mice (**Figure 9**)[217].

b) Elevated plus maze

In the EPM, there were no statistically significant differences ($F_{1,46} = 1.109$, $p = 0.30$) in the amount of time spent in the open arms versus the closed arms between ethanol (94.42 ± 5.66 s) and control mice (86.94 ± 3.96 s) from trimester one. Similarly, in trimester two, there were no significant differences ($F_{1,54} = 0.11$, $p = 0.74$) in the amount of time spent in the open arms versus the closed arms of the EPM between ethanol (69.45 ± 3.89 s) and control mice (68.96 ± 4.17 s).

c) Light/dark box

A LDB was further used to evaluate anxiety-related phenotypes that have been observed in daytime open-field activity data. Trimester one ethanol (146.12 ± 7.58 s) and control (160.90 ± 7.92 s) mice were not significantly different ($F_{1,46} = 1.82$, $p = 0.18$). Trimester two ethanol mice spent significantly ($F_{1,54} = 7.08$, $p = 0.01$) more time (average: 152.46 ± 4.65 s) in the light

area of the box than control mice (average: 134.50 ± 4.89 s) (**Figure 10**)[217]. A comparison between trimester one and two ethanol mice was not performed because data for trimester one and two control mice were statistically different ($p = 0.016$).

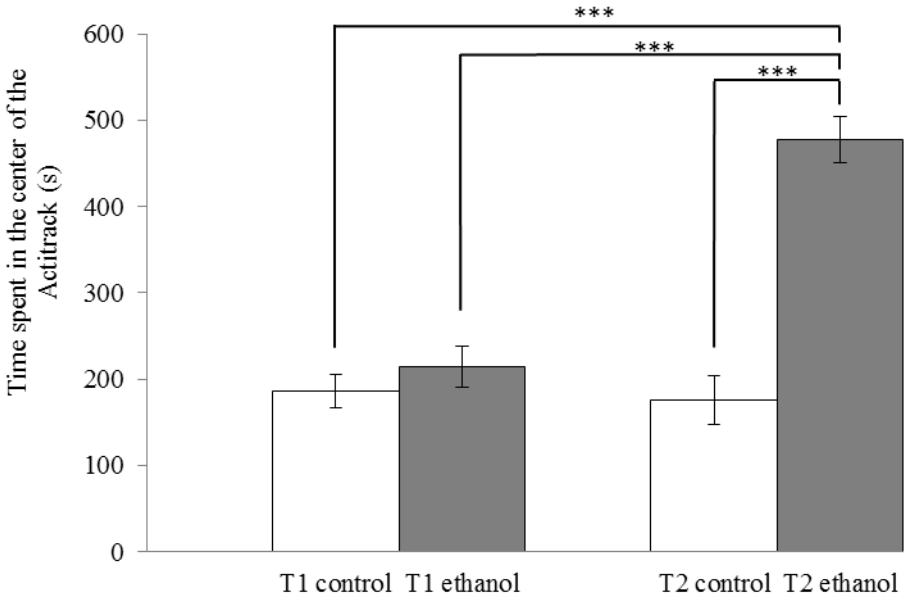

Figure 9. Bar graph of time spent in the centre of a novel, open-field environment in ethanol and control mice. Mean (± SEM) time in seconds (s) spent in the centre of the apparatus of ethanol and control mice from trimester one (T1) and trimester two (T2) over a 15 min period (n = 20-28 mice per group). ***$p < 0.001$.

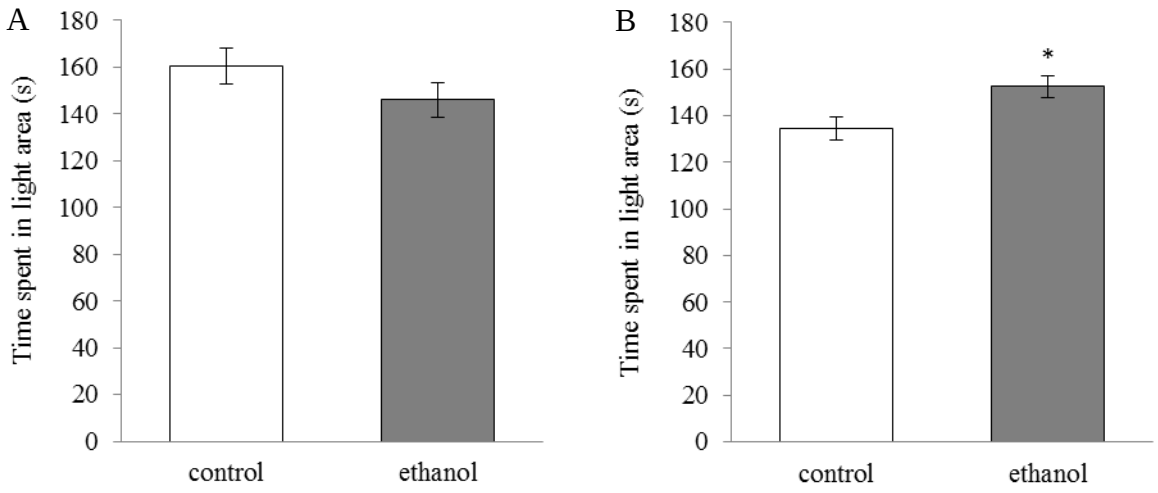

Figure 10. Bar graph of time spent in the light area of a light/dark box in ethanol and control mice. Mean (± SEM) time in seconds (s) spent in the centre of the apparatus of ethanol and control mice from (A) trimester one and (B) trimester two over a 5 min period (n = 20-28 mice per group). *$p < 0.05$.

3.2.4 Ethanol-treated mice exhibit learning and memory deficits in the Barnes maze

a) Learning is disrupted following gestational ethanol exposure

Mixed-model ANOVA showed a significant interaction of treatment by acquisition day on latency to reach the escape box. There was no significant effect of sex or an interaction between sex and treatment observed for any treatment time. Trimester one ethanol mice displayed increased latency (day 3 average: 24.81 ± 2.37; day 4 average: 24.33 ± 2.43 s) to reach the escape box than control mice (day 3 average: 12.68 ± 2.47; day 4 average: 13.29 ± 2.54 s) on acquisition days three ($F_{1,46}$ = 12.54, p = 0.001) and four ($F_{1,46}$ = 9.86, p = 0.003) (**Figure 11A**)[217]. Ethanol mice from trimester two had significantly increased latency (average: 109.09 ± 7.91 s) to reach the target hole on day one ($F_{1,54}$ = 10.60, p = 0.002) versus control mice (average: 71.74 ± 8.31 s), but performed similarly to control mice on days two to four (**Figure 11B**)[217]. A comparison between trimester one and two ethanol mice revealed significant differences on learning days three ($F_{3,100}$ = 10.01, $p < 0.001$) and four ($F_{3,100}$ = 14.36, $p < 0.001$), with trimester two ethanol mice displaying increased latency to the target hole versus trimester one treated mice.

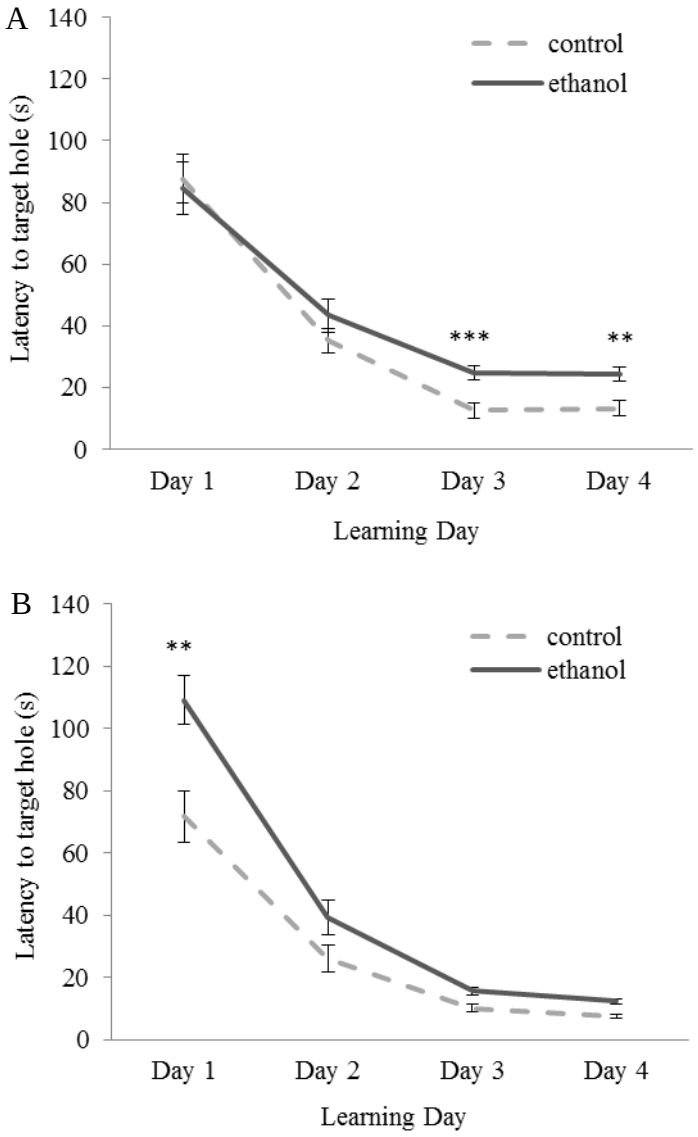

Figure 11. **Line graph of latency to reach the target of the Barnes Maze in ethanol and control mice.** Average latencies in seconds (s) to the target represent mean latencies (± SEM) of four trials per day across four acquisition days for ethanol and control mice from (A) trimester one and (B) trimester two. Data shown are collapsed across sex (n = 20-28 mice per group). ** $p < 0.01$; *** $p < 0.001$.

b) Short-term and long-term recall is delayed in ethanol-treated mice

Short-term and long-term retention of memory in the Barnes Maze was assessed on days 5 and 12, respectively. The number of explorations to each hole was calculated. On probe day 5 (short-term recall), trimester one ethanol mice were not significantly different from control mice in the number of explorations to any holes. A main effect of sex ($F_{1,46}$ = 5.33, p = 0.025) was found, with females (average: 2.46 ± 0.13 explorations) exhibiting significantly more explorations to the target hole than males (average: 2.05 ± 0.12 explorations). No significant interaction between sex and treatment was observed (**Figure 12A**)[217]. On probe day 12 (long-term recall), a significant main effect of sex ($F_{1,46}$ = 4.22, p = 0.046) was found, with females (average: 2.64 ± 0.15 explorations) exhibiting more explorations to the target hole than males (average: 2.21 ± 0.15 explorations). A significant effect of treatment ($F_{1,46}$ = 7.17, $p < 0.05$) was observed at position +2 (near the target hole), with control mice demonstrating more explorations than ethanol mice (**Figure 12B**)[217]. There were no statistically significant differences between trimester one and two ethanol mice.

No significant effects of sex or an interaction between sex and treatment were observed for the number of explorations made by ethanol and control trimester two mice on probe day 5. A significant effect of treatment was observed for the number of explorations to the adjacent hole (position -1) to the target location ($F_{1,54}$ = 14.27, $p < 0.001$), with control mice performing more explorations than ethanol mice. Significant effects of treatment were also observed for positions on the opposite side of the platform, with ethanol mice pursuing significantly more explorations to the opposite side of the target hole than control mice (**Figure 13A**)[217]. Although no main effects of sex were observed, a significant interaction between sex and treatment on probe day 12 ($F_{1,54}$ = 6.03, p = 0.02) was observed. Significant effects of treatment were

observed for the explorations to the target hole ($F_{1,54} = 12.29$, $p = 0.02$) and the hole adjacent to the target (position -1) ($F_{1,54} = 6.17$, $p = 0.002$), with control mice spending significantly more time within the target hole area than ethanol mice (**Figure 13B**)[217]. There were no statistically significant differences between trimester one and two ethanol mice.

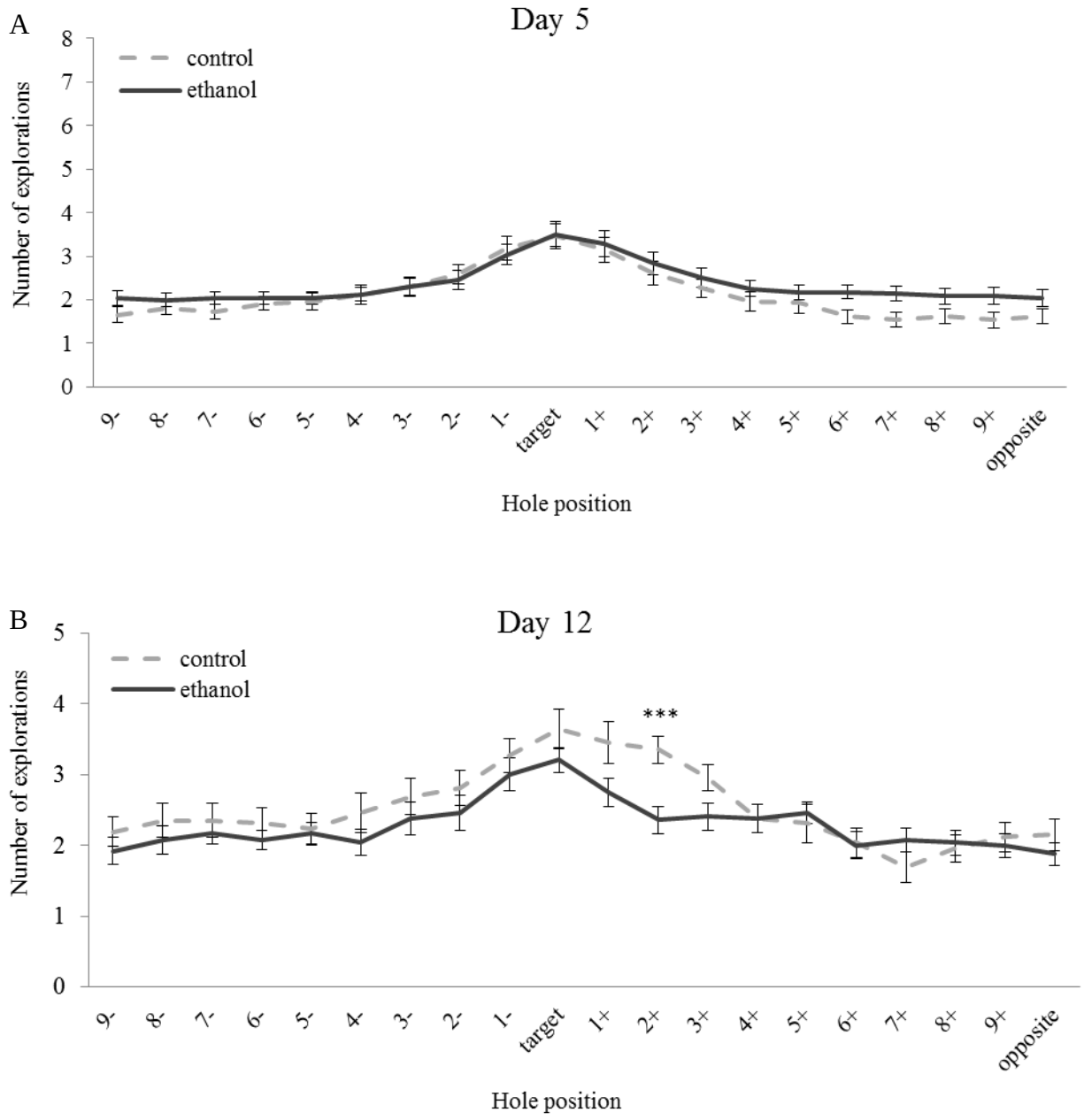

Figure 12. Line graph comparing the number of hole explorations in the Barnes Maze between trimester one ethanol and control mice. Mean (± SEM) number of explorations to each hole of the Barnes Maze for ethanol and control mice on (A) day 5 and (B) day 12. Data shown here are collapsed across sex (n = 20-26 mice per group). ***$p < 0.001$.

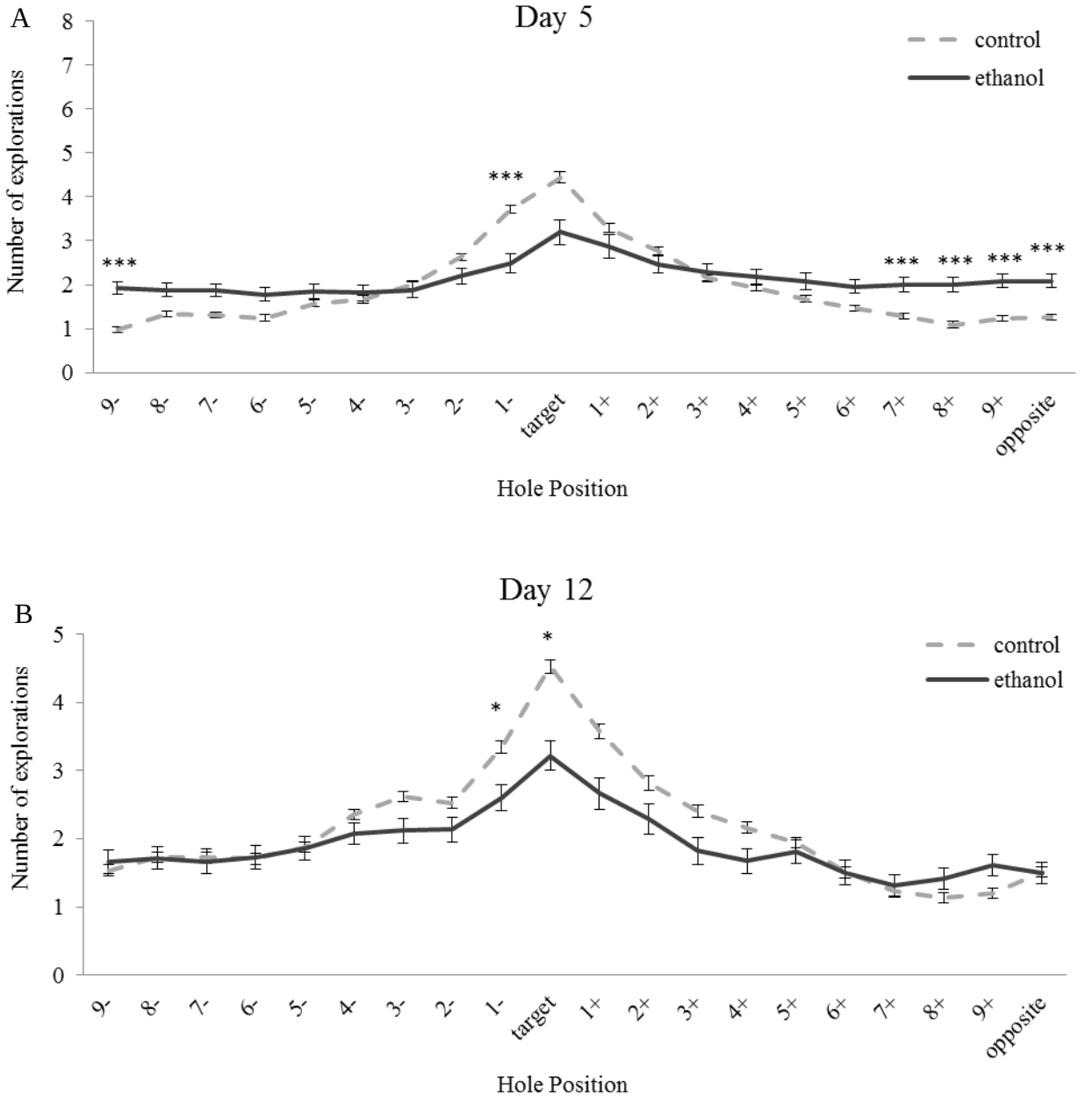

Figure 13. **Line graph comparing the number of hole explorations in the Barnes Maze between trimester two ethanol and control mice.** Mean (± SEM) number of explorations to each hole of the Barnes Maze for ethanol and control mice on (A) day 5 and (B) day 12. Data shown here are collapsed across sex (n = 26-28 mice per group). *$p < 0.05$; ***$p < 0.001$.

3.2.5 Summary of behavioural results

Ethanol exposure during the first and second term of gestation led to a variety of behavioural abnormalities in offspring (**Table 3**). These abnormalities were dependent upon the timing of prenatal ethanol exposure. First and second trimester ethanol exposure resulted in developmental milestone deficits, increased activity levels, and spatial learning delays. Spatial learning delays were not consistent between treatments. In terms of latency to the target hole in the Barnes Maze, trimester-two-ethanol mice were able to "catch up" to control mice by the end of the learning trials. When examining memory using the Barnes Maze, short-term and long-term recall (probe) trials demonstrated that the initial learning delays were persistent in ethanol mice. Trimester one ethanol mice were significantly delayed in reaching the target hole compared to matched controls. However, memory testing revealed that these mice do not exhibit memory deficits. When treated during the first trimester equivalent, ethanol mice were not significantly different from control mice in anxiety-related behaviours. Ethanol exposure during the second trimester appeared to reduce anxiety-related behaviours. These findings indicate that neurodevelopmental timing of ethanol exposure leads to heterogeneity in behaviours reminiscent of FASD.

Table 3. A comparison between trimester one and two ethanol exposure on offspring behaviours.

Behaviours[a]	**Postnatal Day**	**Trimester 1**[b]	**Trimester 2**[b]
Developmental milestones	2-21	Delayed (motor skill)	Delayed (motor skill)
Activity (daytime)	28-30	Increased	Increased
Activity (overnight)	30-35	Increased and decreased	Mostly increased (males)
Anxiety-related (Open-field)	35-40	No difference	Decreased
Anxiety-related (EPM)	35-40	No difference	No difference
Anxiety-related (LDB)	35-40	No difference	Decreased
Spatial learning (Barnes Maze)	45-55	Delayed (days 3-4)	Delayed (day 1)
Short-term memory (Barnes Maze)	50-60	No difference	Delayed
Long-term memory (Barnes Maze)	57-67	Generally no difference	Delayed

[a]Behaviours are listed by day of testing. EPM = Elevated Plus Maze. LDB = Light/Dark Box.
[b]Results are given for ethanol mice compared to control mice. No difference = no observable differences between ethanol and control mice for a behaviour.

3.3 Changes in gene expression following prenatal ethanol exposure

3.3.1 Overall patterns of gene expression changes

The overall patterns of gene expression were assessed in each of the different groups (T2-S, T1-L, and T2-L). The general trend for the Partek analysis resulted in a range from a +3.01-fold increase (*Odorant binding protein 2B*) to a -3.01-fold decrease (*Stomatin (EPB72)-like 3*) in T1-L. In T2-L, DEGs ranged from a +1.65-fold increase (*Olfactory receptor, family 2, subfamily AP, member 1*) to a -1.97-fold decrease (*Myosin, light chain 1, alkali; skeletal, fact*). The ANOVA gene list from T2-S ranged from a +7.49-fold increase (*X (inactive)-specific transcript (non-protein coding)*) from matched controls to a -2.75-fold decrease (*Carbonic anhydrase III, muscle specific*).

There was no overlap of specific genes altered between all three groups when using cut-off values of ± 1.2-fold change and $p < 0.05$ (**Figure 14**). There were no DEGs between ethanol and control mice in any of the groups using a FDR-corrected *p*-value of 0.05 and a ± 1.2-fold change cut-off. Further analysis was restricted to an unadjusted $p < 0.05$ with the same fold change. Using this cut-off, one gene, *Triadin* (*Trdn*), overlapped between T1-L and T2-S (**Figure 14**). Using these criteria, T2-S, T1-L, and T2-L resulted in the altered expression of 48, 55, and 68 genes, respectively (Appendices B-D). These changes ranged from a +1.43-fold increase from matched controls (*SLIT and NTRK-like family, member 2* or *Slitrk2*) to a -1.91-fold decreased (*Trdn*). In T1-L, the range was from a +1.44-fold increase from matched controls (*Predicted gene 3696*) to a -1.39-fold decrease (*Proliferating cell nuclear antigen* or *Pcna*) in T1-L. In T2-L, the range was between a +1.34-fold increase from matched controls (*Predicted gene 9875*) to a -1.78-fold decrease (*Stromal cell-derived factor 2-like-1* or *Sdf2l1*). In this

assessment, the distribution of upregulated and downregulated genes was not equal across groups. In T1-L, 10 genes (18.2%) were increased. In T2-L, 27 genes (39.7%) were increased. And, in group T2-S, 30 genes (62.5%) were increased. Apart from gene annotations identified on the Mouse Gene 1.0 ST arrays, there were various miRNAs discovered. T2-S gene expression analysis resulted in differential expression of Mir-380, Mir-540, Mir-99a, Mir-337 and Mir-665 (Appendix B). As part of the long-term gene lists for T1-L and T2-L, Mir-451 and Mir-342 were identified, respectively (Appendices C-D).

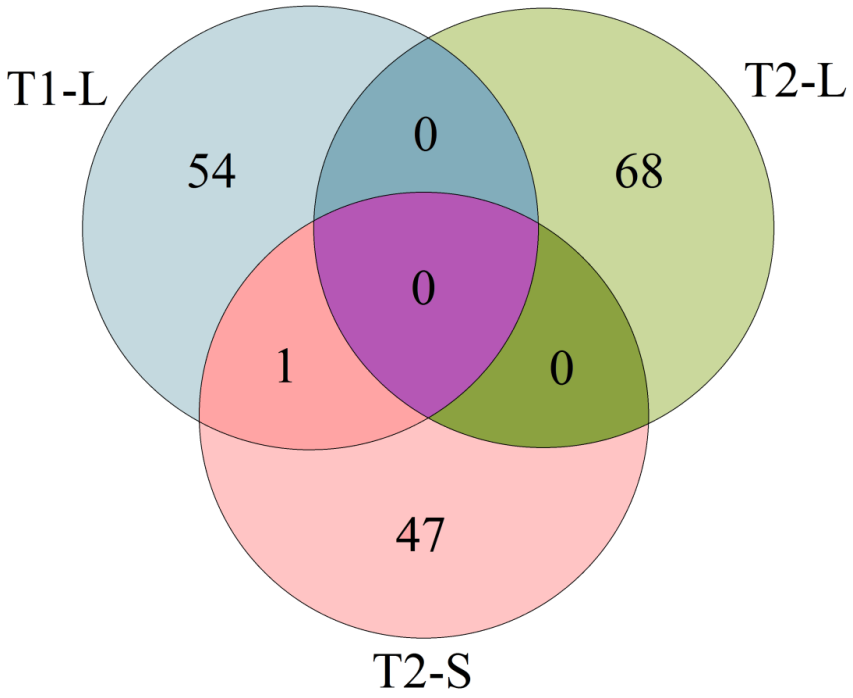

Figure 14. A venn diagram of overlapping differentially-expressed genes (DEGs) compared across trimester two short-term (T2-S), trimester one long-term (T1-L), and trimester two long-term (T2-L) treatments. Adapted from GeneVenn® (http://genevenn.sourceforge.net/). Gene lists included T2-S (pink), T1-L (blue) and T2-L (green). No genes were in common between T2-S, T1-L, and T2-L (purple), or between T1-L and T2-L (dark blue), or between T2-S and T2-L (dark green). One gene (*Triadin*) is in common between T2-S and T1-L (dark pink). ANOVA lists generated from Partek Genomics Suite software using a cut-off of $p < 0.05$ and ± 1.2-fold change.

3.3.2 Molecular analysis of short-term (T2-S) DEGs

a) Immediate effects of ethanol on cellular functions

Functional analysis of T2-S was completed using DAVID, Partek (GE), and IPA. Using DAVID, T2-S data resulted in two significant categories (**Table 4**). Genes identified in the keyword, "Nucleus" are involved in DNA or RNA binding, regulation of p53 transcription and apoptosis, and mismatch repair. The SMART term, Dual specificity phosphatase, catalytic domain ("DSPc") included genes involved in protein-tyrosine phosphorylation, which can affect protein interactions, cellular localization, protein stability, and enzymatic activity.

Analysis of genes disrupted in T2-S using GE revealed 63 significantly disrupted molecular functions. Here, the GO categories were primarily associated with the top function, protein phosphorylation (**Table 5**). These GE results are complementary to DAVID analysis, which implicated *Dual specificity phosphatase 19* (*Dusp19*) and *Slingshot homolog 2 (Drosophila)* (*Ssh2*) in the "DSPc" SMART term. Generally, the GE processes altered in the fetal brain are involved in mitogen-activated protein kinase (MAPK) activity, including calcium stimulation of MAPK. Two processes are involved in each of G-protein coupled receptor activity, and lipid transport. The last three of the top 10 processes are involved in stress response, chromatin binding, and actin cytoskeleton development.

Functional analysis of T2-S using IPA resulted in the identification of five functions in each of three categories: Diseases and Disorders, Molecular and Cellular Functions, and Physiological System Development and Function (**Table 6**). Two miRNAs appear in each of the top five functions of Diseases and Disorders, and are involved in post-transcrpitional regulation of gene expression by affecting the stability and translation of mRNAs.

Table 4. Top significant annotation clusters resulting from The Database for Annotation, Visualization and Integrated Discovery (DAVID) functional analysis of trimester two short-term (T2-S) differentially-expressed genes (DEGs).

Category[a]	**Term**	***p*-value**	**Genes**[b]
SP PIR	Nucleus	0.039	*Gpkow, Jmy, Rybp, Crem, Ccnt1, Zfp600, Magohb, Nol4, Nap1l3, Zc3h18, Tdg, Zmat5*
SMART	DSPc	0.043	*Dusp19, Ssh2*

[a]Category includes information from the Swiss-Prot and Protein Information Resource (SP PIR keyword) and Simple Modular Architecture Research Tool (SMART) genomic database.
[b]Genes included *G patch domain and KOW motifs* (*Gpkow*), *Junction mediating protein, p53 cofactor* (*Jmy*), *RING1 and YY1 binding protein* (*Rybp*), *cAMP responsive element modulator* (*Crem*), *Cyclin T1* (*Ccnt1*), *Zinc finger protein 600* (*Zfp600*), *Mago-nashi homolog B (Drosophila)* (*Magohb*), *Nucleolar protein 4 Nucleosome assembly protein 1-like-3* (*Nol4*), *Zinc finger CCCH-type containing 18* (*Zc3h18*), *Thymine-DNA glycosylase* (*Tdg*), *Zinc finger, matrin-type 5* (*Zmat5*), *Dual specificity phosphatase 19* (*Dusp19*), and *Slingshot homolog 2 (Drosophila)* (*Ssh2*).

Table 5. Top ten functions of short-term (T2-S) differentially-expressed genes (DEGs) identified using Gene Ontology Enrichment (GE).

Gene Ontology Function	Type[a]	Enrichment Score[b]	*p*-value	Genes[c]
Protein tyrosine/serine/threonine phosphatase activity	MF	6.25	0.002	*Dusp19, Ssh2*
Regulation of DNA-dependent transcription in response to stress	BP	5.13	0.006	*Jmy*
Calcium-dependent protein kinase C activity	MF	5.13	0.006	*Ccl3*
Bombesin receptor signaling pathway	BP	5.13	0.006	*Nmbr*
Bombesin receptor activity	MF	5.13	0.006	*Nmbr*
Negative regulation of chromatin binding	BP	5.13	0.006	*Tdg*
Protein tyrosine/threonine phosphatase activity	MF	5.13	0.006	*Dusp19*
Glycolipid transporter activity	MF	4.85	0.008	*Gltpd1*
Glycolipid transport	BP	4.85	0.008	*Gltpd1*
Regulation of lemellipodium assembly	BP	4.85	0.008	*Ssh2*

[a]Type indicates a biological process (BP), cellular component (CC), or molecular function (MF).
[b]Enrichment score = Significant genes in a category/All significant genes, vs All genes in the category/All genes on the chip.
[c]Genes included *Dual-specificity phosphatase 19* (*Dusp19*), *Slingshot homolog 2 (Drosophila)* (*Ssh2*), *Junction mediating protein, p53 cofactor* (*Jmy*), *Chemokine (C-C motif) ligand 3* (*Ccl3*), *Neuromedin B receptor* (*Nmbr*), *Thymine-DNA glycosylase* (*Tdg*), and *Glycolipid transfer protein domain containing 1* (*Gltpd1*).

Table 6. Functional characterization of short-term (T2-S) differentially-expressed genes (DEGs) using Ingenuity Pathway Analysis (IPA).

Diseases and Disorders				
Name	***p*-value**	**# genes**	**Genes**[a]	**Function Annotation**
Developmental Disorder	1.14E-03 – 3.29E-02	5	*mir-379, mir-99, Tdg, Trdn, Crem*	Hypertrophy of skeletal muscle
Hereditary Disorder	1.14E-03 – 2.29E-03	2	*mir-379, mir-99*	Nemaline myopathy
Skeletal and Muscular Disorder	1 .14E-03 – 4.12E-02	5	*mir-379, mir-99, Trdn, Crem, Ccl3*	Muscular hypertrophy
Connective Tissue Disorder	1.34E-03 – 4.12E-02	3	*mir-379, mir-99, Ccl3*	Adjuvant arthritis
Dermatological Diseases	1.34E-03 – 1.34E-03	2	*mir-379, mir-99*	Dermatomyositis
Molecular and Cellular Functions				
Name	***p*-value**	**# genes**	**Genes**[a]	**Function Annotation**
Cell Cycle	2.10E-03 – 4.93E-02	1	*Crem*	Arrest in G2/M phase
Cellular Assembly/Organization	2 .10E-03 – 2.29E-02	1	*Pip5k1b*	Formation of actin comet
Cellular Function/Maintenance	2.10E-03 – 3.11E-02	2	*Pip5k1b, Ccl3*	Formation of microvilli
Antigen Presentation	4 .20E-03 – 8.38E-03	1	*Ccl3*	Migration of dendritic precursors
Cellular Movement	4.20E-03 – 4.93E-02	2	*Ccl3, Ccnt1*	Th1 cell transmigration
Physiological System Development and Function				
Name	***p*-value**	**# genes**	**Genes**[a]	**Function Annotation**
Nervous System Development/Function	2.10E-03 – 1.05E-02	1	*Ccl3*	Astrocyte/microglia accumulation
Tissue Development	2.10E-03 – 2.70E-02	3	*Ccl3, Bcap31, mir-99*	Embryonic stem cell adhesion
Hematological System Development/Function	4.20E-03 – 4.93E-02	3	*Ccl3, Ccnt1, Lair1*	T lymphocyte trafficking
Hematopoiesis	4 .20E-03 – 1.05E-02	1	*Ccl3*	Migration of dendritic precursors
Immune Cell Trafficking	4 .20E-03 – 4.93E-02	2	*Ccl3, Ccnt1*	Natural Killer cell migration

[a]Genes included *microRNA-379* (*mir-379*), *microRNA-99a* (*mir-99*), *Thymine-DNA glycosylase* (*Tdg*), *Triadin* (*Trdn*), *cAMP responsive element modulator* (*Crem*), *Chemokine (C-C motif) ligand 3* (*Ccl3*), *Phosphatidylinositol-4-phosphate 5-kinase, type I, beta* (*Pip5k1b*), *Cyclin T1* (*Ccnt1*), *B-cell receptor-associated protein 31* (*Bcap31*), and *Leukocyte-associated immunoglobulin-like receptor 1* (*Lair1*).

b) Immediate effects of ethanol on cellular pathways

Pathway analysis of T2-S was performed using Pathway Express, Pathway Enrichment, and IPA. T2-S analysis did not result in any statistically significant KEGG pathways in Pathway Express. The top nominally significant pathway "regulation of actin cytoskeleton" (Impact factor = 2.72, p = 0.066), was consistent with functional analysis that implicated *Dusp19* and *Ssh2* in actin cytoskeleton development.

As with Pathway Express, there were no statistically significant T2-S pathways found using PE. The top nominally significant pathways that were identified included: "regulation of actin cytoskeleton" (p = 0.066), with *Phosphatidylinositol-4-phosphate 5-kinase, type I, beta* (*Pip5k1b*) and *Ssh2*, "base excision repair" (p = 0.069), with *Thymine-DNA glycosylase* (*Tdg*), and "nicotine addiction" (p = 0.080), with *Hippocalcin* (*Hpca*).

T2-S exposure was not significantly associated with any canonical pathways in IPA (**Table 7**). However, the top associated pathway, termed, Actin Cytoskeleton Signaling, was nominally significant (p = 7.04E-02), with *Pip5k1b* and *Ssh2*. Other pathways that included immune cell communication, natural killer cell signaling, and p53 signaling were not statistically significant. However, these pathways were complementary to IPA functional analysis (**Table 6**), which implicated each of the genes listed in **Table 7** in such processes.

Table 7. Top canonical pathways resulting from Ingenuity Pathway Analysis (IPA) of short-term (T2-S) differentially-expressed genes (DEGs).

Canonical Pathway Name[a]	***p*-value**	**Genes**[b]
Actin Cytoskeleton Signaling	7.04E-02	*Pip5k1b, Ssh2*
Communication between Innate and Adaptive Immune Cells	1.26E-01	*Ccl3*
Regulation of Actin-based Motility by Rho	0.15	*Pip5k1b*
p53 Signaling	0.17	*Jmy*
Natural Killer Cell Signaling	0.173	*Lair1*

[a]Canonical pathways were identified in Ingenuity Pathway Analysis using the Core Analysis feature. The list of DEGs was generated using Partek software, using a ± 1.2 fold change and $p < 0.05$.
[b]Genes included *Phosphatidylinositol-4-phosphate 5-kinase, type I, beta* (*Pip5k1b*), *Slingshot homolog 2 (Drosophila)* (*Ssh2*), *Chemokine (C-C motif) ligand 3* (*Ccl3*), *Junction mediating protein, p53 cofactor* (*Jmy*), and *Leukocyte-associated immunoglobulin-like receptor 1* (*Lair1*).

c) Immediate effects of ethanol on cellular networks

Network analysis for T2-S was completed using GeneMANIA and IPA's Core Analysis network feature. However, there were no significant GeneMANIA networks identified. The top T2-S IPA networks with a network score > 3 are reported in **Table 8**. The top network was termed: Inflammatory Disease, Neurological Disease, Skeletal and Muscular Disorders (**Figure 15**), and included 13 DEGs out of 34 network genes. Of the DEGs, six genes are downregulated while seven genes are upregulated. The second network, termed, Cellular Development, Cellular Growth and Proliferation, Hematological System Development and Function, was comprised of 35 network genes (**Figure 16**). More genes were upregulated than downregulated in this network, with a 3:2 ratio. The top significant IPA networks from T2-S were merged into one large interacting network to identify "hub" genes. **Figure 17** shows the identified hub molecules that have > 10 interactions with other genes, including those that were differentially-expressed in the fetal brain following GD 16 ethanol exposure.

d) Candidate gene selection and confirmation of specific genes disrupted following immediate ethanol exposure

Based on the criteria given in the Methods and Materials section (**Figure 1**), the selected candidates for confirmation are reported in **Table 9**. Here, the functional (NCBI, DAVID, GO Enrichment, GeneMANIA), pathway (IPA, Partek Pathway, Pathway Express), and network (IPA) characterization of genes was summarized. The resulting expression changes and *p*-values for the eight T2-S genes chosen for confirmation are shown in **Table 10**. No genes from T2-S were confirmed. A series of box plots illustrating the variability across biological replicates in qRT-PCR demonstrates the similarity in ΔC_T values across replicates (**Figure 18**).

Table 8. Top Ingenuity Pathway Analysis (IPA) networks identified in short-term (T2-S) analysis of differentially-expressed genes (DEGs).

Network	No. Focus Molecules[a]	Top Function[b]	Input Genes[c]	Score[d]
1	13	Cellular Compromise, Cell Death, Free Radical Scavenging	*Bcap31, Hpca, Tdg, mir-99, Zc3h18, Crem, mir-379, mir-337, Lair1, Jmy, Ccl3, Nmbr, Rybp*	28
2	5	Cellular Development, Cellular Growth and Proliferation, Hematological System Development and Function	*Ccnt1, Zmat5, Trdn, Sprr2a, Pip5k1b*	8

[a]Number (No.) Focus Molecules indicates the number of genes that were differentially expressed (Partek: ± 1.2 fold change, $p < 0.05$) in fetal brain (GD 16) as a result of ethanol exposure in the second trimester equivalent.
[b]Top Function represents the name of the network in IPA.
[c]Input genes included *B-cell receptor-associated protein 31* (*Bcap31*), *Hippocalcin* (*Hpca*), *Thymine-DNA glycosylase* (*Tdg*), *microRNA 99a* (*mir-99*), *Zinc finger CCCH-type containing 18* (*Zc3h18*), *cAMP responsive element modulator* (*Crem*), *microRNA 379* (*mir-379*), *microRNA 337* (*mir-337*), *Leukocyte-associated immunoglobulin-like receptor 1* (*Lair1*), *Junction mediating protein, p53 cofactor* (*Jmy*), *Chemokine (C-C motif) ligand 3* (*Ccl3*), *Neuromedin B receptor* (*Nmbr*), *RING1 and YY1 binding protein* (*Rybp*), *Cyclin T1* (*Ccnt1), Zinc finger, matrin-type 5* (*Zmat5*), *Triadin* (*Trdn*), *Small proline-rich protein 2A* (*Sprr2a*), and *Phosphatidylinositol-4-phosphate 5-kinase, type I, beta* (*Pip5k1b*).
[d]Score is equal to the negative exponent of the respective p-value such that a score of 3 corresponds to a *p*-value of 10E-3. Network 1 score of 28 is equivalent to $p = 10E-28$. Network 2 score of 8 is equivalent to $p = 10E-8$.

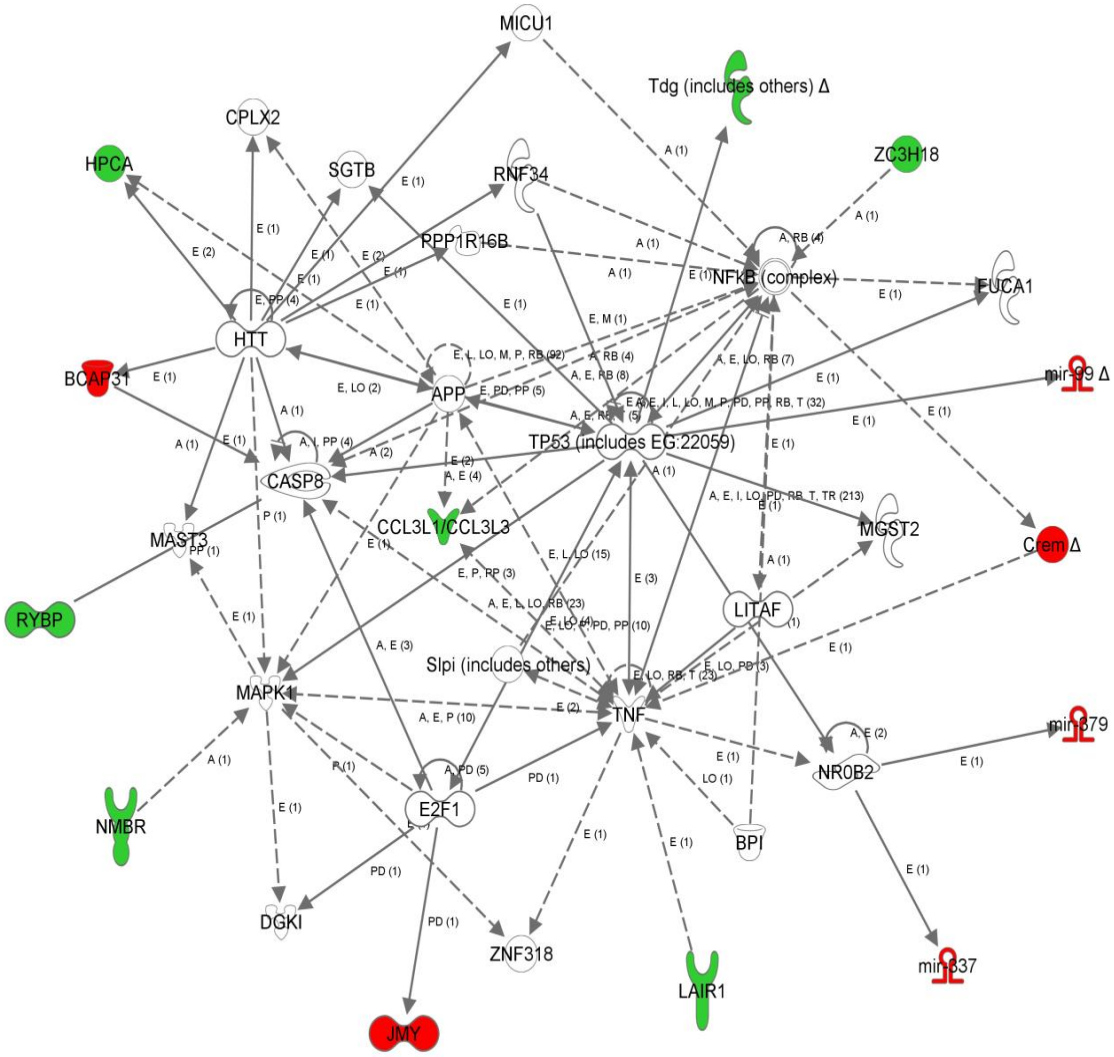

Figure 15. First network resulting from Ingenuity Pathway Analysis (IPA) of short-term (T2-S) differentially-expressed genes (DEGs). Network name: Cellular Compromise, Cell Death, Free Radical Scavenging. Highlighting (red and green) represents input genes. Red indicates downregulation and green indicates upregulation in ethanol mice versus control mice. DEGs were identified using Partek Genomics Suite with a ± 1.2 fold change and $p < 0.05$. A single-headed arrow indicates the action of one gene on another. A double arrow-headed line indicates that the two genes act on each other. Dashed lines indicate an indirect interaction, and solid lines indicate direct interactions. E = expression, L = proteolysis, LO = localization, PD = protein-DNA binding, A = activation, P = phosphorylation/dephosphorylation, PR = protein-RNA binding, PP = protein-protein interaction, I = inhibition, M = biochemical modification, RB = regulation of binding, T = transcription, TR = translocation. Refer to Appendix F for a full IPA legend on relationship types, molecular shapes, and relationships.

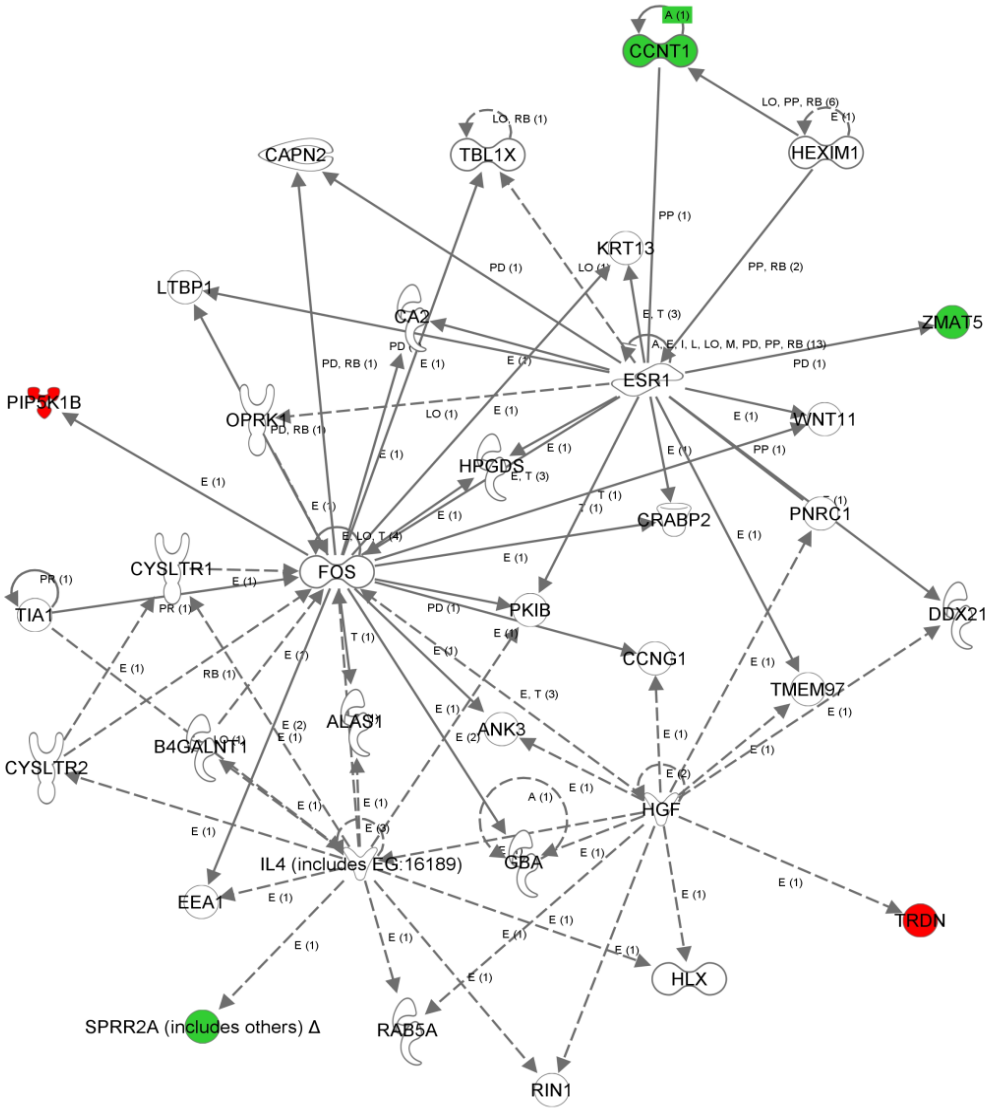

Figure 16. Second network resulting from Ingenuity Pathway Analysis (IPA) of short-term (T2-S) differentially-expressed genes (DEGs). Network term: Cellular Development, Cellular Growth and Proliferation, Hematological System Development and Function. Highlighting (red and green) represents input genes. Red indicates downregulation and green indicates upregulation in ethanol mice versus control mice. DEGs were identified using Partek Genomics Suite with a ± 1.2 fold change and $p < 0.05$. A single-headed arrow indicates the action of one gene on another. A double arrow-headed line indicates that the two genes act on each other. Dashed lines indicate an indirect interaction, and solid lines indicate direct interactions. E = expression, L = proteolysis, LO = localization, PD = protein-DNA binding, A = activation, P = phosphorylation/dephosphorylation, PR = protein-RNA binding, PP = protein-protein interaction, I = inhibition, M = biochemical modification, RB = regulation of binding, T = transcription, TR = translocation. Refer to Appendix F for a full IPA legend on relationship types, molecular shapes, and relationships.

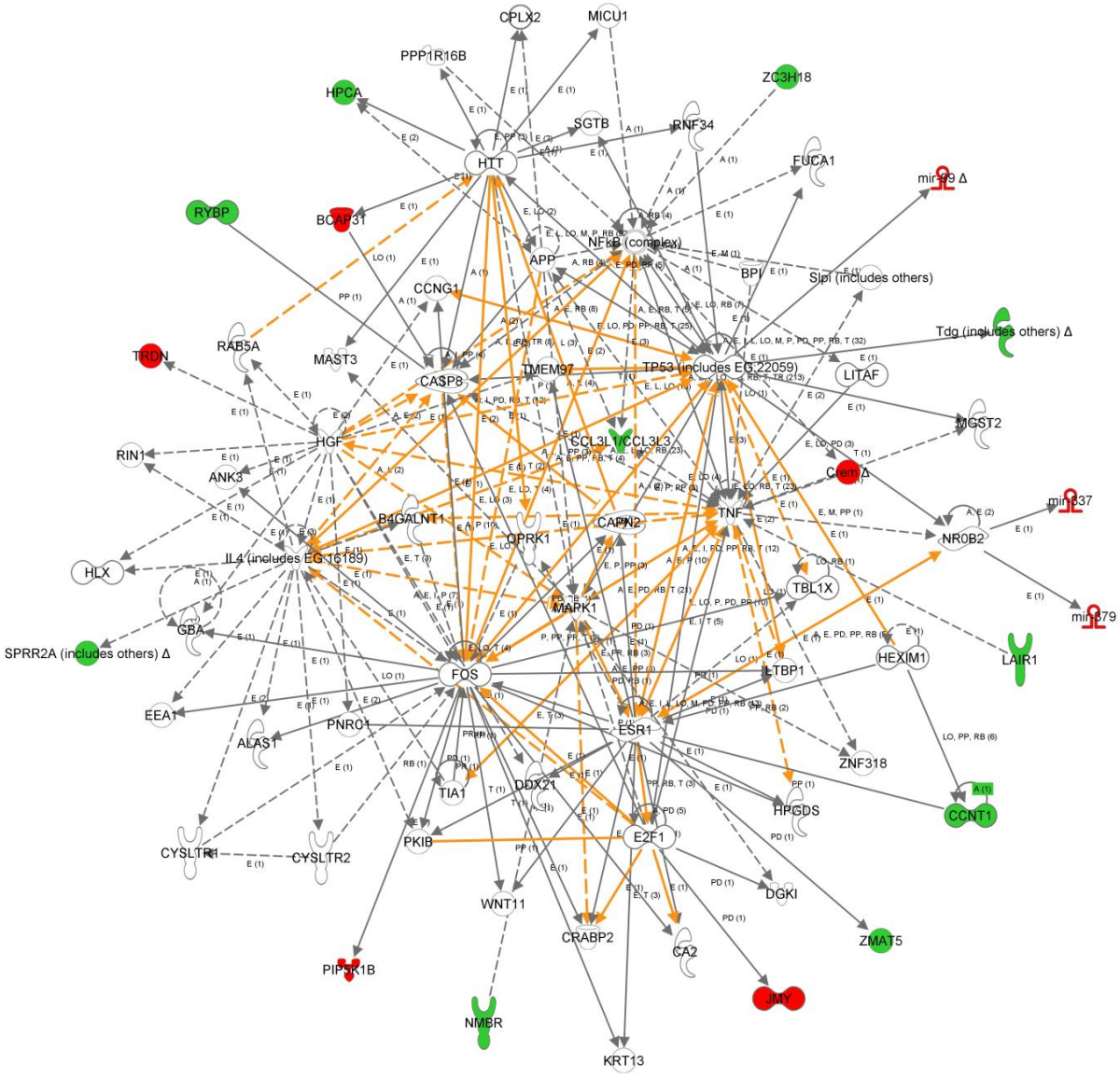

Figure 17. A merged network from Ingenuity Pathway Analysis (IPA) of short-term (T2-S) differentially-expressed genes (DEGs). Highlighting (red and green) represents input genes. Red indicates downregulation and green indicates upregulation in ethanol mice versus control mice. DEGs were identified using Partek Genomics Suite with a ± 1.2 fold change and $p < 0.05$. A single-headed arrow indicates the action of one gene on another. A double arrow-headed line indicates that the two genes act on each other. Dashed lines indicate an indirect interaction, and solid lines indicate direct interactions. E = expression, L = proteolysis, LO = localization, PD = protein-DNA binding, A = activation, P = phosphorylation/dephosphorylation, PR = protein-RNA binding, PP = protein-protein interaction, I = inhibition, M = biochemical modification, RB = regulation of binding, T = transcription, TR = translocation. Refer to Appendix F for a full IPA legend on relationship types, molecular shapes, and relationships.

Table 9. Candidate gene selection criteria for confirmation of specific short-term (T2-S) differentially-expressed genes (DEGs).

Candidate Genes[a]	Neurodevelopment and/or behaviour	Tool[b]	Network (IPA)[c]
Ccl3	facioscapulohumeral musclular dystrophy; microglia, astrocyte and dendrite development; ethanol and taste aversion; immune response osteoclast differentiation[218]	IPA PubMed	1
Ccnt1	immune cell trafficking; cellular movement snRNA binding	IPA Partek GE	2
Gpr50	component of adaptive thermogenesis[219] K/O mice have increased activity levels[220]	PubMed PubMed	None
Lair1	Natural Killer cell signaling feeding behaviour and body weight regulation[221]	IPA PubMed	1
Pip5k1b	regulation of actin cytoskeleton associated with autism[222]	IPA, P. Express PubMed	2
Rybp	histone H2A monoubiquitination required for mouse eye development[223]	Partek GE PubMed	1
Slitrk2	excitatory and inhibitory synapse formation[224] candidate for schizophrenia[225] and bipolar disorder[226]	PubMed PubMed	None
Trdn	hypoplasia of forebrain; hypertrophy of skeletal muscle	IPA	2

[a]Genes are listed alphabetically. Genes include *SLIT and NTRK-like family, member 2* (*Slitrk2*), *Cyclin T1* (*Ccnt1*), *Leukocyte-associated immunoglobulin-like receptor 1* (*Lair1*), *RING1 and YY1 binding protein* (*Rybp*), *G protein-coupled receptor 50* (*Gpr50*), *Triadin* (*Trdn*), *Chemokine (C-C motif) ligand 3* (*Ccl3*), *Phosphatidylinositol-4-phosphate 5-kinase, type I, beta* (*Pip5k1b*).
[b]Tools used to analyse candidate genes (by neurodevelopment and behaviour) include PubMed, Ingenuity Pathway Analysis (IPA), Partek Gene Ontology Enrichment, and Pathway Express.
[c]IPA networks are shown in Figures 15-16.

Table 10. A comparison between short-term (T2-S) qRT-PCR and microarray results for candidate genes.

Genes[a]	Array Fold Change	Array *p*-value	qRT-PCR Fold Change	qRT-PCR *p*-value
Ccl3	1.22	0.034	-1.16	0.414
Ccnt1	1.22	0.014	-0.99	0.541
Gpr50	1.34	0.020	-1.06	0.670
Lair1	1.25	0.019	-0.92	0.355
Pip5k1b	-1.22	0.014	-1.35	0.307
Rybp	1.35	0.030	-1.01	0.218
Slitrk2	1.43	0.046	-0.99	0.684
Trdn	-1.91	0.032	N/A	N/A

[a]Genes are listed alphabetically. Genes include *SLIT and NTRK-like family, member 2* (*Slitrk2*), *Cyclin T1* (*Ccnt1*), *Leukocyte-associated immunoglobulin-like receptor 1* (*Lair1*), *RING1 and YY1 binding protein* (*Rybp*), *G protein-coupled receptor 50* (*Gpr50*), *Triadin* (*Trdn*), *Chemokine (C-C motif) ligand 3* (*Ccl3*), *Phosphatidylinositol-4-phosphate 5-kinase, type I, beta* (*Pip5k1b*).

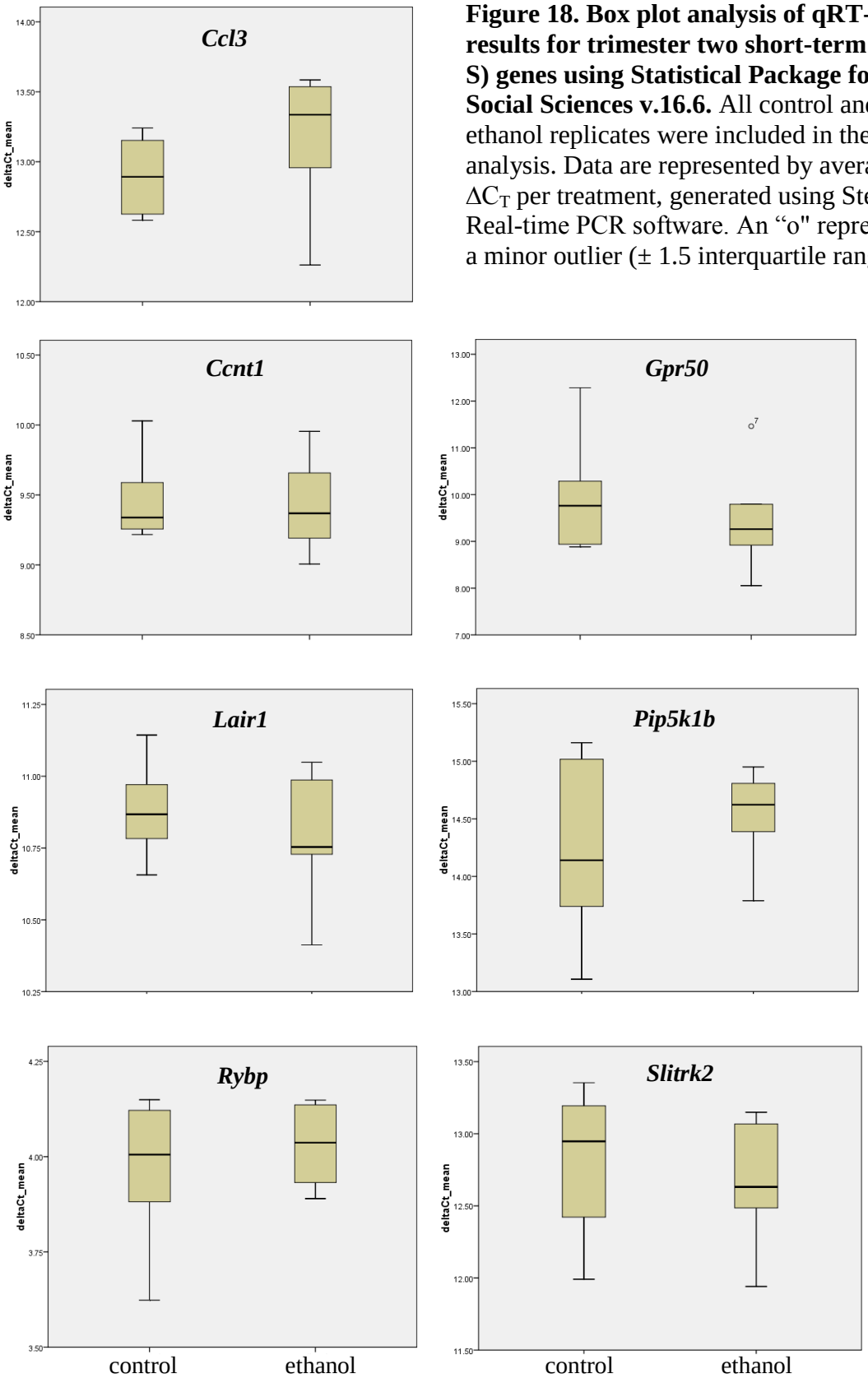

Figure 18. Box plot analysis of qRT-PCR results for trimester two short-term (T2-S) genes using Statistical Package for the Social Sciences v.16.6. All control and ethanol replicates were included in the analysis. Data are represented by average ΔC_T per treatment, generated using StepOne Real-time PCR software. An "o" represents a minor outlier (± 1.5 interquartile range).

3.3.3 Molecular analysis of first trimester long-term (T1-L) DEGs

a) First-trimester effects of ethanol on cellular functions

As outlined for the short-term experiment (T2-S), T1-L gene lists were subjected to functional analysis using DAVID, GE, and IPA. Functional annotation clustering was performed on T1-L DEGs using DAVID (**Table 11**). The SP PIR keyword, "coenzyme A", emphasized a role for synthesis and oxidation of fatty acids in FASD. The three genes that are part of this keyword are involved in processes including ketogenesis and antioxidant detoxification. One of these genes, *N-acetyltransferase 1* (*Nat1*), is involved in folate catabolism. Two of the five categories listed in **Table 11** include genes involved in ribosomal functions. "Base excision repair" was previously identified in T2-S analysis of pathways, albeit not statistically significant.

GO Enrichment was used to evaluate over-represented molecular functions, cellular components, and biological processes using Partek. T1-L GE analysis returned a list of 104 significant functions. The top 10 significant GO categories and shown in **Table 12**. The gene, *Cleavage and polyadenylation factor I subunit 1* (*Clp1*), was identified in three of the top 10 functions, and involved tRNA splicing and mRNA 3'end formation. The gene, *SET domain containing 2* (*Setd2*), was involved in two of the top 10 processes, one of which included histone methylation. In general, the top 10 GE functions were involved in cellular maintenance and protein kinase activity.

Using the Core Analysis tool within IPA, a list of T1-L processes was generated for three different categories: Diseases and Disorders, Molecular and Cellular Functions, and Physiological System Development and Function (**Table 13**). *Carcinoembryonic antigen-related cell adhesion molecular 1 (biliary glycoprotein)* (*Ceacam1*) was the only significant gene in

Diseases and Disorders. *Ceacam1* was also identified in the second significantly GE function, "positive regulation of MAP kinase activity" (**Table 12**). Other genes in this category were previously identified in DAVID analysis (**Table 4**): *Methyl-CpG binding domain protein 4* (*Mbd4*) was part of the GO BP "base excision repair", and *Pleiotropic regulator 1* (*Plrg1*) was involved in the GO CC "ribonucleoprotein"; *Mitogen-activated protein kinase kinase kinase, E3 ubiquitin protein ligase* (*Map3k1*) and *Activating transcription factor 1* (*Atf1*) were involved in "TNF/Stress related signaling". *Ceacam1, Map3k1, Eomesodermin (Xenopus laevis) homolog* (*Eomes*), and *pre-B lymphocyte 1* (*Vpreb1*) appear in at least three of the five top disrupted processes, adding to their importance in cellular disruption following prenatal ethanol exposure in the first trimester equivalent. The function with the highest number of genes implicated in this category included "Tissue Morphology".

Table 11. Top significant annotation clusters resulting from The Database for Annotation, Visualization and Integrated Discovery (DAVID) functional analysis of trimester one long-term (T1-L) differentially-expressed genes (DEGs).

Category[a]	**Term**	***p*-value**	**Genes**[b]
SP PIR keyword	Coenzyme A	0.035	*Hmgcs2, Atf1, Nat1*
GO MF	Structural constituent of ribosome	0.037	*Rpl36a, Gm12191, Gm4987*
BIOCARTA	TNF/Stress related signaling	0.042	*Map3k1, Atf1*
GO CC	Ribonucleoprotein complex	0.043	*Gm12191, Gm4987, Rpl36a, Sfrs1, Clp1, Nat1, Rcl1, Plrg1*
GO BP	Base-excision repair	0.048	*Mbd4, Pcna*

[a]Category includes information from the Swiss-Prot and Protein Information Resource (SP PIR keyword), Gene Ontology's (GO) molecular function (MF), cellular component (CC) and biological process (BP), BioCarta references, and Simple Modular Architecture Research Tool (SMART) genomic database.
[b]Genes included *3-hydroxy-3-methylglutaryl-CoA synthase 2 (mitochondrial)* (*Hmgcs2*), *Activating transcription factor 1* (*Atf1*), *N-acetyltransferase 1 (arylamine N-acetyltransferase)* (*Nat1*), *Ribosomal protein L36a* (*Rpl36a*), predicted genes *Gm12191* and *Gm4987*, *Mitogen-activated protein kinase kinase kinase 1, E3 ubiquitin protein ligase* (*Map3k1*), *Serine/arginine-rich splicing factor 1* (*Sfrs1*), *Cleavage and polyadenylation factor I subunit 1* (*Clp1*), *RNA terminal phosphate cyclase-like 1* (*Rcl1*), *Pleiotropic regulator 1* (*Plrg1*), *Methyl-CpG binding domain protein 4* (*Mbd4*), and *Proliferating cell nuclear antigen* (*Pcna*).

Table 12. Top ten significant functions of trimester one long-term (T1-L) differentially-expressed genes (DEGs) from Gene Ontology Enrichment (GE).

Gene Ontology Function	Type[a]	Enrichment Score[b]	*p*-value	Genes[c]
Homeostasis of number of cells	BP	7.23	0.0007	*Vpreb1, Gcnt4*
Positive regulation of MAP kinase activity	BP	5.43	0.004	*Ceacam1, Map3k1*
Histone H3-K36 methylation	BP	4.96	0.007	*Setd2*
Mesoderm morphogenesis	BP	4.96	0.007	*Setd2*
G-protein coupled receptor signaling pathway, coupled to cyclic nucleotide second messenger	BP	4.96	0.007	*Htr5a*
tRNA-intron endonuclease complex	CC	4.96	0.007	*Clp1*
Targeting of mRNA for destruction involved in RNA interference	BP	4.96	0.007	*Clp1*
ATP-dependent polydeoxyribinucleotide 5'-hydroxyl-kinase activity	MF	4.96	0.007	*Clp1*
mRNA 5'-splice site recognition	BP	4.96	0.007	*Srsf1*
Type 1 melanocortin receptor binding	MF	4.96	0.007	*Mrap2*

[a]Type indicates a biological process (BP), cellular component (CC), or molecular function (MF).
[b]Enrichment score = Significant genes in a category/All significant genes, vs All genes in the category/All genes on the chip.
[c]Genes included *pre-B lymphocyte 1* (*Vpreb1*), *Glucosaminyl (N-acetyl) transferase 4, core 2* (*Gcnt4*), *Carcinoembryonic antigen-related cell adhesion molecule 1 (biliary glycoprotein)* (*Ceacam1*), *Mitogen-activated protein kinase kinase kinase 1, E3 ubiquitin protein ligase* (*Map3k1*), *Serine/arginine-rich splicing factor 1* (*Sfrs1*), *Cleavage and polyadenylation factor I subunit 1* (*Clp1*), *SET domain containing 2* (*Setd2*), *5-hydroxytryptamine (serotonin) receptor 5A, G protein-coupled* (*Htr5a*), and *Melanocortin 2 receptor accessory protein 2* (*Mrap2*).

Table 13. Functional characterization of trimester one long-term (T1-L) differentially-expressed genes (DEGs) using Ingenuity Pathway Analysis (IPA).

Diseases and Disorders				
Name	***p*-value**	**# genes**	**Genes**[a]	**Function Annotation**
Inflammatory Response	5.87E-03 – 4.32E-02	1	*Ceacam1*	Priming of Th1 helper cells
Connective Tissue Disorders	1.17E-02 – 1.17E-02	1	*Ceacam1*	Infection of blood
Hematological Disease	1.17E-02 – 1.17E-02	1	*Ceacam1*	Infection of blood
Infectious Disease	1.17E-02 – 4.32E-02	1	*Ceacam1*	Infection of blood, spleen, liver
Developmental Disorder	1.75E-02 – 3.19E-02	2	*Setd2, Trdn*	Hypoplasia of forebrain
Molecular and Cellular Functions				
Name	***p*-value**	**# genes**	**Genes**[a]	**Function Annotation**
Cell Death/Survival	6.49E-04 – 3.17E-02	4	*Map3k1, Mbd4, Plrg1, Atf1*	Cervical ganglion neuron apoptosis
Cell-To-Cell Signaling and Interaction	2.94E-03 – 5.87E-03	2	*Map3k1, Ceacam1*	Intercellular junction restoration
Cellular Assembly and Organization	2.94E-03 – 8.80E-03	1	*Map3k1*	Permeability of mitochondria
Cellular Development	2.94E-03 – 4.04E-02	3	*Eomes*	Expansion of pre-B2 lymphocytes
Cellular Growth/Proliferation	2.94E-03 – 4.04E-02	2	*Eomes, Vpreb1*	Expansion of thymocytes
Physiological System Development and Function				
Name	***p*-value**	**# genes**	**Genes**[a]	**Function Annotation**
Connective Tissue Development/Function	6.49E-04 – 2.90E-02	4	*Mbd4, Ceacam1, Map3k1, Plrg1*	Cell viability of fibroblasts
Hematological System Development/Function	2.94E-03 – 4.32E-02	5	*Vpreb1, Ceacam1, Eomes, mir-451, H2-T23*	Function of memory T lymphocytes
Hematopoiesis	2.94E-03 – 4.04E-02	3	*Eomes, Vpreb1, mir-451*	Expansion of thymocytes
Humoral Immune Response	2.94E-03 – 1.46E-02	2	*Vpreb1, Map3k1*	Expansion of pre-B2 lymphocytes
Tissue Morphology	2.94E-03 – 4.60E-02	5	*Adamts9, Vpreb1, Eomes, Ceacam1, Map3k1*	Abnormal morphology of trophoectoderm

[a]Genes from Partek Genomics Suite, ± 1.2 fold change, $p < 0.05$; *Carcinoembryonic antigen-related cell adhesion molecule 1 (biliary glycoprotein)* (*Ceacam1*), *SET domain containing 2* (*Setd2*), *Triadin* (*Trdn*), *Mitogen-activated protein kinase kinase kinase 1, E3 ubiquitin protein ligase* (*Map3k1*), *Methyl-CpG binding domain protein 4* (*Mbd4*), *Pleiotropic regulator 1* (*Plrg1*), *Activating transcription factor 1* (*Atf1*), *Eomesodermin* (*Eomes*), *pre-B lymphocyte 1* (*Vpreb1*), *microRNA 451* (*mir-451*), *Major histocompatibility complex, class I, E* (*H2-T23*), and *ADAM metallopeptidase with thrombospondin type 1 motif, 9* (*Adamts9*).

b) First-trimester effects of ethanol on cellular pathways

As in T2-S analysis, the list of T1-L DEGs was subjected to pathway analysis using Pathway Express, PE and IPA's canonical pathway tool. The gene list was subjected to Pathway Express to observe which pathways were enriched. For T1-L, the only significant KEGG pathway was "base excision repair" (Impact factor = 5.92, p = 0.003), with 2 input genes: *Mbd4* and *Pcna*. *Mbd4* and *Pcna* were also identified in DAVID analysis under the GO BP "base excision repair". Given MBD4's role in DNA mismatch repair, and PCNA's role in increasing DNA polymerase processibility, it stands to reason that these two genes play an important role in regulating DNA repair. Of note, the nominally significant pathway "mismatch repair" (Impact factor = 2.99, p = 0.05) was listed as the second pathway altered in the adult brain as a result of trimester one ethanol exposure, with *Pcna* as the only gene implicated in this pathway.

Next, Partek's Pathway Enrichment tool was used to generate KEGG pathways that were significantly altered as a result of prenatal ethanol exposure. The enrichment results for T1-L are presented in **Table 14**, and include four significant pathways. The top pathway was "base excision repair", with *Mbd4* and *Pcna*. *Pcna* was also part of the second significant pathway, "HTLV-I infection", with *Major histocompatibility complex, class I, E* (*H2-T23*). Given its role in cell immunity, *H2-T23* was previously identified in IPA functional analysis as the driver behind, "function of memory T lymphocytes" (**Table 13**). Meanwhile, *3-hydroxy-3-methylglutaryl-CoA synthase 2 (mitochondrial)* (*Hmgcs2*) was implicated in the last pathway, "synthesis and degradation of ketone bodies". Hmgcs2's role in fatty acid synthesis complements results from DAVID that identified this gene in "coenzyme A" function (**Table 11**).

Lastly, using IPA, significant canonical pathways altered in T1-L were identified (**Table 15**). Four of the five pathways were involved in lipid synthesis and other fatty-acid-related processes. The second top pathway, IL-1 Signaling, included *Map3k1*, which has been implicated in PE analysis under "HTLV-I Infection" (**Table 14**). *Map3k1*'s prominence in these pathways signifies its role in immune system response.

Table 14. Significant pathways resulting from Pathway Enrichment (PE) analysis of trimester one long-term (T1-L) differentially-expressed genes (DEGs).

Pathway Name	**Enrichment Score**[a]	***p*-value**	**Genes**[b]
Base excision repair	5.11	0.006	*Mbd4, Pcna*
HTLV-I infection	4.48	0.011	*Atf1, H2-T23, Map3k1, Pcna*
Caffeine metabolism	3.54	0.029	*Nat1*
Synthesis and degradation of ketone bodies	3.44	0.032	*Hmgcs2*

[a]Enrichment score = Significant genes in a category/All significant genes vs All genes in the category/All genes on the chip.
[b]Genes included *Methyl-CpG binding domain protein 4* (*Mbd4*), *Proliferating cell nuclear antigen* (*Pcna*), *Activating transcription factor 1* (*Atf1*), *Major histocompatibility complex, class I, E* (*H2-T23*), *Mitogen-activated protein kinase kinase kinase 1, E3 ubiquitin protein ligase* (*Map3k1*), *N-acetyltransferase 1 (arylamine N-acetyltransferase)* (*Nat1*), and *3-hydroxy-3-methylglutaryl-CoA synthase 2 (mitochondrial)* (*Hmgcs2*).

Table 15. Top canonical pathways resulting from Ingenuity Pathway Analysis (IPA) of trimester one long-term (T1-L) differentially-expressed genes (DEGs).

Canonical Pathway Name[a]	***p*-value**	**Genes**[b]
Pentose Phosphate Pathway (Non-oxidative Branch)	1.75E-02	*Rpe*
IL-1 Signaling	2.81E-02	*Map3k1, Gng4*
Ketogenesis	2.9E-02	*Hmgcs2*
Pentose Phosphate Pathway	2.9E-02	*Rpe*
Mevalonate Pathway I	3.47E-02	*Hmgcs2*

[a]Canonical pathways were identified in Ingenuity Pathway Analysis using the Core Analysis feature. The list of DEGs was generated using Partek Genomics Suite, using a ± 1.2 fold change and $p < 0.05$.
[b]Genes included *Ribulose-5-phosphate-3-epimerase* (*Rpe*), *Mitogen-activated protein kinase kinase kinase 1*, *E3 ubiquitin protein ligase* (*Map3k1*), *Guanine nucleotide binding protein (G protein), gamma 4* (*Gng4*), and *3-hydroxy-3-methylglutaryl-CoA synthase 2 (mitochondrial)* (*Hmgcs2*).

c) First-trimester effects on ethanol on cellular networks

The T1-L gene list was subjected to analysis by the publically available tool, GeneMANIA, to identify disrupted networks. T1-L GeneMANIA analysis resulted in two significant network functions including, "olfactory bulb development" ($p = 0.012$) and "olfactory lobe development" ($p = 0.012$), both with *Eomes* as the only DEG. The nominally significant function, "forebrain development" ($p = 0.059$) included *Eomes* and *Setd2*.

Network analysis was also completed using IPA using the Core Analysis function to identify enriched networks of interest based on literature review. Only one network with a score > 3 was identified from T1-L analysis. This network was termed, Infectious Disease, Organismal Injury and Abnormalities, Cellular Development (score = 22), and was comprised of 11 focus molecules. Focus molecules included: *Hmgcs2, Pcna, Atf1, Ceacam1, Eomes, Map3k1, Hla-e, Tumor necrosis factor receptor superfamily, member 19* (*Tnfrsf19*), *RAS p21 protein activator 2* (*Rasa2*), *CDGSH iron sulfur domain 1* (*Cisd1*), and *Major urinary protein 5* (*Mup5*) (**Figure 19**). Because there were no other significant networks, a merged analysis could not be performed. Instead, this network was analyzed for the presence of any hub molecules that had > 10 interactions with other genes. Hub analysis resulted in three molecules with interactions. These included interferon-gamma (IFNG), peroxisome proliferator-activated receptor gamma (PPARG) and peroxisome proliferator-activated receptor alpha (PPARA). Involved in immunoregulation, IFNG has indirect relationships with HLA-E (H2-T23), MAP3K1 and CEACAM1, which are all downregulated (**Figure 19**).

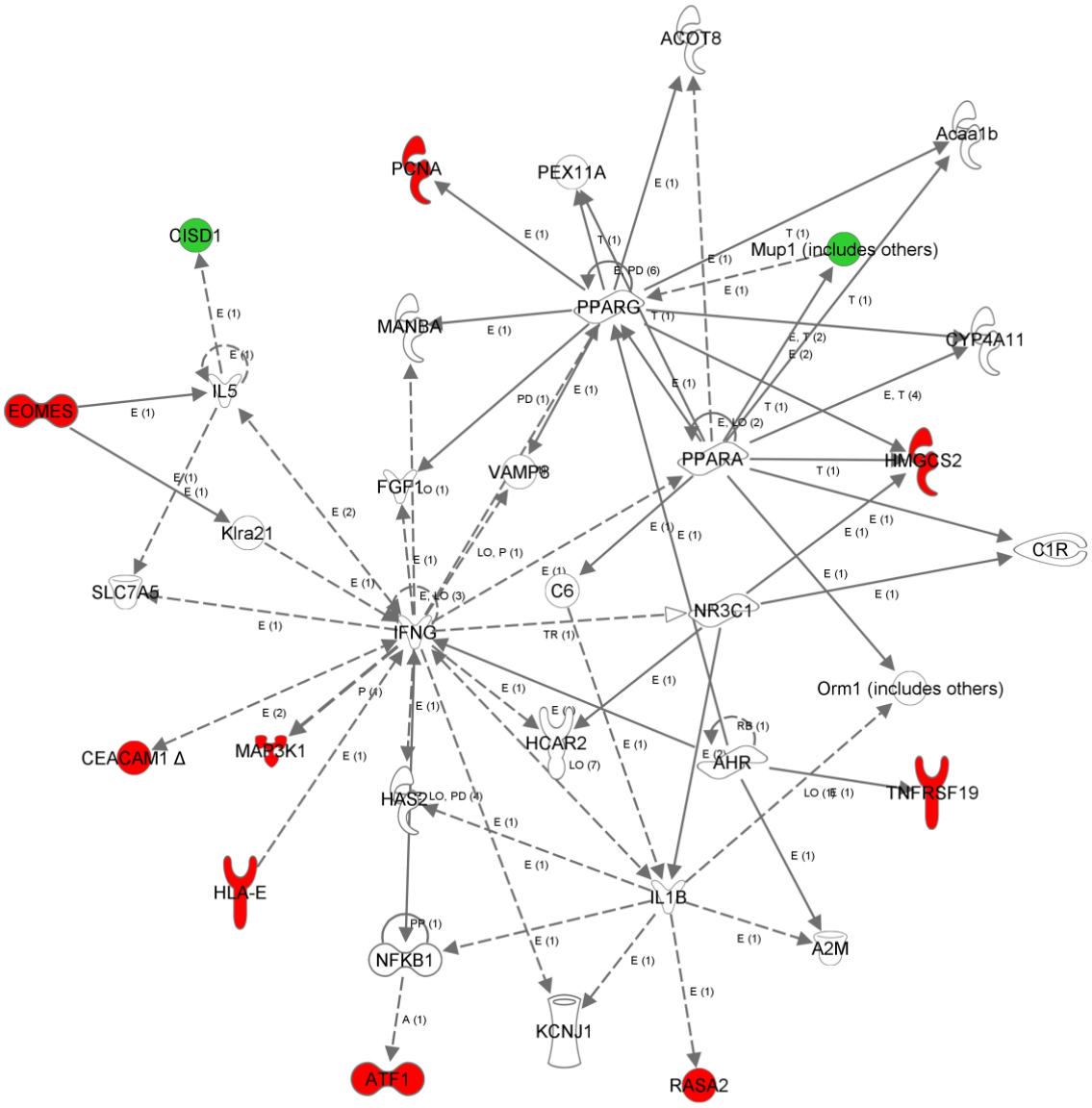

Figure 19. Network resulting from Ingenuity Pathway Analysis (IPA) of trimester one long-term (T1-L) differentially-expressed genes. Network name: Infectious Disease, Organismal Injury and Abnormalities, Cellular Development. Highlighting (red and green) represents input genes. Red indicates downregulation and green indicates upregulation in ethanol mice versus control mice. DEGs were identified using Partek Genomics Suite with a ± 1.2 fold change and $p < 0.05$. A single-headed arrow indicates the action of one gene on another. A double arrow-headed line indicates that the two genes act on each other. Dashed lines indicate an indirect interaction, and solid lines indicate direct interactions. E = expression, LO = localization, PD = protein-DNA binding, A = activation, P = phosphorylation/dephosphorylation, PP = protein-protein interaction, T = transcription, TR = translocation. Refer to Appendix F for a full IPA legend on relationship types, molecular shapes, and relationships.

d) Candidate gene selection and confirmation of specific genes disrupted following first-trimester ethanol exposure

Based on the criteria given in the Methods and Materials section (**Figure 1**), T1-L candidate genes were selected for confirmation by qRT-PCR. The functional (NCBI, DAVID, GE, GeneMANIA), pathway (IPA, PE, Pathway Express), and network (GeneMANIA and IPA) characterizations of DEGs are summarized in **Table 16**. For T1-L, the downregulation of *Tnfrsf19*, *Eomes*, *Map3k1*, and *Synaptoporin* (*Synpr*) was confirmed in six control and six ethanol samples. While the difference between ethanol and control subjects was significant for each of these genes, their degree of fold change was not identical between qRT-PCR are array results (**Table 17**). A series of box plots illustrating the variability across biological replicates in qRT-PCR demonstrates the similarity in ΔC_T values across replicates for *Atf1*, *Ceacam1*, *Htr5a*, and *Stxbp6* (**Figure 20**). Also, given the number of biological replicate outliers present in various samples (eg. *Htr5a*), this may add to properly confirm genes by qRT-PCR.

Table 16. Candidate gene selection criteria for confirmation of specific trimester one long-term (T1-L) differentially-expressed genes (DEGs).

Genes[a]	Neurodevelopment and/or behaviour	Tool[b]	Network (IPA)[c]
Atf1	TNF/Stress related signaling	DAVID	1
	miRNA:gene (miR-1192 and miR-532-5p)	IPA	
Ceacam1	regulation of MAP kinase activity	Partek GE	1
	inflammatory response	IPA	
Eomes	olfactory bulb development; forebrain development	GeneMANIA	1
	embryonic placenta morphogenesis and development	Partek GE	
Htr5a	serotonin signaling	Partek GE	None
	suicide attempts and mood disorders[227]	PubMed	
Map3k1	TNF/Stress related signaling	DAVID	1
	visual system development and function	IPA	
	loss enhances proliferation and apoptosis during retinal development[228]	PubMed	
Stxbp6	linked to ADHD[229]	PubMed	None
	implicated in bipolar disorder[230]	PubMed	
	miRNA:gene (miR-532-5p)	IPA	
Synpr	intrinsic to small synaptic vesicles	PubMed	None
	major depressive disorder link[231]	PubMed	
Tnfrsf19	Regulates differentiation of stromal stem cells[232]	PubMed	1

[a]Genes are listed alphabetically. Genes included *Activating transcription factor 1* (*Atf1*), *Carcinoembryonic antigen-related cell adhesion molecule 1 (biliary glycoprotein)* (*Ceacam1*), *Eomesodermin* (*Eomes*), *5-hydroxytryptamine (serotonin) receptor 5A, G protein-coupled* (*Htr5a*), *Mitogen-activated protein kinase kinase kinase 1, E3 ubiquitin protein ligase* (*Map3k1*), *Syntaxin binding protein 6 (amisyn)* (*Stxbp6*), *Synaptoporin* (*Synpr*), and *Tumor necrosis factor receptor superfamily, member 19* (*Tnfrsf19*).

[b]Tools used to analyse candidate genes (by neurodevelopment and behaviour) include PubMed, Ingenuity Pathway Analysis (IPA), Partek Gene Ontology Enrichment, GeneMANIA (www.genemania.org) and The Database for Annotation, Visualization and Integrated Discovery (DAVID).

[c]IPA network shown in Figure 19.

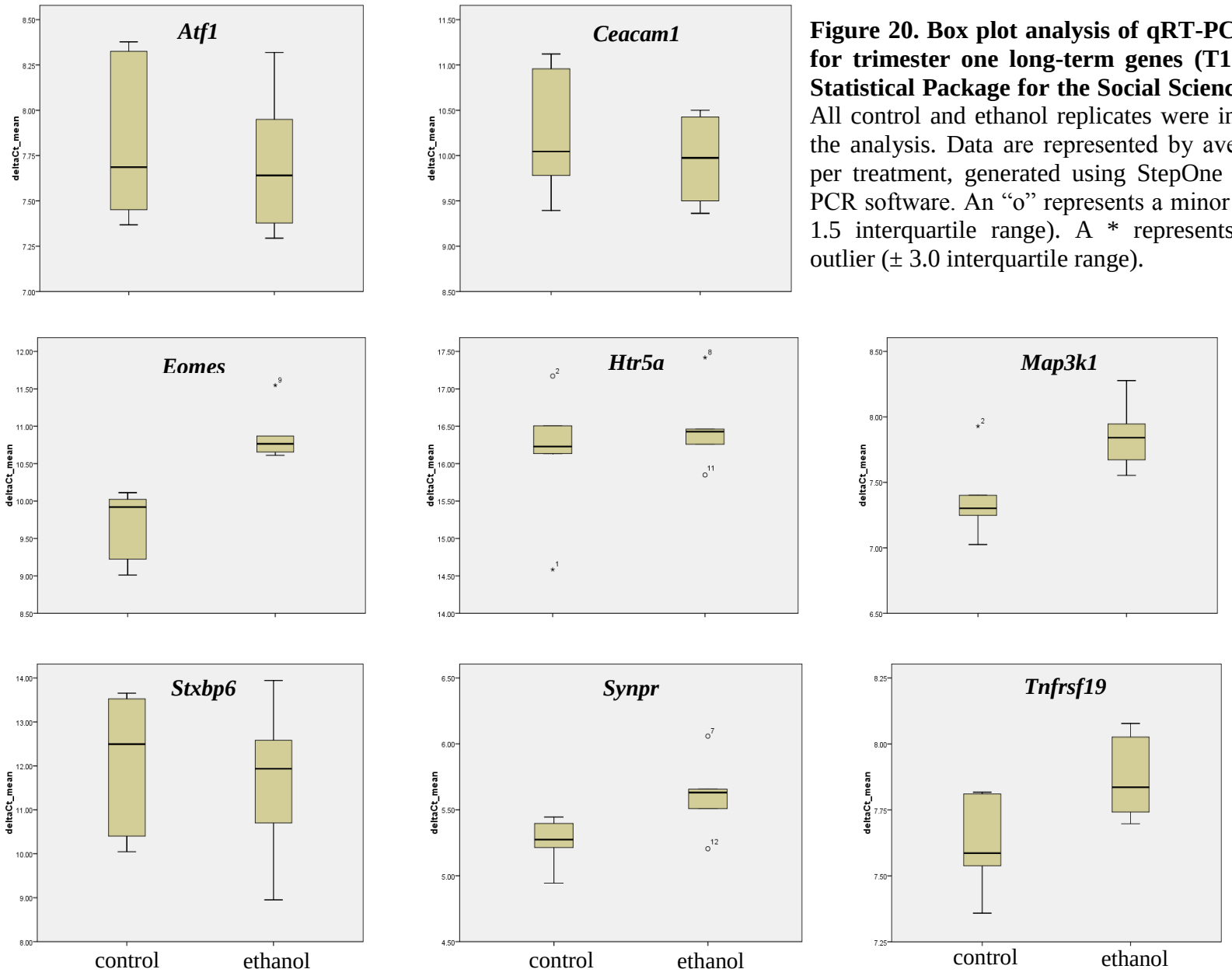

Figure 20. Box plot analysis of qRT-PCR results for trimester one long-term genes (T1-L) using Statistical Package for the Social Sciences v.16.6. All control and ethanol replicates were included in the analysis. Data are represented by average ΔC_T per treatment, generated using StepOne Real-time PCR software. An "o" represents a minor outlier (± 1.5 interquartile range). A * represents a major outlier (± 3.0 interquartile range).

Table 17. A comparison between trimester one long-term (T1-L) qRT-PCR and microarray results for candidate genes.

Genes[a]	Array Fold change	Array *p*-value	qRT-PCR Fold change	qRT-PCR *p*-value
Atf1	-1.32	0.012	-0.93	0.655
Ceacam1	-1.21	0.038	-0.80	0.481
Eomes	-1.20	0.039	-2.21	0.013
Htr5a	-1.24	0.022	-1.42	0.374
Map3k1	-1.25	0.043	-1.36	0.010
Stxbp6	-1.22	0.028	-0.67	0.592
Synpr	-1.25	0.038	-1.29	0.004
Tnfrsf19	-1.20	0.024	-1.19	0.024

[a]Genes are listed alphabetically. Genes in bold font are those that showed differential expression between ethanol and control samples on the array and by qRT-PCR. Genes included *Activating transcription factor 1* (*Atf1*), *Carcinoembryonic antigen-related cell adhesion molecule 1 (biliary glycoprotein)* (*Ceacam1*), *Eomesodermin* (*Eomes*), *5-hydroxytryptamine (serotonin) receptor 5A, G protein-coupled* (*Htr5a*), *Mitogen-activated protein kinase kinase kinase 1, E3 ubiquitin protein ligase* (*Map3k1*), *Syntaxin binding protein 6 (amisyn)* (*Stxbp6*), *Synaptoporin* (*Synpr*), and *Tumor necrosis factor receptor superfamily, member 19* (*Tnfrsf19*).

e) MiRNAs altered in the adult brain following first-trimester ethanol exposure

The results from the mouse miRNA arrays were assessed using Partek. In the global analysis of T1-L, fold change ranged from -12.07-fold (miR-429) to +2.51-fold (miR-21). Of the 1411 miRNAs that were specific to *Mus Musculus*, the ANOVA resulted in 671 miRNAs that were < 1 (47.6%), eight that were unchanged (0.6%) and 732 that were > 1 (51.9%). For consistency with gene expression data, miRNA arrays were assessed using a ± 1.2-fold change cut-off and $p < 0.05$. **Table 18** shows a list of differentially-expressed miRNAs at PD 70, as a result of prenatal ethanol exposure during the first trimester equivalent. Using the established criteria for significance, these results show a total of eight miRNAs that were differentially expressed between control and ethanol samples. These miRNAs include: miR-1192, miR-202, miR-339, miR-532, miR-680, miR-695, miR-743 and miR-764. Their fold changes ranged from -1.46-fold to +1.73-fold. Six of the eight miRNAs (75%) were upregulated in ethanol mice compared to control mice. Detecting upregulation of miRNAs is reasonable given that miRNAs are involved in degradation of messenger RNAs (mRNAs) and are likely to be disrupted in the opposite manner of mRNAs.

Table 18. A list of differentially-expressed microRNAs in trimester one long-term (T1-L) array analysis.

MicroRNA[a]	Fold change	*p*-value
miR-1192	1.43	0.028
miR-202	-1.46	0.033
miR-339	-1.30	0.019
miR-532	1.26	0.040
miR-680	1.38	0.049
miR-695	1.24	0.017
miR-743a	1.26	0.044
miR-764	1.73	0.016

[a]MicroRNAs are listed by numerical ordering. Data generated using a ± 1.2-fold change and $p < 0.05$ in Partek Genomics Suite.

f) Identification and confirmation of specific miRNAs in T1-L and their gene targets

The lists of DEGs from gene expression array analysis (n = 63) and differentially-expressed miRNAs (n = 8) from T1-L were subjected to IPA miRNA and gene interaction analysis using the Target Filter function. Results for T1-L analysis of gene and miRNA interactions are shown in **Table 19**. Genes and miRNA fold changes are shown with their respective expressions. The results demonstrated that only two microRNAs, miR-1191 and miR-532-5p, were implicated in inverse relationships with specific gene targets. Out of the 11 genes implicated in this analysis, *Atf1, Syntaxin binding protein 6 (amisyn)* (*Stxbp6*), and *Centrosome and spindle pole associated protein 1* (*Cspp1*) were inversely expressed with both miRNAs. The relationship between an upregulated miRNA and a downregulated target mRNA is of interest in this study (**Figure 1**). The microRNAs that were in opposing expression to their target genes were used for confirmation by qRT-PCR. This included miR-1192 and miR-532-5p (**Table 19**). The upregulation of miR-532-5p was confirmed using qRT-PCR (-0.45-fold change, p = 7.97e-5; **Figure 21**).

Table 19. Ingenuity Pathway Analysis (IPA) target filtering of differentially-expressed genes (DEGs) and microRNAs from the trimester one long-term (T1-L) group.

Genes[a]		MicroRNAs[b]			
Symbol	**Fold change**	**Symbol**	**Fold change**	**Expression[c] (gene:miRNA)**	**Confidence[d] (predicted)**
Atf1	-1.319	miR-1192	1.432	↓↑	High
Cspp1	1.217	miR-1192	1.432	↑↑	High
Gng4	-1.344	miR-1192	1.432	↓↑	Moderate
Map3k1	-1.247	miR-1192	1.432	↓↑	High
Rpe	-1.206	miR-1192	1.432	↓↑	High
Setd2	-1.202	miR-1192	1.432	↓↑	Moderate
Stxbp6	-1.225	miR-1192	1.432	↓↑	Moderate
Trdn	1.308	miR-1192	1.432	↑↑	High
Zc3h6	-1.232	miR-1192	1.432	↓↑	High
Atf1	-1.319	miR-532-5p	1.263	↓↑	Moderate
Cspp1	1.217	miR-532-5p	1.263	↑↑	Moderate
Itpripl2	-1.211	miR-532-5p	1.263	↓↑	Moderate
Nat2	1.307	miR-532-5p	1.263	↑↑	Moderate
Stxbp6	-1.225	miR-532-5p	1.263	↓↑	Moderate

[a]Genes included *Activating transcription factor 1* (*Atf1*), *Centrosome and spindle pole associated protein 1* (*Cspp1*), *Guanine nucleotide binding protein (G protein), gamma 4* (*Gng4*), *Mitogen-activated protein kinase kinase kinase 1, E3 ubiquitin protein ligase* (*Map3k1*), *Ribulose-5-phosphate-3-epimerase* (*Rpe*), *SET domain containing 2* (*Setd2*), *Syntaxin binding protein 6 (amisyn)* (*Stxbp6*), *Triadin* (*Trdn*), *Zinc finger CCCH-type containing 6* (*Zc3h6*), *Inositol 1,4,5-trisphosphate receptor interacting protein-like 2* (*Itpripl2*), and *N-acetyltransferase 2 (arylamine N-acetyltransferase)* (*Nat2*). DEGs are based on Partek Genomics Suite analysis with ± 1.2-fold change and $p < 0.05$

[b]MicroRNAs are listed by numerical order. MicroRNAs were differentially expressed based on Partek analysis with ± 1.2-fold change and $p < 0.05$.

[c]Expression (gene:miRNA) is highlighted in red if an inverse relationship between gene:miRNA was identified.

[d]Confidence is predicted based on IPA's Target Filter function.

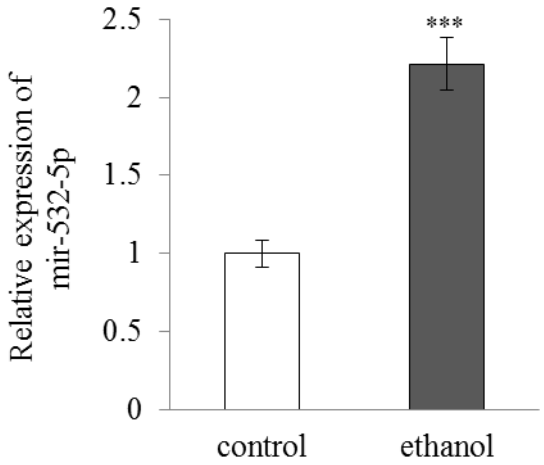

Figure 21. Bar graph of relative expression of microRNA 532-5p (miR-532-5p) between ethanol and control samples. Relative expression is shown. Error bars represent relative expression ± SEM. Statistical significance assessed using a two-tailed *t*-test with ***$p < 0.001$. Biological replicates n = 6 control, n = 6 ethanol. Technical replicates: n = 3.

3.3.4 Molecular analysis of second-trimester long-term (T2-L) DEGs

a) Second-trimester effects of ethanol on cellular functions

Functional analysis of T2-L DEGs was completed by inputting the gene list into three databases: DAVID, GE, and IPA. The top ten DAVID clusters from T2-L are shown in **Table 20**. Three of the top 10 annotations were involved in endoplasmic reticulum (ER)-related functions. Several genes were also implicated in two top functions: "melanosome" and "pigment granule". Two of the top 10 functions also included cellular reduction-oxidation (redox) reaction processes. Another two of the top 10 functions involved chromatin-related processes.

T2-L GE analysis returned a list of 132 significant functions, with the top 10 listed in **Table 21**. Notably, *Protein disulfide isomerase family A, member 4* (*Pdia4*) and *6* (*Pdia6*) were present in four of the top 10 pathways, which included ER-related isomerase activity. In fact, five of the ten categories were involved in ER-related activity, as identified in DAVID functional analysis (**Table 20**). Three of the 10 processes were involved in cellular redox reactions and metabolic processes, which were, again, consistent with DAVID analysis. Together, *Heat shock 70kDa protein 5 (glucose-regulated protein, 78kDa)* (*Hspa5*) and *Heat shock protein 90kDa alpha (cytosolic), class A member 1* (*Hsp90aa1*) were identified in six of the top 10 GE processes. Such processes were involved in ER-related functions including unfolded protein response (UPR), protein folding, and ion channel binding.

Lastly, in T2-L IPA functional analysis, the top affected process in Diseases and Disorders, Molecular and Cellular Functions, and Physiological System Development and Function are given in **Table 22**. "Systemic lupus erythematosus" (SLE) has been previously identified as a top function in DAVID annotation clustering (**Table 20**). In the top three

significant Diseases and Disorders, the genes, *Hspa5*, *X-box binding protein 1* (*Xbp1*), *Early growth response 3* (*Egr3*), *DnaJ (Hsp40) homolog, subfamily B, member 11* (*Dnajb11*), *Protein tyrosine phosphatase, non-receptor type 22 (lymphoid)* (*Ptpn22*), and *Integrin, alpha 4 (antigen CD49D, alpha 4 subunit of VLA-4 receptor)* (*Itga4*) appeared in each of these categories. *Egr3* seemed to be a key player in the Diseases and Disorders category, and along with its role in muscle spindle development, it serves as an important regulator of transcription. The term, SLE, included *Ptpn22*, which was also identified in a KEGG pathway in DAVID analysis (**Table 20**). Of all the implicated genes, *Hspa5* was the only gene appearing in all five significant Diseases and Disorders, which complemented the results of DAVID analysis that implicated *Hspa5* in the top five annotations (**Table 20**). Because *Hspa5* was identified using three different methods of analysis, this signifies the importance of *Hspa5* in ER-related processes including folding and assembly of proteins. The top T2-L process under Molecular and Cellular Functions included the genes: *Ptpn22*, *Xbp1*, and *Cyclin-dependent kinase inhibitor 1a* (*Cdkn1a*) (**Table 22**). Given their roles in cell cycle response, unfolded protein response, and T cell signaling, respectively, these genes are key factors responsible for the development and maintenance of critical cell processes. The top T2-L Physiological System Development and Functions implicated *Cdkn1a, Ptpn22, Xbp1*, *Thromboxane A2 receptor* (*Tbxa2r*), *Peroxiredoxin 1* (*Prdx1*), *Sprouty-related, EVH1 domain containing 2* (*Spred2*), and *Core-binding factor, runt domain, alpha subunit 2; translocated to, 3* (*Cbfa2t3*) in the top three functional categories (**Table 22**).

Table 20. Top ten significant annotation clusters resulting from the Database for Annotation, Visualization and Integrated Discovery (DAVID) functional analysis of trimester two long-term (T2-L) differentially-expressed genes (DEGs).

Category[a]	**Term**	***p*-value**	**Genes**[b]
GO CC	Endoplasmic reticulum lumen	1.3e-6	*Dnajb11, Hspa5, Pdia4, P4ha1, Pdia6, Sdf2l1*
GO CC	Melanosome	2.9e-5	*Hsp90aa1, Gchfr, Hspa5, Prdx1, Pdia4, Pdia6*
GO CC	Pigment granule	7.9e-5	*Hsp90aa1, Gchfr, Hspa5, Prdx1, Pdia4, Pdia6*
INTERPRO	Endoplasmic reticulum, targeting sequence	7.9e-5	*Sdf2l1, Hspa5, Pdia4, Pdia6*
GO CC	Endoplasmic reticulum part	1.9e-4	*Dnajb11, Hspa5, Pdia4, P4ha1, Pdia6, Serinc2, Sdf2l1*
KEGG PATHWAY	Systemic lupus erythematosus	3.7e-4	*Hist1h2bm, Hist1h3a, Hist1h3g, Hist1h3f, Hist1h3d, Hist2h3b, Ighg, Ptpn22*
INTERPRO	Thioredoxin-like	2.7e-3	*Pdia6, Prdx1, Pdia4*
GO BP	Chromatin assembly or disassembly	3.9e-3	*Hist1h3g, Hist1h3f, Hist1h2bm, Hist1h3a, Smarca5, Hist1h3d, Hist2h3b*
SP PIR keyword	Redox-active center	4.3e-3	*Pdia6, Prdx1, Pdia4*
INTERPRO	Histone core	5.1e-3	*Hist1h3a, Hist1h3g, Hist1h2bm, Hist1h3f, Hist1h3d, Hist2h3b*

[a]Category includes information from the Swiss-Prot and Protein Information Resource (SP PIR keyword), Gene Ontology's (GO) cellular component (CC) and biological process (BP), InterPro keywords (www.ebi.ac.uk/interpro/), and Kyoto Encyclopedia of Genes and Genomes (KEGG) database.

[b]Genes included *DnaJ (Hsp40) homolog, subfamily B, member 11* (*Dnajb11*), *Heat shock 90kDa protein 5 (glucose-regulated protein, 78kDa)* (*Hspa5*), *Protein disulfide isomerase family A, member 4* (*Pdia4*), *Prolyl 4-hydroxylase, alpha polypeptide I* (*P4ha1*), *Protein disulfide isomerase family A, member 6* (*Pdia6*), *Stromal cell-derived factor 2-like 1* (*Sdf2l1*), *Heat shock protein 90kDa (cytosolic), class A member 1* (*Hsp90aa1*), *GTP cyclohydrolase I feedback regulator* (*Gchfr*), *Peroxiredoxin 1* (*Prdx1*), *Serine incorporator 2* (*Serinc2*), *Histone cluster 1, H2bm* (*Hist1h2bm*), *Histone cluster 1, H3a* (*Hist1h3a*), *Histone cluster 1, H3g* (*Hist1h3g*), *Histone cluster 1, H3f* (*Hist1h3f*), *Histone cluster 1, H3d* (*Hist1h3d*), *Histone cluster 2, H3b* (*Hist2h3b*), *Immunoglobulin heavy chain (gamma polypeptide)* (*Ighg*), *Protein tyrosine phosphatase, non-receptor type 22 (lymphoid*) (*Ptpn22*), and *SWI/SNF related, matrix associated, actin dependent regulator of chromatin, subfamily a, member 5* (*Smarca5*).

Table 21. Top ten significant functions of trimester two long-term (T2-L) differentially-expressed genes (DEGs) from Gene Ontology Enrichment (GE).

Gene Ontology Function	Type[a]	Enrichment Score[b]	*p*-value	Genes[c]
Endoplasmic reticulum lumen	CC	8.49	0.0002	*Hspa5, Pdia4, Pdia6*
Protein disulfide isomerase activity	MF	8.05	0.0003	*Pdia4, Pdia6*
Glycerol ether metabolic process	BP	7.28	0.0007	*Pdia4, Pdia6*
Unfolded protein binding	MF	6.19	0.002	*Dnajb11, Hspa5, Hsp90aa1*
Protein disulfide oxidoreductase activity	MF	6.12	0.002	*Pdia4, Pdia6*
Isomerase activity	MF	5.37	0.005	*Dnajb11, Hsp90aa1, Fkbp2*
Endoplasmic reticulum-Golgi intermediate compartment	CC	5.35	0.005	*Hspa5, Pdia6*
Protein folding	BP	5.23	0.007	*Dnajb11, Hsp90aa1, Fkbp2*
Positive regulation of fibroblast proliferation	BP	4.94	0.009	*Cdkn1a, Fosl2*
Ion channel binding	MF	4.76	0.009	*Homer1, Hsp90aa1*

[a]Type indicates a biological process (BP), cellular component (CC), or molecular function (MF).
[b]Enrichment score = Significant genes in a category/All significant genes, vs All genes in the category/All genes on the chip.
[c]Genes included *Heat shock 90kDa protein 5 (glucose-regulated protein, 78kDa)* (*Hspa5*), *Protein disulfide isomerase family A, member 4* (*Pdia4*), *Protein disulfide isomerase family A, member 6* (*Pdia6*), *DnaJ (Hsp40) homolog, subfamily B, member 11* (*Dnajb11*), *Heat shock protein 90kDa (cytosolic), class A member 1* (*Hsp90aa1*), *FK506 binding protein 2, 13kDa* (*Fkbp2*), *Cyclin-dependent kinase inhibitor 1A (p21, Cip1)* (*Cdkn1a*), *FOS-like antigen 2* (*Fosl2*), and *Homer homolog 1 (Drosophila)* (*Homer1*).

Table 22. Functional characterization of trimester two long-term (T2-L) differentially-expressed genes (DEGs) using Ingenuity Pathway Analysis (IPA).

Diseases and Disorders				
Name	***p*-value**	**# genes**	**Genes**[a]	**Function Annotation**[b]
Inflammatory Disease	8.78E-05 – 3.11E-02	9	*Dnajb11, Hspa5, Itga4, Ptpn22, Xbp1, Prdx1, Fosl2, Egr3, mir-342*	SLE; Multiple sclerosis
Neurological Disease	8.78E-05 – 2.20E-02	13	*Egr3, Galnt7, Hist1h2bm, Homer1, Xbp1, Dnajb11, Hspa5, Itga4, Ptpn22, Dynlt1, Hsp90aa1, Tufm, P4ha1*	Neuromuscular disease; Schizophrenia
Skeletal and Muscular Disorders	8.78E-05 – 4.33E-02	14	*Egr3, mir-342, Ptpn22, Hsp90aa1, Prdx1, Cdkn1a, Fosl2, Tbxa2r, Dnajb11, Hspa5, Itga4, Xbp1, Dynlt1, Homer1, P4ha1*	SLE; osteosarcoma
Cancer	8.78E-05 – 4.93E-02	8	*Cdkn1a, Prdx1, Itga4, mir-342, Hsp90aa1, Hist1h3a, Hspa5, Ccdc6*	Incidence of lymphoma
Hematological Disease	2.78E-03 – 4.93E-02	6	*Cdkn1a, Itga4, Prdx1, Hspa5, Xbp1, Tbxa2r*	Chronic B-cell leukemia
Molecular and Cellular Functions				
Name	***p*-value**	**# genes**	**Genes**[a]	**Function Annotation**[b]
Cellular Development	5.24E-04 – 4.93E-02	12	*Cdkn1a, Ccdc6, Xbp1, Tbxa2r, Egr3, Smarca5, Klk1b11, Hsp90aa1, Itga4, Ptpn22, Fosl2, Cbfa2t3*	Plasmacytoid dendritic cell development
Cellular Function and Maintenance	5.24E-04 – 4.63E-02	10	*Egr3, Cdkn1a, Hsp90aa1, Itga4, Ptpn22, Hspa5, Tbxa2r, Slc9a3r2, Xbp1, Prdx1*	ER-stress response
Cell Cycle	6.28E-04 – 4.33E-02	3	*Cdkn1a, Ptpn22, Xbp1*	Polyploidization of hepatocytes
Cell Death	8.15E-04 – 4.93E-02	14	*Smarca5, Cdkn1a, Hspa5, Xbp1, Egr3, Tbxa2r, Ptpn22, Ccdc6, Itga4, Prdx1, Slc9a3r2, Camk1g, Manf, Hsp90aa1*	Cell death of immune cells
Cellular Compromise	1.44E-03 – 4.33E-02	5	*Hspa5, Cdkn1a, Prdx1, Hsp90aa1, Xbp1*	Stress response of cells

Physiological System Development and Function				
Name	***p*-value**	**# genes**	**Genes**[a]	**Function Annotation**
Lymphoid Tissue Structure/Development	4.30E-04 – 3.84E-02	10	*Egr3, Cdkn1a, Hsp90aa1, Itga4, Ptpn22, Xbp1, Tbxa2r, Spred2, Cbfa2t3, Prdx1*	Development of plasmacytoid dendritic cells
Organ Morphology	4.30E-04 – 4.93E-02	13	*Cbfa2t3, Cdkn1a, Prdx1, Ptpn22, Tbxa2r, Fosl2, Tnnc1, Hspa5, Spred2, Homer1, Xbp1, Klk1b11, Itga4*	Organization of cerebellum
Tissue Morphology	4.30E-04 – 4.93E-02	12	*Itga4, Xbp1, Tbxa2r, Smarca5, Cdkn1a, Fosl2, Klk1b11, Ptpn22, Spred2, Cbfa2t3, Prdx1, Egr3*	Abnormal morphology of cholinergic neurons
Cell-mediated Immune Response	5.24E-04 – 2.19E-02	5	*Cdkn1a, Egr3, Hsp90aa1, Itga4, Ptpn22*	Metabolism of thymocytes
Embryonic Development	5.24E-04 – 4.93E-02	10	*Cdkn1a, Spred2, Smarca5, Itga4, Egr3, Ptpn22, Fosl2, Xbp1, Hspa5, Otub2*	Cell death of embryonic tissue

[a]Genes from Partek Genomics Suite (± 1.2 fold change, $p < 0.05$). Genes included *DnaJ (Hsp40) homolog, subfamily B, member 11* (*Dnajb11*), *Heat shock 90kDa protein 5 (glucose-regulated protein, 78kDa)* (*Hspa5*), *Integrin, alpha 4 (antigen CD49D, alpha 4 subunit of VLA-4 receptor)* (*Itga4*), *Protein tyrosine phosphatase, non-receptor type 22 (lymphoid*) (*Ptpn22*), *X-box binding protein 1* (*Xbp1*), *Peroxiredoxin 1* (*Prdx1*), *FOS-like antigen 2* (*Fosl2*), *Early growth response 3* (*Egr3*), *microRNA 342* (*mir-342*), *UDP-N-acetyl-alpha-D-galactosamine:polypeptide N-acetylgalactosaminyltransferase 7 (GaINAc-T7)* (*Galnt7*), *Histone cluster 1, H2bm* (*Hist1h2bm*), *Homer homolog 1 (Drosophila)* (*Homer1*), *Dynein, light chain, Tctex-type 1* (*Dynlt1*), *Heat shock protein 90kDa (cytosolic), class A member 1* (*Hsp90aa1*), *Tu translation elongation factor, mitochondrial* (*Tufm*), *Prolyl 4-hydroxylase, alpha polypeptide I* (*P4ha1*), *Cyclin-dependent kinase inhibitor 1A (p21, Cip1)* (*Cdkn1a*), *Thromboxane A2 receptor* (*Tbxa2r*), *Histone cluster 1, H3a* (*Hist1h3a*), *Coiled-coil domain containing 6* (*Ccdc6*), *SWI/SNF related, matrix associated, actin dependent regulator of chromatin, subfamily a, member 5* (*Smarca5*), *Kallikrein 1-related peptidase b11* (*Klk1b11*), *Core-binding factor, runt domain, alpha subunit 2; translocated to, 3* (*Cbfa2t3*), *Solute carrier family 9, subfamily A (NHE3, cation proton antiporter 3), member 3 regulator 2* (*Slc9a3r2*), *Calcium/calmodulin-dependent protein kinase IG* (*Camk1g*), *Mesencephalic astrocyte-derived neurotrophic factor* (*Manf*), *Sprouty-related, EVH1 domain containing 2* (*Spred2*), *Troponin C type 1 (slow)* (*Tnnc1*), and *OTU domain, ubiquitin aldehyde binding 2* (*Otub2*).
[b]Functional annotation s: SLE = Systemic Lupus Erythematosus; ER = endoplasmic reticulum.

b) Second-trimester effects of ethanol on cellular pathways

As in the previous pathway analyses for T2-S and T1-l, Pathway Express, PE, and IPA's canonical pathway tool were used to identify T2-L pathways. T2-L DEGs were inputted into the freely available tool, Pathway Express. The top significant KEGG pathway was "systemic lupus erythematosus" (**Table 23**), which agreed with the T2-L functional analysis results. This pathway included six histone genes, along with *Immunoglobulin heavy chain (gamma polypeptide)* (*Ighg*). The other four disrupted processes were involved in cellular signaling and maintenance.

Partek was used to identify relevant pathways using Pathway Enrichment. PE data for T2-L analysis are shown in **Table 24**. This analysis resulted in six pathways, the top being "systemic lupus erythematosus", with nine histones. Finding SLE using PE complements the Pathway Express results (**Table 23**). The next two pathways also involved all histones (**Table 24**). "Transcriptional regulation of cancer" included the cell cycle regulator, *Cdkn1a*. As with functional analysis, two of the five significant pathways from PE implicated ER-related functions that were disrupted in the adult brain following prenatal ethanol exposure during the second trimester equivalent. *Hspa5* is present in three of the five top functions, which mostly include ER-related processes.

IPA using the canonical pathway tool was used to identify relevant pathways in T2-L (**Table 25**). Canoonical pathways are consistent with GE and PE results, and support the finding that second trimester ethanol exposure was most significantly associated with ER-related damage (**Tables 21, 24**). *Hspa5*, *Hsp90aa1*, and *Cdkn1a* each appeared in more than one of the five canonical pathways. *Xbp1* was present in the top disrupted pathway, Endoplasmic Reticulum

Stress Response. The previously unmentioned genes, *UDP-N-acetyl-alpha-D-galactosamine:polypeptide N-acetylgalactosaminyltransferase 7 (GaINAc-T7)* (*Galnt7*) and *9* (*Galnt9*) comprised the second significant pathway, O-glycan Biosynthesis. These results reveal the importance of altered ER-related stress response following trimester two long-term ethanol exposure. *Cdkn1a* was also an important factor, present in two of the five canonical pathways involved in cell signaling. Previously, *Cdkn1a* was identified in IPA functional analysis as one of the three genes that implicated "Cell Cycle" as a significant Molecular and Cellular Function upon trimester two long-term alcohol exposure (**Table 22**).

Table 23. Top five pathways resulting from Pathway Express analysis of trimester two long-term (T2-L) differentially-expressed genes (DEGs).

Pathway Name	Impact Factor[a]	Corrected *p*-value[b]	Genes[c]
Systemic lupus erythematosus	17.06	3.89e-8	*Hist2h3b, Hist1h2bm, Ighg, Hist1h3g, Hist1h3f, Hist1h2d, Hist1h3a*
Calcium signaling pathway	4.14	0.016	*Ighg, Tbxa2r, Tnnc1*
Hematopoietic cell lineage	3.71	0.025	*Itga4, Ighg*
Antigen processing and presentation	3.69	0.025	*Hsp90aa1, Hspa5*
Prostate cancer	3.58	0.028	*Hsp90aa1, Cdkn1a*

[a]Impact factor = a probabilistic term that takes into consideration the proportion of DEGs on the pathway and gene perturbation factors of all genes in the pathway.
[b]Corrected *p*-value is based on a False-Discover-Rate correction.
[c]Genes were differentially expressed based on Partek Genomics Suite (± 1.2-fold change, $p < 0.05$). Genes included *Histone cluster 2, H3b* (*Hist2h3b*), *Histone cluster 1, H2bm* (*Hist1h2bm*), *Immunoglobulin heavy chain (gamma polypeptide)* (*Ighg*), *Histone cluster 2, H3g* (*Hist1h3g*), *Histone cluster 2, H3f* (*Hist1h3f*), *Histone cluster 2, H3d* (*Hist1h3d*), *Histone cluster 2, H3a* (*Hist1h3a*), *Thromboxane A2 receptor* (*Tbxa2r*), *Troponin C type 1 (slow)* (*Tnnc1*), *Integrin, alpha 4 (antigen CD49D, alpha subunit of VLA-4 receptor)* (*Itga4*), *Heat shock protein 90kDa alpha (cytosolic), class A member 1* (*Hsp90aa1*), *Heat shock 70kDa protein 5 (glucose-regulated protein, 78kDa)* (*Hspa5*), and *Cyclin-dependent kinase inhibitor 1A (p21, Cip1)* (*Cdkn1a*).

Table 24. Significant pathways resulting from Pathway Enrichment (PE) analysis of trimester two long-term (T2-L) differentially-expressed genes (DEGs).

Pathway Name	**Enrichment Score**[a]	***p*-value**	**Genes**[b]
Systemic lupus erythematosus	18.63	8.08E-9	*Hist1h2bm, Hist1h3a, Hist1h3b, Hist1h3c, Hist1h3d, Hist1h3e, Hist1h3g, Hist1h3h, Hist1h3i*
Transcriptional misregulation in cancer	16.56	6.44E-8	*Cdkn1a, Hist1h3a, Hist1h3b, Hist1h3c, Hist1h3d, Hist1h3e, Hist1h3g, Hist1h3h, Hist1h3i*
Alcoholism	16.00	1.12E-7	*Hist1h2bm, Hist1h3a, Hist1h3b, Hist1h3c, Hist1h3d, Hist1h3e, Hist1h3g, Hist1h3h, Hist1h3i*
Protein processing in endoplasmic reticulum	9.24	9.74E-5	*Dnajb11, Hsp90aa1, Hspa5, Pdia4, Pdia6, Xbp1*
Protein export	4.89	0.008	*Hspa5, Immp1l*
Antigen processing and presentation	3.15	0.043	*Hsp90aa1, Hspa5*

[a]Enrichment score = Significant genes in a category/All significant genes vs All genes in the category/All genes on the chip.

[b]Genes included *Histone cluster 1, H2bm* (*Hist1h2bm*), *Histone cluster 2, H3a* (*Hist1h3a*), *Histone cluster 2, H3b* (*Hist1h3b*), *Histone cluster 2, H3c* (*Hist1h3c*), *Histone cluster 2, H3d* (*Hist1h3d*), *Histone cluster 2, H3e* (*Hist1h3e*), *Histone cluster 2, H3g* (*Hist1h3g*), *Histone cluster 2, H3h* (*Hist1h3h*), *Histone cluster 2, H3i* (*Hist1h3i*), *Cyclin-dependent kinase inhibitor 1A (p21, Cip1)* (*Cdkn1a*), *DnaJ (Hsp40) homolog, subfamily B, member 11* (*Dnajb11*), *Heat shock protein 90kDa alpha (cytosolic), class A member 1* (*Hsp90aa1*), *Heat shock 70kDa protein 5 (glucose-regulated protein, 78kDa)* (*Hspa5*), *Protein disulfide isomerase family A, member 4* (*Pdia4*), *Protein disulfide isomerase family A, member 6* (*Pdia6*), *X-box binding protein 1* (*Xbp1*), and *IMP1 inner membrane peptidase-like (S. cerevisiae)* (*Immp1l*).

Table 25. Top canonical pathways resulting from Ingenuity Pathway Analysis (IPA) of trimester two long-term (T2-L) differentially-expressed genes (DEGs).

Canonical Pathway Name[a]	***p*-value**	**Genes**[b]
Endoplasmic reticulum stress pathway	1.44E-03	*Xbp1, Hspa5*
O-glycan biosynthesis	4.26E-03	*Galnt7, Galnt9*
PI3K/AKT Signaling	4.98E-03	*Cdkn1a, Hsp90aa1, Itga4*
Aldosterone Signaling in Epithelial Cells	0.0115	*Dnajb11, Hspa90aa1, Hspa5*
Prostate Cancer Signaling	0.0245	*Cdkn1a, Hsp90aa1*

[a]Canonical pathways were identified in Ingenuity Pathway Analysis® using the Core Analysis feature. The list of DEGs was generated using Partek Genomics Suite using a ± 1.2 fold change and $p < 0.05$.
[b]Genes included *X-box binding protein 1* (*Xbp1*), *Heat shock 70kDa protein 5 (glucose-regulated protein, 78kDa)* (*Hspa5*), *UDP-N-acetyl-alpha-D-galactosamine:polypeptide N-acetylgalactosaminyltransferase 7 (GaINAc-T7)* (*Galnt7*), *UDP-N-acetyl-alpha-D-galactosamine:polypeptide N-acetylgalactosaminyltransferase 9 (GaINAc-T9)* (*Galnt9*), *Cyclin-dependent kinase inhibitor 1A (p21, Cip1)* (*Cdkn1a*), *Heat shock protein 90kDa alpha (cytosolic), class A member 1* (*Hsp90aa1*), *Integrin, alpha 4 (antigen CD49D, alpha subunit of VLA-4 receptor)* (*Itga4*), and *DnaJ (Hsp40) homolog, subfamily B, member 11* (*Dnajb11*).

c) Second-trimester effects of ethanol on cellular networks

The DEG list from T2-L was subjected to network analysis using GeneMANIA and IPA. The results from GeneMANIA are shown in **Table 26**. All six significant functions were involved in ER-related processes, which further indicate the importance of ER-related cellular responses that are altered following second trimester ethanol exposure. The results of GeneMANIA are comparable to DAVID analysis that identified the GO CCs "endoplasmic reticulum lumen" and "endoplasmic reticulum part" (**Table 20**). *Hspa5*, *Hsp90aa1*, and *Dynein, axonemal, heavy chain 3* (*Dnahc3*) are present in all five GeneMANIA functions. Additionally, *Pdia6* and *Xbp1* are each present in two of the five functions.

Network analysis of DEGs in T2-L was performed using the Core Analysis function in IPA. Only those networks with score > 3 are presented (**Table 27**). The T2-L top network was termed: Inflammatory Disease, Neurological Disease, Skeletal and Muscular Disorders. This network included 11 downreguated genes and two upregulated genes out of a total of 35 network genes (**Figure 22**). The second network was termed, Cardiovascular System Development and Function, Cellular Movement, Cell-To-Cell Signaling Interaction. This network included 11 differentially-expressed genes out of 36 network genes, nine of which were downregulated and two of which were upregulated (**Figure 23**). The third network was termed, Amino Acid Metabolism, Lipid Metabolism, Molecular Transport. This network included nine DEGs out of 35 network genes, seven of which were downregulated and two of which were upregulated (**Figure 24**). Similar to their implication in two of the six ER-related GeneMANIA functions, *Hspa5* and *Pdia6* were implicated in the first IPA network. As part of the first IPA network, *Xbp1* was also identified in two of the six GeneMANIA functions that involved "response to unfolded protein" and "response to topologically incorrect protein" (**Table 27**). As part of the

second IPA network, *Hsp90aa1* and *Dnahc3* were also implicated in all six GeneMANIA functions involved in UPR and other ER functions (**Table 27**). The three significant T2-L networks were merged in order to identify relevant hub molecules associated with T2-L ethanol exposure. The merged analysis resulted in one hub molecule in common with trimester one: IFNG. In total, there were 17 hubs with > 10 gene interactions (**Figure 25**). Of the differentially-expressed gene list, XBP1 and CDKN1A were hubs in the merged T2-L network. Hubs common to trimester two ethanol exposure (T2-S and T2-L) included: huntingtin (HTT), FBJ murine osteosarcoma viral oncogene homolog (FOS), and nuclear factor-kappaB (NFkB).

Table 26. Significant network functions resulting from GeneMANIA analysis of trimester two long-term (T2-L) differentially-expressed genes (DEGs).

Network Functions[a]	***p*-value (FDR-corrected)**	**Genes**[a]
Endoplasmic reticulum lumen	1.12e-5	*Erp44*, ***Dnahc3***, ***Hspa5***, ***Hsp90aa1***, ***Pdia6***, *Calr*
Response to unfolded protein	1.36e-3	*Erp44*, ***Dnahc3***, ***Hspa5***, ***Hsp90aa1***, ***Xbp1***
Response to topologically incorrect protein	1.75e-3	*Erp44*, ***Dnahc3***, ***Hspa5***, ***Hsp90aa1***, ***Xbp1***
Endoplasmic reticulum part	2.67e-3	*Erp44*, ***Dnahc3***, ***Hspa5***, ***Hsp90aa1***, *Ostc*, *Magt1*, *Calr*, ***Pdia6***
Endoplasmic reticulum membrane	8.51e-3	*Erp44*, ***Dnahc3***, ***Hspa5***, ***Hsp90aa1***, *Ostc*, *Magt1*, *Calr*
Nuclear outer membrane-endoplasmic reticulum membrane network	0.012	*Erp44*, ***Dnahc3***, ***Hspa5***, ***Hsp90aa1***, *Ostc*, *Magt1*, *Calr*

[a]Network functions were identified by inputting the T2-L DEG list generated from Partek Genomics Suite (± 1.2-fold change and $p < 0.05$).
[b]Genes in bold font indicate those present in the inputted gene list (DEGs). DEGs included *Dynein, axonemal, heavy chain 3* (*Dnahc3*), *Heat shock 70kDa protein 5 (glucose-regulated protein, 78kDa)* (*Hspa5*), *Heat shock protein 90kDa alpha (cytosolic), class A member 1* (*Hsp90aa1*), *Protein disulfide isomerase family A, member 6* (*Pdia6*), and *X-box binding protein 1* (*Xbp1*).

Table 27. Top Ingenuity Pathway Analysis (IPA) networks identified in trimester two long-term (T2-L) analysis of differentially-expressed genes (DEGs).

Network	No. Focus Molecules[a]	Top Network Function[b]	Input Genes[c]	Score[d]
1	13	Inflammatory Disease, Neurological Disease, Skeletal and Muscular Disorders	*Cdkn1a, Dnajb11, Hist1h3a, Hspa5, Itga4, Pdia4, Pdia6, Ptpn22, Sdf2l1, Smarca5, Spred2, Xbp1, Fkbp2*	24
2	11	Cardiovascular System Development and Function, Cellular Movement, Cell-To-Cell Signaling and Interaction	*Hsp90aa1, Dynlt1, Cbfa2t3, Prdx1, Dnahc3, P4ha1, Manf, Tbxa2r, Gchfr, Hist3h3, Slc9a3r2*	20
3	9	Amino Acid Metabolism, Lipid Metabolism, Molecular Transport	*Zhx2, Fosl2, Tufm, Homer1, Klk1b11, Vps13b, Camk1g, Egr3, Tnnc1*	15

[a]Number (No.) Focus Molecules indicates the number of genes that were differentially expressed (Partek Genomics Suite: ± 1.2 fold change, $p < 0.05$) in adult brain (GD 14 and 16) as a result of ethanol exposure in the second trimester equivalent.

[b]Top Function represent the name of the network in IPA.

[c]Input genes included *Cyclin-dependent kinase inhibitor 1A (p21, Cip1)* (*Cdkn1a*), *DnaJ (Hsp40) homolog, subfamily B, member 11* (*Dnajb11*), *Histone cluster 1, H3a* (*Hist1h3a*), *Heat shock 90kDa protein 5 (glucose-regulated protein, 78kDa)* (*Hspa5*), *Integrin, alpha 4 (antigen CD49D, alpha 4 subunit of VLA-4 receptor)* (*Itga4*), *Protein disulfide isomerase family A, member 4* (*Pdia4*), *Protein disulfide isomerase family A, member 6* (*Pdia6*), *Protein tyrosine phosphatase, non-receptor type 22 (lymphoid*) (*Ptpn22*), *Stromal cell-derived factor 2-like 1* (*Sdf2l1*), *SWI/SNF related, matrix associated, actin dependent regulator of chromatin, subfamily a, member 5* (*Smarca5*), *Sprouty-related, EVH1 domain containing 2* (*Spred2*), *X-box binding protein 1* (*Xbp1*), *FK506 binding protein 2, 13kDa* (*Fkbp2*), *Heat shock protein 90kDa (cytosolic), class A member 1* (*Hsp90aa1*), *Dynein, light chain, Tctex-type 1* (*Dynlt1*), *Core-binding factor, runt domain, alpha subunit 2; translocated to, 3* (*Cbfa2t3*), *Peroxiredoxin 1* (*Prdx1*), *Dynein, axonemal, heavy chain 3* (*Dnahc3*), *Prolyl 4-hydroxylase, alpha polypeptide I* (*P4ha1*), *Mesencephalic astrocyte-derived neurotrophic factor* (*Manf*), *Thromboxane A2 receptor* (*Tbxa2r*), *GTP cyclohydrolase I feedback regulator* (*Gchfr*), *Histone cluster 3, H3* (*Hist3h3*), *Solute carrier family 9, subfamily A (NHE3, cation proton antiporter 3), member 3 regulator 2* (*Slc9a3r2*), *Zinc fingers and homeboxes 2* (*Zhx2*), *FOS-like antigen 2* (*Fosl2*), *Tu translation elongation factor, mitochondrial* (*Tufm*), *Homer homolog 1 (Drosophila)* (*Homer1*), *Kallikrein 1-related peptidase b11* (*Klk1b11*), *Vacuolar protein sorting 13 homolog B (yeast)* (*Vps13b*), *Calcium/calmodulin-dependent protein kinase IG* (*Camk1g*), *Early growth response 3* (*Egr3*), and *Troponin C type 1 (slow)* (*Tnnc1*).

[d]Score is equal to the negative exponent of the respective *p*-value such that a score of 3 corresponds to a *p*-value of 10E-3. Network 1 score of 24 is equivalent to $p = 10E\text{-}24$. Network 2 score of 20 is equivalent to $p = 10E\text{-}20$. Network 3 score of 15 is equivalent to $p = 10E\text{-}15$.

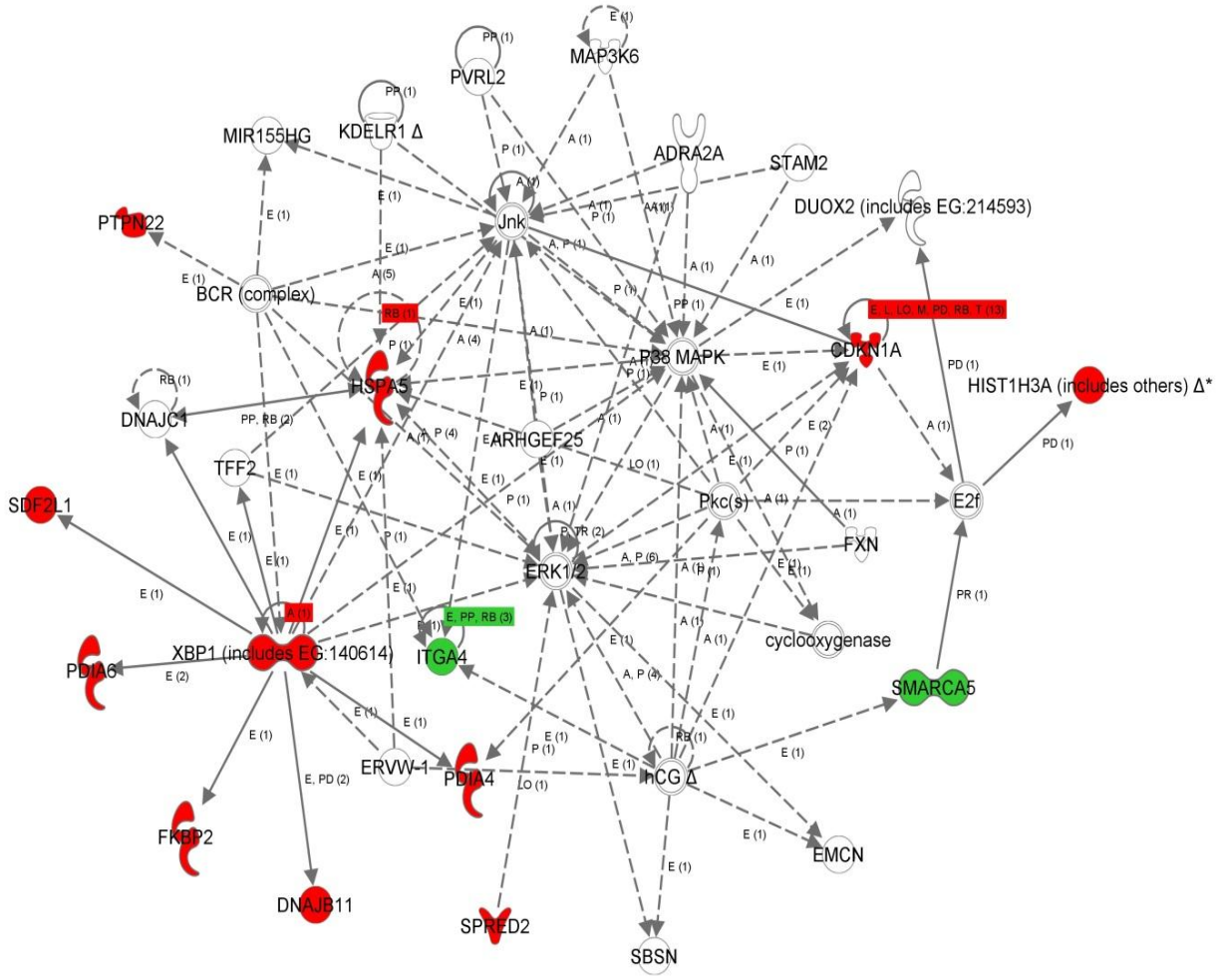

Figure 22. First network resulting from Ingenuity Pathway Analysis of trimester two long-term (T2-L) differentially-expressed genes (DEGs). Network name: Inflammatory Disease, Neurological Disease, Skeletal and Muscular Disorders. Highlighting (red and green) represents input genes. Red indicates downregulation and green indicates upregulation in ethanol mice versus control mice. DEGs were identified using Partek Genomics Suite with a ± 1.2 fold change and $p < 0.05$. A single-headed arrow indicates the action of one gene on another. A double arrow-headed line indicates that the two genes act on each other. Dashed lines indicate an indirect interaction, and solid lines indicate direct interactions. E = expression, L = proteolysis, LO = localization, PD = protein-DNA binding, A = activation, P = phosphorylation/dephosphorylation, PR = protein-RNA binding, PP = protein-protein interaction, I = inhibition, M = biochemical modification, RB = regulation of binding, T = transcription, TR = translocation. Refer to Appendix F for a full IPA legend on relationship types, molecular shapes, and relationships.

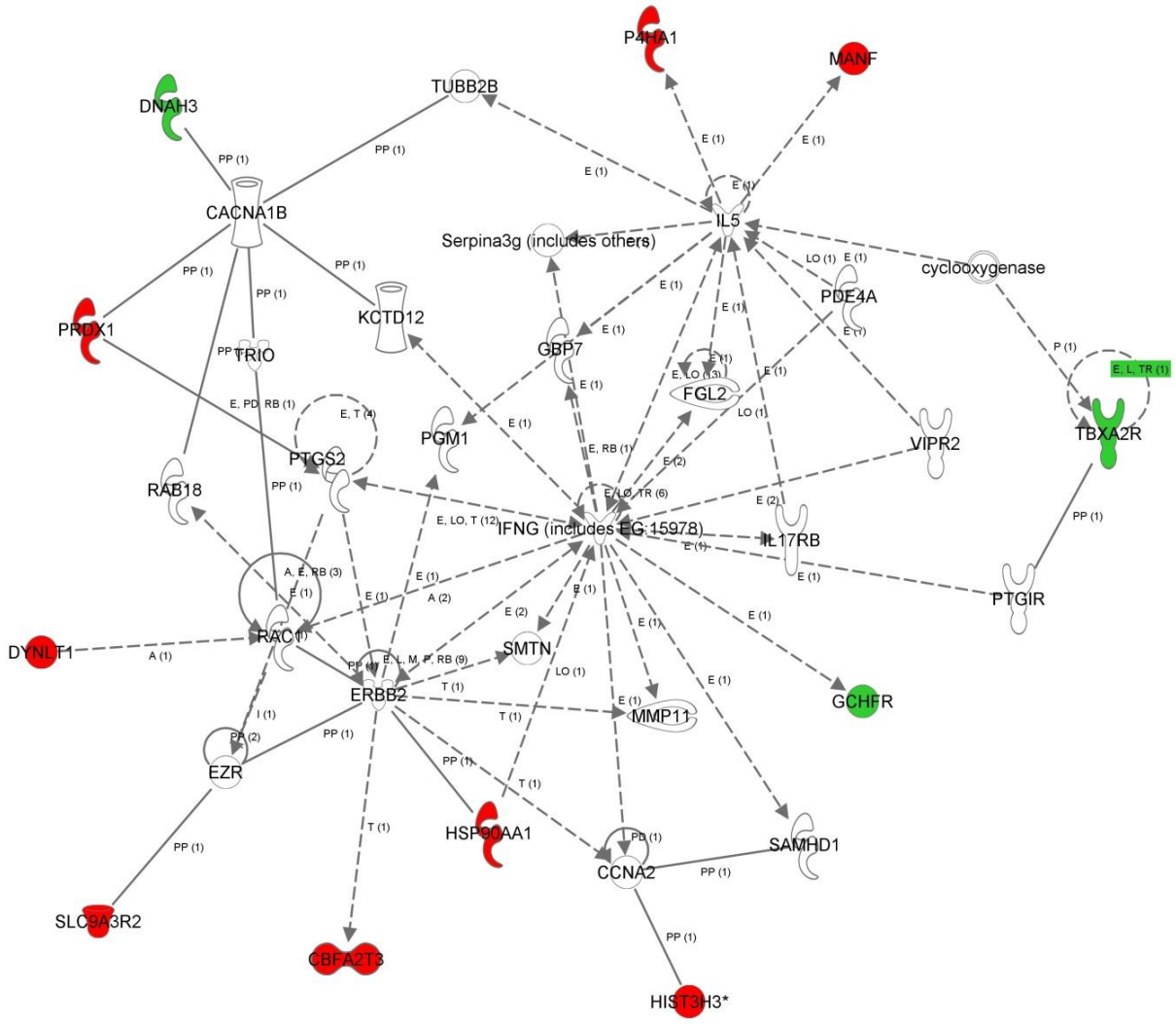

Figure 23. Second network resulting from Ingenuity Pathway Analysis of trimester two long-term (T2-L) differentially-expressed genes (DEGs). Network name: Cardiovascular System Development and Function, Cellular Movement, Cell-To-Cell Signaling and Interaction. Highlighting (red and green) represents input genes. Red indicates downregulation and green indicates upregulation in ethanol mice versus control mice. DEGs were identified using Partek Genomics Suite with a ± 1.2 fold change and $p < 0.05$. A single-headed arrow indicates the action of one gene on another. A double arrow-headed line indicates that the two genes act on each other. Dashed lines indicate an indirect interaction, and solid lines indicate direct interactions. E = expression, L = proteolysis, LO = localization, PD = protein-DNA binding, A = activation, P = phosphorylation/dephosphorylation, PR = protein-RNA binding, PP = protein-protein interaction, I = inhibition, M = biochemical modification, RB = regulation of binding, T = transcription, TR = translocation. Refer to Appendix F for a full IPA legend on relationship types, molecular shapes, and relationships.

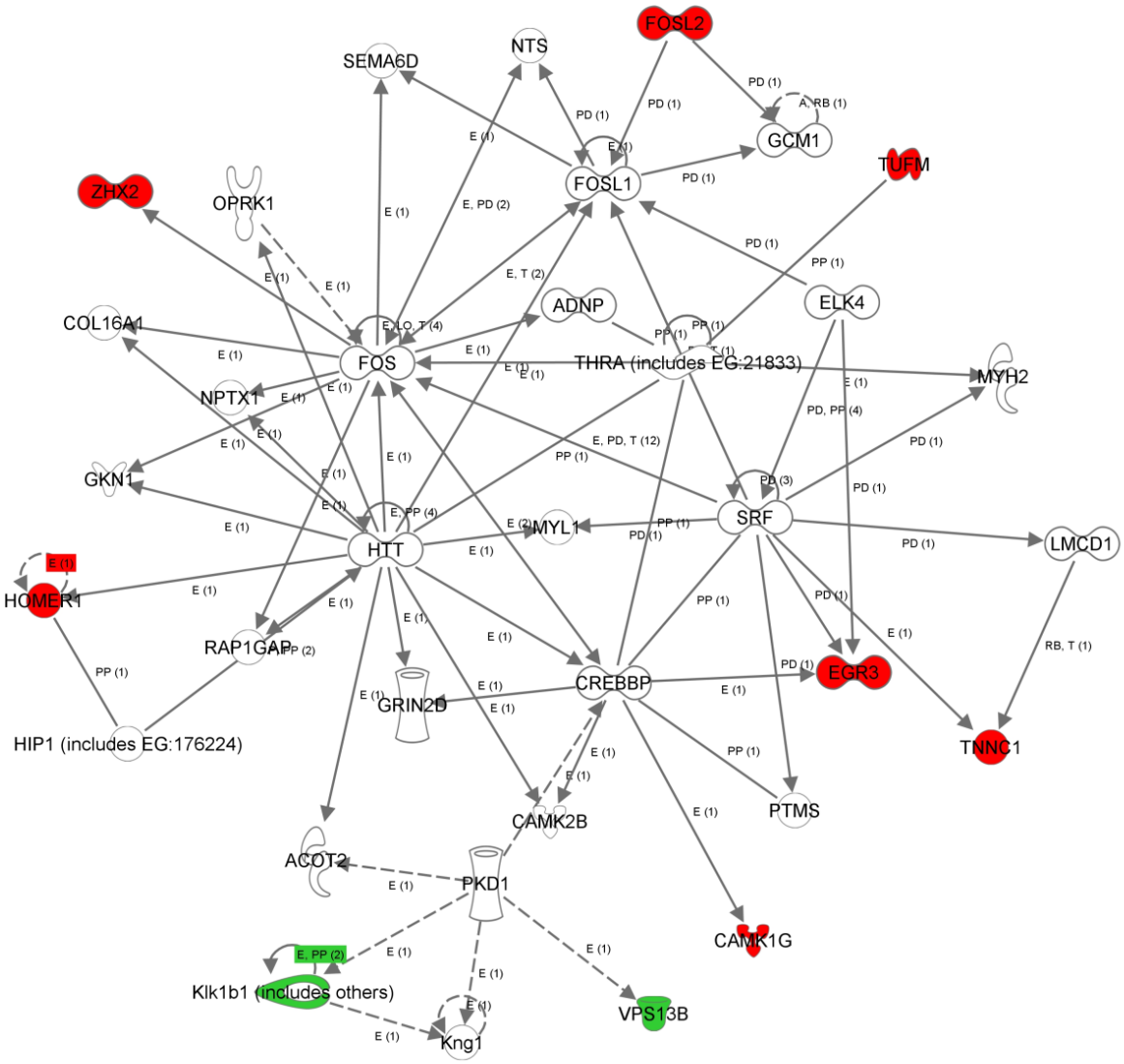

Figure 24. Third network resulting from Ingenuity Pathway Analysis of trimester two long-term (T2-L) differentially-expressed genes (DEGs). Network name: Amino Acid Metabolism, Lipid Metabolism, Molecular Transport. Highlighting (red and green) represents input genes. Red indicates downregulation and green indicates upregulation in ethanol mice versus control mice. DEGs were identified using Partek Genomics Suite with a ± 1.2 fold change and $p < 0.05$. A single-headed arrow indicates the action of one gene on another. A double arrow-headed line indicates that the two genes act on each other. Dashed lines indicate an indirect interaction, and solid lines indicate direct interactions. E = expression, L = proteolysis, LO = localization, PD = protein-DNA binding, A = activation, P = phosphorylation/dephosphorylation, PR = protein-RNA binding, PP = protein-protein interaction, I = inhibition, M = biochemical modification, RB = regulation of binding, T = transcription, TR = translocation. Refer to Appendix F for a full IPA legend on relationship types, molecular shapes, and relationships.

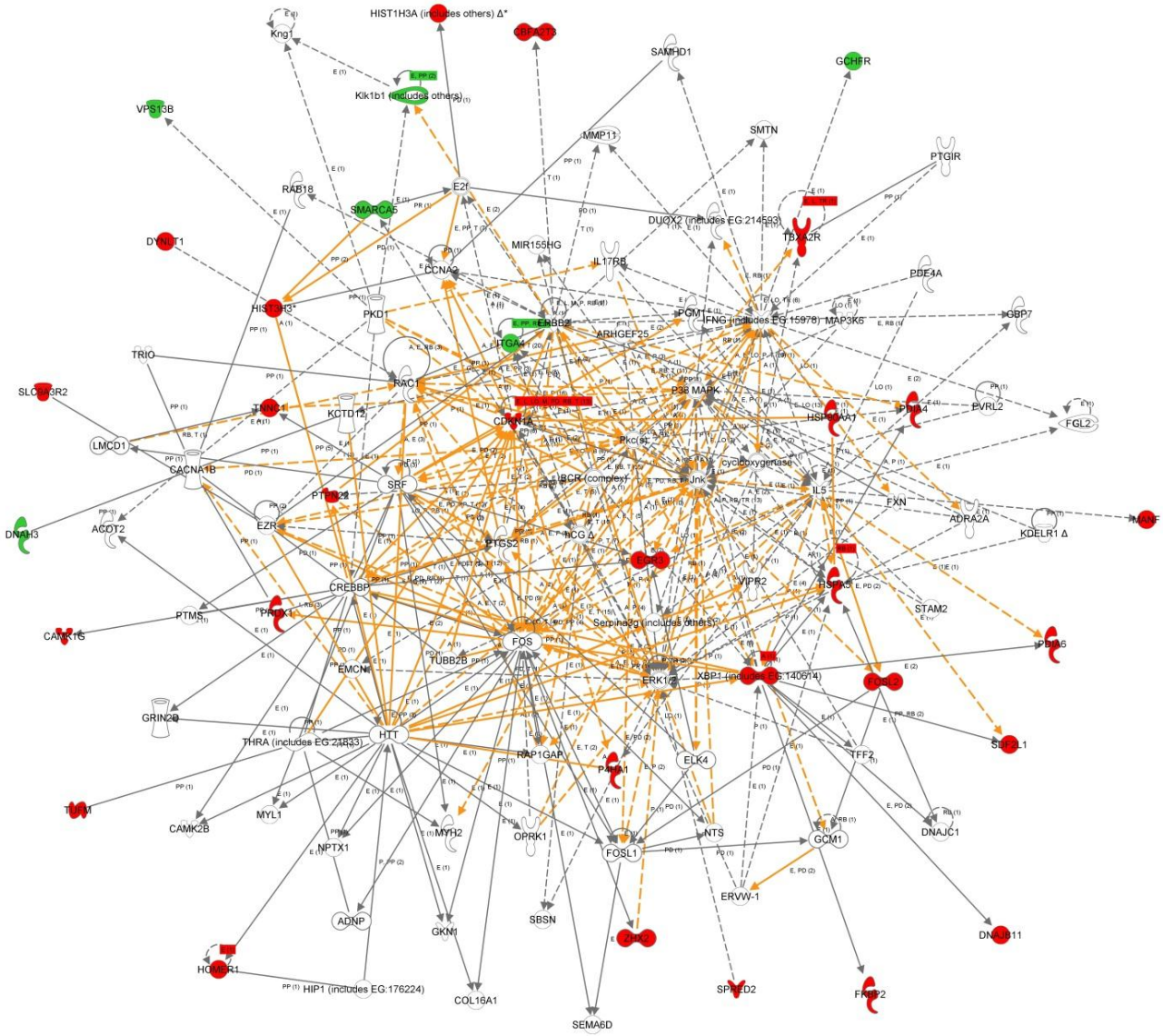

Figure 25. A merged network from Ingenuity Pathway Analysis (IPA) of trimester two long-term (T2-L) differentially-expressed genes (DEGs). Highlighting (red and green) represents input genes. Red indicates downregulation and green indicates upregulation in ethanol mice versus control mice. DEGs were identified using Partek Genomics Suite with a ± 1.2 fold change and $p < 0.05$. A single-headed arrow indicates the action of one gene on another. A double arrow-headed line indicates that the two genes act on each other. Dashed lines indicate an indirect interaction, and solid lines indicate direct interactions. E = expression, L = proteolysis, LO = localization, PD = protein-DNA binding, A = activation, P = phosphorylation/dephosphorylation, PR = protein-RNA binding, PP = protein-protein interaction, I = inhibition, M = biochemical modification, RB = regulation of binding, T = transcription, TR = translocation. Refer to Appendix F for a full IPA legend on relationship types, molecular shapes, and relationships.

d) Candidate gene selection and confirmation of specific genes disrupted following second-trimester ethanol exposure

The selected T2-L gene candidates are shown in **Table 28**, which specifies the criteria used for qRT-PCR confirmation experiments. The criteria were based on functional analysis (DAVID, GE, IPA), pathway analysis (Pathway Express, PE, canonical pathways), and network analysis (GeneMANIA, IPA). Selected genes were subjected to qRT-PCR for confirmation, and the results are shown in **Table 29**. The downregulation of T2-L genes including, *Calcium/calmodulin-dependent protein kinase IG* (*Camk1g*), *Coiled-coil domain containing 6* (*Ccdc6*), *Mesencephalic astrocyte-derived neurotrophic factor* (*Manf*), *Cdkn1a*, *Egr3*, *Hspa5*, and *Xbp1* was confirmed. *Homer homolog 1 (Drosophila)* (*Homer1*) and *Hspa90aa1* qRT-PCR fold-changes, albeit statistically significant, were opposite to the array fold-changes. A series of box plots illustrating the variability across biological replicates in qRT-PCR demonstrates the similarity in ΔC_T values across replicates, and the presence of major and minor outliers, for *Tbxa2r* samples (**Figure 26**). Comparing the *Tbxa2r* box plot to those of other genes, the data suggest that all other genes from this group show between-group variability in order to reach statistical significance.

Table 28. Candidate gene selection criteria for confirmation of specific trimester two long-term (T2-L) differentially-expressed genes (DEGs).

Genes[a]	Neurodevelopment and/or behaviour	Tool[b]	Network (IPA)[c]
Camk1g	pathophysiology of sleep disorders[233]	PubMed	3
Ccdc6	responsive to genotoxic stress (DNA damage)[234] miRNA:gene (miR-302c)	PubMed IPA	None
Cdkn1a	PI3K/AKT signaling; prostate cancer signaling misregulation in cancer	IPA GE	1 (hub)
Egr3	attack behaviour[235] neuromuscular synaptic transmission association with schizophrenia[236]	IPA, PubMed GE PubMed	3
Homer1	working memory; navigation skeletal muscle contraction enhanced behavioural despair and anxiety[237]	IPA GE NCBI	3
Hsp90aa1	protein refolding; nitric-oxide synthase regulator altered expression in autism post-mortem brains[238]	P.Express PubMed	2
Hspa5	ER response (to unfolded proteins) pathogenesis of spinocerebellar ataxis[239]	DAVID PubMed	1
Manf	reduces ER stress (neuroprotective); recovery of motor functions[240]	PubMed	2
Tbxa2r	contraction of skeletal muscle asthma-related symptoms[241]	IPA PubMed	2
Xbp1	ER stress response UPR in neurites[242] association with schizophrenia[243]	IPA, GeneMANIA PubMed	1 (hub)

[a]Genes listed alphabetically; DEGs: *Calcium/calmodulin-dependent protein kinase IG* (*Camk1g*), *Coiled-coil domain containing 6* (*Ccdc6*), *Cyclin-dependent kinase inhibitor 1A (p21, Cip1)* (*Cdkn1a*), *Early growth response 3* (*Egr3*), *Homer homolog 1 (Drosophila)* (*Homer1*), *Heat shock protein 90kDa (cytosolic), class A member 1* (*Hsp90aa1*), *Heat shock 90kDa protein 5 (glucose-regulated protein, 78kDa)* (*Hspa5*), *Mesencephalic astrocyte-derived neurotrophic factor* (*Manf*), *Thromboxane A2 receptor* (*Tbxa2r*), and *X-box binding protein 1* (*Xbp1*).
[b]Tools used to analyse candidate genes (by neurodevelopment and behaviour) include PubMed, Ingenuity Pathway Analysis, Partek Gene Ontology Enrichment (GE), National Center for Biotechnology Information (NCBI), GeneMANIA (www.genemania.org), The Database for Annotation, Visualization and Integrated Discovery (DAVID), and Pathway Express (P. Express).
[c]IPA networks listed are shown in Figure 22-24. "Hub" = molecule that appears in a top IPA network with strong intramodule connectivity to all other genes in the same network. Connectivity of a hub > 10 interaction.

Table 29. A comparison of trimester two long-term (T2-L) qRT-PCR and microarray results for candidate genes.

Genes[a]	Array Fold change	Array *p*-value	qRT-PCR Fold change	qRT-PCR *p*-value
Camk1g	-1.27	0.023	-1.66	3.0e-4
Ccdc6	-1.25	0.019	-1.19	0.049
Cdkn1a	-1.43	0.021	-2.23	0.003
Egr3	-1.21	0.040	-1.29	0.026
Homer1	-1.20	0.021	-0.74	0.005
Hsp90aa1	-1.21	0.041	-0.89	0.025
Hspa5	-1.36	0.005	-1.61	0.029
Manf	-1.35	0.009	-1.70	0.006
Tbxa2r	1.21	0.033	-1.18	0.079
Xbp1	-1.37	0.028	-1.54	0.018

[a]Genes are listed alphabetically. Genes included *Calcium/calmodulin-dependent protein kinase IG* (*Camk1g*), *Coiled-coil domain containing 6* (*Ccdc6*), *Cyclin-dependent kinase inhibitor 1A (p21, Cip1)* (*Cdkn1a*), *Early growth response 3* (*Egr3*), *Homer homolog 1 (Drosophila)* (*Homer1*), *Heat shock protein 90kDa (cytosolic), class A member 1* (*Hsp90aa1*), *Heat shock 90kDa protein 5 (glucose-regulated protein, 78kDa)* (*Hspa5*), *Mesencephalic astrocyte-derived neurotrophic factor* (*Manf*), *Thromboxane A2 receptor* (*Tbxa2r*), and *X-box binding protein 1* (*Xbp1*). Genes with bold font represent those that were differentially expressed in array and qRT-PCR results. An underline indicates opposing results between array and qRT-PCR results.

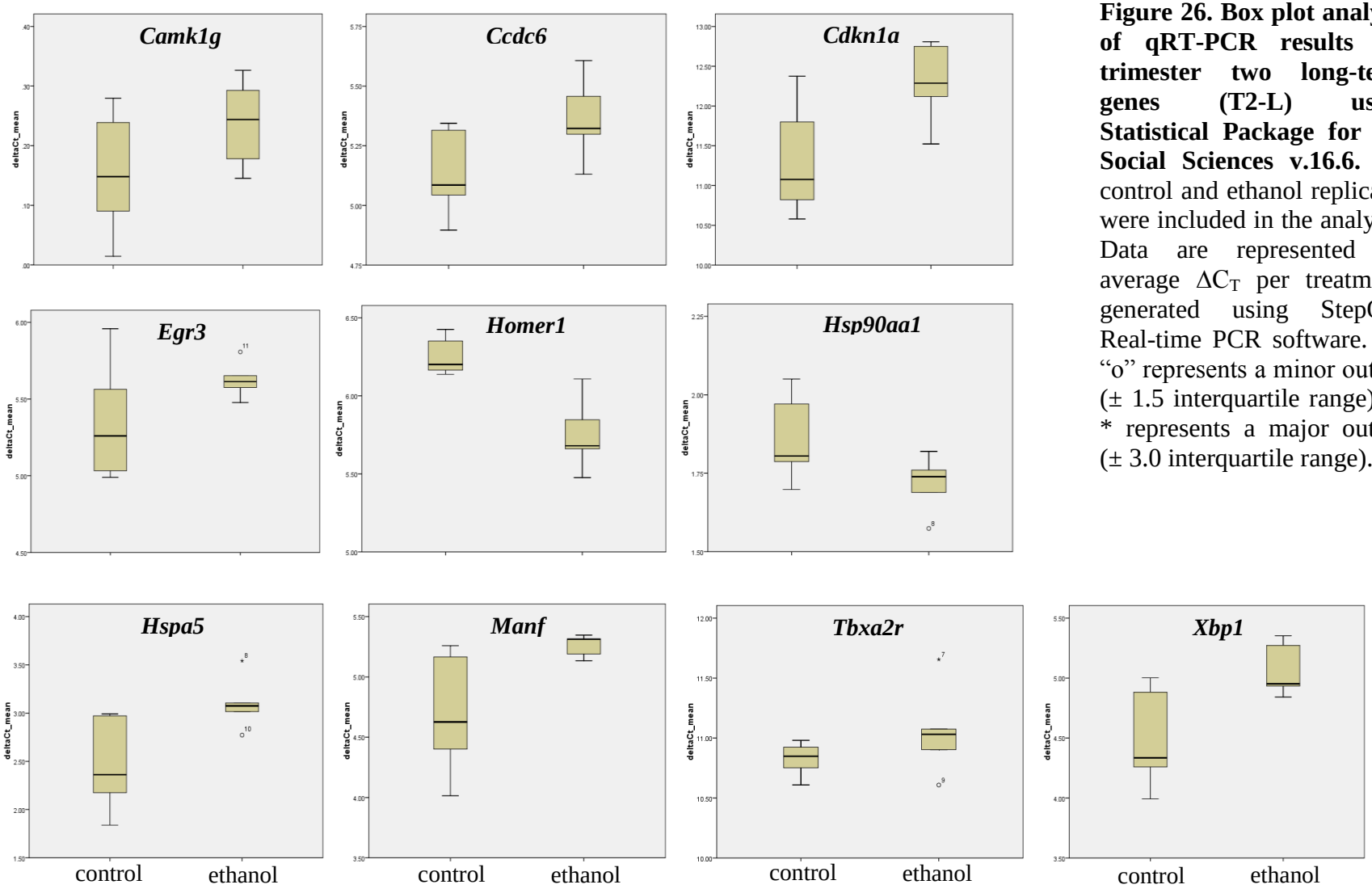

Figure 26. Box plot analysis of qRT-PCR results for trimester two long-term genes (T2-L) using Statistical Package for the Social Sciences v.16.6. All control and ethanol replicates were included in the analysis. Data are represented by average ΔC_T per treatment, generated using StepOne Real-time PCR software. An "o" represents a minor outlier (± 1.5 interquartile range). A * represents a major outlier (± 3.0 interquartile range).

e) MiRNAs altered in the adult brain following second-trimester ethanol exposure

In the global analysis of T2-L miRNAs, fold change ranged from -476-fold (miR-704) to +1.96-fold (miR-467e). Of the 1407 miRNAs on the T2-L arrays that were specific to *Mus Musculus*, the ANOVA resulted in 790 that were < 1 (56.2%), four that were unchanged (0.3%) and 613 that were < 1 (43.6%). T2-L analysis resulted in 20 differentially-expressed miRNAs (± 1.2-fold change, $p < 0.05$) listed in **Table 30**. Only seven of 20 (35%) were found to be upregulated in ethanol mice compared to control mice. None of the miRNAs found in T2-L were in common with those in T1-L. However, miR-342-5p, identified in miRNA T2-L analysis (± 1.2-fold change, $p < 0.05$), was also found in the T2-L long-term gene list (Appendix D).

f) Identification and Confirmation of Specific MiRNAs in T2-L and their Gene Targets

For T2-L analysis of miRNA and gene expression levels, the target filtering results are shown in **Table 31**. Six miRNAs were implicated in the results including: miR-146b, miR-208b, miR-302c, miR-335, miR-449 and miR-455. Contrary to T1-L, all miRNAs except for miR-302c were downregulated, which was surprising since it opposes the notion that an upregulated miRNA(s) leads to decreased expression of mRNAs. There were 10 genes identified in target filtering analysis, which were all downregulated. The only miRNA:gene inverse relationship included miR-302c and *Ccdc6*. Mir-302c was subjected to confirmation by qRT-PCR. The upregulation of miR-302c **—** along with the previously mentioned corresponding downregulation of its target gene, *Ccdc6* **—** was confirmed (**Figure 27**).

Table 30. A list of differentially-expressed microRNAs in trimester two long-term (T2-L) array analysis.

MicroRNA[a]	Fold change	*p*-value
miR-10b	-1.47	0.002
miR-1194	-1.30	0.006
miR-146b	-1.24	0.049
miR-184	-1.44	0.001
miR-1942	1.38	0.029
miR-1952	1.25	0.018
miR-1964	1.26	0.032
miR-208b	-1.37	0.040
miR-2145	1.39	0.029
miR-302c	1.27	0.011
miR-335-5p	-1.35	0.038
miR-342-5p	-1.27	0.025
miR-343	1.27	0.018
miR-369-5p	1.29	0.003
miR-449b	-1.27	0.043
miR-455	-1.48	0.037
miR-466b-3p	-1.35	0.038
miR-466c-3p	-1.90	0.030
miR-466e-3p	-1.49	2.5e-4
miR-684	-1.28	0.021

[a]MicroRNAs are listed by numerical ordering. Data generated using a ± 1.2-fold change and $p < 0.05$ in Partek Genomics Suite.

Table 31. Ingenuity Pathway Analysis (IPA) target filtering of differentially-expressed genes (DEGs) and microRNAs from the trimester two long-term (T2-L) group.

Genes[a]		MicroRNA[b]			
Symbol	**Fold change**	**Symbol**	**Fold change**	**Expression[c] (gene:miRNA)**	**Confidence[d] (predicted)**
Ccdc6	-1.254	miR-146b	-1.243	↓↓	High
Cdkn1a	-1.425	miR-208b	-1.373	↓↓	Moderate
Dynlt1	-1.208	miR-208b	-1.373	↓↓	High
Ccdc6	-1.254	miR-302c	1.265	↓↑	Moderate
Fam107b	-1.245	miR-335-5p	-1.349	↓↓	High
Ptpn22	-1.216	miR-335-5p	-1.349	↓↓	Moderate
Cbfa2t3	-1.203	miR-449b	-1.268	↓↓	High
Galnt7	-1.212	miR-449b	-1.268	↓↓	High
Xbp1	-1.367	miR-449b	-1.268	↓↓	Moderate
Zhx2	-1.221	miR-449b	-1.268	↓↓	High
Cdkn1a	-1.425	miR-455	-1.477	↓↓	Moderate
Otub2	-1.314	miR-455	-1.477	↓↓	Moderate

[a]Genes included *Coiled-coil domain containing 6* (*Ccdc6*), *Cyclin-dependent kinase inhibitor 1A (p21, Cip1)* (*Cdkn1a*), *Dynein, light chain, Tctex-type 1* (*Dynlt1*), *Family with sequence similarity 107, member B* (*Fam107b*), *Protein tyrosine phosphatase, non-receptor type 22 (lymphoid*) (*Ptpn22*), *Core-binding factor, runt domain, alpha subunit 2; translocated to, 3* (*Cbfa2t3*), *UDP-N-acetyl-alpha-D-galactosamine:polypeptide-N-acetylgalactosaminyltransferase 7 (GaINAc-T7)* (*Galnt7*), *X-box binding protein 1* (*Xbp1*), *Zinc fingers and homeboxes 2* (*Zhx2*), and *OUT domain, ubiquitin aldehyde binding 2* (*Otub2*). DEGs are based on Partek Genomics Suite analysis with ± 1.2-fold change and $p < 0.05$

[b]MicroRNAs are listed by numerical order. MicroRNAs were differentially expressed based on Partek analysis with ± 1.2-fold change and $p < 0.05$.

[c]Expression (gene:miRNA) is highlighted in red if an inverse relationship between gene:miRNA was identified.

[d]Confidence predicted based on IPA's Target Filter function.

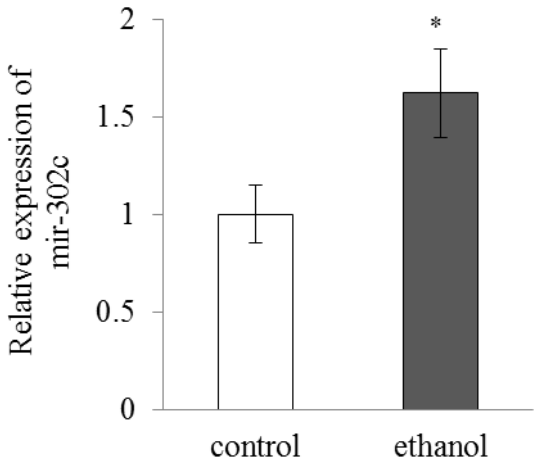

Figure 27. Bar graph of relative expression of miR-302c between ethanol and control samples. Error bars represent relative expression ± SEM. Statistical significance assessed using a two-tailed *t*-test with $*p < 0.05$. Biological replicates: n = 5 control, n = 6 ethanol. Technical replicates: n = 3.

4. Discussion

My central hypothesis stated that, *prenatal alcohol exposure during the first and second term of gestation causes FASD-related behavioural abnormalities and may involve immediate and lifelong changes in brain gene expression, affecting specific pathways*. The results presented in this thesis show that B6 mice exhibit behavioural delays and alterations to the brain transcriptome, both immediately following ethanol treatment and into adulthood, regardless of neurodevelopmental timing. More specifically, I established that prenatal ethanol exposure alters developmental milestones, particularly those associated with motor skill, and leads to learning abnormalities associated with FASD. Immediate (fetal) and long-term (adult) effect of binge-like exposure in B6 mice involves genome-wide gene expression in the brain. Such changes are specific to cellular pathways and networks related to neurodevelopment and FASD-relevant behaviours. I also investigated a role for miRNAs in the long-term maintenance of gene expression changes in response to prenatal ethanol exposure.

The discussion interprets the behavioural and transcriptomic results in the context of neurodevelopment and FASD. In the behaviour section of the discussion, long-term effects (treated during trimester one or two) phenotypic explanations are organized by specific behaviours analysed comparatively to the results. In the molecular section of the discussion, an interpretation of the immediate effects of prenatal alcohol exposure (T2-S) is presented. Next, the long-term effects (T1-L and T2-L) on mRNA and miRNA changes resulting from prenatal ethanol exposure are reported. For each of the groups in the molecular section (T2-S, T1-L, and T2-L), the discussion includes the interpretation of functions, pathways, and networks, and their importance to specific cellular processes.

4.1 Binge-like prenatal ethanol exposure leads to behavioural alterations in exposed offspring

4.1.1 Gestational ethanol exposure leads to motor skill deficits

The results from behavioural analysis demonstrate that ethanol exposure during the first and second trimester equivalent may cause delays in specific developmental milestones. When pups are exposed during the first trimester equivalent, the effects appear to be subtle, with four of the nine milestones affected. Trimester-one-exposed males and females show significant deficits in surface righting, forelimb grasping, open-field traversal, and air righting, which follows the literature[8]. Such phenotypes are early indicators of the rostro-caudal gradient of limb coordination maturation[244]. Limb and musculoskeletal defects have been reported in children with FASD, at early infancy[245]. Poor limb coordination has been observed in ethanol-affected animals, including mice[91,246]. Ethanol exposure during the second trimester equivalent produces delays in six of nine developmental milestones in males and females including: surface righting, negative geotaxis, cliff aversion, open-field traversal, eye opening, and air righting. Trimester two ethanol mice are delayed in reflex (eg. negative geotaxis) and sensory coordination (eg. cliff aversion). Similar to trimester one results, motor skill and coordination deficits are persistent in trimester two ethanol mice compared to control mice. Trimester two ethanol mice were significantly delayed in forelimb grasping (which measures balance, coordination, and motoric strength) compared to trimester one ethanol mice.

The reported motor strength, reflex, and coordination deficits have been observed in other studies assessing developmental milestones in FASD[247,248]. These patterns may suggest that the brain regions responsible for the development of these neuro-motor skills may be sensitive to

ethanol at early stages of development, at which time neurulation and cell proliferation occur[2]. Motor activity behaviours have been closely correlated with serotonin function[249]. Serotonin function is important for neurogenesis; and, its levels are altered by alcohol exposure[250]. Serotonin may be important in the disrupted development of motor skills. Fetal ethanol exposure can cause cell death and neuronal reduction, which may lead to motor impairments[61,93,251,252]. The impairments caused by late gestation ethanol exposure may be attributed to interference during specific brain region development including synapse formation in the cerebellum and prefrontal cortex[93,253–256]. Such results are relevant to FASD, as young children with FASD show delayed motor development and fine-motor dysfunction including weak grasp, poor hand-eye coordination, and poor balance[19,257,258]. Deficits in fine-motor skills are thought to result from damage to the cerebellum, due to its involvement in motor learning[259]. The cerebellum is also sensitive to the apoptotic effects of ethanol, particularly during later neurodevelopmental stages[53]. My results support these findings, and suggest that ethanol exposure, particularly when given at late gestation, may be detrimental to the development of motor skills, reflexes, and coordination.

4.1.2 Prenatal ethanol exposure leads to increased activity

The literature is divided on the impact of prenatal alcohol exposure on activity levels[1,78,260,261]. In my study, novelty-based activity levels (movements) are increased in trimesters one and two ethanol mice compared to control mice, which follows the literature[1,68,262]. Trimester two ethanol mice were significantly more active than trimester one ethanol mice (**Figure 6**), suggesting that second trimester ethanol exposure may lead to more severe deficits in activity levels in offspring than early ethanol exposure. Increased activity are common in children with FASD, and in animal models of FASD[1,14,263,264].

In the open-field activity analysis, I sought to differentiate the effects of alcohol on activity versus novelty-induced stress by measuring overnight activity of the mouse. Overnight activity levels, plotted hour-by-hour, were not consistent between males and females from trimesters one and two. Results suggest that alterations to activity levels in a familiar environment may be due, at least in part, to the timing of exposure during neurodevelopment. Trimester one ethanol females were significantly less active than control females at three time-points during the night; whereas, at one time-point, ethanol females were more active than control females (**Figure 7A**). Trimester one ethanol males were significantly more active than control males at the beginning and ending time-points of overnight testing; ethanol males were significantly less active than control males for one hour during the night (**Figure 7B**). The results suggest that prenatal ethanol exposure during the first trimester equivalent results in generally altered (whether increased or decreased) levels of activity in ethanol mice. The results also point to the complexity of locomotor behaviours associated with FASD. These findings are consistent with studies that have observed differences in activity in animals following ethanol administration during early stages of fetal development[1,68,262,263]. Trimester two ethanol females were hyper-active for two hours during the nocturnal phase, and hypo-active for one hour (**Figure 8B**). Ethanol males showed altered activity levels compared to their control counterparts at certain peaks throughout the night. Trimester two ethanol males displayed increased activity for four hours, and significantly decreased activity for two hours (**Figure 8A**). Such disturbances in activity levels follow the results from trimester one. Ultimately, both early- and mid-gestation ethanol exposures led to changes in nocturnal behaviour in ethanol-exposed adolescent mice. These abnormalities may represent sporadic alterations in activity following prenatal ethanol exposure.

Researchers have reported on altered locomotor activity of mice, and its association with 5-hydroxytryptophan (5-HT) transporter mRNA levels in neurons[266]. Serotonin, a neurotransmitter involved in behaviour and CNS development, is decreased in the forebrains of ethanol mice compared to control counterparts[267]. Prenatal ethanol exposure leads to differential long-term effects on 5-HT-mediated neuroendocrine function in males and females[268]. Timester one is important for neural progenitor development and forebrain development[64,65]. Altered activity levels in ethanol mice could be maintained into adulthood due to altered serotonin signaling in the brain. Trimester two is a critical period for neuroepithelial cell proliferation, differentiation, and migration[69]. Ethanol exposure during this stage alters neuronal migration and, similar to first trimester exposure, reduces the number of neurons and glial cells in the neocortex, hippocampus, and sensory nucleus[64,70]; these reductions are associated with alterations in locomotor activity[269]. A correlation between neuronal reduction and disturbed locomtor activity is logical, given that the hippocampus ― one of the prominent limbic system structures ― contributes to exploratory locomotion behaviour[270]. Prenatal ethanol exposure has been reported to lead to a 25-30% decline in the number of hippocampal cornu ammonis area 1 (CA1) pyramidal cells, which corresponded to a significant increase in activity levels in ethanol subjects[269]. Long-term abnormalities in the cerebral cortex, a region important for the control of voluntary movement, have been noted in motor-impaired individuals with FAS and FASD[48,271].

4.1.3 Ethanol leads to changes in anxiety-related traits when offspring are exposed during the second trimester

The results from anxiety testing indicate that anxiety-related traits may confound analysis of locomotor behaviours in FASD models, particularly when assessed in novel environments. In my study, three measures of anxiety-related traits were used including an open field test, a LDB,

and an EPM. Thigmotaxis is an index of anxiety in mice, and is observed when a mouse has a tendency to remain close to walls or in the dark, i.e., away from open and light areas[272]. Trimester one ethanol mice and control mice were not significantly different, which suggests that mice exposed to ethanol during the beginning of gestation have no observable anxiety-related deficits. Although others have agreed that there may be no changes in anxiety-related traits following prenatal alcohol exposure[102], they have not focussed on the first trimester, leading to the novelty of the findings in this thesis.

Trimester two ethanol mice showed significantly lower levels of thigmotaxis, indicated by significantly increased time, compared to control mice, in the center zone and light arena of the open-field test and LDB, respectively (**Figures 9-10**). Additionally, trimester two ethanol mice show lower levels of thigmotaxis in the open field than trimester one ethanol mice. No changes in activity between trimester two ethanol and control mice were observed in the EPM. It is possible that using multiple anxiety tests may lead to unreliable estimates of the similarities between the tests; a physical integration of these tests into one apparatus may prove to be more useful in the assessment of anxiety-related traits[115]. From the open field and LDB results, one can infer that second-trimester ethanol mice show significantly lower levels of anxiety-related traits than control mice. A decrease in anxiety-related behaviour does not follow previous reports in the literature. However, it is possible that trimester two exposure may not reduce anxiety in offspring, per se, but may instead increase the risk of other FASD-related phenotypes, such as impulsivity[273]. In such a way, the lowered anxiety-related phenotype may actually represent high impulsivity or risk-taking behaviour, which have been reported in animal models of FASD[274,275]. Children with FASD are known to be impulsive and to take risks[11,276–278]. Risky behaviour and low impulse control is associated with damage to the ventromedial prefrontal cortex (VPC)[279,280].

The VPC undergoes massive neuronal migration of cells, which may contribute to this phenotype[281]. The second possibility to observing lowered anxiety-like behaviours is an anxiolytic effect of alcohol during the second trimester. Previous studies have identified a similar phenomenon resulting in anxiolytic effects in prenatally ethanol mice[282]. Such findings give evidence to the sedative effects of ethanol[283]. Further behavioural testing — that deciphers between anxiety-related behaviours and impulsivity or risky behaviour — would allow for more comprehensive conclusions regarding the results of anxiety-related behaviours during second trimester ethanol exposure.

4.1.4 Deficits in spatial learning and memory result from prenatal ethanol exposure

Ethanol mice from trimester one and two showed impairments in spatial learning and memory, albeit not to the same degree. Trimester one ethanol mice did not learn the location of a target hole by the final learning day (**Figure 11A**). During short-term recall trials, ethanol mice made the same number of explorations around the target hole than control mice (**Figure 12A**). No changes in exploration indicates the adsence of short-term memory deficits in trimester one ethanol mice. Control mice displayed an increased number of explorations to a position near the target hole in long-term recall trials (**Figure 12B**). Although there was a general trend of increased explorations to the target hole by control mice versus ethanol mice, the findings were not significant. These results indicate the presence of learning deficits in ethanol mice; however, trimester one exposed mice do not have severe memory delays. My results on learning trials support those from other studies, which have demonstrated that ethanol mice show significant impairments in spatial learning[78,91,284]. Observing no memory deficits following early-gestational alcohol exposure is novel in the literature. However, the results should be interpreted with

caution. A general trend of increased latency to the target hole was observed in ethanol mice, and these results may be significant with increased sample size.

Young adults with FASD often have cognitive functioning abnormalities in the following areas: intellectual ability, attention and speed of information processing, executive functioning, language, visual perception and visual construction, number processing, and learning[9,285–288]. Akin to mice that did not learn the spatial orientation of the target in the Barnes Maze, individuals with FASD may have difficulty in developing spatial navigation and require consistent repetition to reinforce learning[15]. Ethanol decreases the spatial specificity of hippocampal place cells, suggesting that ethanol affects learning and memory by altering, directly or indirectly, neuronal activity in the hippocampus and related structures[289]. The hippocampus is critical for spatial information in guiding and organizing behaviours[290]. Given that the hippocampus becomes visible during the first trimester and is vulnerable to external cues (eg. ethanol), hippocampal abnormalities may lead to the observed spatial learning deficits[291].

Although second trimester ethanol mice took longer than control mice to reach the target on the first learning day, they were able to "catch up" by the end of the trials (**Figure 11B**). On learning days three and four, trimester two ethanol mice spent signifcnatly less time searching for the target hole than trimester one ethanol mice. The difference between early- and late-gestational alcohol exposures suggests that reinforced learning in the Barnes Maze allowed trimester-two-exposed mice to catch up to control mice by the final trial day. On the other hand, early-gestational alcohol exposure impairs learning in offspring into adulthood, even with repeated trials. Others have agreed that repeated learning can result in ethanol animals reaching a similar performance level to that of control animals[292]. Repeated learning in children with FASD may help to improve spatial learning when children are given an implicit learning strategy[15,293].

The late second trimester is the beginning of rapid brain growth, a time when neuroteratogens can exert adverse effects[294]. Ethanol exposure during the second trimester leads to reductions in the number of neurons and glial cells in the hippocampus[2,70,295]. Any spatial deficits resulting from ethanol exposure during this time may result from hippocampal neuronal damage. In the Barnes Maze, short-term recall trials resulted in lower numbers of explorations to the target area by trimester two ethanol mice than control mice. Ethanol mice also made more explorations to the opposite side of the maze than control mice (**Figure 12A**). Long-term recall trials resulted in lower numbers of explorations in the target area by ethanol mice compared to control mice (**Figure 12B**). These findings are contradictory, since repeated learning led to an improvement in learning performance in ethanol mice. However, the results suggest that even repeated learning trials may not necessarily lead to improved short-term or long-term memory following mid-gestational ethanol exposure.

4.1.5 Caveats to behaviour modeling of complex disorders

a) General use of mice as a model

Modeling complex disorders using the mouse is not without limitations. The first caveat to mouse behavioural phenotyping is the resulting comparison to human subjects. This limitation represents an issue pertaining to face validity in animal models, which addresses the extent to which a test is subjectively viewed as covering the concept it purports to measure[186]. Essentially, there must be similarity between the behaviour exhibited by the animal model, and the specific symptom of the human condition. Establishing face validity of a model is impossible, because claims for face validity of a model almost invariably involve subjective arbitrary arguments that are not necessarily accepted by all investigators in the field[186]. As proper characterization of

many complex disorders still remains to be properly elucidated in human studies, the validity of specific behavioural tests to measure animal behaviour will also require revision. Another aspect of animal model validity includes predictive validity. Predictive validity involves the identification of potential treatments or pharmacotherapies for reducing physical or behavioural abnormalities[186]. This feature of animal model validity was not addresses in my thesis, and remains to be observed in future studies. Lastly, construct validity must be established in an animal model of human complex disorders in order to remain valid. Construct validity refers to whether a test measures that which it is intended to measure[186]. Although a necessary component in establishing the reliability and validity of animal models, it is rarely established. For instance, I measured anxiety-related traits using three testing apparatuses for mice, with inconsistent results. Given this, complex behaviours may not be properly characterized using available testing apparatuses, and the results could be misrepresented.

Other than addressing the validity of mouse models of complex disorders, there are other limitations to behavioural research on animals. These may include: 1. varying results across different labs using the same behavioural test, 2. experimenter's influence (eg. odour cues) on animal performance, 3. early-life environment of the mouse (eg. stress, maternal care), 4. variation across mouse strains, 5. influences from previous behaviour tests . Each of these factors may alter the outcome of behavioural analysis. However, although these issues may confound behavioural testing, the mouse was chosen for this project based on the extensive availability of behavioural and analytical tools.

b) Technical considerations in the FASD project

In my project, the first caveat was the use of cardboard material in the construction of the LDB (enclosure), EPM (closed arms), and Barnes Maze (hole covers). Cardboard has been used by other researchers in construction of behavior apparatuses[100]. However, odour cues are used as scent marks for communication between mice[296]. It is possible that olfactory cues could have remained on the testing apparatus and influenced the results. Another limitation to behaviour testing involves measurement of human traits in animal models. In my study, I found inconsistent results across three tests that apparently measure anxiety-related behaviours (open field, LDB, EPM). Such discrepancies may have been due to the mouse's familiarization to anxiety-related experiments with time, or the inability of the apparatuses to reliably measure the same aspect of anxiety. A final source of concern in behaviour testing included reliance on previous BAC studies in B6 mice. Given the amount of ethanol injected, I can predict that BACs remained above a critical threshold of neurodegeneration, described by Ikonomidou and colleagues[21]. However, because the exact BACs were unknown, there may be inconsistencies in the treatments. Such caveats are intrinsic to behavioural testing, and the results from my studies should be interpreted with caution.

4.1.6 Prenatal ethanol exposure leads to behavioural disabilities in mice

Prenatal ethanol exposure in the first and second trimester equivalents in mice leads to delays in the achievement of developmental milestones, increased activity levels in a novel environment, altered activity in a home cage environment, and deficits in spatial learning and memory. However, abnormalities in anxiety-related behaviours are dependent on the timing of gestational alcohol exposure. Mice treated at the second trimester equivalent show decreased

anxiety-like traits compared to matched control mice. Whereas, mice treated at the first trimester equivalent are not statistically different from matched controls. Given the nature of the neurodevelopmental processes that occur during each stage, it is likely that behavioural abnormalities are resultant from differential timing of gestational ethanol exposure. However, the results also provide evidence that neither time is safe from the teratogenic effects of alcohol on the developing brain. Herein, the timing of gestational ethanol exposure is an important factor in the development of a spectrum of abnormalities associated with FASD.

4.2 Molecular search for the mechanisms that may govern FASD

4.2.1 Prenatal ethanol exposure leads to gene expression changes that are subtle, timing-dependent, and developmental stage-specific

The developing brain is highly susceptible to the teratogenic effects of ethanol[54,297]. Researchers have demonstrated that prenatal ethanol exposure can lead to long-term behavioural abnormalities that characterize FASD[7,17,91,217]. These long-term behavioural consequences are associated with changes in gene expression that are maintained into adulthood[158,217]. The mechanisms maintaining alterations in gene expression may be a result of epigenetic mechanisms, including "fine tuning" of the genome by miRNAs[95,165]. In my thesis, I took a novel approach by comparing the short-term (fetal) and long-term (adult) transcriptomic changes resulting from gestational ethanol exposure during the second trimester equivalent in the B6 mouse. I also compared the long-term changes in gene expression between two time points: first trimester and second trimester. Furthermore, the role of miRNAs was explored in the maintenance of the observed long-term (T1-L and T2-L) gene expression changes.

The resulting list of T1-L and T2-L DEGs from microarray analysis provides evidence that ethanol exposure during neurodevelopment significantly alters the transcriptome of the adult brain, regardless of timing. In addition, prenatal ethanol exposure at T2-S also produces subtle, immediate changes in the transcriptome of the fetal brain. Researchers argue that subtle changes to the transcriptome are relevant to the idenitification of altered biological processes[298]. Because there was close to no gene overlap across groups, this may suggest that major contributors to the DEGs — aside from ethanol itself — are the timing and developmental stage of ethanol exposure. Gestational timing may result in different sets of genes being implicated due to changes that occur in the transcriptome as the brain develops. The resulting affected gene-sets are based on the biological processes occuring at the time of exposure. Depending on the timing (i.e. trimester), ethanol would likely disrupt different sets of biological pathways. Depending on the developmental stage (fetal brain versus adult brain), the genes and pathways corresponding to these stages will reflect differences in ethanol's targets during brain development in the womb versus in adulthood. Changes in gene expression could result from ethanol-induced apoptosis of specific cell types, which may lead to an overall change in the cellular composition of the brain and, subsequently, the overall pattern of brain gene expression[21,53,54,297,299]. Ethanol may disrupt specific developmental processes that are sensitive to external cues, such as cell growth, proliferation, migration, or differentiation[10,300,301]. These mechanisms may represent immediate effects of ethanol. Ethanol may not directly alter gene expression, but rather, it may act indirectly by altering cellular identity or physiology of the brain such that the appropriate balance of neural gene expression is not maintained. If proper patterning is not maintained into adulthood, this may explain why gene expression changes are still persistent in adult mice, thereby leaving a molecular "footprint"[158]. Interestingly, even low blood alcohol levels can trigger apoptosis in the

developing brain[54]. Also, FASD-relevant behaviours are observed in individuals with no obvious brain abnormalities[27]. These observations suggest that a reduction in brain cell populations does not account for all of the variation in FASD. Epigenetic modification may be another mechanism responsible for altered gene expression following prenatal ethanol exposure.

It is important to note that the overall patterns of gene expression in T1-L and T2-L have inverse numbers of upregulated versus downregulated genes from T2-S. More genes (~63%) from T2-S analyses were upregulated than downregulated. In agreement with this finding, others have shown that more transcripts are upregulated than downregulated as a result of inhibition of proteins related to cell growth, differentiation, and modification[302]. This is reasonable given that the second trimester is important for cell growth, proliferation, migration, and differentiation[2,69]. Also, the higher percentage of upregulated genes in T2-S may be a result of an immediate compensatory response to fetal teratogen (i.e. ethanol) exposure. More genes from T1-L (~82%) and T2-L (~60%) were downregulated than upregulated. These overall patterns represent developmental-stage-specific changes in the transcriptomes. Downregulation and upregulation of different sets of genes and pathways likely depends on which biological processes are affected by prenatal alcohol exposure at two developmental times. Ethanol has been shown to result in downregulation of neurotransmitter-related genes in the brain, even in adult mice[91,102]. The results suggest that certain genes remain dysregulated into adulthood, leading to long-term maintenance of FASD-related behavioural abnormalities.

4.2.2 The effects of second-trimester ethanol exposure on molecular processes in the fetal brain (T2-S)

a) Short-term (T1-S) process 1: neuroinflammation

Functional, pathway, and network characterization of T2-S genes resulted in neurinflammation as an affected process. The neutrophil-derived, Chemokine (C-C motif) ligand 3 (CCL3), is essential for the rapid recruitment of dendritic cells to sites of microbial infection[303]. Given its role in inflammation of the nervous system, *Ccl3* may have an integral and immediate reaction to ethanol. Another gene, *Leukocyte-associated immunoglobulin-like receptor 1* (*Lair1*) was implicated in natural killer cell proliferation, and is involved in inhibitory regulation of the immune system to prevent cell lysis[304]. Studies show that *in utero* alcohol exposure can result in immune deficiencies, including impaired adaptive immune responses to influenza virus infection, in neonates and adults[305,306]. Immune system-related genes affected immediately following gestational ethanol exposure can lead to compromised immune system response into adulthood. An ongoing neuroinflammatory process in the cerebral cortex and cerebellum of post-mortem autistic brain samples[307]. Comorbidity of cognitive and behavioural deficits in autistic children and individuals with FASD is quickly becoming a new avenue of investigation. FASD and autism share similarities with regard to social and communicative functioning[308]. Researchers have also supported the position of compromised immunity and neuroinflammation in the autistic brain[309]. Of the two networks identified by IPA analysis, the top pathway included *Lair1* and *Ccl3* (**Figure 15**). *Ccl3* and *Lair1* may be upregulated immediately following prenatal ethanol exposure in an attempt to mediate the effects of neuroinflammation by alcohol on the sensitive brain. A loss of LAIR1 results in altered immune cell phenotypes[310]. CCL3 functions to traffic inflammatory cells across the blood brain barrier in

CNS inflammation[311]. As a result, *Lair1* and *Ccl3* expression may increase in order to facilitate proper immune function in an attempt to elicit a response following ethanol-induced inflammation. It is possible that neuroinflammation could be a potential cause of cognitive decline in individuals with neurodevelopmental disorders[194].

b) Short-term (T2-S) process 2: chromatin stability

A second process that is disrupted in the fetal brain following acute ethanol administration in the second trimester is chromatin stability. GE analysis identified chromatin stability, specifically histone-related processes, with *Tdg* and *RING1 and YY1 binding protein* (*Rybp*) (**Table 4**). Given that *Tdg*'s main function is repairing DNA mismatches, the finding of "base excision repair" as the top pathway (albeit not statistically significant) from Pathway Express is reasonable. Base excision repair mechanisms must function correctly to enable efficient repair, and subsequent repackaging of DNA into nucleosomes[312]. Network analysis using IPA showed *Tdg* and *Rybp* involved in the top network (**Figure 15**). Given its association with TP53, *Tdg* may be upregulated immediately following fetal ethanol exposure in order to compensate for cell death. The upregulated *Rybp*, involved in degradation of TP53, may additionally compensate for the damaging effects of ethanol on the developing brain. Damage to DNA resulting from oxidation generates single stranded breaks that must be repaired[313]. Chromatin instability could be promoted if these breaks are left unrepaired. RYBP interacts with E2 transcription factors (E2fs). E2fs play a major role in the cell cycle as checkpoint regulators and DNA repair and replication proteins[314,315]. These factors also interact with histone acetyltransferases to facilitate proper gene expression in the cell cycle[316]. An alteration in transcript levels of *Rybp*, whether increased or decreased, may interrupt histone interaction and lead to improper chromatin regulation. Improper chromatin regulation may lead to a loss in

control of gene regulation and cell cycle response. Another gene, *Jmy*, was also identified in T2-S functional and pathway analysis as a regulator of DNA-dependent transcription in response to stress (**Tables 3-6**). As a transcriptional cofactor, *Jmy* is a key player that can impact p53 activity[317]. If disrupted, the DNA damage response may be altered, which could impact the regulation of a variety of genes involved in cell cycle control and apoptosis. Ethanol exposure can lead to DNA damage, specifically by disrupting chromatin remodeling[318]. Given that chromatin remodeling is important in the regulation, unfolding, and activity of genes, any deficiencies in this process may have severe implications on neural development and plasticity[319].

c) Short-term (T2-S) process 3: signal transduction

Another disrupted process in the fetal brain immediately following second trimester ethanol administration is signal transduction. In the second trimester, neuroepithelial cell proliferation and migration occurs[2,69]. Hence, cell-to-cell communication via signalling pathways may be impacted as a result of ethanol exposure. Functional analysis using DAVID resulted in the keyword, Dual specificity phosphatase (catalytic domain) or "DSPc" (**Table 3**). DSPcs are key regulatory components in signal transduction pathways (eg. MAPK pathway) involved in cellular localisation, growth, proliferation, differentiation, and transformation[320]. In this DAVID category, *Dusp19* and *Ssh2* were implicated (**Table 3**). A knock down of SSH2 was found to induce apoptotic cell death through cell cycle arrest[321]. Apoptotic cell death may be mediated by changes in chromatin, resulting from damage to the DNA-histone interactions[322,323]. DSPcs, such as *Dusp19*, have been previously implicated in major depressive disorder (MDD)[324]. MDD and other depressive disorders often occur comorbid with anxiety[325]. These disorders may also share similar phenotypes with FASD. Of the canonical pathways identified in IPA, "p53 signaling",

driven by *Jmy*, is associated with signal transduction pathways that mediate apoptosis. *Jmy* and *Bcap31* are identified in the top network from IPA (**Figure 15**). The downregulation of *Bcap31* and *Jmy* may be a result of ethanol's effect on signaling, leading to cellular compromise in the fetal brain. Signaling pathways, including MAPK, are involved in synaptic plasticity and learning[326,327]. Ethanol's immediate effects may disrupt genes relevant to these processes. Differential regulation of cell signaling, specifically MAPK1/ERK2 signaling, may contribute to genetic susceptibility to FASD[328]. Other studies agree with my findings that signaling pathways are disrupted following prenatal ethanol exposure in the fetal brain.

d) Short-term (T2-S) process 4: actin cytoskeleton development

Another process disrupted immediately following second trimester ethanol exposure is actin cytoskeleton development. Specifically, *Trdn* was identified in the IPA function, hypertrophy of skeletal muscle; *Crem* (*cAMP responsive element modulator*) and *Trdn* were both involved in muscular hypertrophy (**Table 5**). Given that actin cytoskeleton development has been identified as a disrupted process in a mouse model of FAS[82], these results are relevant to my model. Thyroid hormone and its receptor, TRDN, have been implicated in limb development[329]. Other factors involved in cytoskeleton development are miRNAs; miRNA importance in cytoskeleton development is supported in the literature[330]. In the top IPA network, *Hpca* is upregulated while *Crem*, *miR-397* and *miR-99* are downregulated (**Figure 15**). Although mature miRNAs are usually upregulated in order to downregulate their target mRNAs, they themselves can be downregulated following prenatal ethanol exposure[331]. Skeletal abnormalities are often observed in children with FAS[46,332–334]. Also, deformities of the joints, limbs, and fingers have been observed in individuals with FAS[257]. It is presumable that genes involved in

cytoskeleton development are altered immediately following prenatal ethanol exposure in this model.

e) Inability to confirm short-term genes using qRT-PCR

None of the selected genes from T2-S analysis were confirmed by qRT-PCR. The inability of qRT-PCR to detect low-fold changes is a possibility[335]. The likelihood that all eight genes may be false positives is questionable, especially given that four of the genes have a relatively high (±1.34) fold change. There was no bias in confirmation of upregulated versus downregulated genes. An important next step to determining the problem with confirmation would be to repeat the microarray experiment and confirm specific genes. Another step could be to use a newer technology such as RNA sequencing (RNAseq) to further investigate candidate genes. Another idea could be to use a more rigorous method to quantify mRNA transcript levels, particularly if some of the genes were false positives. This could be achieved using well-established technology such as, Northern Blotting, ribonuclease protection assays, or droplet digital PCR, which can confirm low fold-changes[336]. Using a different algorithm to assess microarray data is another possibility. Dallas and colleagues reported a high correlation of microarray and qRT-PCR experiments using Partek's RMA algorithm[337]. The RMA algorithm could be applied to my dataset, and the top DEGs could then be confirmed by qRT-PCR.

4.2.3 Ethanol exposure during trimester one (T1-L) leads to long-term changes to the adult brain transcriptome

a) Long-term (T1-L) process 1: tissue morphology

Functional, pathway, and network characterization of T1-L ethanol-responsive genes resulted in the disruption of a variety of cellular processes. One of these processes included

tissue morphology. Gastrulation — the early phase in embryonic development during which germ layers begin to form — takes place during trimester one[2]. Herein, it is reasonable that the embryonic stage is disrupted following early prenatal alcohol exposure. Functional characterization of significant genes using GE resulted in "mesoderm morphogenesis" with *Setd2* and *Eomes* implicated (**Table 11**). *Eomes* interacted with an interleukin in the only significant IPA network (**Figure 19**). Studies have shown that *Eomes* is required for trophoblast differentiation and mesoderm formation during gastrulation[338]. This lends credence to the likelihood that first trimester ethanol exposure interferes with tissue morphology in the fetus, which could be mediated by tissue-specific genes such as *Eomes*. Another gene, *Map3k1*, was implicated in IPA functional analysis, in "Tissue Morphology" (**Table 12**). Loss of MAP3K1, an enzyme involved in cellular responses to stimuli, enhances proliferation and apoptosis during retinal morphology[339]. A role in developmental eyelid closure during fetal development is among the most obvious functions of MAP3K1[340]. The only significant T1-L IPA network included nine downregulated genes (**Figure 19**), including *RAS p21 protein activator 2* (*Rasa2*), which is part of several known Ras GTPase activating proteins involved in tissue distribution[341]. Spruce and colleagues have implicated *Rasa2*, along with *Eomes*, in mouse embryogenesis[342]. Children with FASD are often characterized with malformations of various organs, facial abnormalities, and malformations of the optic discs and retinal vessels[25]. Previous mouse models have consistently resulted in craniofacial malformations and anomalies of the face and eyes following trimester one ethanol exposure[334,343–345]. It is logical that biological processes involved in tissue morphology and organogenesis are disrupted following early gestational ethanol exposure in this model.

b) Long-term (T1-L) process 2: adaptive immunity

Similar to T2-S, genes and pathways disrupted in T1-L were also involved in immune system response. Functional characterization of gene annotations using DAVID resulted in a significant term, "TNF/stress related signaling", with *Map3k1* and *Atf1* implicated. Various Tumor necrosis factor (TNF) receptor family members are involved in lymphoid development and/or peripheral immune system response[346]. One of the essential roles of *Map3k1* includes regulation of immune system development and function[347,348]. Given the diverse roles of *Map3k1*, its disruption in the brain following ethanol exposure in the first trimester leads to compromised immune system response. *Eomes* also plays a role in cell immunity, as per its interaction with interleukin 5 (IL5) in the IPA network (**Figure 19**). Interleukins are cytokines that regulate immune and inflammatory responses. *Eomes* controls IL5 production in memory T helper 2 cells; T helper 2 cells play an important role in the clearance of different pathogens, including toxins[349]. The downregulation of *Eomes* may directly impact immunity to infection by disrupting interleukins, such as IL5. GE analysis complemented DAVID analysis, with the identification of *H2-T23* in T cell proliferation (**Table 10**). Given that B and T lymphocytes have central roles in cell-mediated immunity, their identification in T1-L is well-founded. H2-T23 is a homologue of Major histocompatibility complex, class I molecule human leukocyte antigen, E (HLA-E), which is involved in the innate and adaptive immune systems[350]. My findings are consistent with animal models of FASD that have identified deficits in adaptive immunity following prenatal ethanol exposure[351,352]. Individuals with FAS can exhibit immune deficiencies, specifically decreased lymphocytes, and diminished mitogen-induced stimulation responses to mitogens[353]. It is possible that defects in host defense to infection could be attributable to prenatal exposure to high levels of ethanol during early gestation. *Tnfrsf19* also

plays a role in immunotoxicity. *Tnfrsf19* is downregulated by Aryl hydrocarbon receptor (AhR) (**Figure 19**), which mediates biochemical and toxic effects of halogenated aromatic hydrocarbons[354]. AhR is also involved in cell cycle regulation and development and maturation of many tissues. The disruption of AhR by *Tnfrsf19* may lead to compromised immune system following toxicity. *Ceacam1*, identified in functional analysis, is responsible for a variety of functions, one of which includes modulation of innate and adaptive immune responses. Given its disruption following ethanol exposure, *Ceacam1* may lead to lifelong changes in dendritic and natural killer cells, which are part of the innate immune system. Adaptive immunity refers to the adaptability of cells to infectious agents, mediated by B or T lymphocytes. Both processes may be altered into adulthood following exposure to toxins, such as ethanol.

c) Long-term (T1-L) process 3: fatty acid synthesis

Lipid synthesis is another process that is disrupted in the adult brain following first trimester ethanol exposure. The top functional annotation from DAVID analysis was "coenzyme A", with *Hmgcs2* (**Table 10**). PE identified *Hmgcs2* in the significant pathway, "synthesis and degradation of ketone bodies". Meanwhile, three of five top IPA canonical pathways were relevant to fatty acid synthesis, with *Rpe* and *Hmgcs2* included as key players. HMGCS2 is known to regulate mitochondrial fatty acid oxidation[355]. *Hmgcs2*'s downregulation in the T1-L network suggests that ethanol may inhibit lipid synthesis. Fatty acids contribute to regulation of hepatic acid oxidation and synthesis in adults; fatty acids also accumulate in fetal and infant liver in variable amounts depending on maternal diet fat composition[356]. My results suggest that disruption in fatty acid production during the first trimester may lead to lifelong impairments to similar processes in the adult. Furthermore, the role of fatty acids in FASD is recognized. Placental fatty acid ethyl esters (FAEEs) are well-known biomarkers of heavy prenatal ethanol

exposure[357]. FAEEs may be a useful screening tool for the identification of newborns at risk for FASD[358]. This screening tool would be a biological attempt to facilitate proper characterization of FASD. Results from my study are in-line with previous reports that have identified fatty acid biosynthesis as a disrupted process following *in utero* ethanol exposure, and may help to elucidate the key players involved in FASD.

d) Long-term (T1-L) process 4: DNA repair

An analysis of T1-L ethanol exposure has also implicated DNA repair as a disrupted process. DAVID clustering of functional annotations resulted in "base-excision repair" as a significantly affected process dependent on two genes: *Mbd4* and *Pcna* (**Table 10**). "Base-excision repair" was also the top pathway resulting from PE analysis, and also included *Mbd4* and *Pcna* (**Table 13**). It is well known that ethanol is a toxic substance. The most obvious line of evidence that ethanol produces DNA damage is the positive association between alcohol intake and an increased risk for cancer[359]. Brooks and colleagues were the first to provide direct evidence that neurons in the adult mammalian brain have the capacity to carry out DNA mismatch repair[360]. Formation of the neural plate begins on GD 7 in mice[345], which allows for the compairons of these reports to my findings. Genes involved in DNA mismatch repair have decreased expression following hypoxic stress in mammalian cells[361]. Herein, one can speculate that perhaps mismatch repair proteins, i.e. PCNA are dysregulated upon gestational insults (i.e. ethanol) and remain decreased even into adulthood[362]. By doing so, such proteins maintain changes in the brain resulting from abnormalities in DNA repair.

e) Confirmation of T1-L-specific genes using qRT-PCR

The qRT-PCR results for T1-L included the confirmation of four genes: *Tnfrsf19, Eomes, Synpr*, and *Map3k1* ($p < 0.05$). The differential expressions of *Atf1, Stxbp6, Ceacam1* and *5-hydroxytryptamine (serotonin) receptor 5A, G-protein coupled* (*Htr5a*) were not reproducible by qRT-PCR (**Table 16**). Given that the gene lists generated from microarray analysis did not correct for a FDR, there may be false positives in the results, particularly for genes at low-fold changes.

f) Alteration of miRNAs following first-trimester ethanol exposure

i. General trends in alteration of mouse-specific miRNAs

Mouse miRNA arrays were completed on the long-term (T1-L and T2-L) samples. The results from T1-L mouse miRNA arrays demonstrate that ethanol exposure during early neurodevelopment affects miRNA expression in the adult brain. Since only eight mouse-specific miRNAs out of ~1000 were significantly affected (± 1.2-fold change, $p < 0.05$), the results are not stringent enough to make conclusions on array data. The findings from the miRNA arrays should be examined with caution. It is important to note that others have also observed low numbers of miRNAs disrupted using expression arrays[363,364]. Given that one miRNA has the potential to downregulate hundreds of target mRNAs[365], my findings may be relevant. In fact, a miRNA:mRNA relationship may result in subtle, rather than drastic, changes to the transcriptome[366]. A disruption in miRNAs usually leads to low-fold changes in gene expression. Such an association is why miRNAs are often referred to as, "fine turners of gene expression"[165]. Although global miRNA profiling has not been widely-used in FASD research, recent studies report that ethanol does alter miRNA expression[175,176,182,367]. In my study, miRNA analysis was

undertaken at postnatal day 70, i.e. young adulthood; therefore, the disrupted miRNAs represent altered biological processes that are maintained into adulthood. These altered miRNAs and processes may have lasting effects on gene expression and behavioural phenotypes.

ii. Candidate mouse-specific miRNAs in T1-L

In general, if a miRNA is upregulated, its target gene(s) is likely to be post-transcriptionally downregulated. IPA target filtering was performed on the eight T1-L differentially-expressed miRNAs, along with their respective DEGs to identify potential targets of the miRNAs. Two miRNAs, miR-1192 and miR-532-5p were identified in target filtering, along with 11 genes (**Table 18**). Downregulation of miR-532-5p is reported to alter the macrophage inflammatory response to lipopolysaccharide stimulation[368]. MiR-532-5p is also involved in suppression of a Runt-related transcription factor (RUNX), which is involved in a variety of cellular processes including: cell differentiation, development, angiogenesis, cell adhesion and invasion, DNA repair, and immunity[369,370]. A RUNX transcription factor (TF) is a downstream effector of the Transforming growth factor beta (TGF-β) signaling pathway[371]. The role of miR-532-5p may be relevant to the development and/or maintenance of neurodevelopmental abnormalities, specifically those that are related to cellular maintenance and signal transduction, particularly if its target gene is involved in one of these processes. In my thesis, the upregulation of miR-532-5p was confirmed using qRT-PCR. The second disrupted miRNA, miR-1192, was previously reported to be upregulated in PPARγ dominant negative individuals[372]. PPARs are involved in lipid metabolism; PPARγ and PPARα are hubs in T1-L network analysis (**Figure 19**). Given that I have identified fatty acid synthesis as a disrupted process following trimester one ethanol exposure, the involvement of miR-1192 in FASD is intriguing. However, miR-1192 was not confirmed using qRT-PCR.

Of the 14 miRNA:mRNA interactions, ten of these have decreased mRNA fold changes and increased miRNA fold changes (**Table 18**). These results demonstrate that one microRNA (i.e. miR-532-5p) has the potential to target multiple genes (i.e. *Atf1*, *Cspp1*, *Itpripl2*, *Nat2*, *Stxbp6*). Similarly, one gene (i.e. *Atf1*) can be targeted by multiple miRNAs (i.e. miR-1192 and miR-532-5p). Other researchers have found that a single gene can be targeted by various miRNAs[373]. Predicted genes that may be disrupted by miR-1192 and miR-532-5p include *Atf1*, *Itpripl2*, and *Stxbp6*. From gene functional analysis, *Atf1* was found to be involved in TNF/stress related signaling (**Tables 10**). *Atf1*'s role in cell differentiation, immunity, cell survival, and neurite outgrowth during early mouse development is well-established in the literature[374,375]. *Atf1*'s function is relevant to the elucidated roles of miR-532-5p, and was a meaningful candidate for confirmation by qRT-PCR. Another role for *Atf1* is its involvement in the cellular fatty acid homeostasis[376]. *Atf1*'s downregulation — particularly in the context of upregulation of miR-1192, which is involved in fatty acid biosynthesis — would be relevant to FASD. However, given that miR-1192 was not confirmed by qRT-PCR, no direct conclusions can be made. A model for the molecular interaction between each of miR-1192 and miR-532-5p with *Atf1*, *Itpripl2*, and *Stxbp6* is shown in **Figure 28**.

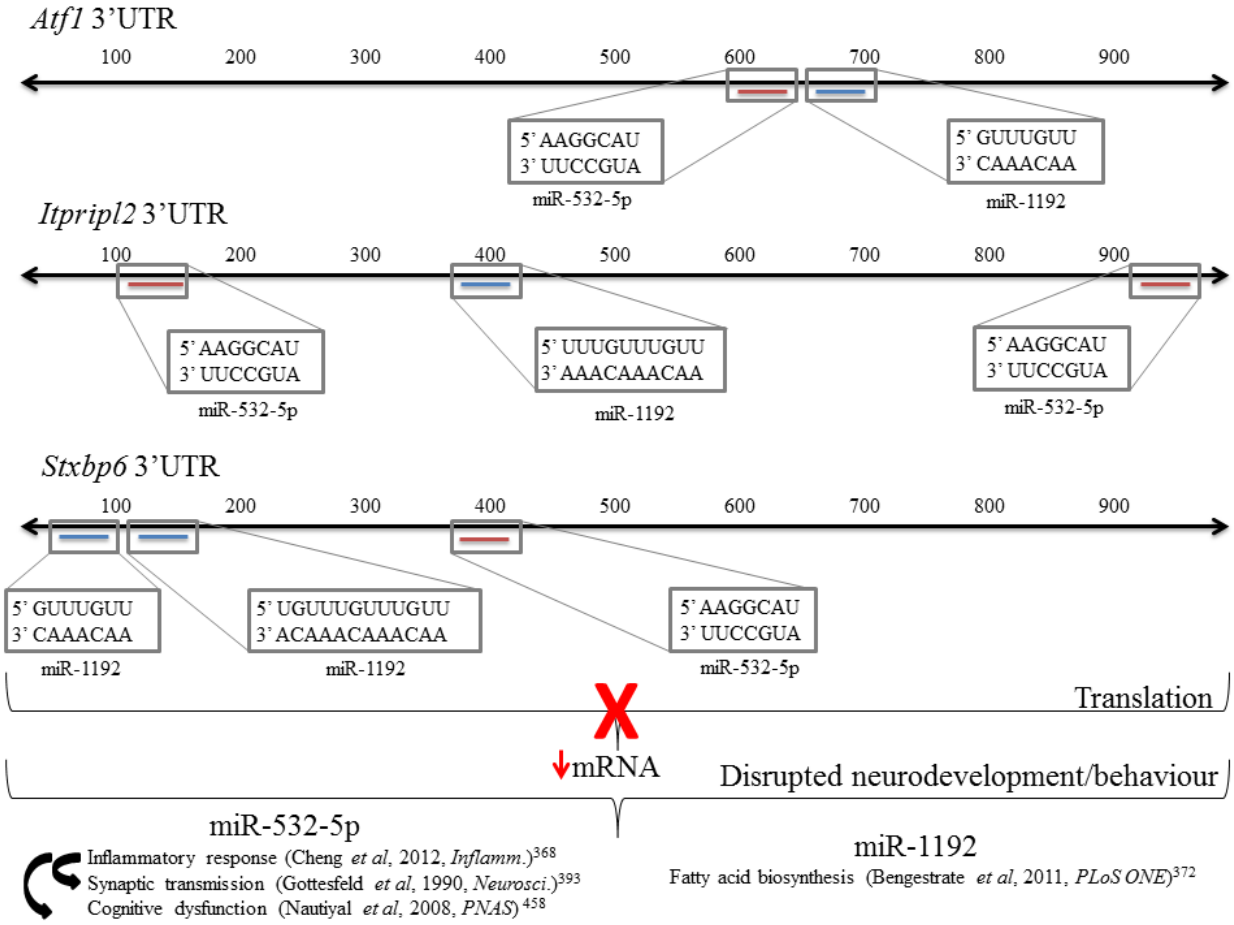

Figure 28. The molecular interaction between each of miR-1192 and miR-532-5p with *Atf1*, *Itpripl2*, and *Stxbp6*, and their potential implication for FASD-relevant cellular processes and behaviours. Alignment sequences of microRNAs 1192 (miR-1192) and 532-5p (miR-532-5p) with *Activating transcription factor 1* (*Atf1*), *Inositol 1,4,5-triphosphate receptor interacting protein-like 2* (*Itpripl2*), and *Syntaxin binding protein 6 (amisyn)* (*Stxbp6*) were idenitifed using the microRNA.org – Targets and Expression database (http://www.microrna.org/microrna/home.do/). Prediction of binding between microRNAs and targets was performed using microRNA.org. Red arrows indicate expression. A red "X" indicated blocking. Dashed arrows indicate a potential correlation. UTR = untranslated region.

4.2.4 Ethanol exposure during trimester two (T2-L) leads to long-term maintenance of molecular changes in the adult brain

a) Long-term (T2-L) process 1: unfolded protein response

Functional, pathway, and network analysis of T2-L ethanol-responsive genes resulted in a variety of disrupted biological processes. Second trimester treatment with ethanol resulted in alterations to UPR, which occurs in the ER. The ER quality control system recognizes unfolded or misfolded proteins and activates stress-signaling pathways (UPR pathways) via ER stress sensors[377]. Altered ER stress response signaling, resulting from promoter polymorphisms in HSPA5, has been previously implicated in bipolar disorder[378]. Changes in ER-related stress response have also been implicated in a variety of other neurodevelopmental disorders including myopathy and Alzheimer's Disease[379,380]. Presence of *Homer1* in the third IPA network (**Figure 24**), along with *Homer1*'s vast roles in working memory and spatial navigation, make this gene a suitable candidate for FASD. Isoforms of *Homer1* are involved in mediation of behaviour, maintenance of basal extracellular glutamate, and regulation of the prefrontal cortex (PFC) glutamate release relevant to schizophrenia and stimulant abuse comorbidity[381]. Modulation of glutamatergic transmission by ethanol has also been demonstrated in a rat model of FASD[382]. Perinatal alcohol exposure induces subtle differences in hippocampus-dependent spatial learning, accompanied by glutamate transmission-related gene expression in the adult hippocampus[383]. The UPR regulates glutamate receptor export in the ER[384]; glutamate regulation is important for FASD-related behaviours. Genes such as *Homer1* are relevant in the maintenance of FASD-related phenotypes, such as spatial learning. The ER is also involved in storing and releasing calcium for the biosynthesis of lipids and sterols. This is relevant given that calcium signaling was identified as a disrupted process in T2-L using IPA and Pathway Express. *Tbxa2r*, *Ighg*, and

Troponin C type 1 (slow) (*Tnnc1*) are each implicated in calcium signaling. Calcium signaling is related to FASD since prenatal ethanol exposure alters calcium signaling in neurons that are responsible for directing cellular activity and survival, thereby leading to apoptosis in the developing brain[385]. Given that neural cell proliferation and migration occurs in the second trimester, it is likely that calcium signaling may be disturbed. The top IPA network contains most of the genes that were characterized in ER- and protein-related functions including: *Hspa5, Dnajb11, Pdia4, Pdia6, Xbp1*, and *FK506 binding protein 2, 12kDa* (*Fkbp2*) (**Figure 22**). In this network, it appears that the downregulation of *Xbp1* may lead to the downregulation of other genes including, *Hspa5, Sdf2l1, Pdia4, Pdia6, Dnajb11* and *Fkbp2*. Given these interactions, *Xbp1*'s regulation may be important in the maintenance of FASD-related phenotypes. A network-based model for this interaction is shown in **Figure 29**. XBP1 is reported to regulate a subset of ER resident chaperone genes, including *Hsp40*-like genes (*Dnajb11*), in the UPR[386]. Given that *Xbp1* is highly expressed in neurites during neurodevelopment, through the induction of Brain-derived neurotropic factor (BDNF)[387], its role in the maintenance of FASD is possible. ER stress plays a role in the pathogenesis of several other neurological diseases such as Alzheimer's Disease and Parkinson's Disease[388,389]. As a key TF in the UPR pathway, XBP1 has been implicated in the pathophysiology of many neurodevelopmental disorders, such as schizophrenia[390]. Another gene, *Manf,* is downregulated in the second IPA network (**Figure 23**). Given that MANF acts as a neuroprotective molecule by reducing ER stress[240], MANF's downregulation could contribute to maintenance of FASD-related features impacted by ER stress.

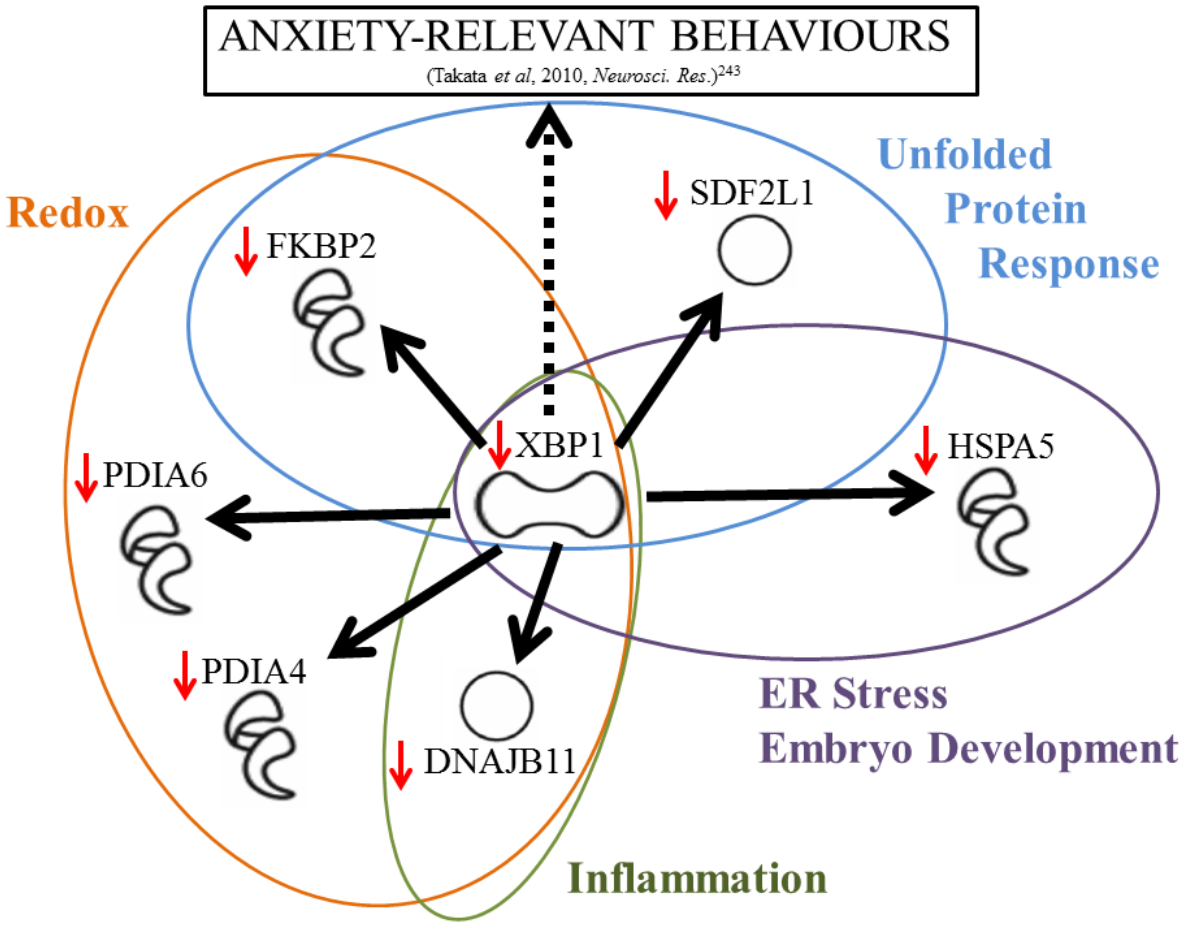

Figure 29. A network-based model for the interaction of second-trimester disrupted molecules and their implication in FASD-relevant cellular processes and behaviours. Black arrows indicate a molecule's interaction. A dashed arrow represents a correlation between a molecule and a behaviour. Red arrows indicate downregulation. Redox = reduction/oxidation. ER = endoplasmic reticulum. Molecular symbols are generated from Ingenuity Pathway Analysis (IPA). Refer to Appendix F for a full legend of molecular shapes from Ingenuity Pathway Analysis. X-box binding protein (XBP1) is represented by a "transcription factor" IPA symbol. FK506 binding protein 2, 13kDa (FKBP2), Protein disulfide isomerase family A, member 6 (PDIA6), Protein disulfide isomerase family A, member 4 (PDIA4), and Heat shock 70kDa protein 5 (glucose-regulated protein, 78kDa) (HSPA) are represented by an "enzyme" IPA symbol. Stromal cell-derived factor 2-like 1 (SDF2L1) and DnaJ (Hsp40) homolog, subfamily B, member 11 (DNAJB11) are represented by an "other" IPA symbol.

b) Long-term (T2-L) process 2: immunity

Immune system response is another disrupted process following second trimester ethanol exposure. Given that the immune response is also compromised following ethanol treatment in the first trimester (T1-L), and immediately following ethanol administration in the second trimester (T2-S), this may represent a general process that is disputed no matter the timing or developmental stage of exposure. **Figure 30** illustrates the T2-S, T1-L, and T2-L DEGs that were involved in immune response. DAVID clustering analysis resulted in "systemic lupus erythematosus" as a significantly affected KEGG pathway, which included several histone genes, *Ighg*, and *Ptpn22* (**Table 19**). These results are consistent with IPA functional analysis that implicated SLE as a top function under "Inflammatory Disease" (**Table 21**). T cells are defective in individuals with SLE[391]. Researchers have reported lowered T cell numbers in fetal mice exposed to ethanol; however, the ability of T cell levels to "catch up" to normal levels was reinstated in adulthood[392]. Other have reported that, as young adults, mice prenatally exposed to ethanol displayed immunological changes including depressed ability to produce cellular immune responses and altered synaptic transmission[393]. Such studies support my hypothesis that the immune system is compromised, even into adulthood, following *in utero* ethanol exposure. Of the top three networks in T2-L, the first network is relevant to immunity, and includes, *Cdkn1a*, *Xbp1*, *Ptpn22*, *Hist1h3a* and all other histone genes, which are all downregulated (**Figure 22**). XBP1 is a downstream target of Inositol-requiring transmembrane kinase/endonuclease-1 (IRE1α), which is a UPR element that senses bacterial proteins invading the ER to activate innate immune signaling[394]. Mice deficient in XBP1 show greater bacterial burden than control mice once infected with a pathogen, which implicates XBP1 in mammalian host defense[395]. Herein, *Xbp1* — possibly influenced by other factors such as IRE1α — may be

an important player in maintaining a compromised immune system into adulthood. Downregulation of other genes resulting from downregulation of *Xbp1* may represent an important cascade of events that together lead to compromised immunity in FASD. Another gene, *Homer1*, was downregulated in the third IPA network (**Figure 24**). Its interaction with IL-5, which is a cytokine that participates in the regulation of immune response, may suggest that immunity is compromised by IL-5's action on *Homer1*.

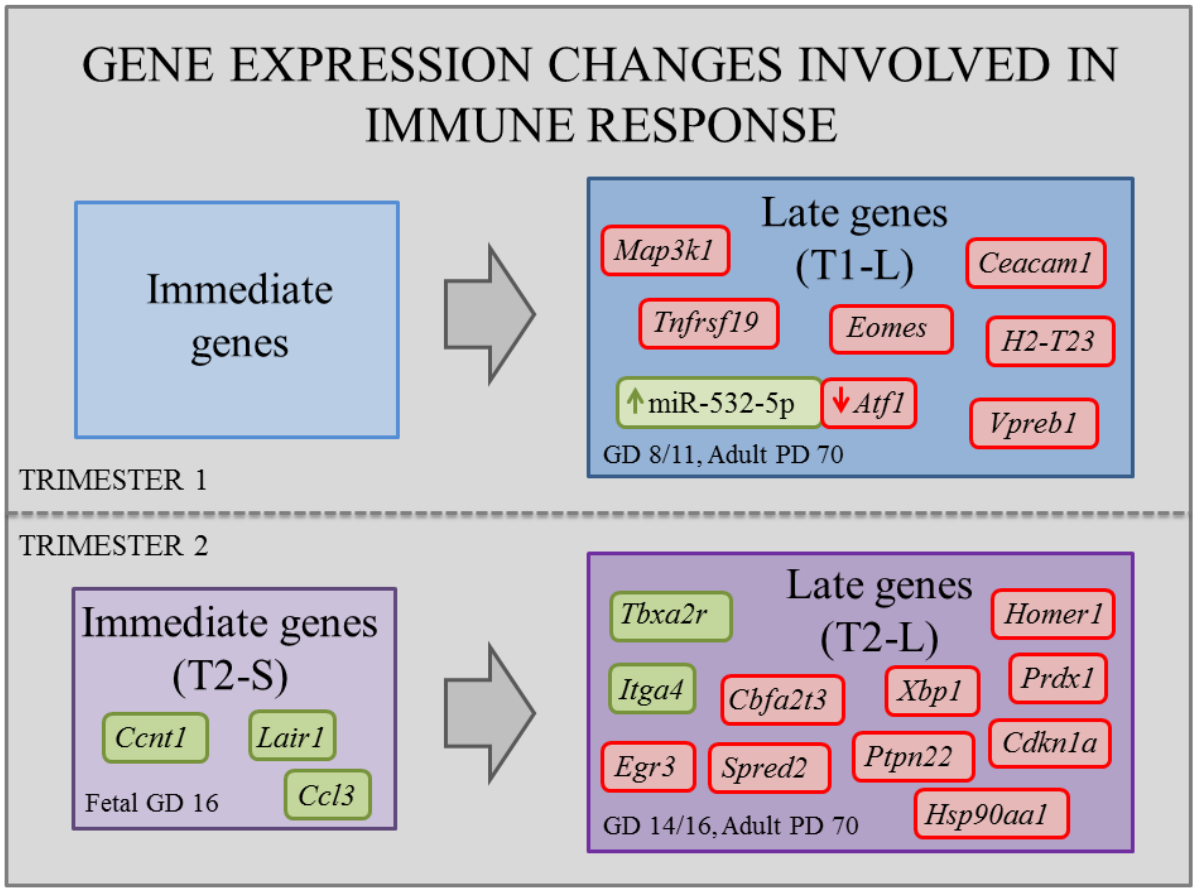

Figure 30. Immune genes altered in the fetal (immediate) and adult (late) brains following binge ethanol exposure in the first and second trimesters. Differentially-expressed genes identified using Partek Genomics Suite. Upregulated (green) and downregulated (red) genes are shown for each group. T2-S = trimester two treatment, short-term exposure. Fetuses were exposed to ethanol at gestational day (GD) 16, and fetal brains were isolated two hours post maternal injections. T2-S genes included: *Chemokine (C-C motif) ligand 3* (*Ccl3*), *Cyclin T1* (*Ccnt1*), and *Leukocyte-associated immunoglobulin-like receptor 1* (*Lair1*). T1-L = trimester one treatment, long-term exposure. Fetuses were exposed to ethanol at GD 8 and 11. T1-L genes included: (*Atf1*), *Carcinoembryonic antigen-related cell adhesion molecular 1 (biliary glycoprotein)* (*Ceacam1*), *Eomesodermin (Xenopus laevis) homolog* (*Eomes*), *Major histocompatibility complex, class I, E* (*H2-T23*), *Mitogen-activated protein kinase kinase kinase, E3 ubiquitin protein ligase* (*Map3k1*), *Tumor necrosis factor receptor superfamily, member 19* (*Tnfrsf19*), and *pre-B lymphocyte 1* (*Vpreb1*). T2-L = trimester two treatment, long-term exposure. Fetuses were exposed to ethanol at GD 14 and 16. T2-L genes included: *Core-binding factor, runt domain, alpha subunit 2; translocated to, 3* (*Cbfa2t3*), *Cyclin-dependent kinase inhibitor 1a* (*Cdkn1a*), *Early growth response 3* (*Egr3*), *Homer homolog 1 (Drosophila)* (*Homer1*), *Heat shock protein 90kDa alpha (cytosolic), class A member 1* (*Hsp90aa1*), *Integrin, alpha 4 (antigen CD49D, alpha 4 subunit of VLA-4 receptor)* (*Itga4*), *Protein tyrosine phosphatase, non-receptor type 22 (lymphoid)* (*Ptpn22*), *Peroxiredoxin 1* (*Prdx1*), *Sprouty-related, EVH1 domain containing 2* (*Spred2*), *Thromboxane A2 receptor* (*Tbxa2r*), and *X-box binding protein 1* (*Xbp1*). Adult brains from T1-L and T2-L were isolated at postnatal day (PD) 70.

c) Long-term (T2-L) process 3: chromatin stability

Evidence for the role of epigenetics and histone modifications in FASD arises from T2-L functional and pathway analysis. As identified in the fetal brain following second trimester ethanol exposure (T2-S), chromatin stability is also a disrupted process in the adult brain following trimester two ethanol exposure (T1-L). Along with all histone genes, *SWI/SNF related, matrix associated, actin dependent regulator of chromatin, subfamily A, member 5* (*Smarca5*) is involved in the maintenance of chromatin structures during DNA replication (**Table 19**). The histones, along with *Cdkn1a*, are also involved in "transcriptional misregulation in cancer" (**Table 23**). The role of chromatin remodeling has been implicated in genome stability[396], and has been heavily discussed in terms of cancer[397,398]. Like cancer, damage to cellular development and organization occurs following prenatal alcohol exposure. Identification of pathways involved in cancer is reasonable. IPA network analysis of T2-L genes resulted in *Cdkn1a*, *Smarca5*, and several histones implicated in the first network (**Figure 22**). Given each of their interactions with the E2f transcription factor complex, their dysregulation may affect each other's regulation. *Smarca5* is upregulated and directly acts on E2f, which leads to a downregulation in histones. *Cdkn1a* indirectly acts on E2f, which may also lead to the downregulation of histones. The combination of a decrease in *Cdkn1a* and an increase in *Smarca5* may, through E2f, lead to a disruption in histones. Given that E2f members play important roles in the cell cycle, it is presumable that histones, *Cdkn1a*, and *Smarca5* — which are involved in chromatin formation — would be disrupted. Mutations in $SMARCB_1$, which is the a member from the same family as SMARCA5, leads to epigenetic dysregulation of chromatin in individuals with intellectual disabilities[399]. Similarly, *Smarca5* could play a role in regulation of chromatin structure, which may be disrupted following damage due to ethanol. The role of chromatin remodeling in

neurodevelopmental disorders has not been extensively examined to date. Researchers have reported disruption of chromatin-remodeling factors in studies on prenatal alcohol exposure and FASD[400,401]. Only recently have researchers investigated epigenetic modification of chromatin structure — which controls gene transcription — in neurons, as a mechanism in the etiology of intellectual disability[399,402]. Further studies examining ethanol's effect on chromatin stability may offer insight into the biological underpinnings of FASD.

d) Long-term (T2-L) process 4: free radical signaling

A final mechanism that is disrupted in the adult brain following second trimester ethanol exposure is free radical signaling. Proper cellular maintenance is disrupted following prenatal alcohol exposure. *Pdia4*, *Pdia6* and *Prdx1* have been implicated in reduction-oxidation (redox) processes from DAVID and GE analyses (**Tables 19-20**). Knockout of *Prdx1* results in an increased need for double stranded break repair due to increased accumulation of highly reactive OH• radicals[403]. Given *Prdx1*'s role in erythrocyte antioxidant defence and tumor suppression[404], its downregulation as a result of ethanol exposure is reasonable. Researchers have yet to examine whether ethanol disrupts *Prdx1* levels directly. Polymorphisms in another gene, *Itga4*, have been associated with susceptibility to multiple sclerosis (MS) and autism, which show comorbidity with FASD[405,406]. Both MS and autism have been linked to oxidative damage[407,408]. The PI3K/AKT signaling pathway was implicated as a top canonical pathway from IPA (**Table 24**). Reactive oxygen species (ROS) via redox signaling to the PI3K/AKT pathway contribute to mammalian growth of epithelial cells[409]. The PI3K/AKT pathway may be an important disrupted process in the adult brain following gestational ethanol exposure. Alterations to free radical signaling, associated with oxidative stress, are mechanisms by which ethanol exerts its long-term effects on the brain following mid-gestation ethanol exposure. The role of oxidative stress in

FASD is well-established in the literature[44,45,410,411]. Prenatal ethanol exposure causes an increase in oxidative stress, particularly in the brain[410,411]. Even a brief exposure to ethanol during gestation can produce an imbalance in the brain's intracellular redox state[412]. Such imbalances in proper brain-related redox maintenance correlate with FASD-relevant spatial learning deficits[413]. Therefore, FASD-related behavioural deficits may result from damage to cellular redox, including ROS.

e) Confirmation of T2-L-specific genes using qRT-PCR

Quantitative RT-PCR resulted in confirmation of DEGs from T2-L analysis (**Table 28**). The downregulation of *Calcium/calmodulin-dependent protein kinase 1G* (*Camk1g*), *Cdkn1a*[158], *Manf*[158], *Egr3, Ccdc6, Xbp1*, and *Hspa5* was confirmed. Although statistically significant by qRT-PCR, *Homer1* and *Hsp90aa1* were increased in ethanol samples compared to control samples, which is opposite to the array results. *Tbxa2r* was the only gene that did not confirm. Other researchers suggest that qRT-PCR is not sensitive to detect fold changes lower than 2.0[414,415], which could be a potential contributing factor to these results.

f) Alteration of microRNAs following second-trimester ethanol exposure

i. General trends in alteration of mouse-specific miRNAs

The results from mouse miRNA arrays show that second trimester ethanol exposure affects miRNA expression in the adult brain. Since only 20 mature, mouse-specific miRNAs out of ~1000 were significantly affected (± 1.2-fold change, $p < 0.05$), the results are not stringent enough to make conclusions on array data, as discussed for T1-L. The results from T1-L and T2-L analyses suggest that alterations to specific miRNAs are dependent on the timing of gestational

ethanol exposure. There were no miRNAs in common between T1-L and T2-L, which signified the timing-specific effects of ethanol on miRNA expression.

ii. Candidate mouse-specific miRNAs in T2-L

In T2-L, target filtering using IPA resulted in six differentially-expressed miRNAs known to interact with mRNAs (**Table 30**). Ten genes were identified to interact with these six miRNAs, all of which were downregulated. Twelve interactions were found between genes and miRNAs. Only one interaction exhibited an inverse relationship between mRNA and miRNA: decreased *Ccdc6* and increased miR-302c. The upregulation of miR-302c was confirmed by qRT-PCR. Similar to T1-L, one miRNA (i.e. miR-449b) can have multiple target mRNAs (i.e. *Cbfa2t3*, *Galnt7*, and *Xbp1*), and one gene (i.e. *Ccdc6*) can be regulated by multiple miRNAs (i.e. miR-146b and miR-302c). Unlike T1-L miRNA results, most miRNAs in target filtering analysis were downregulated. This inconsistency lends to the timing-specific effects of prenatal ethanol exposure. The downregulation of miRNAs as a result of ethanol exposure has been reported by other researchers[174,367].

Given that in T2-L analysis, *Ccdc6* is the only gene with an inverse relationship to a miRNA, its confirmation by qRT-PCR was pursued. Recently, Merolla and colleagues identified CCDC6, a pro-apoptotic phosphoroprotein, to be responsive to genotoxic stress; genotoxic stress is defined as damage to the genome of an organism as a result of a genotoxin[234]. Increased genotoxic stress has been linked to teratogenic substances, including ethanol[416]. Increased stress can lead to disruption of signal transduction pathways that regulate cell cycle progression and DNA stability[417]. DNA stability, specifically chromatin stability, and cellular redox, were disrupted processes following prenatal ethanol administration during the second trimester. As the

only target-filtered miRNA, miR-302c was confirmed using qRT-PCR (**Figure 27**). The miR-302 cluster has been identified as a key family of miRNAs involved in embryonic stem cell-specific cell cycle regulation and reprogramming of both human and mouse embryonic fibroblasts[418,419]. MiR-302c and *Ccdc6* are involved in DNA damage and stability, which is impacted in trimester two following *in utero* ethanol exposure; thus, their relationship is relevant to FASD. MiR-302c directly contributes to regulation of p21 (CKDN1A) expression in human embryonic stem cells, thus illuminating its role in governing G1/S transition checkpoint during DNA damage[420]. *Cdkn1a*, whose expression was confirmed by qRT-PCR, was also identified in target filtering analysis, albeit not for its relationship with miR-302c.

4.2.5 Hub genes may identify gene sets altered following prenatal ethanol exposure

Following the interpretation of specific cellular processes that are disrupted in each treatment (T2-S, T1-L, and T2-L), I further examined the hub molecules in a merged network analysis of each group. An investigation of these hubs, and their interactions with DEGs, may illuminate potential cellular processes that are relevant to FASD. Some of the mechanisms of these hub genes may overlap with processes identified in functional, pathway, and network analyses. Examination of hubs may help to identify any overarching gene sets that are disrupted following prenatal ethanol exposure. Identification of specific gene sets and processes via hub molecules may help to elucidate the underlying mechanisms governing FASD.

a) Short-term hub molecules following second-trimester ethanol exposure (T2-S)

The top two merged networks from short-term analysis with > 10 genes showed that FOS and HTT were hub molecules (**Figure 17**). FOS was found to directly interact with PIP5K1B, which is involved in postsynaptic neuronal signaling and has been implicated in autism spectrum

disorders[222]. HTT directly interacts with two factors: HPCA and BCAP31. *Bcap31* is involved in a variety of cellular processes including fragmentation of mitochondria, mitochondrial calcium ion concentration, embryonic development, free radical scavenging, apoptosis, and immune response. Given that HTT directly affects both upregulated (HPCA) and downregulated (BCAP31) molecules, this lends to the complexity of gene expression alterations underlying FASD. FOS and HTT are involved in apoptosis in the developing brain, and neuronal survival during brain development, respectively; their immediate responses to heavy doses of ethanol are expected.

Another hub molecule from T2-S is Interleukin 4 (IL-4), which is an inflammatory interleukin linked with autism[421]. Disruption of proinflammatory cytokines may impair cognition[422,423]. Compromised immune activity in the CNS is considered detrimental to cognitive function. An IL-4 deficiency in mice leads to severe cognitive impairment and reductions of BDNF mRNA production in astrocytes[424]. IL-4 acts on Small proline-rich protein 2A (SPRR2A) and CCL3, which are upregulated in the merged network. *Ccl3* is involved in many functions including: muscular dystrophy; microglial, astrocyte and dendrite development; and immune response. CCL3's interaction with interleukins may be an important mechanism by which ethanol exerts its effects. Or, IL-4 may result in increased expression of *Sprr2a* and *Ccl3* as a protective mechanism against ethanol teratogenicity.

Other hubs in the T2-S network, such as TNF, NFkB, and Amyloid beta (A4) precursor protein (APP) also act on the upregulated factor, CCL3. TNF, NFkB and APP are involved in regulation of hippocampal synaptic plasticity and synapse formation[425,426]. Studies suggest that NFkB and APP also have important roles in learning and memory in mice by modulation of synaptic plasticity and growth of dendrites[426,427]. Because of their roles in hippocampal memory

formation, TNF, NFkB, and APP are prime candidates for FASD. Cellular processes related to TNF, NFkB, and APP are consistent with the known processes of disrupted genes (eg. *Ccl3*). APP's well-defined role in cognitive decline in Alzheimer's disease also makes it a suitable candidate for other neurodevelopmental disorders[428]. Both TNF and NFkB also interact with *Crem*, which is one of the few downregulated genes in the IPA network. The interactions between these genes point to the complexity in immediate responses of the fetal brain as a result of ethanol exposure. Another apoptosis factor affected in T2-S, Tumor protein 53 (TP53), has direct effects on TDG, which is upregulated. TP53 is a tumor suppressor protein that functions in apoptosis and genomic stability, and is often associated with cancer[429]. This hub directly affects TDG, an enzyme that corrects DNA mismatches. An upregulation in *Tdg* likely occurs immediately following ethanol exposure, particularly if cells are attempting to increase this repair enzyme. Ethanol exposure can result in DNA damage[430]. An increase in *Tdg*, which interacts with a central regulator of DNA damage (TP53), may be beneficial to the fetus, as an attempt to decrease DNA damage.

b) Long-term hub molecules following first-trimester ethanol exposure (T1-L)

Merged network analysis of T1-L was not carried out, given that only one network with > 10 genes was implicated (**Figure 19**). Network one contained three hub molecules, one of which was IFNG. IFNG has 18 interactions with other genes, three of which include the downregulated molecules, CEACAM1, MAP3K1and HLA-E (i.e. H2-T23). H2-T23 acts indirectly on IFNG. IFNG itself acts indirectly on CEACAM1 and MAP3K1. Along with interleukins, Interferon gamma, an inflammatory cytokine, has been implicated in neurodevelopmental disorders including autism and schizophrenia[431–433]. IFNG is increased at mid-gestation in women bearing children with autism[421]. The immune system is compromised in children with FASD[353,434], and in

animal models of FASD[435,436]. Given its role in immunity, IFNG may be a key player in the maintenance of alcohol-related transcriptome changes. H2-T23 and MAP3K1 are involved in HTLV-I Infection, while CEACAM1 and MAP3K1 are involved in regulation of MAPK activity. Downregulation of H2-T23 and MAP3K1 in this network, through IFNG, may lead to compromised cell immunity.

Also considered as hubs in T1-L, PPARα and PPARγ have > 10 interactions with other genes in the network. The upregulated molecule, *Major urinary protein 5* (*Mup5*), is directly acted upon by PPARα, whereas *Mup5*, itself, acts indirectly on PPARγ. PPARα and PPARγ both act directly on HMGCS2, which is downregulated, and PPARγ also acts directly on PCNA. PPARs function in metabolic pathways as transcription regulators of gene expression, and play important roles in cellular differentiation, development, tumorigenesis, and metabolism[437]. PPARs provide nuclear control of lipid metabolism and inflammation[437,438]. PPARs have been implicated in cancer, and, most recently, childhood obesity[439,440]. Following prenatal ethanol exposure, these hub molecules could disrupt other genes. In this network, PPARs may contribute to the downregulation of HMGCS2 and PCNA. HMGCS2 and PCNA are involved in ketogenesis (fatty acid breakdown) and base-excision repair (DNA damage, cancer), respectively. Tumor Necrosis Factor-alpha, Extracellular signal-regulated kinases (ERK), c-Jun NH(2)-terminal kinases (JNK) and p38 MAPKs each regulate PPARs. The regulation between these factors adds to PPARs' diverse roles in cell signaling[441]. *Mup5*, which is involved in fatty-acid binding, is upregulated in coordination with the downregulation of PPARs. This relationship further illustrates the complexity of adult genetic interactions disrupted following prenatal ethanol exposure in the first trimester.

c) Long-term hub molecules following second-trimester ethanol exposure (T2-L)

Merged network analysis of the top three networks from T2-L by IPA included a list of 11 hub molecules (**Figure 25**). The hubs included CDKN1A and XBP1. Previous functional analysis identified that CDKN1A plays a role in PI3K/AKT signaling. PI3K/AKT signaling is an important pathway for apoptosis, so CDKN1A's importance as a central hub molecule is relevant especially since neuronal apoptosis occurs following prenatal ethanol exposure[50,53,54,442]. XBP1 is important for initiating UPR in neurites[242]. Dysregulation of XBP1 can affect neurite outgrowth during the first trimester. In the merged network, CDKN1A was found to bind to HSP90AA1, and interact indirectly with Prolyl 4-hydroxylase, alpha polypeptide I (P4HA1). XBP1 was found to interact directly with six genes (**Figure 25**). The downregulation of XBP1 may be influencing the downregulation of multiple genes, some of which are involved in ER-related functions, particularly ER stress response. This cascade would likely contribute to ER-induced damage following mid-gestation ethanol exposure, which is maintained into adulthood.

Similar to T1-L, IFNG is a hub molecule in T2-L analysis that includes interactions with three downregulated genes including: GCHFR, CDKN1A, and EGR3. Given its previously discussed role in inflammation, it is logical that prenatal ethanol exposure at any gestational time during would compromise the immune system. Of the hub molecules in **Figure 25**, FOS, HTT, ERK1/2, IL5, v-erb-b2 erythroblastic leukemia viral oncogene homolog 2, neruo/glioblastoma derived oncogene homolog (avian) (ERBB2), and Polyketide synthase (Pkc) interacted with give or more input genes (DEGs), signifying the dynamic reach of each of these hubs. Erbb2 is a receptor for neuregulins. Erbb2 has been implicated as a regulator of neuromuscular synapse formation and is an essential component for muscle spindle development[443]. In T2-L functional analysis, muscle spindle development was a disrupted process. As described for T1-L and T2-S,

interleukins are important for proper immune system response[431]. In addition to IL-4 (T2-S), IL-5 was implicated in children with autism[421]. Given that IL5 has been associated with neurobehavioural and motor disturbances upon neonatal infection[444], its role as a central hub molecule in second trimester ethanol exposure is reasonable. Another set of hubs includes the PKS genes, which are involved in fatty acid biosynthesis[445,446], which is an affected process in T1-L. The PKS hub genes may be relevant in establishing ethanol-induced abnormalities in the fetus following both early and late-gestation exposure.

ERK1 and ERK2 are part of another hub in T2-L (**Figure 25**). These kinases comprise a specific subset of MAPKs that are involved in cell proliferation and growth signaling[447]. Disruption of ERK genes is common in cancers[448]. Trimester two is an important time for cell growth and proliferation. Some of the merged network interactions between ERK1/2 and DEGs involve those implicated in cellular development, cell death and cellular compromise (*Xbp1*, *Cdkn1a*, *Hspa5*). The importance of the ERK pathway is relevant in the maintenance of neurodevelopmental outcomes.

Commonly referred to as c-Fos, FOS is also a central hub molecule in this merged T2-L network. FOS was also a hub in T2-S. Given that ethanol was administered at GD 16 for both treatments, this similarity is understood. It is interesting to find that the same hub genes are affected during the fetal stage, and even into the adult stage. As a proto-oncogene, *c-Fos* contributes to apoptosis in the frontal cortex and hippocampus[449]. Apoptosis in these brain regions is relevant to the pathogenesis of schizophrenia, particularly in negative symptoms including decreases in reactivity, volition (will) and goal-directed activity upon stress[450,451]. In the merged network, FOS interacts with XBP1, in which polymorphisms have been implicated in the pathogenesis of schizophrenia in humans[390,452] and in mouse models of schizophrenia[243].

Given that XBP1 may downregulate other genes implicated in neurodevelopmental disorders, it is reasonable that its apoptotic properties are important in the development and maintenance of FASD.

Another interesting hub molecule in T2-L, HTT, interacts directly with five DEGs, and binds with P4HA1 (**Figure 25**). HTT is involved in neuronal migration and survival during brain development[453]; its implication as a central hub in FASD is both novel, and not surprising, given its brain-related role. Its interaction with HOMER1, which is involved in working memory and spatial navigation, along with its implication in behavioural despair and anxiety, further adds to the evidence surrounding its importance in the pathogenesis of neurodevelopmental disorders[237]. Each of the T2-L hub molecules play relevant roles in brain-related functions and their implications in FASD are well-founded.

4.3 Limitations of molecular studies on FASD

Using a mouse model to study molecular mechanisms underlying complex disorders, i.e. FASD, has limitations. Although minimal guidelines are set out for microarray-based gene expression studies[454,455], it is difficult to find consistency in array design. For instance, I used two biological replicates (arrays) for my experimental design, whereas three biological replicates are considered as the minimum standard amongst researchers. To overcome such limitations, I pooled three samples on each array. In addition to biological replicates, the industry standard requires technical replicates. It was not feasible to include more than one technical replicate in the array design. However, qRT-PCR of specific genes included three technical replicates per biological sample, which offers reproducibility of results[456]. Another caveat to my study includes the exclusion of one biological replicate (ethanol, T2-L) in qRT-PCR confirmation experiments.

I chose to discount this sample due to a low A260/A280, indicating possible contamination or degradation of RNA. Given that six samples are standard in qRT-PCR confirmation[456], my results from this analysis do not meet industry guidelines. A final caveat to molecular studies includes disuse of a FDR-corrected *p*-value to create the ANOVA gene lists. A FDR is a standard correction for multiple testing (i.e. false positives), which is a key issue in microarrays[457]. The exclusion of a FDR was necessary in my study because there were no differentially-expressed genes using a 1.1-fold change cut-off with an FDR-corrected $p < 0.05$. Because I did not use a multiple testing correction strategy, my array results likely contain > 5% false positives. Although these sources of error may impact the results, I have attempted to overcome these limitations, and caution the reader on the existence of such caveats.

Other than the technical limitations of my study, it should also be noted that a different set of genes was identified in a downstream analysis of 12 arrays. These 12 arrays included my eight long-term arrays (n=4 trimester one, n=4 trimester two) that were analyzed in Partek with another set of four long-term (trimester three) arrays. A 12-array analysis was pubished by our group in the *Journal of Neurodevelopmental Disorders* (see Co-authorship statement for details)[158]. Although the methods in this publication included the use of the same eight long-term arrays that were discussed in this thesis, the 12-array analysis resulted in the identification of substantially more DEGs. Since 12-array data was included in a single analysis in the publication — whereas data from each trimester was generated separately for this thesis — the results differ. Even with a FDR correction for multiple testing, our publication reported 195 and 231 DEGs in trimester one and two, respectively, using the same cut off criteria ($p < 0.05$, ± 1.2-fold change). Given the inconsistency of the results, it is relevant to comment on why such differences may be observed. A 12-array comparison across ethanol and control arrays would

provide greater statistical power to generate real differences between groups. The specific genes that were differentially-expressed were largely different from those reported in this thesis. This inconsistency reflects increased statistical power in detecting real differences that resulted from increased sample size (3-fold). It must also be noted that, although the number of DEGs was increased in our publication, the fold-changes were subtle (most 1.1-1.5-fold), which is similar to the pattern of differential expression in my thesis. Also, a 12-array comparison is more robust than a 4-array comparison. The findings from our publication may represent a more robust gene-set, whereas those from my thesis may represent a more relaxed gene-set, with increased potential for false positives.

It is difficult to rectify the discrepany across results from two different sets of analyses. However, although different gene-sets were established, a comparison at the network-level (IPA) may offer an encouraging explanation. In both 12-array and 4-array analyses, trimester one pathways and networks were involved in cellular development, cell death, G-protein coupled receptor signaling, and fatty acid biosynthesis. Again in both sets of analyses, trimester two networks were involved in neurological disease, with APP, HTT and FOS as hub molecules. Furthermore, common trimester two canonical pathways included ER stress response and calcium signaling. Given the comprehensive nature of the results using a 12-array analysis, one may expect larger networks with a greater number of hub genes. The results from my thesis are functionally similar to those in our publication, but on a smaller scale. The downstream network analyses in my thesis are therefore consistent with those in our publication. It should also be noted that the results from both sets of analyses represent subtle changes to the brain transcriptome, affecting similar functions, pathways, networks, and cellular processes. Given the robust nature of our publication results, one might expect that confirmation of specific genes

using qRT-PCR would be more in-line with our publication results. However, the opposite may also be true. Comparing my 4-array analyses with the 12-array analysis, there were four genes (*Tnfrsf19*, *Trdn*, *Vpreb1*, *Zfp763*) in common for trimester one, and three genes (*Cdkn1a*, *Hist1h2bm*, *Manf*) in common for trimester two. Therefore, one must interpret microarray data with caution, no matter the stringency of the criteria. It is possible that false positives may occur regardless of statistical procedures. Given the inconsistent nature of microarray data, confirmation techniques are necessary to provide reliable and reproducible results. Ultimately, the main goal of microarrays is to identify functional relationships and cellular processes that are disrupted following a specific treatment, and not necessarily the identification of specific genes.

4.4 Prenatal ethanol exposure and its relevance to behaviours, genes, and miRNAs

In the long-term analyses, a relationship between FASD-relevant behaviours and changes in the transcriptome can be inferred. Behavioural deficits including, developmental milestones, activity, and spatial learning are generally impaired no matter the timing of gestational ethanol exposure. However, there are some behavioural differences. Trimester two ethanol exposure resulted in timing-specific behaviours including decreased anxiety-like behaviours and consistent spatial learning deficits in ethanol versus control mice. Whereas, trimester one ethanol mice had no changes in anxiety-related behaviours compared to control counterparts. In T1-L, specific genes (*Atf1* and *Stxbp6*) were found to have an inverse relationship with miR-532-5p. Given that miR-532-5p is involved in inflammatory response[368], and may downregulate a variety of genes including *Atf1*, *Stxbp6*, and *Itpripl2*, this may lead to the overwhelming support for compromised immune system following early gestational ethanol exposure. Compromised immune system has been associated with a range of cognitive and emotional effects in offspring[458]. Given the disruptions in activity-related traits in trimester one ethanol mice, these results may point to

maintained transcriptome changes, including specific miRNAs, which may govern these behaviours into adulthood. In T2-L, only one gene, *Ccdc6*, was found to have an inverse relationship with the upregulated miRNA, miR-302c. Given miR-302c's role in DNA damage, specifically in the maintenance of embryonic stem-cell cycle regulation of fibroblasts[419,459], this miRNA can interfere with second trimester specific processes that involve cellular maintenance and development. Also, the upregulation of miR-302c could lead to a downregulation in specific genes such as *Ccdc6*. Given *Ccdc*'s role as a pro-apoptotic phosphoprotein in response to genotoxic (i.e. ethanol) stress[234], the commonality of DNA damage in this miRNA:mRNA relationship is apparent. Furthermore, researchers have suggested that DNA damage in brain cells can produce locomotor disturbances and learning and memory delays[460]. My results are consistent with these findings, and point to a relationship between specific behaviours (locomotor activity, learning and memory), genes (*Ccdc6*), and miRNAs (miR-302c) that may play a role in maintaining disrupted cellular processes (DNA damage). A model of the interaction between miR-302c and *Ccdc6*, and their potential influence of neurodevelopment and behaviour is shown in **Figure 31**.

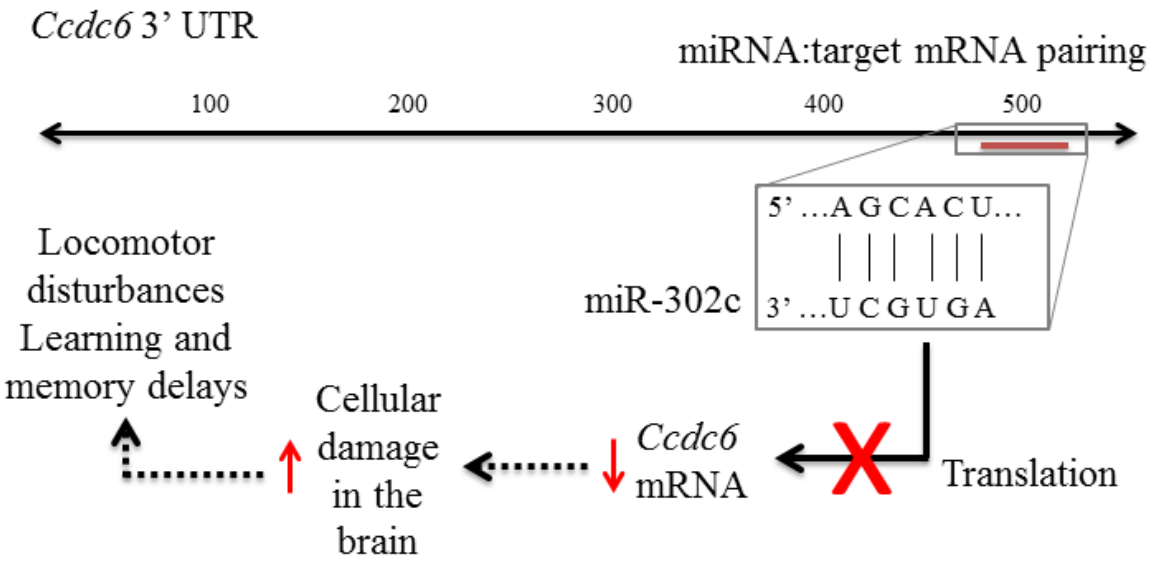

Figure 31. The molecular interaction between miR-302c and *Ccdc6*, and their potential implication for FASD-relevant cellular processes and behaviours. Alignment equences of microRNA 302c (miR-302c) and *Coiled-coil domain containing 6* (*Ccdc6*) were idenitifed using TargetScanMouse 5.2 (http://www.targetscan.org/mmu_50/). Binding of miR-302c to *Ccdc6* was predicted using TargetScanMouse. Red arrows indicate expression. A red "X" indicates blocking. Dashed arrows indicate correlation. Dark red line represents miR-302c. UTR = untranslated region.

4.5 Conclusions and implications

4.5.1 Prenatal ethanol exposure leads to behavioural and transcriptomic alterations in the mouse brain

From the behavioural experiments gathered in this report, prenatal alcohol exposure, independent on timing of exposure, leads to FASD-relevant behavioural abnormalities in B6 mice. These mice are delayed in the achievement of developmental milestones, particularly those related to motor coordination, and show increased activity levels in response to their placement in a novel environment. Although all ethanol mice exhibit deficits in spatial learning and memory, their extent depends on timing of gestational alcohol exposure. It appears that, when exposed at late-gestation, ethanol young adults can "catch up" following repeated learning trials. Anxiety-related traits are not consistent between treatments, with second trimester exposed mice showing lowered anxiety-like behaviour compared to control mice; meanwhile, first trimester ethanol and control mice are not significantly different. Such a marked difference in timing of exposure is consistent with the spectrum of disabilities observed in individuals with FASD.

The second set of experiments provided evidence that prenatal ethanol exposure leads to general alterations in the brain transcriptome, independent of timing of exposure. However, the specific genes that are altered are dependent upon timing of exposure. Furthermore, the characterized functions, pathways, and networks associated with the DEGs are consistent with disruptions of cellular and neurodevelopmental processes that occur at comparable stages of brain development. When comparing transcript levels between immediate exposure (fetal brain) and long-term (adult brain) effects of exposure, common processes related to DNA/chromatin stability, apoptosis, and inflammation are affected. Functioning of the immune system is a

disrupted process in all three treatments, indicating that it is compromised no matter of the timing or term of ethanol exposure. The confirmation of specific long-term genes involved in neurodevelopment and FASD-related behavioural phenotypes lends evidence to the functions that are maintained into adulthood. The results from gene expression analysis in this report provide further evidence that no time during gestation is safe from the teratogenic effects of alcohol on gene expression, and subsequent behavioural dysfunction.

The final sets of experiments in this thesis included the analysis of global miRNA levels in the long-term brains of ethanol mice and resulted in relatively low numbers of affected miRNAs. However, given that miRNAs can target multiple genes, it is not unlikely that only a few key miRNAs would be affected, particularly long after ethanol had been introduced to the fetus. The relationship between miRNAs and their target mRNAs revealed the importance of processes involved in cellular development, proliferation, differentiation, and repair in the pathogenesis of FASD. Although these processes peak in middle to late gestation, the results show that they are extremely important developmental mechanisms that can be disrupted at any time following prenatal alcohol exposure and may lead to FASD-related abnormalities. The experiments completed in this thesis could be adapted to studying other complex disorders.

4.5.2 Implications for FASD: from mouse models to humans

The comprehensive nature of these results, which include behavioural testing and transcriptome — including miRNA — analysis of multiple treatment groups, allow for some conclusions to be made regarding the implications to FASD. The results generated from this study have helped to elucidate the molecular mechanisms that may take place immediately following gestational ethanol exposure, and transform into changes in adulthood. Genes and

processes affected in the short-term exposure may represent direct effects of ethanol. Meanwhile, genes and processes disrupted in the long-term may result from the indirect effect of ethanol on gene expression via microRNAs. These long-term alterations may lead to a molecular "footprint" in the adult. These results help to provide evidence that no time is safe from the consumption of alcohol during pregnancy. Furthermore, although there are differences in timing of ethanol exposure, the results still point to deficits in cognitive functions and brain-related transcriptome alterations that have the potential to last a lifetime. The developing brain undergoes an immediate response to an environmental teratogen (ethanol), and will never be the same, thereby leading to life-long impairments in motor skills, activity, and spatial learning in mice. Some of these abnormalities are reminiscent to those characterizing children with FASD. Also, certain brain-related processes, including inflammation and DNA damage, are disrupted in the fetal brains of mice exposed to ethanol in the womb. The results may further help to elucidate the molecular mechanisms underlying FASD-related abnormalities. Given that these experiments were successful in determining functions, networks, and miRNAs that are disrupted following ethanol exposure, they could be developed as biomarkers for identifying individuals with FASD.

4.5.3 Future directions

The results included in this thesis implicate gene expression alterations and miRNA disruptions in FASD-related abnormalities in mice. Such results offer novel approaches toward unraveling the biological mechanisms underlying FASD. The identified miRNAs and mRNAs related to the behavioural abnormalities may present novel targets for understanding of the mechanism involved in FASD. The disrupted miRNAs and mRNA may lead to the development of biological diagnosis, via biological markers, and subsequent therapies for individuals affected with this disorder. Biological markers such as hub genes or disrupted cellular processes, coupled

with maternal education and early, multidisciplinary intervention, may provide avenues to better prognosis of families and children with FASD. Early intervention, including environmental enrichment and improved maternal care have been reported to ameliorate some of the deficits associated with prenatal alcohol exposure[35,71,187]. Multidisciplinary therapy refers to the participation of multiple individuals in helping a child with FASD. Such individuals may include parents, teachers, psychologists, and other health care professionals. Children with FASD who have a strong, multidisciplinary support-system have improved performance in the classroom[30]. The coupling of maternal education, and early and multidisciplinary intervention, with a molecular seach for biological markers in FASD will lead to better diagnosis and prognosis for individuals suffering from this disorder. This approach can be applied to other complex disorders with fetal origin.

I hypothesize that the observed changes in behaviours such as spatial learning are likely specific to particular brain regions. One of the candidate regions involves the hippocampus, which has been implicated in learning and memory[290,461]. Performing histological analysis of specific brain regions, staining for apoptotic neurons, and measuring transcriptomic and behavioural changes between control and ethanol-treated mice in a specific brain region may help to identify regional cell processes involved in specific behaviours. Once specific genes (eg. disrupted hubs) and microRNAs are identified, luciferase reporter assays or immunohistochemistry techniques, along with qRT-PCR confirmation, would provide evidence for specific miRNA:mRNA relationships altered as a result of prenatal ethanol exposure. Subsequent knockdown and transient overexpression experiments would further our understanding of specific molecular consequences on the developing fetal brain. Another brain region disrupted following prenatal ethanol exposure includes the cerebellum[53].The cerebellum

is involved in motor control and cognitive functions including attention and language[259]. Performing a similar protocol on cerebellum samples from control and ethanol-exposed adult mice may help to explain the prolonged molecular effects of ethanol on life-long motor skill disabilities related to FASD.

As mentioned, my findings may open avenues of correction by molecular manipulation of specific cellular pathways or network hubs (eg. MAPK signaling, PI3K/AKT signaling) in specific brain regions. Such manipulations may involve epigenetic regulation, as already suggested by other researchers[42,95,462,463]. Along with the disrupted miRNAs identified during the course of this research, additional results of DNA methylation and histone modifications could be insightful. Indeed, the involvement of miRNAs, DNA methylation, and histone modifications in prenatal ethanol exposure has been reported[95,464,465]. Epigenetic modifications may help to explain the underlying cause(s) of FASD, given their regulation of gene expression. In my study, I was able to identify and correlate specific neurodevelopmental genes and microRNAs with potential contributions to disruption in cellular processes and FASD-relevant behaviours. This brought-together a unifying theory that involved gene expression changes and gene regulation at the transcriptional level by microRNAs. It is well-known that the central dogma of molecular biology includes multiple gene regulatory levels. DNA methylation and histone modifications exert their effects on gene regulation at the post-transcriptional level. Post-translational modifications may also impact the stability of a protein once it is translated from a mRNA. An altered set of proteins may have consequences on neurodevelopment. It would be relevant to assess specific protein functioning following prenatal ethanol exposure using a Western blot. Additionally, a yeast-2-hybrid screen may provide relevant information regarding protein-protein dynamics, and how such interactions may lead to altered behaviours.

For inclusion in this thesis, I have examined the behavioural and gene expression changes associated with prenatal ethanol exposure. Furthermore, I have assessed gene regulation at the transcriptional level (miRNAs). As outlined, an important next step would be to investigate other epigenetic mechanisms at differing levels of gene regulation. Epigenetic manipulation of genetic pathways that are disrupted following prenatal ethanol exposure may be useful in the development of novel corrective measures for individuals with FASD.

References

1. Becker HC, Randall CL. Effects of prenatal ethanol exposure in C57BL mice on locomotor activity and passive avoidance behavior. *Psychopharmacology (Berl)* 1989; 97(1): 40-4.

2. Guerri C, Bazinet A, Riley EP. Foetal Alcohol Spectrum Disorders and alterations in brain and behaviour. *Alcohol Alcohol* 2009; **44**(2): 108-14. doi:10.1093/alcalc/agn105.

3. Abel EL, Sokol RJ. Incidence of fetal alcohol syndrome and economic impact of FAS-related anomalies. *Drug Alcohol Depend* 1987; **19**(1): 51-70.

4. Bertrand J, Floyd LL, Weber MK, Fetal Alcohol Syndrome Prevention Team, Division of Birth Defects and Developmental Disabilities, National Center on Birth Defects and Developmental Disabilities, Centers for Disease Control and Prevention (CDC). Guidelines for identifying and referring persons with fetal alcohol syndrome. *MMWR Recomm Rep* 2005; **54**(RR-11): 1-14.

5. Stade B, Ali A, Bennett D, et al. The burden of prenatal exposure to alcohol: revised measurement of cost. *Can J Clin Pharmacol* 2009; **16**(1): e91-102.

6. Steinhausen HC, Willms J, Spohr HL. Long-term psychopathological and cognitive outcome of children with fetal alcohol syndrome. *J Am Acad Child Adolesc Psychiatry* 1993; **32**(5): 990-4. doi:10.1097/00004583-199309000-00016.

7. Chudley AE, Conry J, Cook JL, Loock C, Rosales T, LeBlanc N, Public Health Agency of Canada's National Advisory Committee on Fetal Alcohol Spectrum Disorder. Fetal alcohol spectrum disorder: Canadian guidelines for diagnosis. *CMAJ* 2005; **172**(5 Suppl): S1-S21. doi:10.1503/cmaj.1040302.

8. Kalberg WO, Provost B, Tollison SJ, et al. Comparison of motor delays in young children with fetal alcohol syndrome to those with prenatal alcohol exposure and with no prenatal alcohol exposure. *Alcohol Clin Exp Res* 2006; **30**(12): 2037-45. doi:10.1111/j.1530-0277.2006.00250.x.

9. Kodituwakku PW. Defining the behavioral phenotype in children with fetal alcohol spectrum disorders: a review. *Neurosci Biobehav Rev* 2007; **31**(2): 192-201. doi:10.1016/j.neubiorev.2006.06.020.

10. Guerri C. Neuroanatomical and neurophysiological mechanisms involved in central nervous system dysfunctions induced by prenatal alcohol exposure. *Alcohol Clin Exp Res* 1998; **22**(2): 304-12.

11. Bhatara V, Loudenberg R, Ellis R. Association of attention deficit hyperactivity disorder and gestational alcohol exposure: an exploratory study. *J Atten Disord* 2006; **9**(3): 515-22. doi:10.1177/1087054705283880.

12. Colorado RA, Shumake J, Conejo NM, Gonzalez-Pardo H, Gonzalez-Lima F. Effects of maternal separation, early handling, and standard facility rearing on orienting and impulsive

behavior of adolescent rats. *Behav Processes* 2006; **71**(1): 51-8. doi:10.1016/j.beproc.2005.09.007.

13. Herman LE, Acosta MC, Chang PN. Gender and attention deficits in children diagnosed with a Fetal Alcohol Spectrum Disorder. *Can J Clin Pharmacol* 2008; **15**(3): e411-9.

14. Hellemans KG, Sliwowska JH, Verma P, Weinberg J. Prenatal alcohol exposure: fetal programming and later life vulnerability to stress, depression and anxiety disorders. *Neurosci Biobehav Rev* 2010; **34**(6): 791-807. doi:10.1016/j.neubiorev.2009.06.004.

15. Engle JA, Kerns KA. Reinforcement learning in children with FASD. *J Popul Ther Clin Pharmacol* 2011; **18**(1): e17-27.

16. Mattson SN, Riley EP, Gramling L, Delis DC, Jones KL. Neuropsychological comparison of alcohol-exposed children with or without physical features of fetal alcohol syndrome. *Neuropsychology* 1998; **12**(1): 146-53.

17. Jirikowic T, Olson HC, Kartin D. Sensory processing, school performance, and adaptive behavior of young school-age children with fetal alcohol spectrum disorders. *Phys Occup Ther Pediatr* 2008; **28**(2): 117-36.

18. Green CR, Mihic AM, Nikkel SM, Stade BC, Rasmussen C, Munoz DP, Reynolds JN. Executive function deficits in children with fetal alcohol spectrum disorders (FASD) measured using the Cambridge Neuropsychological Tests Automated Battery (CANTAB). *J Child Psychol Psychiatry* 2009; **50**(6): 688-97. doi:10.1111/j.1469-7610.2008.01990.x.

19. Steinhausen HC, Willms J, Metzke CW, Spohr HL. Behavioural phenotype in foetal alcohol syndrome and foetal alcohol effects. *Dev Med Child Neurol* 2003; **45**(3): 179-82.

20. Manning MA, Eugene Hoyme H. Fetal alcohol spectrum disorders: a practical clinical approach to diagnosis. *Neurosci Biobehav Rev* 2007; **31**(2): 230-8. doi:10.1016/j.neubiorev.2006.06.016.

21. Ikonomidou C, Bittigau P, Ishimaru MJ, et al. Ethanol-induced apoptotic neurodegeneration and fetal alcohol syndrome. *Science* 2000; **287**(5455): 1056-60.

22. Kvigne VL, Leonardson GR, Neff-Smith M, Brock E, Borzelleca J, Welty TK. Characteristics of children who have full or incomplete fetal alcohol syndrome. *J Pediatr* 2004; **145**(5): 635-40. doi:10.1016/j.jpeds.2004.07.015.

23. Clarke ME, Gibbard WB. Overview of fetal alcohol spectrum disorders for mental health professionals. *Can Child Adolesc Psychiatr Rev* 2003; **12**(3): 57-63.

24. Peadon E, Fremantle E, Bower C, Elliott EJ. International survey of diagnostic services for children with Fetal Alcohol Spectrum Disorders. *BMC Pediatr* 2008; **8**: 12. doi:10.1186/1471-2431-8-12.

25. Moore ES, Ward RE, Wetherill LF, et al. Unique facial features distinguish fetal alcohol syndrome patients and controls in diverse ethnic populations. *Alcohol Clin Exp Res* 2007; **31**(10): 1707-13. doi:10.1111/j.1530-0277.2007.00472.x.

26. Henry J, Sloane M, Black-Pond C. Neurobiology and neurodevelopmental impact of childhood traumatic stress and prenatal alcohol exposure. *Lang Speech Hear Serv Sch* 2007; **38**(2): 99-108. doi:10.1044/0161-1461(2007/010).

27. Mattson SN, Riley EP. A review of the neurobehavioral deficits in children with fetal alcohol syndrome or prenatal exposure to alcohol. *Alcohol Clin Exp Res* 1998; **22**(2): 279-94.

28. Mattson SN, Goodman AM, Caine C, Delis DC, Riley EP. Executive functioning in children with heavy prenatal alcohol exposure. *Alcohol Clin Exp Res* 1999; **23**(11): 1808-15.

29. Kodituwakku PW, Kalberg W, May PA. The effects of prenatal alcohol exposure on executive functioning. *Alcohol Res Health* 2001; **25**(3): 192-8.

30. Kalberg WO, Buckley D. FASD: what types of intervention and rehabilitation are useful? *Neurosci Biobehav Rev* 2007; **31**(2): 278-85. doi:10.1016/j.neubiorev.2006.06.014.

31. O'Connor MJ, Frankel F, Paley B, Schonfeld AM, Carpenter E, Laugeson EA, Marquardt R. A controlled social skills training for children with fetal alcohol spectrum disorders. *J Consult Clin Psychol* 2006; **74**(4): 639-48. doi:10.1037/0022-006X.74.4.639.

32. Peadon E, Elliott EJ. Distinguishing between attention-deficit hyperactivity and fetal alcohol spectrum disorders in children: clinical guidelines. *Neuropsychiatr Dis Treat* 2010; **6**: 509-15.

33. Rasmussen C, Benz J, Pei J, et al. The impact of an ADHD co-morbidity on the diagnosis of FASD. *Can J Clin Pharmacol* 2010; **17**(1): e165-76.

34. Nash K, Rovet J, Greenbaum R, Fantus E, Nulman I, Koren G. Identifying the behavioural phenotype in Fetal Alcohol Spectrum Disorder: sensitivity, specificity and screening potential. *Arch Womens Ment Health* 2006; **9**(4): 181-6. doi:10.1007/s00737-006-0130-3.

35. Chiodo LM, Janisse J, Delaney-Black V, Sokol RJ, Hannigan JH. A metric of maternal prenatal risk drinking predicts neurobehavioral outcomes in preschool children. *Alcohol Clin Exp Res* 2009; **33**(4): 634-44. doi:10.1111/j.1530-0277.2008.00878.x; 10.1111/j.1530-0277.2008.00878.x.

36. Barr HM, Bookstein FL, O'Malley KD, Connor PD, Huggins JE, Streissguth AP. Binge drinking during pregnancy as a predictor of psychiatric disorders on the Structured Clinical Interview for DSM-IV in young adult offspring. *Am J Psychiatry* 2006; **163**(6): 1061-5. doi:10.1176/appi.ajp.163.6.1061.

37. Caetano R, Ramisetty-Mikler S, Floyd LR, McGrath C. The epidemiology of drinking among women of child-bearing age. *Alcohol Clin Exp Res* 2006; **30**(6): 1023-30. doi:10.1111/j.1530-0277.2006.00116.x.

38. Kelly-Weeder S. Binge drinking in college-aged women: framing a gender-specific prevention strategy. *J Am Acad Nurse Pract* 2008; **20**(12): 577-84. doi:10.1111/j.1745-7599.2008.00357.x.

39. Mulford HA, Miller DE. Drinking in Iowa. III. A scale of definitions of alcohol related to drinking behavior. *Q J Stud Alcohol* 1960; **21**: 267-78.

40. Sulik KK, Johnston MC, Webb MA. Fetal alcohol syndrome: embryogenesis in a mouse model. *Science* 1981; **214**(4523): 936-8.

41. Streissguth AP, Sampson PD, Olson HC, et al. Maternal drinking during pregnancy: attention and short-term memory in 14-year-old offspring--a longitudinal prospective study. *Alcohol Clin Exp Res* 1994; **18**(1): 202-18.

42. Kelly SJ, Goodlett CR, Hannigan JH. Animal models of fetal alcohol spectrum disorders: impact of the social environment. *Dev Disabil Res Rev* 2009; **15**(3): 200-8. doi:10.1002/ddrr.69.

43. Gemma S, Vichi S, Testai E. Metabolic and genetic factors contributing to alcohol induced effects and fetal alcohol syndrome. *Neurosci Biobehav Rev* 2007; **31**(2): 221-9. doi:10.1016/j.neubiorev.2006.06.018.

44. Li Y, Wang H. In utero exposure to tobacco and alcohol modifies neurobehavioral development in mice offspring: consideration a role of oxidative stress. *Pharmacol Res* 2004; **49**(5): 467-73. doi:10.1016/j.phrs.2003.11.002.

45. Brocardo PS, Gil-Mohapel J, Christie BR. The role of oxidative stress in fetal alcohol spectrum disorders. *Brain Res Rev* 2011; **67**(1-2): 209-25. doi:10.1016/j.brainresrev.2011.02.001.

46. Jones KL, Smith DW. The fetal alcohol syndrome. *Teratology* 1975; **12**(1): 1-10. doi:10.1002/tera.1420120102.

47. Bhatara VS, Lovrein F, Kirkeby J, Swayze V,2nd, Unruh E, Johnson V. Brain function in fetal alcohol syndrome assessed by single photon emission computed tomography. *S D J Med* 2002; **55**(2): 59-62.

48. Sowell ER, Thompson PM, Mattson SN, Tessner KD, Jernigan TL, Riley EP, Toga AW. Regional brain shape abnormalities persist into adolescence after heavy prenatal alcohol exposure. *Cereb Cortex* 2002; **12**(8): 856-65.

49. Ma X, Coles CD, Lynch ME, Laconte SM, Zurkiya O, Wang D, Hu X. Evaluation of corpus callosum anisotropy in young adults with fetal alcohol syndrome according to diffusion tensor imaging. *Alcohol Clin Exp Res* 2005; **29**(7): 1214-22.

50. Olney JW, Ishimaru MJ, Bittigau P, Ikonomidou C. Ethanol-induced apoptotic neurodegeneration in the developing brain. *Apoptosis* 2000; **5**(6): 515-21.

51. Olney JW. Fetal alcohol syndrome at the cellular level. *Addict Biol* 2004; **9**(2): 137,49; discussion 151. doi:10.1080/13556210410001717006.

52. Wozniak DF, Hartman RE, Boyle MP, et al. Apoptotic neurodegeneration induced by ethanol in neonatal mice is associated with profound learning/memory deficits in juveniles followed by progressive functional recovery in adults. *Neurobiol Dis* 2004; **17**(3): 403-14. doi:10.1016/j.nbd.2004.08.006.

53. Dikranian K, Qin YQ, Labruyere J, Nemmers B, Olney JW. Ethanol-induced neuroapoptosis in the developing rodent cerebellum and related brain stem structures. *Brain Res Dev Brain Res* 2005; **155**(1): 1-13. doi:10.1016/j.devbrainres.2004.11.005.

54. Young C, Olney JW. Neuroapoptosis in the infant mouse brain triggered by a transient small increase in blood alcohol concentration. *Neurobiol Dis* 2006; **22**(3): 548-54. doi:10.1016/j.nbd.2005.12.015.

55. Hamilton GF, Whitcher LT, Klintsova AY. Postnatal binge-like alcohol exposure decreases dendritic complexity while increasing the density of mature spines in mPFC Layer II/III pyramidal neurons. *Synapse* 2009; **64**(2): 127-35. doi:10.1002/syn.20711.

56. Substance Abuse and Mental Health Services Administration. *2006 National Survey on Drug Use and Health: national findings*. 2006; Avalable at: http://www.oas.samhsa.gov/NSDUH/2k6NSDUH/2k6results.cfm#Ch3. Accessed 04/30, 2013.

57. May PA, Gossage JP, Marais AS, et al. Maternal risk factors for fetal alcohol syndrome and partial fetal alcohol syndrome in South Africa: a third study. *Alcohol Clin Exp Res* 2008; **3**2(5): 738-53. doi:10.1111/j.1530-0277.2008.00634.x; 10.1111/j.1530-0277.2008.00634.x.

58. Abel EL. Fetal alcohol syndrome in families. *Neurotoxicol Teratol* 1988; **1**0(1): 1-2.

59. Livy DJ, Miller EK, Maier SE, West JR. Fetal alcohol exposure and temporal vulnerability: effects of binge-like alcohol exposure on the developing rat hippocampus. *Neurotoxicol Teratol* 2003; **2**5(4): 447-58.

60. Liu W, Redmond EM, Morrow D, Cullen JP. Differential effects of daily-moderate versus weekend-binge alcohol consumption on atherosclerotic plaque development in mice. *Atherosclerosis* 2011; **21**9(2): 448-54. doi:10.1016/j.atherosclerosis.2011.08.034; 10.1016/j.atherosclerosis.2011.08.034.

61. Bonthius DJ, West JR. Alcohol-induced neuronal loss in developing rats: increased brain damage with binge exposure. *Alcohol Clin Exp Res* 1990; **1**4(1): 107-18.

62. Frezza M, di Padova C, Pozzato G, Terpin M, Baraona E, Lieber CS. High blood alcohol levels in women. The role of decreased gastric alcohol dehydrogenase activity and first-pass metabolism. *N Engl J Med* 1990; **32**2(2): 95-9. doi:10.1056/NEJM199001113220205.

63. Parker DA, Harford TC, Rosenstock IM. Alcohol, other drugs, and sexual risk-taking among young adults. *J Subst Abuse* 1994; 6(1): 87-93.

64. Rubert G, Minana R, Pascual M, Guerri C. Ethanol exposure during embryogenesis decreases the radial glial progenitorpool and affects the generation of neurons and astrocytes. *J Neurosci Res* 2006; **8**4(3): 483-96. doi:10.1002/jnr.20963.

65. Ashwell KW, Zhang LL. Forebrain hypoplasia following acute prenatal ethanol exposure: quantitative analysis of effects on specific forebrain nuclei. *Pathology* 1996; **2**8(2): 161-6.

66. Mooney SM, Miller MW. Time-specific effects of ethanol exposure on cranial nerve

nuclei: gastrulation and neuronogenesis. *Exp Neurol* 2007; **20**5(1): 56-63. doi:10.1016/j.expneurol.2007.01.016.

67. Ernhart CB, Sokol RJ, Martier S, Moron P, Nadler D, Ager JW, Wolf A. Alcohol teratogenicity in the human: a detailed assessment of specificity, critical period, and threshold. *Am J Obstet Gynecol* 1987; **15**6(1): 33-9.

68. Astley SJ, Magnuson SI, Omnell LM, Clarren SK. Fetal alcohol syndrome: changes in craniofacial form with age, cognition, and timing of ethanol exposure in the macaque. *Teratology* 1999; **5**9(3): 163-72. doi:2-8.

69. Suzuki K. Neuropathology of developmental abnormalities. *Brain Dev* 2007; **2**9(3): 129-41. doi:10.1016/j.braindev.2006.08.006.

70. Miller MW. Effect of pre- or postnatal exposure to ethanol on the total number of neurons in the principal sensory nucleus of the trigeminal nerve: cell proliferation and neuronal death. *Alcohol Clin Exp Res* 1995; **1**9(5): 1359-63.

71. Ornoy A, Ergaz Z. Alcohol abuse in pregnant women: effects on the fetus and newborn, mode of action and maternal treatment. *Int J Environ Res Public Health* 2010; 7(2): 364-79. doi:10.3390/ijerph7020364; 10.3390/ijerph7020364.

72. Pierce DR, West JR. Blood alcohol concentration: a critical factor for producing fetal alcohol effects. *Alcohol* 1986; 3(4): 269-72.

73. The Jackson Laboratory. *Jax® Mouse Database*. 2013; Avalable at: http://jaxmice.jax.org/strain/000664.html. Accessed 05/02, 2013.

74. Garro AJ, McBeth DL, Lima V, Lieber CS. Ethanol consumption inhibits fetal DNA methylation in mice: implications for the fetal alcohol syndrome. *Alcohol Clin Exp Res* 1991; **1**5(3): 395-8.

75. Belknap JK, Crabbe JC, Young ER. Voluntary consumption of ethanol in 15 inbred mouse strains. *Psychopharmacology (Berl)* 1993; **11**2(4): 503-10.

76. Kitagawa K, Kawamoto T, Kunugita N, et al. Aldehyde dehydrogenase (ALDH) 2 associates with oxidation of methoxyacetaldehyde; in vitro analysis with liver subcellular fraction derived from human and Aldh2 gene targeting mouse. *FEBS Lett* 2000; **47**6(3): 306-11.

77. Datta S, Turner D, Singh R, Ruest LB, Pierce WM,Jr, Knudsen TB. Fetal alcohol syndrome (FAS) in C57BL/6 mice detected through proteomics screening of the amniotic fluid. *Birth Defects Res A Clin Mol Teratol* 2008; **8**2(4): 177-86. doi:10.1002/bdra.20440.

78. Brady ML, Allan AM, Caldwell KK. A Limited Access Mouse Model of Prenatal Alcohol Exposure that Produces Long-Lasting Deficits in Hippocampal-Dependent Learning and Memory. *Alcohol Clin Exp Res* 2011; . doi:10.1111/j.1530-0277.2011.01644.x; 10.1111/j.1530-0277.2011.01644.x.

79. Shukla PK, Sittig LJ, Ullmann TM, Redei EE. Candidate placental biomarkers for

intrauterine alcohol exposure. *Alcohol Clin Exp Res* 2011; **3**5(3): 559-65. doi:10.1111/j.1530-0277.2010.01373.x; 10.1111/j.1530-0277.2010.01373.x.

80. Hard ML, Abdolell M, Robinson BH, Koren G. Gene-expression analysis after alcohol exposure in the developing mouse. *J Lab Clin Med* 2005; **14**5(1): 47-54. doi:10.1016/j.lab.2004.11.011.

81. Lombard Z, Tiffin N, Hofmann O, Bajic VB, Hide W, Ramsay M. Computational selection and prioritization of candidate genes for fetal alcohol syndrome. *BMC Genomics* 2007; 8: 389. doi:10.1186/1471-2164-8-389.

82. Green ML, Singh AV, Zhang Y, Nemeth KA, Sulik KK, Knudsen TB. Reprogramming of genetic networks during initiation of the Fetal Alcohol Syndrome. *Dev Dyn* 2007; **23**6(2): 613-31. doi:10.1002/dvdy.21048.

83. Singh SM, Treadwell J, Kleiber ML, Harrison M, Uddin RK. Analysis of behavior using genetical genomics in mice as a model: from alcohol preferences to gene expression differences. *Genome* 2007; **5**0(10): 877-97. doi:10.1139/g06-118.

84. Ponomarev I, Wang S, Zhang L, Harris RA, Mayfield RD. Gene coexpression networks in human brain identify epigenetic modifications in alcohol dependence. *J Neurosci* 2012; **3**2(5): 1884-97. doi:10.1523/JNEUROSCI.3136-11.2012.

85. Mouse Genome Sequencing Consortium, Waterston RH, Lindblad-Toh K, et al. Initial sequencing and comparative analysis of the mouse genome. *Nature* 2002; **42**0(6915): 520-62. doi:10.1038/nature01262.

86. Liao BY, Zhang J. Evolutionary conservation of expression profiles between human and mouse orthologous genes. *Mol Biol Evol* 2006; **2**3(3): 530-40. doi:10.1093/molbev/msj054.

87. Singh SM, Treadwell J, Kleiber ML, Harrison M, Uddin RK. Analysis of behavior using genetical genomics in mice as a model: from alcohol preferences to gene expression differences. *Genome* 2007; **5**0(10): 877-97. doi:10.1139/g06-118.

88. Poot M, Badea A, Williams RW, Kas MJ. Identifying human disease genes through cross-species gene mapping of evolutionary conserved processes. *PLoS One* 2011; 6(5): e18612. doi:10.1371/journal.pone.0018612; 10.1371/journal.pone.0018612.

89. Sunyer B, Patil S, Hoger H, Lubec G. Barnes maze, a useful task to assess spatial reference memory in the mice. *Nat Protoc* 2007; : doi:10.1038/nprot.2007.390.

90. Caldwell KK, Sheema S, Paz RD, et al. Fetal alcohol spectrum disorder-associated depression: evidence for reductions in the levels of brain-derived neurotrophic factor in a mouse model. *Pharmacol Biochem Behav* 2008; **9**0(4): 614-24. doi:10.1016/j.pbb.2008.05.004.

91. Kleiber ML, Wright E, Singh SM. Maternal voluntary drinking in C57BL/6J mice: advancing a model for fetal alcohol spectrum disorders. *Behav Brain Res* 2011; **22**3(2): 376-87. doi:10.1016/j.bbr.2011.05.005.

92. Zhou FC, Sari Y, Zhang JK, Goodlett CR, Li T. Prenatal alcohol exposure retards the

migration and development of serotonin neurons in fetal C57BL mice. *Brain Res Dev Brain Res* 2001; **12**6(2): 147-55.

93. Mayock DE, Ness D, Mondares RL, Gleason CA. Binge alcohol exposure in the second trimester attenuates fetal cerebral blood flow response to hypoxia. *J Appl Physiol* 2007; **10**2(3): 972-7. doi:10.1152/japplphysiol.00956.2006.

94. Kleiber ML, Laufer BI, Wright E, Diehl EJ, Singh SM. Long-term alterations to the brain transcriptome in a maternal voluntary consumption model of fetal alcohol spectrum disorders. *Brain Res* 2012; **145**8: 18-33. doi:10.1016/j.brainres.2012.04.016; 10.1016/j.brainres.2012.04.016.

95. Laufer BI, Mantha K, Kleiber ML, Diehl EJ, Addison SM, Singh SM. Long lasting alterations to DNA methylation and ncRNAs may underlie the effects of fetal alcohol exposure. *Dis Model Mech* 2013; . doi:10.1242/dmm.010975.

96. Murphy BC, Chiu T, Harrison M, Uddin RK, Singh SM. Examination of ethanol responsive liver and brain specific gene expression, in the mouse strains with variable ethanol preferences, using cDNA expression arrays. *Biochem Genet* 2002; **40**(11-12): 395-410.

97. Treadwell JA, Singh SM. Microarray analysis of mouse brain gene expression following acute ethanol treatment. *Neurochem Res* 2004; **29**(2): 357-69.

98. Hashimoto-Torii K, Kawasawa YI, Kuhn A, Rakic P. Combined transcriptome analysis of fetal human and mouse cerebral cortex exposed to alcohol. *Proc Natl Acad Sci U S A* 2011; **108**(10): 4212-7. doi:10.1073/pnas.1100903108.

99. Lister RG. The use of a plus-maze to measure anxiety in the mouse. *Psychopharmacology (Berl)* 1987; **92**(2): 180-5.

100. Bourin M, Hascoet M. The mouse light/dark box test. *Eur J Pharmacol* 2003; **463**(1-3): 55-65.

101. Hill JM, Lim MA, Stone MM. Developmental Milestones in the Newborn Mouse. In: Gozes I, editor. Neuropeptide Techniques. Totowa, N.J: Humana Press; 2008. p.149.

102. Carneiro LM, Diogenes JP, Vasconcelos SM, Aragao GF, Noronha EC, Gomes PB, Viana GS. Behavioral and neurochemical effects on rat offspring after prenatal exposure to ethanol. *Neurotoxicol Teratol* 2005; **27**(4): 585-92. doi:10.1016/j.ntt.2005.06.006.

103. Camarini R, Hodge CW. Ethanol preexposure increases ethanol self-administration in C57BL/6J and DBA/2J mice. *Pharmacol Biochem Behav* 2004; **79**(4): 623-32. doi:10.1016/j.pbb.2004.09.012.

104. Wolstenholme JT, Warner JA, Capparuccini MI, Archer KJ, Shelton KL, Miles MF. Genomic analysis of individual differences in ethanol drinking: evidence for non-genetic factors in C57BL/6 mice. *PLoS One* 2011; **6**(6): e21100. doi:10.1371/journal.pone.0021100; 10.1371/journal.pone.0021100.

105. Leenaars M, Hendriksen CF. Influence of Route of Injection on Efficacy and Side Effects of Immunisation. *ALTEX* 1998; **15**(5): 87.

106. Harris SR, Osborn JA, Weinberg J, Loock C, Junaid K. Effects of prenatal alcohol exposure on neuromotor and cognitive development during early childhood: a series of case reports. *Phys Ther* 1993; **73**(9): 608-17.

107. Connor PD, Sampson PD, Streissguth AP, Bookstein FL, Barr HM. Effects of prenatal alcohol exposure on fine motor coordination and balance: A study of two adult samples. *Neuropsychologia* 2006; **44**(5): 744-51. doi:10.1016/j.neuropsychologia.2005.07.016.

108. Jirikowic T, Olson HC, Kartin D. Sensory processing, school performance, and adaptive behavior of young school-age children with fetal alcohol spectrum disorders. *Phys Occup Ther Pediatr* 2008; **28**(2): 117-36.

109. Butchbach ME, Edwards JD, Burghes AH. Abnormal motor phenotype in the SMNDelta7 mouse model of spinal muscular atrophy. *Neurobiol Dis* 2007; **27**(2): 207-19. doi:10.1016/j.nbd.2007.04.009.

110. Lim MA, Stack CM, Cuasay K, Stone MM, McFarlane HG, Waschek JA, Hill JM. Regardless of genotype, offspring of VIP-deficient female mice exhibit developmental delays and deficits in social behavior. *Int J Dev Neurosci* 2008; **26**(5): 423-34. doi:10.1016/j.ijdevneu.2008.03.002; 10.1016/j.ijdevneu.2008.03.002.

111. Clarkson J, Herbison AE. Postnatal development of kisspeptin neurons in mouse hypothalamus; sexual dimorphism and projections to gonadotropin-releasing hormone neurons. *Endocrinology* 2006; **147**(12): 5817-25. doi:10.1210/en.2006-0787.

112. August GJ, Braswell L, Thuras P. Diagnostic stability of ADHD in a community sample of school-aged children screened for disruptive behavior. *J Abnorm Child Psychol* 1998; **26**(5): 345-56.

113. Pastor PN, Reuben CA. Diagnosed attention deficit hyperactivity disorder and learning disability: United States, 2004-2006. *Vital Health Stat 10* 2008; **(237)**(237): 1-14.

114. Beesdo K, Knappe S, Pine DS. Anxiety and anxiety disorders in children and adolescents: developmental issues and implications for DSM-V. *Psychiatr Clin North Am* 2009; **32**(3): 483-524. doi:10.1016/j.psc.2009.06.002; 10.1016/j.psc.2009.06.002.

115. Ramos A. Animal models of anxiety: do I need multiple tests? *Trends Pharmacol Sci* 2008; **29**(10): 493-8. doi:10.1016/j.tips.2008.07.005; 10.1016/j.tips.2008.07.005.

116. Nowoslawski L, Klocke BJ, Roth KA. Molecular regulation of acute ethanol-induced neuron apoptosis. *J Neuropathol Exp Neurol* 2005; **64**(6): 490-7.

117. Dildy-Mayfield JE, Mihic SJ, Liu Y, Deitrich RA, Harris RA. Actions of long chain alcohols on GABAA and glutamate receptors: relation to in vivo effects. *Br J Pharmacol* 1996; **118**(2): 378-84.

118. Mihic SJ, Harris RA. Inhibition of rho1 receptor GABAergic currents by alcohols and volatile anesthetics. *J Pharmacol Exp Ther* 1996; **277**(1): 411-6.

119. Thibault C, Hassan S, Miles M. Using in vitro models for expression profiling studies on ethanol and drugs of abuse. *Addict Biol* 2005; **10**(1): 53-62. doi:10.1080/13556210412331308949.

120. Crabbe JC, Phillips TJ, Harris RA, Arends MA, Koob GF. Alcohol-related genes: contributions from studies with genetically engineered mice. *Addict Biol* 2006; **11**(3-4): 195-269. doi:10.1111/j.1369-1600.2006.00038.x.

121. Harris RA, Trudell JR, Mihic SJ. Ethanol's molecular targets. *Sci Signal* 2008; **1**(28): re7. doi:10.1126/scisignal.128re7.

122. Becker KG. The common variants/multiple disease hypothesis of common complex genetic disorders. *Med Hypotheses* 2004; **62**(2): 309-17. doi:10.1016/S0306-9877(03)00332-3.

123. Tabor HK, Risch NJ, Myers RM. Candidate-gene approaches for studying complex genetic traits: practical considerations. *Nat Rev Genet* 2002; **3**(5): 391-7. doi:10.1038/nrg796.

124. Hacia JG, Brody LC, Chee MS, Fodor SP, Collins FS. Detection of heterozygous mutations in BRCA1 using high density oligonucleotide arrays and two-colour fluorescence analysis. *Nat Genet* 1996; **14**(4): 441-7. doi:10.1038/ng1296-441.

125. Lewohl JM, Wang L, Miles MF, Zhang L, Dodd PR, Harris RA. Gene expression in human alcoholism: microarray analysis of frontal cortex. *Alcohol Clin Exp Res* 2000; **24**(12): 1873-82.

126. Mirnics K, Middleton FA, Marquez A, Lewis DA, Levitt P. Molecular characterization of schizophrenia viewed by microarray analysis of gene expression in prefrontal cortex. *Neuron* 2000; **28**(1): 53-67.

127. Weindruch R, Kayo T, Lee CK, Prolla TA. Microarray profiling of gene expression in aging and its alteration by caloric restriction in mice. *J Nutr* 2001; **131**(3): 918S-23S.

128. Reimer T, Koczan D, Gerber B, Richter D, Thiesen HJ, Friese K. Microarray analysis of differentially expressed genes in placental tissue of pre-eclampsia: up-regulation of obesity-related genes. *Mol Hum Reprod* 2002; **8**(7): 674-80.

129. Small SA, Kent K, Pierce A, et al. Model-guided microarray implicates the retromer complex in Alzheimer's disease. *Ann Neurol* 2005; **58**(6): 909-19. doi:10.1002/ana.20667.

130. Ronald A, Butcher LM, Docherty S, Davis OS, Schalkwyk LC, Craig IW, Plomin R. A genome-wide association study of social and non-social autistic-like traits in the general population using pooled DNA, 500 K SNP microarrays and both community and diagnosed autism replication samples. *Behav Genet* 2010; **40**(1): 31-45. doi:10.1007/s10519-009-9308-6; 10.1007/s10519-009-9308-6.

131. Zhou FC, Zhao Q, Liu Y, et al. Alteration of gene expression by alcohol exposure at early neurulation. *BMC Genomics* 2011; **12**: 124,2164-12-124. doi:10.1186/1471-2164-12-124; 10.1186/1471-2164-12-124.

132. Lee CK, Klopp RG, Weindruch R, Prolla TA. Gene expression profile of aging and its retardation by caloric restriction. *Science* 1999; **285**(5432): 1390-3.

133. de Wilde J, Mohren R, van den Berg S, et al. Short-term high fat-feeding results in morphological and metabolic adaptations in the skeletal muscle of C57BL/6J mice. *Physiol Genomics* 2008; **32**(3): 360-9. doi:10.1152/physiolgenomics.00219.2007.

134. Mulligan MK, Rhodes JS, Crabbe JC, Mayfield RD, Adron Harris R, Ponomarev I. Molecular profiles of drinking alcohol to intoxication in C57BL/6J mice. *Alcohol Clin Exp Res* 2011; **35**(4): 659-70. doi:10.1111/j.1530-0277.2010.01384.x; 10.1111/j.1530-0277.2010.01384.x.

135. Schulze A, Downward J. Navigating gene expression using microarrays--a technology review. *Nat Cell Biol* 2001; **3**(8): E190-5. doi:10.1038/35087138.

136. Dennis G,Jr, Sherman BT, Hosack DA, Yang J, Gao W, Lane HC, Lempicki RA. DAVID: Database for Annotation, Visualization, and Integrated Discovery. *Genome Biol* 2003; **4**(5): P3.

137. Huang da W, Sherman BT, Lempicki RA. Systematic and integrative analysis of large gene lists using DAVID bioinformatics resources. *Nat Protoc* 2009; **4**(1): 44-57. doi:10.1038/nprot.2008.211; 10.1038/nprot.2008.211.

138. Partek Tutorials. Partek GO Enrichment Tutorial. 2009; Avalable at: http://www.partek.com/Tutorials/microarray/GO_Enrichment/GO_Enrichment.pdf. Accessed 05/01, 2013.

139. Ingenuity Systems. Calculating and Interpreting the p-values for Functions, Pathways and Lists in IPA. ; Avalable at: http://www.ingenuity.com/wp-content/themes/ingenuitytheme/pdf/ipa/functions-pathways-pval-whitepaper.pdf. Accessed 05/01, 2013.

140. Huang da W, Sherman BT, Lempicki RA. Bioinformatics enrichment tools: paths toward the comprehensive functional analysis of large gene lists. *Nucleic Acids Res* 2009; **3**7(1): 1-13. doi:10.1093/nar/gkn923; 10.1093/nar/gkn923.

141. Draghici S, Khatri P, Tarca AL, et al. A systems biology approach for pathway level analysis. *Genome Res* 2007; **1**7(10): 1537-45. doi:10.1101/gr.6202607.

142. Partek Pathway Tutorial. Pathway Analysis using Partek Genomics Suite™ 6.6 and Partek Pathway. 2011; Avalable at: http://www.partek.com/Tutorials/microarray/User_Guides/Pathway_Tutorial.pdf. Accessed 05/01, 2013.

143. Savli H, Szendroi A, Romics I, Nagy B. Gene network and canonical pathway analysis in prostate cancer: a microarray study. *Exp Mol Med* 2008; **4**0(2): 176-85.

144. Mostafavi S, Ray D, Warde-Farley D, Grouios C, Morris Q. GeneMANIA: a real-time multiple association network integration algorithm for predicting gene function. *Genome Biol* 2008; **9 Suppl** 1: S4,2008-9-s1-s4. Epub 2008 Jun 27. doi:10.1186/gb-2008-9-s1-s4; 10.1186/gb-2008-9-s1-s4.

145. Liu Y, Balaraman Y, Wang G, Nephew KP, Zhou FC. Alcohol exposure alters DNA methylation profiles in mouse embryos at early neurulation. *Epigenetics* 2009; 4(7): 500-11.

146. Kaminen-Ahola N, Ahola A, Flatscher-Bader T, Wilkins SJ, Anderson GJ, Whitelaw E, Chong S. Postnatal growth restriction and gene expression changes in a mouse model of fetal alcohol syndrome. *Birth Defects Res A Clin Mol Teratol* 2010; **88**(10): 818-26. doi:10.1002/bdra.20729; 10.1002/bdra.20729.

147. Zhou FC, Balaraman Y, Teng M, Liu Y, Singh RP, Nephew KP. Alcohol alters DNA methylation patterns and inhibits neural stem cell differentiation. *Alcohol Clin Exp Res* 2011; **35**(4): 735-46. doi:10.1111/j.1530-0277.2010.01391.x; 10.1111/j.1530-0277.2010.01391.x.

148. Mason S, Anthony B, Lai X, et al. Ethanol exposure alters protein expression in a mouse model of fetal alcohol spectrum disorders. *Int J Proteomics* 2012; **2012**: 867141. doi:10.1155/2012/867141; 10.1155/2012/867141.

149. Spirin V, Mirny LA. Protein complexes and functional modules in molecular networks. *Proc Natl Acad Sci U S A* 2003; **100**(21): 12123-8. doi:10.1073/pnas.2032324100.

150. Ma HW, Zhao XM, Yuan YJ, Zeng AP. Decomposition of metabolic network into functional modules based on the global connectivity structure of reaction graph. *Bioinformatics* 2004; **20**(12): 1870-6. doi:10.1093/bioinformatics/bth167.

151. Ingenuity Systems. IPA Network Generation Algorithm. 2005; Avalable at: http://www.ingenuity.com/wp-content/themes/ingenuitytheme/pdf/ipa/IPA-netgen-algorithm-whitepaper.pdf. Accessed 05/01, 2013.

152. Shanley TP, Cvijanovich N, Lin R, et al. Genome-level longitudinal expression of signaling pathways and gene networks in pediatric septic shock. *Mol Med* 2007; **1**3(9-10): 495-508. doi:10.2119/2007-00065.Shanley.

153. Calvano SE, Xiao W, Richards DR, et al. A network-based analysis of systemic inflammation in humans. *Nature* 2005; **43**7(7061): 1032-7. doi:10.1038/nature03985.

154. Shen R, Ghosh D, Chinnaiyan A, Meng Z. Eigengene-based linear discriminant model for tumor classification using gene expression microarray data. *Bioinformatics* 2006; **2**2(21): 2635-42. doi:10.1093/bioinformatics/btl442.

155. Han JD, Bertin N, Hao T, et al. Evidence for dynamically organized modularity in the yeast protein-protein interaction network. *Nature* 2004; **43**0(6995): 88-93. doi:10.1038/nature02555.

156. Patil A, Nakamura H. Disordered domains and high surface charge confer hubs with the ability to interact with multiple proteins in interaction networks. *FEBS Lett* 2006; **58**0(8): 2041-5. doi:10.1016/j.febslet.2006.03.003.

157. Lu X, Jain VV, Finn PW, Perkins DL. Hubs in biological interaction networks exhibit low changes in expression in experimental asthma. *Mol Syst Biol* 2007; 3: 98. doi:10.1038/msb4100138.

158. Kleiber ML, Mantha K, Stringer RL, Singh SM. Neurodevelopmental alcohol exposure elicits long-term changes to gene expression that alter distinct molecular pathways dependent on timing of exposure. *J Neurodev Disord* 2013; 5(1): 6. doi:10.1186/1866-1955-5-6.

159. Bartel DP. MicroRNAs: genomics, biogenesis, mechanism, and function. *Cell* 2004; **11**6(2): 281-97.

160. Kloosterman WP, Plasterk RH. The diverse functions of microRNAs in animal development and disease. *Dev Cell* 2006; **1**1(4): 441-50. doi:10.1016/j.devcel.2006.09.009.

161. O'Carroll D, Schaefer A. General principals of miRNA biogenesis and regulation in the brain. *Neuropsychopharmacology* 2013; **3**8(1): 39-54. doi:10.1038/npp.2012.87; 10.1038/npp.2012.87.

162. Amaral DG. Emerging principles of intrinsic hippocampal organization. *Curr Opin Neurobiol* 1993; 3(2): 225-9.

163. Li XG, Somogyi P, Ylinen A, Buzsaki G. The hippocampal CA3 network: an in vivo intracellular labeling study. *J Comp Neurol* 1994; **33**9(2): 181-208. doi:10.1002/cne.903390204.

164. Tamamaki N, Abe K, Nojyo Y. Three-dimensional analysis of the whole axonal arbors originating from single CA2 pyramidal neurons in the rat hippocampus with the aid of a computer graphic technique. *Brain Res* 1988; **45**2(1-2): 255-72.

165. Sevignani C, Calin GA, Siracusa LD, Croce CM. Mammalian microRNAs: a small world for fine-tuning gene expression. *Mamm Genome* 2006; **1**7(3): 189-202. doi:10.1007/s00335-005-0066-3.

166. Pasquinelli AE, Reinhart BJ, Slack F, et al. Conservation of the sequence and temporal expression of let-7 heterochronic regulatory RNA. *Nature* 2000; **40**8(6808): 86-9. doi:10.1038/35040556.

167. Lagos-Quintana M, Rauhut R, Meyer J, Borkhardt A, Tuschl T. New microRNAs from mouse and human. *RNA* 2003; 9(2): 175-9.

168. Kim J, Krichevsky A, Grad Y, Hayes GD, Kosik KS, Church GM, Ruvkun G. Identification of many microRNAs that copurify with polyribosomes in mammalian neurons. *Proc Natl Acad Sci U S A* 2004; **10**1(1): 360-5. doi:10.1073/pnas.2333854100.

169. Sempere LF, Freemantle S, Pitha-Rowe I, Moss E, Dmitrovsky E, Ambros V. Expression profiling of mammalian microRNAs uncovers a subset of brain-expressed microRNAs with possible roles in murine and human neuronal differentiation. *Genome Biol* 2004; 5(3): R13. doi:10.1186/gb-2004-5-3-r13.

170. Abelson JF, Kwan KY, O'Roak BJ, et al. Sequence variants in SLITRK1 are associated with Tourette's syndrome. *Science* 2005; **31**0(5746): 317-20. doi:10.1126/science.1116502.

171. Kim AH, Reimers M, Maher B, et al. MicroRNA expression profiling in the prefrontal cortex of individuals affected with schizophrenia and bipolar disorders. *Schizophr Res* 2010; **12**4(1-3): 183-91. doi:10.1016/j.schres.2010.07.002; 10.1016/j.schres.2010.07.002.

172. Sarachana T, Zhou R, Chen G, Manji HK, Hu VW. Investigation of post-transcriptional gene regulatory networks associated with autism spectrum disorders by microRNA expression profiling of lymphoblastoid cell lines. *Genome Med* 2010; 2(4): 23. doi:10.1186/gm144; 10.1186/gm144.

173. Wu H, Tao J, Chen PJ, et al. Genome-wide analysis reveals methyl-CpG-binding protein 2-dependent regulation of microRNAs in a mouse model of Rett syndrome. *Proc Natl Acad Sci U S A* 2010; **10**7(42): 18161-6. doi:10.1073/pnas.1005595107; 10.1073/pnas.1005595107.

174. Sathyan P, Golden HB, Miranda RC. Competing interactions between micro-RNAs determine neural progenitor survival and proliferation after ethanol exposure: evidence from an ex vivo model of the fetal cerebral cortical neuroepithelium. *J Neurosci* 2007; **2**7(32): 8546-57. doi:10.1523/JNEUROSCI.1269-07.2007.

175. Wang LL, Zhang Z, Li Q, et al. Ethanol exposure induces differential microRNA and target gene expression and teratogenic effects which can be suppressed by folic acid supplementation. *Hum Reprod* 2009; **2**4(3): 562-79. doi:10.1093/humrep/den439; 10.1093/humrep/den439.

176. Guo Y, Chen Y, Carreon S, Qiang M. Chronic intermittent ethanol exposure and its removal induce a different miRNA expression pattern in primary cortical neuronal cultures. *Alcohol Clin Exp Res* 2012; **3**6(6): 1058-66. doi:10.1111/j.1530-0277.2011.01689.x; 10.1111/j.1530-0277.2011.01689.x.

177. Bak M, Silahtaroglu A, Moller M, et al. MicroRNA expression in the adult mouse central nervous system. *RNA* 2008; **1**4(3): 432-44. doi:10.1261/rna.783108; 10.1261/rna.783108.

178. Leucht C, Stigloher C, Wizenmann A, Klafke R, Folchert A, Bally-Cuif L. MicroRNA-9 directs late organizer activity of the midbrain-hindbrain boundary. *Nat Neurosci* 2008; **1**1(6): 641-8. doi:10.1038/nn.2115; 10.1038/nn.2115.

179. Packer AN, Xing Y, Harper SQ, Jones L, Davidson BL. The bifunctional microRNA miR-9/miR-9* regulates REST and CoREST and is downregulated in Huntington's disease. *J Neurosci* 2008; **2**8(53): 14341-6. doi:10.1523/JNEUROSCI.2390-08.2008; 10.1523/JNEUROSCI.2390-08.2008.

180. Shibata M, Nakao H, Kiyonari H, Abe T, Aizawa S. MicroRNA-9 regulates neurogenesis in mouse telencephalon by targeting multiple transcription factors. *J Neurosci* 2011; **3**1(9): 3407-22. doi:10.1523/JNEUROSCI.5085-10.2011; 10.1523/JNEUROSCI.5085-10.2011.

181. Balaraman S, Winzer-Serhan UH, Miranda RC. Opposing actions of ethanol and nicotine on microRNAs are mediated by nicotinic acetylcholine receptors in fetal cerebral cortical-derived neural progenitor cells. *Alcohol Clin Exp Res* 2012; **3**6(10): 1669-77. doi:10.1111/j.1530-0277.2012.01793.x; 10.1111/j.1530-0277.2012.01793.x.

182. Miranda RC. MicroRNAs and Fetal Brain Development: Implications for Ethanol Teratology during the Second Trimester Period of Neurogenesis. *Front Genet* 2012; 3: 77. doi:10.3389/fgene.2012.00077; 10.3389/fgene.2012.00077.

183. Flicek P, Aken BL, Beal K, et al. Ensembl 2008. *Nucleic Acids Res* 2008; **3**6(Database issue): D707-14. doi:10.1093/nar/gkm988.

184. Sethupathy P, Megraw M, Hatzigeorgiou AG. A guide through present computational approaches for the identification of mammalian microRNA targets. *Nat Methods* 2006; 3(11): 881-6. doi:10.1038/nmeth954.

185. Kuhn DE, Martin MM, Feldman DS, Terry AV,Jr, Nuovo GJ, Elton TS. Experimental validation of miRNA targets. *Methods* 2008; **4**4(1): 47-54. doi:10.1016/j.ymeth.2007.09.005.

186. K oob GF. Animal models of psychiatric disorders. *Handb. Clin Neurol* 2012; **106**: 137-66. doi: 10.1016/B978-0-444-52002-9.00009-7; 10.1016/B978-0-444-52002-9.00009.7.

187. Hannigan JH, O'Leary-Moore SK, Berman RF. Postnatal environment or experimental amelioration of neurobehavioral effects of perinatal alcohol exposure in rats. Neurosci Biobeh Rev 2007; 31(2): 202-11. doi: 10.1016/j.neubiorev.2006.06.019.

188. Li N, Bates DJ, An J, Terry DA, Wang E. Up-regulation of key microRNAs, and inverse down-regulation of their predicted oxidative phosphorylation target genes, during aging in mouse brain. *Neurobiol Aging* 2011; **3**2(5): 944-55. doi:10.1016/j.neurobiolaging.2009.04.020; 10.1016/j.neurobiolaging.2009.04.020.

189. Affymetrix Data Sheet. GeneChip® miRNA 2.0 Array. 2011; Avalable at: http://media.affymetrix.com/support/technical/datasheets/miRNA_2_datasheet.pdf. Accessed 04/30, 2013.

190. Grucza RA, Norberg KE, Bierut LJ. Binge drinking among youths and young adults in the United States: 1979-2006. *J Am Acad Child Adolesc Psychiatry* 2009; **4**8(7): 692-702. doi:10.1097/CHI.0b013e3181a2b32f; 10.1097/CHI.0b013e3181a2b32f.

191. Mitka M. College binge drinking still on the rise. *JAMA* 2009; **30**2(8): 836-7. doi:10.1001/jama.2009.1154; 10.1001/jama.2009.1154.

192. Naimi TS, Lipscomb LE, Brewer RD, Gilbert BC. Binge drinking in the preconception period and the risk of unintended pregnancy: implications for women and their children. *Pediatrics* 2003; **111**(5 Pt 2): 1136-41.

193. Dobbing J, Sands J. Comparative aspects of the brain growth spurt. *Early Hum Dev* 1979; **3**(1): 79-83.

194. De Miranda J, Yaddanapudi K, Hornig M, Villar G, Serge R, Lipkin WI. Induction of Toll-like receptor 3-mediated immunity during gestation inhibits cortical neurogenesis and causes behavioral disturbances. *MBio* 2010; **1**(4): e00176-10. doi:10.1128/mBio.00176-10.

195. Bake S, Tingling JD, Miranda RC. Ethanol Exposure During Pregnancy Persistently Attenuates Cranially Directed Blood Flow in the Developing Fetus: Evidence from Ultrasound

Imaging in a Murine Second Trimester Equivalent Model. *Alcohol Clin Exp Res* 2011; . doi:10.1111/j.1530-0277.2011.01676.x; 10.1111/j.1530-0277.2011.01676.x.

196. Crimins JL, Rocher AB, Peters A, Shultz P, Lewis J, Luebke JI. Homeostatic responses by surviving cortical pyramidal cells in neurodegenerative tauopathy. *Acta Neuropathol* 2011; **122**(5): 551-64. doi:10.1007/s00401-011-0877-0; 10.1007/s00401-011-0877-0.

197. Walf AA, Frye CA. The use of the elevated plus maze as an assay of anxiety-related behavior in rodents. *Nat Protoc* 2007; **2**(2): 322-8. doi:10.1038/nprot.2007.44.

198. Harrison FE, Reiserer RS, Tomarken AJ, McDonald MP. Spatial and nonspatial escape strategies in the Barnes maze. *Learn Mem* 2006; **13**(6): 809-19. doi:10.1101/lm.334306.

199. Imbeaud S, Graudens E, Boulanger V, et al. Towards standardization of RNA quality assessment using user-independent classifiers of microcapillary electrophoresis traces. *Nucleic Acids Res* 2005; **33**(6): e56. doi:10.1093/nar/gni054.

200. Irizarry RA, Hobbs B, Collin F, Beazer-Barclay YD, Antonellis KJ, Scherf U, Speed TP. Exploration, normalization, and summaries of high density oligonucleotide array probe level data. *Biostatistics* 2003; **4**(2): 249-64. doi:10.1093/biostatistics/4.2.249.

201. Wu Z, Irizarry RA. Preprocessing of oligonucleotide array data. *Nat Biotechnol* 2004; **22**(6): 656,8; author reply 658. doi:10.1038/nbt0604-656b.

202. Vardhanabhuti S, Blakemore SJ, Clark SM, Ghosh S, Stephens RJ, Rajagopalan D. A comparison of statistical tests for detecting differential expression using Affymetrix oligonucleotide microarrays. *OMICS* 2006; **10**(4): 555-66. doi:10.1089/omi.2006.10.555.

203. Gharaibeh RZ, Fodor AA, Gibas CJ. Background correction using dinucleotide affinities improves the performance of GCRMA. *BMC Bioinformatics* 2008; **9**: 452,2105-9-452. doi:10.1186/1471-2105-9-452; 10.1186/1471-2105-9-452.

204. Choe SE, Boutros M, Michelson AM, Church GM, Halfon MS. Preferred analysis methods for Affymetrix GeneChips revealed by a wholly defined control dataset. *Genome Biol* 2005; **6**(2): R16. doi:10.1186/gb-2005-6-2-r16.

205. Downey T. Analysis of a multifactor microarray study using Partek genomics solution. *Methods Enzymol* 2006; **411**: 256-70. doi:10.1016/S0076-6879(06)11013-7.

206. Churchill GA. Using ANOVA to analyze microarray data. *BioTechniques* 2004; **37**(2): 173,5, 177.

207. Storey JD, Tibshirani R. Statistical significance for genomewide studies. *Proc Natl Acad Sci U S A* 2003; **100**(16): 9440-5. doi:10.1073/pnas.1530509100.

208. Dennis G,Jr, Sherman BT, Hosack DA, Yang J, Gao W, Lane HC, Lempicki RA. DAVID: Database for Annotation, Visualization, and Integrated Discovery. *Genome Biol* 2003; **4**(5): P3.

209. DAVID Bioinformatics Resources 6.7. National Institute of Allergy and Infectious Diseases (NIAID), NIH
Functional Annotation Tool. 2007; Avalable at: http://david.abcc.ncifcrf.gov/content.jsp?file=functional_annotation.html. Accessed 04/30, 2013.

210. Schultz J, Milpetz F, Bork P, Ponting CP. SMART, a simple modular architecture research tool: identification of signaling domains. *Proc Natl Acad Sci U S A* 1998; **9**5(11): 5857-64.

211. Letunic I, Doerks T, Bork P. SMART 7: recent updates to the protein domain annotation resource. *Nucleic Acids Res* 2012; **4**0(Database issue): D302-5. doi:10.1093/nar/gkr931; 10.1093/nar/gkr931.

212. Pena-Castillo L, Tasan M, Myers CL, et al. A critical assessment of Mus musculus gene function prediction using integrated genomic evidence. *Genome Biol* 2008; **9 Suppl** 1: S2,2008-9-s1-s2. Epub 2008 Jun 27. doi:10.1186/gb-2008-9-s1-s2; 10.1186/gb-2008-9-s1-s2.

213. Schmittgen TD, Livak KJ. Analyzing real-time PCR data by the comparative C(T) method. *Nat Protoc* 2008; 3(6): 1101-8.

214. Vergoulis T, Vlachos IS, Alexiou P, et al. TarBase 6.0: capturing the exponential growth of miRNA targets with experimental support. *Nucleic Acids Res* 2012; **4**0(Database issue): D222-9. doi:10.1093/nar/gkr1161; 10.1093/nar/gkr1161.

215. Gao J, Wang WY, Mao YW, et al. A novel pathway regulates memory and plasticity via SIRT1 and miR-134. *Nature* 2010; **46**6(7310): 1105-9. doi:10.1038/nature09271; 10.1038/nature09271.

216. Schmittgen TD, Lee EJ, Jiang J, Sarkar A, Yang L, Elton TS, Chen C. Real-time PCR quantification of precursor and mature microRNA. *Methods* 2008; **4**4(1): 31-8. doi:10.1016/j.ymeth.2007.09.006.

217. Mantha,K., Kleiber,M.L. and Singh,S.M. Neurodevelopmental timing of ethanol exposure may contribute to observed heterogeneity of behavioral deficits in a mouse model of Fetal Alcohol Spectrum Disorder (FASD). *J Beh Brain Sci* 2013; 3: 85,85-99.

218. Tsutsumi T, Kajiya H, Goto KT, Takahashi Y, Okabe K. Hyperocclusion up-regulates CCL3 expression in CCL2- and CCR2-deficient mice. *J Dent Res* 2013; **9**2(1): 65-70. doi:10.1177/0022034512467803; 10.1177/0022034512467803.

219. Bechtold DA, Sidibe A, Saer BR, et al. A role for the melatonin-related receptor GPR50 in leptin signaling, adaptive thermogenesis, and torpor. *Curr Biol* 2012; **2**2(1): 70-7. doi:10.1016/j.cub.2011.11.043; 10.1016/j.cub.2011.11.043.

220. Ivanova EA, Bechtold DA, Dupre SM, Brennand J, Barrett P, Luckman SM, Loudon AS. Altered metabolism in the melatonin-related receptor (GPR50) knockout mouse. *Am J Physiol Endocrinol Metab* 2008; **29**4(1): E176-82. doi:10.1152/ajpendo.00199.2007.

221. Mercader JM, Lozano JJ, Sumoy L, Dierssen M, Visa J, Gratacos M, Estivill X. Hypothalamus transcriptome profile suggests an anorexia-cachexia syndrome in the anx/anx

mouse model. *Physiol Genomics* 2008; **3**5(3): 341-50. doi:10.1152/physiolgenomics.90255.2008; 10.1152/physiolgenomics.90255.2008.

222. Cusco I, Medrano A, Gener B, et al. Autism-specific copy number variants further implicate the phosphatidylinositol signaling pathway and the glutamatergic synapse in the etiology of the disorder. *Hum Mol Genet* 2009; **1**8(10): 1795-804. doi:10.1093/hmg/ddp092; 10.1093/hmg/ddp092.

223. Pirity MK, Wang WL, Wolf LV, Tamm ER, Schreiber-Agus N, Cvekl A. Rybp, a polycomb complex-associated protein, is required for mouse eye development. *BMC Dev Biol* 2007; 7: 39. doi:10.1186/1471-213X-7-39.

224. Yim YS, Kwon Y, Nam J, et al. Slitrks control excitatory and inhibitory synapse formation with LAR receptor protein tyrosine phosphatases. *Proc Natl Acad Sci U S A* 2013; **11**0(10): 4057-62. doi:10.1073/pnas.1209881110; 10.1073/pnas.1209881110.

225. Piton A, Gauthier J, Hamdan FF, et al. Systematic resequencing of X-chromosome synaptic genes in autism spectrum disorder and schizophrenia. *Mol Psychiatry* 2011; **1**6(8): 867-80. doi:10.1038/mp.2010.54; 10.1038/mp.2010.54.

226. Smith EN, Bloss CS, Badner JA, et al. Genome-wide association study of bipolar disorder in European American and African American individuals. *Mol Psychiatry* 2009; **1**4(8): 755-63. doi:10.1038/mp.2009.43; 10.1038/mp.2009.43.

227. Brezo J, Bureau A, Merette C, et al. Differences and similarities in the serotonergic diathesis for suicide attempts and mood disorders: a 22-year longitudinal gene-environment study. *Mol Psychiatry* 2010; **1**5(8): 831-43. doi:10.1038/mp.2009.19; 10.1038/mp.2009.19.

228. Mongan M, Wang J, Liu H, Fan Y, Jin C, Kao WY, Xia Y. Loss of MAP3K1 enhances proliferation and apoptosis during retinal development. *Development* 2011; **13**8(18): 4001-12. doi:10.1242/dev.065003; 10.1242/dev.065003.

229. Romanos M, Freitag C, Jacob C, et al. Genome-wide linkage analysis of ADHD using high-density SNP arrays: novel loci at 5q13.1 and 14q12. *Mol Psychiatry* 2008; **1**3(5): 522-30. doi:10.1038/mp.2008.12; 10.1038/mp.2008.12.

230. Lopez de Lara C, Jaitovich-Groisman I, Cruceanu C, et al. Implication of synapse-related genes in bipolar disorder by linkage and gene expression analyses. *Int J Neuropsychopharmacol* 2010; **1**3(10): 1397-410. doi:10.1017/S1461145710000714; 10.1017/S1461145710000714.

231. Lee PH, Perlis RH, Jung JY, et al. Multi-locus genome-wide association analysis supports the role of glutamatergic synaptic transmission in the etiology of major depressive disorder. *Transl Psychiatry* 2012; 2: e184. doi:10.1038/tp.2012.95; 10.1038/tp.2012.95.

232. Qiu W, Hu Y, Andersen TE, Jafari A, Li N, Chen W, Kassem M. Tumor necrosis factor receptor superfamily member 19 (TNFRSF19) regulates differentiation fate of human mesenchymal (stromal) stem cells through canonical Wnt signaling and C/EBP. *J Biol Chem* 2010; **28**5(19): 14438-49. doi:10.1074/jbc.M109.052001; 10.1074/jbc.M109.052001.

233. Yang S, Wang K, Valladares O, Hannenhalli S, Bucan M. Genome-wide expression profiling and bioinformatics analysis of diurnally regulated genes in the mouse prefrontal cortex. *Genome Biol* 2007; 8(11): R247. doi:10.1186/gb-2007-8-11-r247.

234. Merolla F, Luise C, Muller MT, Pacelli R, Fusco A, Celetti A. Loss of CCDC6, the first identified RET partner gene, affects pH2AX S139 levels and accelerates mitotic entry upon DNA damage. *PLoS One* 2012; 7(5): e36177. doi:10.1371/journal.pone.0036177; 10.1371/journal.pone.0036177.

235. Gallitano-Mendel A, Wozniak DF, Pehek EA, Milbrandt J. Mice lacking the immediate early gene Egr3 respond to the anti-aggressive effects of clozapine yet are relatively resistant to its sedating effects. *Neuropsychopharmacology* 2008; **3**3(6): 1266-75. doi:10.1038/sj.npp.1301505.

236. Zhang R, Lu S, Meng L, et al. Genetic evidence for the association between the early growth response 3 (EGR3) gene and schizophrenia. *PLoS One* 2012; 7(1): e30237. doi:10.1371/journal.pone.0030237; 10.1371/journal.pone.0030237.

237. Szumlinski KK, Lominac KD, Kleschen MJ, et al. Behavioral and neurochemical phenotyping of Homer1 mutant mice: possible relevance to schizophrenia. *Genes Brain Behav* 2005; **4**(5): 273-88. doi:10.1111/j.1601-183X.2005.00120.x.

238. Anitha A, Nakamura K, Thanseem I, et al. Brain region-specific altered expression and association of mitochondria-related genes in autism. *Mol Autism* 2012; **3**(1): 12,2392-3-12. doi:10.1186/2040-2392-3-12; 10.1186/2040-2392-3-12.

239. Lee LC, Chen CM, Chen FL, et al. Altered expression of HSPA5, HSPA8 and PARK7 in spinocerebellar ataxia type 17 identified by 2-dimensional fluorescence difference in gel electrophoresis. *Clin Chim Acta* 2009; **400**(1-2): 56-62. doi:10.1016/j.cca.2008.10.013; 10.1016/j.cca.2008.10.013.

240. Airavaara M, Shen H, Kuo CC, Peranen J, Saarma M, Hoffer B, Wang Y. Mesencephalic astrocyte-derived neurotrophic factor reduces ischemic brain injury and promotes behavioral recovery in rats. *J Comp Neurol* 2009; **515**(1): 116-24. doi:10.1002/cne.22039; 10.1002/cne.22039.

241. Kavalar MS, Balantic M, Silar M, Kosnik M, Korosec P, Rijavec M. Association of ORMDL3, STAT6 and TBXA2R gene polymorphisms with asthma. *Int J Immunogenet* 2012; **39**(1): 20-5. doi:10.1111/j.1744-313X.2011.01051.x; 10.1111/j.1744-313X.2011.01051.x.

242. Ringhoff DN, Cassimeris L. Gene expression profiles in mouse embryo fibroblasts lacking stathmin, a microtubule regulatory protein, reveal changes in the expression of genes contributing to cell motility. *BMC Genomics* 2009; **10**: 343,2164-10-343. doi:10.1186/1471-2164-10-343; 10.1186/1471-2164-10-343.

243. Takata A, Kakiuchi C, Ishiwata M, Kanba S, Kato T. Behavioral and gene expression analyses in heterozygous XBP1 knockout mice: Possible contribution of chromosome 11qA1 locus to prepulse inhibition. *Neurosci Res* 2010; **68**(3): 250-5. doi:10.1016/j.neures.2010.07.2042; 10.1016/j.neures.2010.07.2042.

244. Altman J, Sudarshan K. Postnatal development of locomotion in the laboratory rat. *Anim Behav* 1975; **23**(4): 896-920.

245. Jones KL, Smith DW. Recognition of the fetal alcohol syndrome in early infancy. *Lancet* 1973; **302**(7836): 999-1001.

246. Thomas JD, Garrison M, O'Neill TM. Perinatal choline supplementation attenuates behavioral alterations associated with neonatal alcohol exposure in rats. *Neurotoxicol Teratol* 2004; **26**(1): 35-45. doi:10.1016/j.ntt.2003.10.002.

247. Thomas JD, Burchette TL, Dominguez HD, Riley EP. Neonatal alcohol exposure produces more severe motor coordination deficits in high alcohol sensitive rats compared to low alcohol sensitive rats. *Alcohol* 2000; **20**(1): 93-9.

248. Thomas JD, Abou EJ, Dominguez HD. Prenatal choline supplementation mitigates the adverse effects of prenatal alcohol exposure on development in rats. *Neurotoxicol Teratol* 2009; **31**(5): 303-11. doi:10.1016/j.ntt.2009.07.002; 10.1016/j.ntt.2009.07.002.

249. Cheetham SC, Heal DJ. Evidence that RU 24969-induced locomotor activity in C57/B1/6 mice is specifically mediated by the 5-HT1B receptor. *Br J Pharmacol* 1993; **110**(4): 1621-9.

250. Zhou FC, Sari Y, Li TK, Goodlett C, Azmitia EC. Deviations in brain early serotonergic development as a result of fetal alcohol exposure. *Neurotox Res* 2002; **4**(4): 337-42. doi:10.1080/10298420290030532.

251. Cudd TA, Chen WJ, Parnell SE, West JR. Third trimester binge ethanol exposure results in fetal hypercapnea and acidemia but not hypoxemia in pregnant sheep. *Alcohol Clin Exp Res* 2001; **25**(2): 269-76.

252. Burke MW, Palmour RM, Ervin FR, Ptito M. Neuronal reduction in frontal cortex of primates after prenatal alcohol exposure. *Neuroreport* 2009; **20**(1): 13-7. doi:10.1097/WNR.0b013e32831b449c.

253. West JR, Hamre KM. Effects of alcohol exposure during different periods of development: changes in hippocampal mossy fibers. *Brain Res* 1985; **349**(1-2): 280-4.

254. West JR, Kelly SJ, Pierce DR. Severity of alcohol-induced deficits in rats during the third trimester equivalent is determined by the pattern of exposure. *Alcohol Alcohol Suppl* 1987; **1**: 461-5.

255. Diamond A. Close interrelation of motor development and cognitive development and of the cerebellum and prefrontal cortex. *Child Dev* 2000; **71**(1): 44-56.

256. Matsumura M, Sadato N, Kochiyama T, et al. Role of the cerebellum in implicit motor skill learning: a PET study. *Brain Res Bull* 2004; **63**(6): 471-83. doi:10.1016/j.brainresbull.2004.04.008.

257. Jones KL, Smith DW, Ulleland CN, Streissguth P. Pattern of malformation in offspring of chronic alcoholic mothers. *Lancet* 1973; **1**(7815): 1267-71.

258. Streissguth AP, Barr HM, Martin DC, Herman CS. Effects of maternal alcohol, nicotine, and caffeine use during pregnancy on infant mental and motor development at eight months. *Alcohol Clin Exp Res* 1980; **4**(2): 152-64.

259. Ito M. Mechanisms of motor learning in the cerebellum. *Brain Res* 2000; **886**(1-2): 237-45.

260. Allan AM, Chynoweth J, Tyler LA, Caldwell KK. A mouse model of prenatal ethanol exposure using a voluntary drinking paradigm. *Alcohol Clin Exp Res* 2003; **27**(12): 2009-16. doi:10.1097/01.ALC.0000100940.95053.72.

261. Downing C, Balderrama-Durbin C, Hayes J, Johnson TE, Gilliam D. No effect of prenatal alcohol exposure on activity in three inbred strains of mice. *Alcohol Alcohol* 2009; **44**(1): 25-33. doi:10.1093/alcalc/agn082.

262. Marche K, Danel T, Bordet R. Fetal alcohol-induced hyperactivity is reversed by treatment with the PPARalpha agonist fenofibrate in a rat model. *Psychopharmacology (Berl)* 2011; **214**(1): 285-96. doi:10.1007/s00213-010-1960-2.

263. Mothes HK, Opitz B, Werner R, Clausing P. Effects of prenatal ethanol exposure and early experience on home-cage and open-field activity in mice. *Neurotoxicol Teratol* 1996; **18**(1): 59-65.

264. Fryer SL, McGee CL, Matt GE, Riley EP, Mattson SN. Evaluation of psychopathological conditions in children with heavy prenatal alcohol exposure. *Pediatrics* 2007; **119**(3): e733-41. doi:10.1542/peds.2006-1606.

265. Gilbertson RJ, Barron S. Neonatal ethanol and nicotine exposure causes locomotor activity changes in preweanling animals. *Pharmacol Biochem Behav* 2005; **81**(1): 54-64. doi:10.1016/j.pbb.2005.02.002.

266. Collin M, Hakansson-Ovesjo ML, Misane I, Ogren SO, Meister B. Decreased 5-HT transporter mRNA in neurons of the dorsal raphe nucleus and behavioral depression in the obese leptin-deficient ob/ob mouse. *Brain Res Mol Brain Res* 2000; **81**(1-2): 51-61.

267. Sari Y, Powrozek T, Zhou FC. Alcohol deters the outgrowth of serotonergic neurons at midgestation. *J Biomed Sci* 2001; **8**(1): 119-25. doi:54022.

268. Hofmann CE, Ellis L, Yu WK, Weinberg J. Hypothalamic-pituitary-adrenal responses to 5-HT1A and 5-HT2A/C agonists are differentially altered in female and male rats prenatally exposed to ethanol. *Alcohol Clin Exp Res* 2007; **31**(2): 345-55. doi:10.1111/j.1530-0277.2006.00316.x.

269. Gibson MA, Butters NS, Reynolds JN, Brien JF. Effects of chronic prenatal ethanol exposure on locomotor activity, and hippocampal weight, neurons, and nitric oxide synthase activity of the young postnatal guinea pig. *Neurotoxicol Teratol* 2000; **22**(2): 183-92.

270. Mogenson GJ, Nielsen M. A study of the contribution of hippocampal-accumbens-subpallidal projections to locomotor activity. *Behav Neural Biol* 1984; **42**(1): 38-51.

271. Sowell ER, Thompson PM, Mattson SN, Tessner KD, Jernigan TL, Riley EP, Toga AW. Voxel-based morphometric analyses of the brain in children and adolescents prenatally exposed to alcohol. *Neuroreport* 2001; **12**(3): 515-23.

272. Simon P, Dupuis R, Costentin J. Thigmotaxis as an index of anxiety in mice. Influence of dopaminergic transmissions. *Behav Brain Res* 1994; **61**(1): 59-64.

273. Whaley SE, O'Connor And MJ, Gunderson B. Comparison of the adaptive functioning of children prenatally exposed to alcohol to a nonexposed clinical sample. *Alcohol Clin Exp Res* 2001; **25**(7): 1018-24.

274. Hausknecht KA, Acheson A, Farrar AM, Kieres AK, Shen RY, Richards JB, Sabol KE. Prenatal alcohol exposure causes attention deficits in male rats. *Behav Neurosci* 2005; **119**(1): 302-10. doi:10.1037/0735-7044.119.1.302.

275. Kim P, Park JH, Choi CS, et al. Effects of ethanol exposure during early pregnancy in hyperactive, inattentive and impulsive behaviors and MeCP2 expression in rodent offspring. *Neurochem Res* 2013; **38**(3): 620-31. doi:10.1007/s11064-012-0960-5; 10.1007/s11064-012-0960-5.

276. Mattson SN, Riley EP. Parent ratings of behavior in children with heavy prenatal alcohol exposure and IQ-matched controls. *Alcohol Clin Exp Res* 2000; **24**(2): 226-31.

277. Rasmussen C. Executive functioning and working memory in fetal alcohol spectrum disorder. *Alcohol Clin Exp Res* 2005; **29**(8): 1359-67.

278. O'Connor MJ, Frankel F, Paley B, Schonfeld AM, Carpenter E, Laugeson EA, Marquardt R. A controlled social skills training for children with fetal alcohol spectrum disorders. *J Consult Clin Psychol* 2006; **74**(4): 639-48. doi:10.1037/0022-006X.74.4.639.

279. Clark L, Cools R, Robbins TW. The neuropsychology of ventral prefrontal cortex: decision-making and reversal learning. *Brain Cogn* 2004; **55**(1): 41-53. doi:10.1016/S0278-2626(03)00284-7.

280. Naccache L, Dehaene S, Cohen L, Habert MO, Guichart-Gomez E, Galanaud D, Willer JC. Effortless control: executive attention and conscious feeling of mental effort are dissociable. *Neuropsychologia* 2005; **43**(9): 1318-28. doi:10.1016/j.neuropsychologia.2004.11.024.

281. Bunney WE, Bunney BG. Evidence for a compromised dorsolateral prefrontal cortical parallel circuit in schizophrenia. *Brain Res Brain Res Rev* 2000; **31**(2-3): 138-46.

282. Pohorecky LA. The interaction of alcohol and stress. A review. *Neurosci Biobehav Rev* 1981; **5**(2): 209-29.

283. Frye GD, Chapin RE, Vogel RA, Mailman RB, Kilts CD, Mueller RA, Breese GR. Effects of acute and chronic 1,3-butanediol treatment on central nervous system function: a comparison with ethanol. *J Pharmacol Exp Ther* 1981; **216**(2): 306-14.

284. Goodlett CR, Johnson TB. Neonatal binge ethanol exposure using intubation: timing and dose effects on place learning. *Neurotoxicol Teratol* 1997; **19**(6): 435-46.

285. Streissguth AP, Barr HM, Sampson PD, Parrish-Johnson JC, Kirchner GL, Martin DC. Attention, distraction and reaction time at age 7 years and prenatal alcohol exposure. *Neurobehav Toxicol Teratol* 1986; **8**(6): 717-25.

286. Becker M, Warr-Leeper GA, Leeper HA,Jr. Fetal alcohol syndrome: a description of oral motor, articulatory, short-term memory, grammatical, and semantic abilities. *J Commun Disord* 1990; **23**(2): 97-124.

287. Streissguth AP, Barr HM, Sampson PD. Moderate prenatal alcohol exposure: effects on child IQ and learning problems at age 7 1/2 years. *Alcohol Clin Exp Res* 1990; **14**(5): 662-9.

288. Streissguth AP, Barr HM, Olson HC, Sampson PD, Bookstein FL, Burgess DM. Drinking during pregnancy decreases word attack and arithmetic scores on standardized tests: adolescent data from a population-based prospective study. *Alcohol Clin Exp Res* 1994; **18**(2): 248-54.

289. Scoville WB, Milner B. Loss of recent memory after bilateral hippocampal lesions. 1957. *J Neuropsychiatry Clin Neurosci* 2000; **12**(1): 103-13.

290. Jarrard LE. On the role of the hippocampus in learning and memory in the rat. *Behav Neural Biol* 1993; **60**(1): 9-26.

291. Kier EL, Kim JH, Fulbright RK, Bronen RA. Embryology of the human fetal hippocampus: MR imaging, anatomy, and histology. *AJNR Am J Neuroradiol* 1997; **18**(3): 525-32.

292. Dursun I, Jakubowska-Dogru E, Uzbay T. Effects of prenatal exposure to alcohol on activity, anxiety, motor coordination, and memory in young adult Wistar rats. *Pharmacol Biochem Behav* 2006; **85**(2): 345-55. doi:10.1016/j.pbb.2006.09.001.

293. Roebuck-Spencer TM, Mattson SN. Implicit strategy affects learning in children with heavy prenatal alcohol exposure. *Alcohol Clin Exp Res* 2004; **28**(9): 1424-31.

294. Bonthius DJ, West JR. Permanent neuronal deficits in rats exposed to alcohol during the brain growth spurt. *Teratology* 1991; **44**(2): 147-63. doi:10.1002/tera.1420440203.

295. Tran TD, Cronise K, Marino MD, Jenkins WJ, Kelly SJ. Critical periods for the effects of alcohol exposure on brain weight, body weight, activity and investigation. *Behav Brain Res* 2000; **116**(1): 99-110.

296. Arakawa H, Blanchard DC, Arakawa K, Dunlap C, Blanchard RJ. Scent marking behavior as an odorant communication in mice. *Neurosci Biobehav Rev* 2008; **32**(7): 1236-48. doi:10.1016/j.neubiorev.2008.05.012; 10.1016/j.neubiorev.2008.05.012.

297. Olney JW, Tenkova T, Dikranian K, Qin YQ, Labruyere J, Ikonomidou C. Ethanol-induced apoptotic neurodegeneration in the developing C57BL/6 mouse brain. *Brain Res Dev Brain Res* 2002; **133**(2): 115-26.

298. Subramanian A, Tamayo P, Mootha VK, et al. Gene set enrichment analysis: a

knowledge-based approach for interpreting genome-wide expression profiles. *Proc Natl Acad Sci U S A* 2005; **102**(43): 15545-50. doi:10.1073/pnas.0506580102.

299. Wang X, Gomutputra P, Wolgemuth DJ, Baxi LV. Acute alcohol exposure induces apoptosis and increases histone H3K9/18 acetylation in the mid-gestation mouse lung. *Reprod Sci* 2010; **17**(4): 384-90. doi:10.1177/1933719109356984.

300. Rice D, Barone S,Jr. Critical periods of vulnerability for the developing nervous system: evidence from humans and animal models. *Environ Health Perspect* 2000; **108 Suppl 3**: 511-33.

301. Camarillo C, Miranda RC. Ethanol exposure during neurogenesis induces persistent effects on neural maturation: evidence from an ex vivo model of fetal cerebral cortical neuroepithelial progenitor maturation. *Gene Expr* 2008; **14**(3): 159-71.

302. Garriga J, Xie H, Obradovic Z, Grana X. Selective control of gene expression by CDK9 in human cells. *J Cell Physiol* 2010; **222**(1): 200-8. doi:10.1002/jcp.21938; 10.1002/jcp.21938.

303. Charmoy M, Brunner-Agten S, Aebischer D, et al. Neutrophil-derived CCL3 is essential for the rapid recruitment of dendritic cells to the site of Leishmania major inoculation in resistant mice. *PLoS Pathog* 2010; **6**(2): e1000755. doi:10.1371/journal.ppat.1000755; 10.1371/journal.ppat.1000755.

304. Brondijk TH, de Ruiter T, Ballering J, et al. Crystal structure and collagen-binding site of immune inhibitory receptor LAIR-1: unexpected implications for collagen binding by platelet receptor GPVI. *Blood* 2010; **115**(7): 1364-73. doi:10.1182/blood-2009-10-246322; 10.1182/blood-2009-10-246322.

305. Gauthier TW, Drews-Botsch C, Falek A, Coles C, Brown LA. Maternal alcohol abuse and neonatal infection. *Alcohol Clin Exp Res* 2005; **29**(6): 1035-43.

306. McGill J, Meyerholz DK, Edsen-Moore M, et al. Fetal exposure to ethanol has long-term effects on the severity of influenza virus infections. *J Immunol* 2009; **182**(12): 7803-8. doi:10.4049/jimmunol.0803881; 10.4049/jimmunol.0803881.

307. Vargas DL, Nascimbene C, Krishnan C, Zimmerman AW, Pardo CA. Neuroglial activation and neuroinflammation in the brain of patients with autism. *Ann Neurol* 2005; **57**(1): 67-81. doi:10.1002/ana.20315.

308. Stevens SA, Nash K, Koren G, Rovet J. Autism characteristics in children with fetal alcohol spectrum disorders. *Child Neuropsychol* 2012; . doi:10.1080/09297049.2012.727791.

309. El-Ansary A, Al-Ayadhi L. Neuroinflammation in autism spectrum disorders. *J Neuroinflammation* 2012; **9**: 265,2094-9-265. doi:10.1186/1742-2094-9-265; 10.1186/1742-2094-9-265.

310. Tang X, Tian L, Esteso G, et al. Leukocyte-associated Ig-like receptor-1-deficient mice have an altered immune cell phenotype. *J Immunol* 2012; **188**(2): 548-58. doi:10.4049/jimmunol.1102044; 10.4049/jimmunol.1102044.

311. Chui R, Dorovini-Zis K. Regulation of CCL2 and CCL3 expression in human brain endothelial cells by cytokines and lipopolysaccharide. *J Neuroinflammation* 2010; **7**: 1,2094-7-1. doi:10.1186/1742-2094-7-1; 10.1186/1742-2094-7-1.

312. Odell ID, Wallace SS, Pederson DS. Rules of engagement for base excision repair in chromatin. *J Cell Physiol* 2013; **228**(2): 258-66. doi:10.1002/jcp.24134; 10.1002/jcp.24134.

313. Breen AP, Murphy JA. Reactions of oxyl radicals with DNA. *Free Radic Biol Med* 1995; **18**(6): 1033-77.

314. Garcia E, Marcos-Gutierrez C, del Mar Lorente M, Moreno JC, Vidal M. RYBP, a new repressor protein that interacts with components of the mammalian Polycomb complex, and with the transcription factor YY1. *EMBO J* 1999; **18**(12): 3404-18. doi:10.1093/emboj/18.12.3404.

315. Schlisio S, Halperin T, Vidal M, Nevins JR. Interaction of YY1 with E2Fs, mediated by RYBP, provides a mechanism for specificity of E2F function. *EMBO J* 2002; **21**(21): 5775-86.

316. Macaluso M, Montanari M, Giordano A. Rb family proteins as modulators of gene expression and new aspects regarding the interaction with chromatin remodeling enzymes. *Oncogene* 2006; **25**(38): 5263-7. doi:10.1038/sj.onc.1209680.

317. Coutts AS, La Thangue N. The p53 response during DNA damage: impact of transcriptional cofactors. *Biochem Soc Symp* 2006; **(73)**(73): 181-9.

318. Knezovich JG, Ramsay M. The effect of preconception paternal alcohol exposure on epigenetic remodeling of the h19 and rasgrf1 imprinting control regions in mouse offspring. *Front Genet* 2012; **3**: 10. doi:10.3389/fgene.2012.00010; 10.3389/fgene.2012.00010.

319. Hsieh J, Gage FH. Chromatin remodeling in neural development and plasticity. *Curr Opin Cell Biol* 2005; **17**(6): 664-71. doi:10.1016/j.ceb.2005.09.002.

320. Paul S, Lombroso PJ. Receptor and nonreceptor protein tyrosine phosphatases in the nervous system. *Cell Mol Life Sci* 2003; **60**(11): 2465-82. doi:10.1007/s00018-003-3123-7.

321. Lu X, Boora U, Seabra L, et al. Knockdown of Slingshot 2 (SSH2) serine phosphatase induces Caspase3 activation in human carcinoma cell lines with the loss of the Birt-Hogg-Dube tumour suppressor gene (FLCN). *Oncogene* 2013; . doi:10.1038/onc.2013.27; 10.1038/onc.2013.27.

322. Zamzami N, Kroemer G. Condensed matter in cell death. *Nature* 1999; **401**(6749): 127-8. doi:10.1038/43591.

323. Frankfurt OS, Krishan A. Identification of apoptotic cells by formamide-induced dna denaturation in condensed chromatin. *J Histochem Cytochem* 2001; **49**(3): 369-78.

324. Duric V, Banasr M, Licznerski P, et al. A negative regulator of MAP kinase causes depressive behavior. *Nat Med* 2010; **16**(11): 1328-32. doi:10.1038/nm.2219; 10.1038/nm.2219.

325. Aina Y, Susman JL. Understanding comorbidity with depression and anxiety disorders. *J Am Osteopath Assoc* 2006; **106**(5 Suppl 2): S9-14.

326. Keifer J, Zheng ZQ, Zhu D. MAPK signaling pathways mediate AMPA receptor trafficking in an in vitro model of classical conditioning. *J Neurophysiol* 2007; **97**(3): 2067-74. doi:10.1152/jn.01154.2006.

327. Medina AE. Fetal alcohol spectrum disorders and abnormal neuronal plasticity. *Neuroscientist* 2011; **17**(3): 274-87. doi:10.1177/1073858410383336; 10.1177/1073858410383336.

328. Dou X, Wilkemeyer MF, Menkari CE, Parnell SE, Sulik KK, Charness ME. Mitogen-activated protein kinase modulates ethanol inhibition of cell adhesion mediated by the L1 neural cell adhesion molecule. *Proc Natl Acad Sci U S A* 2013; **110**(14): 5683-8. doi:10.1073/pnas.1221386110; 10.1073/pnas.1221386110.

329. Brown DD, Cai L, Das B, Marsh-Armstrong N, Schreiber AM, Juste R. Thyroid hormone controls multiple independent programs required for limb development in Xenopus laevis metamorphosis. *Proc Natl Acad Sci U S A* 2005; **102**(35): 12455-8. doi:10.1073/pnas.0505989102.

330. Cui XS, Sun SC, Kang YK, Kim NH. Involvement of microRNA-335-5p in cytoskeleton dynamics in mouse oocytes. *Reprod Fertil Dev* 2013; **25**(4): 691-9. doi:10.1071/RD12138; 10.1071/RD12138.

331. Wang LL, Zhang Z, Li Q, et al. Ethanol exposure induces differential microRNA and target gene expression and teratogenic effects which can be suppressed by folic acid supplementation. *Hum Reprod* 2009; **24**(3): 562-79. doi:10.1093/humrep/den439; 10.1093/humrep/den439.

332. Lowry RB. The Klippel-Feil anomalad as part of the fetal alcohol syndrome. *Teratology* 1977; **16**(1): 53-6. doi:10.1002/tera.1420160109.

333. Herrmann J, Pallister PD, Opitz JM. Tetraectrodactyly and other skeletal manifestations in the fetal alcohol syndrome. *Eur J Pediatr* 1980; **133**(3): 221-6.

334. Sulik KK, Johnston MC. Sequence of developmental alterations following acute ethanol exposure in mice: craniofacial features of the fetal alcohol syndrome. *Am J Anat* 1983; **166**(3): 257-69. doi:10.1002/aja.1001660303.

335. Ringhoff DN, Cassimeris L. Gene expression profiles in mouse embryo fibroblasts lacking stathmin, a microtubule regulatory protein, reveal changes in the expression of genes contributing to cell motility. *BMC Genomics* 2009; **10**: 343,2164-10-343. doi:10.1186/1471-2164-10-343; 10.1186/1471-2164-10-343.

336. Hindson BJ, Ness KD, Masquelier DA, et al. High-throughput droplet digital PCR system for absolute quantitation of DNA copy number. *Anal Chem* 2011; **83**(22): 8604-10. doi:10.1021/ac202028g; 10.1021/ac202028g.

337. Dallas PB, Gottardo NG, Firth MJ, et al. Gene expression levels assessed by oligonucleotide microarray analysis and quantitative real-time RT-PCR -- how well do they correlate? *BMC Genomics* 2005; **6**: 59. doi:10.1186/1471-2164-6-59.

338. Russ AP, Wattler S, Colledge WH, et al. Eomesodermin is required for mouse trophoblast development and mesoderm formation. *Nature* 2000; **404**(6773): 95-9. doi:10.1038/35003601.

339. Mongan M, Wang J, Liu H, Fan Y, Jin C, Kao WY, Xia Y. Loss of MAP3K1 enhances proliferation and apoptosis during retinal development. *Development* 2011; **138**(18): 4001-12. doi:10.1242/dev.065003; 10.1242/dev.065003.

340. Geh E, Meng Q, Mongan M, et al. Mitogen-activated protein kinase kinase kinase 1 (MAP3K1) integrates developmental signals for eyelid closure. *Proc Natl Acad Sci U S A* 2011; **108**(42): 17349-54. doi:10.1073/pnas.1102297108; 10.1073/pnas.1102297108.

341. King PD, Lubeck BA, Lapinski PE. Nonredundant functions for Ras GTPase-activating proteins in tissue homeostasis. *Sci Signal* 2013; **6**(264): re1. doi:10.1126/scisignal.2003669; 10.1126/scisignal.2003669.

342. Spruce T, Pernaute B, Di-Gregorio A, Cobb BS, Merkenschlager M, Manzanares M, Rodriguez TA. An early developmental role for miRNAs in the maintenance of extraembryonic stem cells in the mouse embryo. *Dev Cell* 2010; **19**(2): 207-19. doi:10.1016/j.devcel.2010.07.014; 10.1016/j.devcel.2010.07.014.

343. Sulik KK, Johnston MC, Webb MA. Fetal alcohol syndrome: embryogenesis in a mouse model. *Science* 1981; **214**(4523): 936-8.

344. Sulik KK. Genesis of alcohol-induced craniofacial dysmorphism. *Exp Biol Med (Maywood)* 2005; **230**(6): 366-75.

345. Godin EA, O'Leary-Moore SK, Khan AA, et al. Magnetic resonance microscopy defines ethanol-induced brain abnormalities in prenatal mice: effects of acute insult on gestational day 7. *Alcohol Clin Exp Res* 2010; **34**(1): 98-111. doi:10.1111/j.1530-0277.2009.01071.x; 10.1111/j.1530-0277.2009.01071.x.

346. Gravestein LA, Borst J. Tumor necrosis factor receptor family members in the immune system. *Semin Immunol* 1998; **10**(6): 423-34. doi:10.1006/smim.1998.0144.

347. Gao M, Labuda T, Xia Y, Gallagher E, Fang D, Liu YC, Karin M. Jun turnover is controlled through JNK-dependent phosphorylation of the E3 ligase Itch. *Science* 2004; **306**(5694): 271-5. doi:10.1126/science.1099414.

348. Gallagher E, Enzler T, Matsuzawa A, et al. Kinase MEKK1 is required for CD40-dependent activation of the kinases Jnk and p38, germinal center formation, B cell proliferation and antibody production. *Nat Immunol* 2007; **8**(1): 57-63. doi:10.1038/ni1421.

349. Endo Y, Iwamura C, Kuwahara M, et al. Eomesodermin controls interleukin-5 production in memory T helper 2 cells through inhibition of activity of the transcription factor GATA3. *Immunity* 2011; **35**(5): 733-45. doi:10.1016/j.immuni.2011.08.017; 10.1016/j.immuni.2011.08.017.

350. Sullivan LC, Clements CS, Rossjohn J, Brooks AG. The major histocompatibility complex class Ib molecule HLA-E at the interface between innate and adaptive immunity. *Tissue*

Antigens 2008; **72**(5): 415-24. doi:10.1111/j.1399-0039.2008.01138.x; 10.1111/j.1399-0039.2008.01138.x.

351. Steven WM, Stewart GL, Seelig LL. The effects of maternal ethanol consumption on lactational transfer of immunity to Trichinella spiralis in rats. *Alcohol Clin Exp Res* 1992; **16**(5): 884-90.

352. Seelig LL,Jr, Steven WM, Stewart GL. Effects of maternal ethanol consumption on the subsequent development of immunity to Trichinella spiralis in rat neonates. *Alcohol Clin Exp Res* 1996; **20**(3): 514-22.

353. Johnson S, Knight R, Marmer DJ, Steele RW. Immune deficiency in fetal alcohol syndrome. *Pediatr Res* 1981; **15**(6): 908-11. doi:10.1203/00006450-198106000-00005.

354. Iwano S, Ichikawa M, Takizawa S, Hashimoto H, Miyamoto Y. Identification of AhR-regulated genes involved in PAH-induced immunotoxicity using a highly-sensitive DNA chip, 3D-Gene Human Immunity and Metabolic Syndrome 9k. *Toxicol In Vitro* 2010; **24**(1): 85-91. doi:10.1016/j.tiv.2009.08.030; 10.1016/j.tiv.2009.08.030.

355. Vila-Brau A, De Sousa-Coelho AL, Mayordomo C, Haro D, Marrero PF. Human HMGCS2 regulates mitochondrial fatty acid oxidation and FGF21 expression in HepG2 cell line. *J Biol Chem* 2011; **286**(23): 20423-30. doi:10.1074/jbc.M111.235044; 10.1074/jbc.M111.235044.

356. Novak EM, Keller BO, Innis SM. Metabolic development in the liver and the implications of the n-3 fatty acid supply. *Am J Physiol Gastrointest Liver Physiol* 2012; **302**(2): G250-9. doi:10.1152/ajpgi.00189.2011; 10.1152/ajpgi.00189.2011.

357. Chan D, Knie B, Boskovic R, Koren G. Placental handling of fatty acid ethyl esters: perfusion and subcellular studies. *J Pharmacol Exp Ther* 2004; **310**(1): 75-82. doi:10.1124/jpet.104.066597.

358. Goh YI, Chudley AE, Clarren SK, et al. Development of Canadian screening tools for fetal alcohol spectrum disorder. *Can J Clin Pharmacol* 2008; **15**(2): e344-66.

359. Longnecker MP. Alcohol consumption and risk of cancer in humans: an overview. *Alcohol* 1995; **12**(2): 87-96.

360. Brooks PJ, Marietta C, Goldman D. DNA mismatch repair and DNA methylation in adult brain neurons. *J Neurosci* 1996; **16**(3): 939-45.

361. Mihaylova VT, Bindra RS, Yuan J, et al. Decreased expression of the DNA mismatch repair gene Mlh1 under hypoxic stress in mammalian cells. *Mol Cell Biol* 2003; **23**(9): 3265-73.

362. Masih PJ, Kunnev D, Melendy T. Mismatch Repair proteins are recruited to replicating DNA through interaction with Proliferating Cell Nuclear Antigen (PCNA). *Nucleic Acids Res* 2008; **36**(1): 67-75. doi:10.1093/nar/gkm943.

363. Krichevsky AM, King KS, Donahue CP, Khrapko K, Kosik KS. A microRNA array

reveals extensive regulation of microRNAs during brain development. *RNA* 2003; **9**(10): 1274-81.

364. Dreher A, Rossing M, Kaczkowski B, Nielsen FC, Norrild B. Differential expression of cellular microRNAs in HPV-11 transfected cells. An analysis by three different array platforms and qRT-PCR. *Biochem Biophys Res Commun* 2010; **403**(3-4): 357-62. doi:10.1016/j.bbrc.2010.11.035; 10.1016/j.bbrc.2010.11.035.

365. Lim LP, Lau NC, Garrett-Engele P, et al. Microarray analysis shows that some microRNAs downregulate large numbers of target mRNAs. *Nature* 2005; **433**(7027): 769-73. doi:10.1038/nature03315.

366. Mukherji S, Ebert MS, Zheng GX, Tsang JS, Sharp PA, van Oudenaarden A. MicroRNAs can generate thresholds in target gene expression. *Nat Genet* 2011; **43**(9): 854-9. doi:10.1038/ng.905; 10.1038/ng.905.

367. Miranda RC, Pietrzykowski AZ, Tang Y, et al. MicroRNAs: master regulators of ethanol abuse and toxicity? *Alcohol Clin Exp Res* 2010; **34**(4): 575-87. doi:10.1111/j.1530-0277.2009.01126.x.

368. Cheng Y, Kuang W, Hao Y, et al. Downregulation of miR-27a* and miR-532-5p and upregulation of miR-146a and miR-155 in LPS-induced RAW264.7 macrophage cells. *Inflammation* 2012; **35**(4): 1308-13. doi:10.1007/s10753-012-9443-8; 10.1007/s10753-012-9443-8.

369. Kitago M, Martinez SR, Nakamura T, Sim MS, Hoon DS. Regulation of RUNX3 tumor suppressor gene expression in cutaneous melanoma. *Clin Cancer Res* 2009; **15**(9): 2988-94. doi:10.1158/1078-0432.CCR-08-3172; 10.1158/1078-0432.CCR-08-3172.

370. Collins A, Hewitt SL, Chaumeil J, et al. RUNX transcription factor-mediated association of Cd4 and Cd8 enables coordinate gene regulation. *Immunity* 2011; **34**(3): 303-14. doi:10.1016/j.immuni.2011.03.004; 10.1016/j.immuni.2011.03.004.

371. Ito Y. Oncogenic potential of the RUNX gene family: 'overview'. *Oncogene* 2004; **23**(24): 4198-208. doi:10.1038/sj.onc.1207755.

372. Bengestrate L, Virtue S, Campbell M, Vidal-Puig A, Hadaschik D, Hahn P, Bielke W. Genome-wide profiling of microRNAs in adipose mesenchymal stem cell differentiation and mouse models of obesity. *PLoS One* 2011; **6**(6): e21305. doi:10.1371/journal.pone.0021305; 10.1371/journal.pone.0021305.

373. Thomson DW, Bracken CP, Goodall GJ. Experimental strategies for microRNA target identification. *Nucleic Acids Res* 2011; **39**(16): 6845-53. doi:10.1093/nar/gkr330; 10.1093/nar/gkr330.

374. Shimomura A, Okamoto Y, Hirata Y, et al. Dominant negative ATF1 blocks cyclic AMP-induced neurite outgrowth in PC12D cells. *J Neurochem* 1998; **70**(3): 1029-34.

375. Bleckmann SC, Blendy JA, Rudolph D, Monaghan AP, Schmid W, Schutz G. Activating

transcription factor 1 and CREB are important for cell survival during early mouse development. *Mol Cell Biol* 2002; **22**(6): 1919-25.

376. Mason AB, Dufour JP. Alcohol acetyltransferases and the significance of ester synthesis in yeast. *Yeast* 2000; **16**(14): 1287-98. doi:2-I.

377. Sitia R, Braakman I. Quality control in the endoplasmic reticulum protein factory. *Nature* 2003; **426**(6968): 891-4. doi:10.1038/nature02262.

378. Kakiuchi C, Ishiwata M, Nanko S, et al. Functional polymorphisms of HSPA5: possible association with bipolar disorder. *Biochem Biophys Res Commun* 2005; **336**(4): 1136-43. doi:10.1016/j.bbrc.2005.08.248.

379. Anttonen AK, Mahjneh I, Hamalainen RH, et al. The gene disrupted in Marinesco-Sjogren syndrome encodes SIL1, an HSPA5 cochaperone. *Nat Genet* 2005; **37**(12): 1309-11. doi:10.1038/ng1677.

380. Hsu WC, Wang HK, Lee LC, et al. Promoter polymorphisms modulating HSPA5 expression may increase susceptibility to Taiwanese Alzheimer's disease. *J Neural Transm* 2008; **115**(11): 1537-43. doi:10.1007/s00702-008-0117-5; 10.1007/s00702-008-0117-5.

381. Lominac KD, Oleson EB, Pava M, et al. Distinct roles for different Homer1 isoforms in behaviors and associated prefrontal cortex function. *J Neurosci* 2005; **25**(50): 11586-94. doi:10.1523/JNEUROSCI.3764-05.2005.

382. Sanderson JL, Donald Partridge L, Valenzuela CF. Modulation of GABAergic and glutamatergic transmission by ethanol in the developing neocortex: an in vitro test of the excessive inhibition hypothesis of fetal alcohol spectrum disorder. *Neuropharmacology* 2009; **56**(2): 541-55. doi:10.1016/j.neuropharm.2008.10.012.

383. Zink M, Ferbert T, Frank ST, Seufert P, Gebicke-Haerter PJ, Spanagel R. Perinatal exposure to alcohol disturbs spatial learning and glutamate transmission-related gene expression in the adult hippocampus. *Eur J Neurosci* 2011; **34**(3): 457-68. doi:10.1111/j.1460-9568.2011.07776.x; 10.1111/j.1460-9568.2011.07776.x.

384. Shim J, Umemura T, Nothstein E, Rongo C. The unfolded protein response regulates glutamate receptor export from the endoplasmic reticulum. *Mol Biol Cell* 2004; **15**(11): 4818-28. doi:10.1091/mbc.E04-02-0108.

385. Mah SJ, Fleck MW, Lindsley TA. Ethanol alters calcium signaling in axonal growth cones. *Neuroscience* 2011; **189**: 384-96. doi:10.1016/j.neuroscience.2011.05.042.

386. Lee AH, Iwakoshi NN, Glimcher LH. XBP-1 regulates a subset of endoplasmic reticulum resident chaperone genes in the unfolded protein response. *Mol Cell Biol* 2003; **23**(21): 7448-59.

387. Hayashi A, Kasahara T, Iwamoto K, et al. The role of brain-derived neurotrophic factor (BDNF)-induced XBP1 splicing during brain development. *J Biol Chem* 2007; **282**(47): 34525-34. doi:10.1074/jbc.M704300200.

388. Silva RM, Ries V, Oo TF, et al. CHOP/GADD153 is a mediator of apoptotic death in

substantia nigra dopamine neurons in an in vivo neurotoxin model of parkinsonism. *J Neurochem* 2005; **95**(4): 974-86. doi:10.1111/j.1471-4159.2005.03428.x.

389. Scheper W, Hoozemans JJ. Endoplasmic reticulum protein quality control in neurodegenerative disease: the good, the bad and the therapy. *Curr Med Chem* 2009; **16**(5): 615-26.

390. Jonsson EG, Cichon S, Schumacher J, et al. Association study of a functional promoter polymorphism in the XBP1 gene and schizophrenia. *Am J Med Genet B Neuropsychiatr Genet* 2006; **141B**(1): 71-5. doi:10.1002/ajmg.b.30262.

391. Nagy G, Koncz A, Perl A. T- and B-cell abnormalities in systemic lupus erythematosus. *Crit Rev Immunol* 2005; **25**(2): 123-40.

392. Ewald SJ. T lymphocyte populations in fetal alcohol syndrome. *Alcohol Clin Exp Res* 1989; **13**(4): 485-9.

393. Gottesfeld Z, Christie R, Felten DL, LeGrue SJ. Prenatal ethanol exposure alters immune capacity and noradrenergic synaptic transmission in lymphoid organs of the adult mouse. *Neuroscience* 1990; **35**(1): 185-94.

394. Hetz C, Martinon F, Rodriguez D, Glimcher LH. The unfolded protein response: integrating stress signals through the stress sensor IRE1alpha. *Physiol Rev* 2011; **91**(4): 1219-43. doi:10.1152/physrev.00001.2011; 10.1152/physrev.00001.2011.

395. Martinon F, Chen X, Lee AH, Glimcher LH. TLR activation of the transcription factor XBP1 regulates innate immune responses in macrophages. *Nat Immunol* 2010; **11**(5): 411-8. doi:10.1038/ni.1857; 10.1038/ni.1857.

396. Barkess G. Chromatin remodeling and genome stability. *Genome Biol* 2006; **7**(6): 319. doi:10.1186/gb-2006-7-6-319.

397. Wolffe AP. Chromatin remodeling: why it is important in cancer. *Oncogene* 2001; **20**(24): 2988-90. doi:10.1038/sj.onc.1204322.

398. Davis PK, Brackmann RK. Chromatin remodeling and cancer. *Cancer Biol Ther* 2003; **2**(1): 22-9.

399. Kleefstra T, Kramer JM, Neveling K, et al. Disruption of an EHMT1-associated chromatin-modification module causes intellectual disability. *Am J Hum Genet* 2012; **91**(1): 73-82. doi:10.1016/j.ajhg.2012.05.003; 10.1016/j.ajhg.2012.05.003.

400. Sari Y, Segu ZM, YoussefAgha A, Karty JA, Isailovic D. Neuroprotective peptide ADNF-9 in fetal brain of C57BL/6 mice exposed prenatally to alcohol. *J Biomed Sci* 2011; **18**: 77,0127-18-77. doi:10.1186/1423-0127-18-77; 10.1186/1423-0127-18-77.

401. Downing C, Flink S, Florez-McClure ML, Johnson TE, Tabakoff B, Kechris KJ. Gene expression changes in C57BL/6J and DBA/2J mice following prenatal alcohol exposure. *Alcohol Clin Exp Res* 2012; **36**(9): 1519-29. doi:10.1111/j.1530-0277.2012.01757.x; 10.1111/j.1530-0277.2012.01757.x.

402. Zollino M, Orteschi D, Murdolo M, et al. Mutations in KANSL1 cause the 17q21.31 microdeletion syndrome phenotype. *Nat Genet* 2012; **44**(6): 636-8. doi:10.1038/ng.2257; 10.1038/ng.2257.

403. Rani V, Neumann CA, Shao C, Tischfield JA. Prdx1 deficiency in mice promotes tissue specific loss of heterozygosity mediated by deficiency in DNA repair and increased oxidative stress. *Mutat Res* 2012; **735**(1-2): 39-45. doi:10.1016/j.mrfmmm.2012.04.004; 10.1016/j.mrfmmm.2012.04.004.

404. Neumann CA, Krause DS, Carman CV, et al. Essential role for the peroxiredoxin Prdx1 in erythrocyte antioxidant defence and tumour suppression. *Nature* 2003; **424**(6948): 561-5. doi:10.1038/nature01819.

405. O'Doherty C, Roos IM, Antiguedad A, Aransay AM, Hillert J, Vandenbroeck K. ITGA4 polymorphisms and susceptibility to multiple sclerosis. *J Neuroimmunol* 2007; **189**(1-2): 151-7. doi:10.1016/j.jneuroim.2007.07.006.

406. Correia C, Coutinho AM, Almeida J, et al. Association of the alpha4 integrin subunit gene (ITGA4) with autism. *Am J Med Genet B Neuropsychiatr Genet* 2009; **150B**(8): 1147-51. doi:10.1002/ajmg.b.30940; 10.1002/ajmg.b.30940.

407. Sajdel-Sulkowska EM, Xu M, McGinnis W, Koibuchi N. Brain region-specific changes in oxidative stress and neurotrophin levels in autism spectrum disorders (ASD). *Cerebellum* 2011; **10**(1): 43-8. doi:10.1007/s12311-010-0223-4; 10.1007/s12311-010-0223-4.

408. Fischer MT, Sharma R, Lim JL, et al. NADPH oxidase expression in active multiple sclerosis lesions in relation to oxidative tissue damage and mitochondrial injury. *Brain* 2012; **135**(Pt 3): 886-99. doi:10.1093/brain/aws012; 10.1093/brain/aws012.

409. Okoh VO, Felty Q, Parkash J, Poppiti R, Roy D. Reactive oxygen species via redox signaling to PI3K/AKT pathway contribute to the malignant growth of 4-hydroxy estradiol-transformed mammary epithelial cells. *PLoS One* 2013; **8**(2): e54206. doi:10.1371/journal.pone.0054206; 10.1371/journal.pone.0054206.

410. Heaton MB, Paiva M, Mayer J, Miller R. Ethanol-mediated generation of reactive oxygen species in developing rat cerebellum. *Neurosci Lett* 2002; **334**(2): 83-6.

411. Chu J, Tong M, de la Monte SM. Chronic ethanol exposure causes mitochondrial dysfunction and oxidative stress in immature central nervous system neurons. *Acta Neuropathol* 2007; **113**(6): 659-73. doi:10.1007/s00401-007-0199-4.

412. Dong J, Sulik KK, Chen SY. The role of NOX enzymes in ethanol-induced oxidative stress and apoptosis in mouse embryos. *Toxicol Lett* 2010; **193**(1): 94-100. doi:10.1016/j.toxlet.2009.12.012; 10.1016/j.toxlet.2009.12.012.

413. Vink J, Auth J, Abebe DT, Brenneman DE, Spong CY. Novel peptides prevent alcohol-induced spatial learning deficits and proinflammatory cytokine release in a mouse model of fetal alcohol syndrome. *Am J Obstet Gynecol* 2005; **193**(3 Pt 1): 825-9. doi:10.1016/j.ajog.2005.02.101.

414. Peirson SN, Butler JN. Quantitative polymerase chain reaction. *Methods Mol Biol* 2007; **362**: 349-62. doi:10.1007/978-1-59745-257-1_25.

415. Vikalo, H., Hassibi, B. and Hassibi, A. Limits of performance of quantitative polymerase chain reaction systems. In: Information Theory, IEEE Transactions on. ; 2010. p.688,689, 690, 691, 692, 693, 694, 695.

416. Phillips BJ, Jenkinson P. Is ethanol genotoxic? A review of the published data. *Mutagenesis* 2001; **16**(2): 91-101.

417. Shackelford RE, Kaufmann WK, Paules RS. Cell cycle control, checkpoint mechanisms, and genotoxic stress. *Environ Health Perspect* 1999; **107 Suppl 1**: 5-24.

418. Barroso-del Jesus A, Lucena-Aguilar G, Menendez P. The miR-302-367 cluster as a potential stemness regulator in ESCs. *Cell Cycle* 2009; **8**(3): 394-8.

419. Subramanyam D, Lamouille S, Judson RL, Liu JY, Bucay N, Derynck R, Blelloch R. Multiple targets of miR-302 and miR-372 promote reprogramming of human fibroblasts to induced pluripotent stem cells. *Nat Biotechnol* 2011; **29**(5): 443-8. doi:10.1038/nbt.1862; 10.1038/nbt.1862.

420. Dolezalova D, Mraz M, Barta T, et al. MicroRNAs regulate p21(Waf1/Cip1) protein expression and the DNA damage response in human embryonic stem cells. *Stem Cells* 2012; **30**(7): 1362-72. doi:10.1002/stem.1108; 10.1002/stem.1108.

421. Goines PE, Croen LA, Braunschweig D, et al. Increased midgestational IFN-gamma, IL-4 and IL-5 in women bearing a child with autism: A case-control study. *Mol Autism* 2011; **2**: 13,2392-2-13. doi:10.1186/2040-2392-2-13; 10.1186/2040-2392-2-13.

422. Kipnis J, Cohen H, Cardon M, Ziv Y, Schwartz M. T cell deficiency leads to cognitive dysfunction: implications for therapeutic vaccination for schizophrenia and other psychiatric conditions. *Proc Natl Acad Sci U S A* 2004; **101**(21): 8180-5. doi:10.1073/pnas.0402268101.

423. Brynskikh A, Warren T, Zhu J, Kipnis J. Adaptive immunity affects learning behavior in mice. *Brain Behav Immun* 2008; **22**(6): 861-9. doi:10.1016/j.bbi.2007.12.008; 10.1016/j.bbi.2007.12.008.

424. Derecki NC, Cardani AN, Yang CH, Quinnies KM, Crihfield A, Lynch KR, Kipnis J. Regulation of learning and memory by meningeal immunity: a key role for IL-4. *J Exp Med* 2010; **207**(5): 1067-80. doi:10.1084/jem.20091419; 10.1084/jem.20091419.

425. Albensi BC, Mattson MP. Evidence for the involvement of TNF and NF-kappaB in hippocampal synaptic plasticity. *Synapse* 2000; **35**(2): 151-9. doi:2-P.

426. Turner PR, O'Connor K, Tate WP, Abraham WC. Roles of amyloid precursor protein and its fragments in regulating neural activity, plasticity and memory. *Prog Neurobiol* 2003; **70**(1): 1-32.

427. Kaltschmidt B, Ndiaye D, Korte M, et al. NF-kappaB regulates spatial memory formation

and synaptic plasticity through protein kinase A/CREB signaling. *Mol Cell Biol* 2006; **26**(8): 2936-46. doi:10.1128/MCB.26.8.2936-2946.2006.

428. Jonsson T, Atwal JK, Steinberg S, et al. A mutation in APP protects against Alzheimer's disease and age-related cognitive decline. *Nature* 2012; **488**(7409): 96-9. doi:10.1038/nature11283; 10.1038/nature11283.

429. Hollstein M, Sidransky D, Vogelstein B, Harris CC. P53 Mutations in Human Cancers. *Science* 1991; **253**(5015): 49-53.

430. Fowler AK, Hewetson A, Agrawal RG, et al. Alcohol-induced one-carbon metabolism impairment promotes dysfunction of DNA base excision repair in adult brain. *J Biol Chem* 2012; **287**(52): 43533-42. doi:10.1074/jbc.M112.401497; 10.1074/jbc.M112.401497.

431. Singh VK. Plasma increase of interleukin-12 and interferon-gamma. Pathological significance in autism. *J Neuroimmunol* 1996; **66**(1-2): 143-5.

432. Kim YK, Myint AM, Lee BH, Han CS, Lee HJ, Kim DJ, Leonard BE. Th1, Th2 and Th3 cytokine alteration in schizophrenia. *Prog Neuropsychopharmacol Biol Psychiatry* 2004; **28**(7): 1129-34. doi:10.1016/j.pnpbp.2004.05.047.

433. Sweeten TL, Posey DJ, Shankar S, McDougle CJ. High nitric oxide production in autistic disorder: a possible role for interferon-gamma. *Biol Psychiatry* 2004; **55**(4): 434-7. doi:10.1016/j.biopsych.2003.09.001.

434. Zhang X, Sliwowska JH, Weinberg J. Prenatal alcohol exposure and fetal programming: effects on neuroendocrine and immune function. *Exp Biol Med (Maywood)* 2005; **230**(6): 376-88.

435. Redei E, Clark WR, McGivern RF. Alcohol exposure in utero results in diminished T-cell function and alterations in brain corticotropin-releasing factor and ACTH content. *Alcohol Clin Exp Res* 1989; **13**(3): 439-43.

436. Grossmann A, Astley SJ, Liggitt HD, et al. Immune function in offspring of nonhuman primates (Macaca nemestrina) exposed weekly to 1.8 g/kg ethanol during pregnancy: preliminary observations. *Alcohol Clin Exp Res* 1993; **17**(4): 822-7.

437. Moraes LA, Piqueras L, Bishop-Bailey D. Peroxisome proliferator-activated receptors and inflammation. *Pharmacol Ther* 2006; **110**(3): 371-85. doi:10.1016/j.pharmthera.2005.08.007.

438. Varga T, Czimmerer Z, Nagy L. PPARs are a unique set of fatty acid regulated transcription factors controlling both lipid metabolism and inflammation. *Biochim Biophys Acta* 2011; **1812**(8): 1007-22. doi:10.1016/j.bbadis.2011.02.014; 10.1016/j.bbadis.2011.02.014.

439. Belfiore A, Genua M, Malaguarnera R. PPAR-gamma agonists and their effects on IGF-I receptor signaling: Implications for cancer. *PPAR Res* 2009; **2009**: 830501. doi:10.1155/2009/830501; 10.1155/2009/830501.

440. Akyurek N, Aycan Z, Cetinkaya S, Akyurek O, Yilmaz Agladioglu S, Ertan U. Peroxisome proliferator activated receptor (PPAR)-gamma concentrations in childhood obesity. *Scand J Clin Lab Invest* 2013; . doi:10.3109/00365513.2013.786121.

441. Ye J. Regulation of PPARgamma function by TNF-alpha. *Biochem Biophys Res Commun* 2008; **374**(3): 405-8. doi:10.1016/j.bbrc.2008.07.068; 10.1016/j.bbrc.2008.07.068.

442. Kim N, Han JY, Roh GS, et al. Nuclear clusterin is associated with neuronal apoptosis in the developing rat brain upon ethanol exposure. *Alcohol Clin Exp Res* 2012; **36**(1): 72-82. doi:10.1111/j.1530-0277.2011.01588.x; 10.1111/j.1530-0277.2011.01588.x.

443. Leu M, Bellmunt E, Schwander M, Farinas I, Brenner HR, Muller U. Erbb2 regulates neuromuscular synapse formation and is essential for muscle spindle development. *Development* 2003; **130**(11): 2291-301.

444. Hornig M, Weissenbock H, Horscroft N, Lipkin WI. An infection-based model of neurodevelopmental damage. *Proc Natl Acad Sci U S A* 1999; **96**(21): 12102-7.

445. Khosla C, Gokhale RS, Jacobsen JR, Cane DE. Tolerance and specificity of polyketide synthases. *Annu Rev Biochem* 1999; **68**: 219-53. doi:10.1146/annurev.biochem.68.1.219.

446. Jenke-Kodama H, Sandmann A, Muller R, Dittmann E. Evolutionary implications of bacterial polyketide synthases. *Mol Biol Evol* 2005; **22**(10): 2027-39. doi:10.1093/molbev/msi193.

447. Lefloch R, Pouyssegur J, Lenormand P. Single and combined silencing of ERK1 and ERK2 reveals their positive contribution to growth signaling depending on their expression levels. *Mol Cell Biol* 2008; **28**(1): 511-27. doi:10.1128/MCB.00800-07.

448. Vantaggiato C, Formentini I, Bondanza A, Bonini C, Naldini L, Brambilla R. ERK1 and ERK2 mitogen-activated protein kinases affect Ras-dependent cell signaling differentially. *J Biol* 2006; **5**(5): 14. doi:10.1186/jbiol38.

449. Preston GA, Lyon TT, Yin Y, et al. Induction of apoptosis by c-Fos protein. *Mol Cell Biol* 1996; **16**(1): 211-8.

450. Abdel-Naby Sayed M, Noda Y, Mahmoud Hamdy M, Mamiya T, Nagai T, Furukawa H, Nabeshima T. Enhancement of immobility induced by repeated phencyclidine injection: association with c-Fos protein in the mouse brain. *Behav Brain Res* 2001; **124**(1): 71-6.

451. Keilhoff G, Becker A, Grecksch G, Wolf G, Bernstein HG. Repeated application of ketamine to rats induces changes in the hippocampal expression of parvalbumin, neuronal nitric oxide synthase and cFOS similar to those found in human schizophrenia. *Neuroscience* 2004; **126**(3): 591-8. doi:10.1016/j.neuroscience.2004.03.039.

452. Kakiuchi C, Ishiwata M, Umekage T, Tochigi M, Kohda K, Sasaki T, Kato T. Association of the XBP1-116C/G polymorphism with schizophrenia in the Japanese population. *Psychiatry Clin Neurosci* 2004; **58**(4): 438-40. doi:10.1111/j.1440-1819.2004.01280.x.

453. Tong Y, Ha TJ, Liu L, Nishimoto A, Reiner A, Goldowitz D. Spatial and temporal

requirements for huntingtin (Htt) in neuronal migration and survival during brain development. *J Neurosci* 2011; **31**(41): 14794-9. doi:10.1523/JNEUROSCI.2774-11.2011; 10.1523/JNEUROSCI.2774-11.2011.

454. Brazma A, Hingamp P, Quackenbush J, et al. Minimum information about a microarray experiment (MIAME)-toward standards for microarray data. *Nat Genet* 2001; **29**(4): 365-71. doi:10.1038/ng1201-365.

455. Brazma A. Minimum Information About a Microarray Experiment (MIAME)--successes, failures, challenges. *ScientificWorldJournal* 2009; **9**: 420-3. doi:10.1100/tsw.2009.57; 10.1100/tsw.2009.57.

456. Fleige S, Pfaffl MW. RNA integrity and the effect on the real-time qRT-PCR performance. *Mol Aspects Med* 2006; **27**(2-3): 126-39. doi:10.1016/j.mam.2005.12.003.

457. Ge Y, Sealfon SC, Speed TP. Multiple testing and its applications to microarrays. *Stat Methods Med Res* 2009; **18**(6): 543-63. doi:10.1177/0962280209351899; 10.1177/0962280209351899.

458. Nautiyal KM, Ribeiro AC, Pfaff DW, Silver R. Brain mast cells link the immune system to anxiety-like behavior. *Proc Natl Acad Sci U S A* 2008; **105**(46): 18053-7. doi:10.1073/pnas.0809479105; 10.1073/pnas.0809479105.

459. Zheng GX, Ravi A, Calabrese JM, et al. A latent pro-survival function for the mir-290-295 cluster in mouse embryonic stem cells. *PLoS Genet* 2011; **7**(5): e1002054. doi:10.1371/journal.pgen.1002054; 10.1371/journal.pgen.1002054.

460. Kaefer V, Semedo JG, Silva Kahl VF, et al. DNA damage in brain cells and behavioral deficits in mice after treatment with high doses of amantadine. *J Appl Toxicol* 2010; **30**(8): 745-53. doi:10.1002/jat.1550; 10.1002/jat.1550.

461. Izquierdo I, Medina JH. Memory formation: the sequence of biochemical events in the hippocampus and its connection to activity in other brain structures. *Neurobiol Learn Mem* 1997; **68**(3): 285-316. doi:10.1006/nlme.1997.3799.

462. Haycock PC. Fetal alcohol spectrum disorders: the epigenetic perspective. *Biol Reprod* 2009; **81**(4): 607-17. doi:10.1095/biolreprod.108.074690.

463. Ramsay M. Genetic and epigenetic insights into fetal alcohol spectrum disorders. *Genome Med* 2010; **2**(4): 27. doi:10.1186/gm148.

464. Park PH, Lim RW, Shukla SD. Involvement of histone acetyltransferase (HAT) in ethanol-induced acetylation of histone H3 in hepatocytes: potential mechanism for gene expression. *Am J Physiol Gastrointest Liver Physiol* 2005; **289**(6): G1124-36. doi:10.1152/ajpgi.00091.2005.

465. Bekdash RA, Zhang C, Sarkar DK. Gestational Choline Supplementation Normalized Fetal Alcohol-Induced Alterations in Histone Modifications, DNA Methylation, and Proopiomelanocortin (POMC) Gene Expression in beta-Endorphin-Producing POMC Neurons of the Hypothalamus. *Alcohol Clin Exp Res* 2013; . doi:10.1111/acer.12082; 10.1111/acer.12082.

Appendix A. Animal use protocol approvals from Animal Care and Veterinary Services at the University of Western Ontario.

November 1, 2009
***This is the 2nd Renewal of this protocol**
*A Full Protocol submission will be required in **2011**

Western

Dear Dr. **Singh:**

Your Animal Use Protocol form entitled:

Genetic Regulatory Mechanisms

has had its yearly renewal approved by the Animal Use Subcommittee.

This approval is valid from **November 1, 2009 to October 31, 2010**

The protocol number for this project remains as **2007-059**

1. This number must be indicated when ordering animals for this project.
2. Animals for other projects may not be ordered under this number.
3. If no number appears please contact this office when grant approval is received.
   If the application for funding is not successful and you wish to proceed with the project, request that an internal scientific peer review be performed by the Animal Use Subcommittee office.
4. Purchases of animals other than through this system must be cleared through the ACVS office. Health certificates will be required.

REQUIREMENTS/COMMENTS

Please ensure that individual(s) performing procedures on live animals, as described in this protocol, are familiar with the contents of this document.

The holder of this Animal Use Protocol is responsible to ensure that all associated safety components (biosafety, radiation safety, general laboratory safety) comply with institutional safety standards and have received all necessary approvals. Please consult directly with your institutional safety officers.

c.c. Approved Protocol - S. Singh, W. Lagerwerf, S. Waring
Approval Letter - S. Singh, W. Lagerwerf, S. Waring

Western

Nov.1, 2010
***This is the 3rd Renewal of this protocol**
*A Full Protocol submission will be required in **2011**

Dear Dr. **Singh**

Your Animal Use Protocol form entitled:

Genetic Regulatory Mechanisms: Genes Determining Ethanol Preference in Mice

has had its yearly renewal approved by the Animal Use Subcommittee.

This approval is valid from **Nov.1, 2010 to Oct.31, 2011**

The protocol number for this project remains as **2007-059**

1. This number must be indicated when ordering animals for this project.
2. Animals for other projects may not be ordered under this number.
3. If no number appears please contact this office when grant approval is received.
   If the application for funding is not successful and you wish to proceed with the project, request that an internal scientific peer review be performed by the Animal Use Subcommittee office.
4. Purchases of animals other than through this system must be cleared through the ACVS office. Health certificates will be required.

REQUIREMENTS/COMMENTS

Please ensure that individual(s) performing procedures on live animals, as described in this protocol, are familiar with the contents of this document.

The holder of this *Animal Use Protocol* is responsible to ensure that all associated safety components (biosafety, radiation safety, general laboratory safety) comply with institutional safety standards and have received all necessary approvals. Please consult directly with your institutional safety officers.

c.c. M. Kleiber, W. Lagerwerf

Subject: eSirius Notification - Annual Protocol Renewal APPROVED by the AUS 2007-059-10::5

Western

2007-059-10::5:

AUP Number: 2007-059-10
AUP Title: Genetic Regulatory Mechanisms: Genes Determining Ethanol Preference in Mice

Approval Date: 10/27/2011

The YEARLY RENEWAL to Animal Use Protocol (AUP) 2007-059-10 has been approved.

1. This AUP number must be indicated when ordering animals for this project.
2. Animals for other projects may not be ordered under this AUP number.
3. Purchases of animals other than through this system must be cleared through the ACVS office. Health certificates will be required.

REQUIREMENTS/COMMENTS
Please ensure that individual(s) performing procedures on live animals, as described in this protocol, are familiar with the contents of this document.

The holder of this Animal Use Protocol is responsible to ensure that all associated safety components (biosafety, radiation safety, general laboratory safety) comply with institutional safety standards and have received all necessary approvals. Please consult directly with your institutional safety officers.

Submitted by: Kinchlea, Will D
on behalf of the Animal Use Subcommittee

The University *of* Western Ontario
Animal Use Subcommittee / University Council on Animal Care
Health Sciences Centre, • London, Ontario • CANADA – N6A 5C1
PH: 519-661-2111 ext. 86768 • FL 519-661-2028

Appendix B. Differentially expressed genes (DEGs) in the fetal brain following prenatal ethanol exposure during the second trimester equivalent (T2-S).

Transcript ID	Gene Symbol[a]	mrna_assignment	*p*-value	Fold-Change[b]
10599884	*Slitrk2*	NM_001161431 // RefSeq // Mus musculus SLIT and NTRK-like family, member 2	0.046	1.429
10592186	*Gm9896*	ENSMUST00000065197 // Gm9896 // predicted gene 9896	0.004	1.392
10510191	*Zfp600*	NM_001177545 // RefSeq // Mus musculus zinc finger protein 600	0.049	1.355
10546706	*Rybp*	NM_019743 // RefSeq // Mus musculus RING1 and YY1 binding protein	0.030	1.351
10600024	*Gpr50*	NM_010340 // RefSeq // Mus musculus G-protein-coupled receptor 50	0.020	1.336
10473224	*Dusp19*	ENSMUST00000028384 // ENSEMBL // cdna:known chromosome:NCBIM37:2:80457202:80471818:1gene	0.045	1.302
10387816	*Rnasek*	NM_173742 // RefSeq // Mus musculus ribonuclease, RNase K (Rnasek)	0.010	1.301
10460582	*AI837181*	ENSMUST00000159759 // ENSEMBL // cdna:known chromosome:NCBIM37:19:5425157:5427313:1 gene	0.036	1.296
10445107	*Gm4831*	ENSMUST00000174626 // ENSEMBL // cdna:pseudogene chromosome:NCBIM37:17:37250800:3725139	0.022	1.279
10519219	*Gltpd1*	NM_024472 // RefSeq // Mus musculus glycolipid transfer protein domain containing 1	0.034	1.276
10548565	*Magohb*	NM_025564 // RefSeq // Mus musculus mago-nashi homolog B (Drosophila)	0.047	1.249
10559486	*Lair1*	NM_001113474 // RefSeq // Mus musculus leukocyte-associated Ig-like receptor 1	0.019	1.247
10493860	*Sprr2b*	NM_011469 // RefSeq // Mus musculus small proline-rich protein 2B	0.030	1.242
10516544	*Hpca*	ENSMUST00000095807 // ENSEMBL // cdna:known chromosome:NCBIM37:4:128788814:128796211:-1	0.033	1.234
10455112	*Pcdhb17*	NM_053142 // RefSeq // Mus musculus protocadherin beta 17	0.008	1.234

10473464	*Olfr1015*	NM_146571 // RefSeq // Mus musculus olfactory receptor 1015	0.032	1.229
10378855	*Ssh2*	NM_177710 // RefSeq // Mus musculus slingshot homolog 2 (Drosophila)	0.049	1.228
10389231	*Ccl3*	NM_011337 // RefSeq // Mus musculus chemokine (C-C motif) ligand 3	0.034	1.225
10361818	*Nmbr*	ENSMUST00000020015 // ENSEMBL // cdna:known chromosome:NCBIM37:10:14480027:14490389:1 gene	0.040	1.223
10605507	*Zc3h18*	NM_001029993 // RefSeq // Mus musculus zinc finger CCCH-type containing 18	0.042	1.223
10432180	*Ccnt1*	NM_009833 // RefSeq // Mus musculus cyclin T1	0.014	1.223
10498500	*Vmn2r1*	NM_019918 // RefSeq // Mus musculus vomeronasal 2, receptor 1	0.036	1.222
10373944	*Zmat5*	NM_026015 // RefSeq // Mus musculus zinc finger, matrin type 5	0.022	1.218
10598169	*4930449I24Rik*	NM_001243109 // RefSeq // Mus musculus predicted gene 3404	0.023	1.218
10584252	*Gm9513*	NM_001128510 // RefSeq // Mus musculus predicted gene 9513	0.026	1.214
10352119	*Pppde1*	NM_024282 // RefSeq // Mus musculus PPPDE peptidase domain containing 1	0.004	1.212
10350188	*Tmem9*	NM_025439 // RefSeq // Mus musculus transmembrane protein 9	0.003	1.208
10606554	*Nap1l3*	NM_138742 // RefSeq // Mus musculus nucleosome assembly protein 1-like 3	0.028	1.207
10360664	*Gm10001*	NM_001081227 // RefSeq // Mus musculus RIKEN cDNA 6330403A02 gene	0.037	1.206
10430871	*Tdg*	NM_011561 // RefSeq // Mus musculus thymine DNA glycosylase	0.042	1.203
10362426	*Trdn*	NM_029726 // Trdn // triadin // 10 A4 // 76757	0.032	-1.907
10457778	*Gm10551*	AK162814 // GenBank HTC // Mus musculus 16 days neonate thymus cDNA, RIKEN full-length	0.007	-1.333
10398388	*Mir380*	NR_029881 // RefSeq // Mus musculus microRNA 380, microRNA	0.006	-1.331
10398336	*Mir540*	NR_030260 // RefSeq // Mus musculus microRNA 540, microRNA	0.042	-1.323
10436600	*Mir99a*	NR_029535 // RefSeq // Mus musculus microRNA 99a, microRNA	0.003	-1.309
10411126	*Jmy*	NM_021310 // RefSeq // Mus musculus	0.023	-1.302

		junction-mediating and regulatory protein		
10423505	*Cmbl*	NM_181588 // RefSeq // Mus musculus carboxymethylenebutenolidase-like (Pseudomonas)	0.039	-1.298
10398334	*Mir337*	NR_029765 // RefSeq // Mus musculus microRNA 337, microRNA	0.008	-1.296
10398338	*Mir665*	NR_030425 // RefSeq // Mus musculus microRNA 665, microRNA	0.021	-1.271
10605081	*Bcap31*	NM_012060 // RefSeq // Mus musculus B cell receptor associated protein 31	0.026	-1.229
10457834	*Nol4*	NM_199024 // RefSeq // Mus musculus nucleolar protein 4	0.015	-1.222
10466779	*Pip5k1b*	NM_008846 // RefSeq // Mus musculus phosphatidylinositol-4-phosphate 5-kinase, type 1 b	0.014	-1.222
10513082	*D730040F13Rik*	NM_175518 // D730040F13Rik // RIKEN cDNA D730040F13 gene // 4 B3 // 242474 /// E	0.033	-1.214
10577152	*E330037G11Rik*	AK087889 // E330037G11Rik // RIKEN cDNA E330037G11 gene // 8 A1.1 // 102220	0.027	-1.214
10449111	*Wdr90*	NM_001163766 // RefSeq // Mus musculus WD repeat domain 90	0.012	-1.211
10457205	*Crem*	NM_001110856 // RefSeq // Mus musculus cAMP responsive element modulator	0.047	-1.211
10598381	*Gpkow*	NM_173747 // RefSeq // Mus musculus G patch domain and KOW motifs	0.002	-1.205
10579508	*Ano8*	NM_001164679 // RefSeq // Mus musculus anoctamin 8	0.032	-1.203

[a]List of DEGs generated using Partek Genomics Suite Software with a ± 1.2-fold change cut off and $p < 0.05$.
[b]DEGs are listed from highest to lowest fold change.

Appendix C. Differentially expressed genes (DEGs) in the adult brain following prenatal ethanol exposure during the first trimester equivalent (T1-L).

Transcript ID	Gene Symbol[a]	mrna_assignment	*p*-value	Fold-Change[b]
10417371	*Gm3696*	NM_001024712 // RefSeq // Mus musculus predicted gene 3696	0.035	1.438
10367497	*Olfr787*	NM_001011822 // RefSeq // Mus musculus olfactory receptor 787	0.044	1.325
10362428	*Trdn*	NM_029726 // RefSeq // Mus musculus triadin	0.015	1.308
10433902	*Gm12191*	NR_028101 // RefSeq // Mus musculus predicted gene 12191, non-coding	0.027	1.302
10406452	*Gm10759*	AY344585 // GenBank // Mus musculus hypothetical protein (Arzc)	0.024	1.301
10604342	*Gm4987*	NM_001085510 // RefSeq // Mus musculus predicted gene 4987	0.006	1.291
10546238	*Vmn1r48*	NM_053218 // RefSeq // Mus musculus vomeronasal 1 receptor 48	0.008	1.266
10344805	*Cspp1*	NM_026493 // RefSeq // Mus musculus centrosome and spindle pole associated protein 1	0.036	1.217
10513514	*Mup5*	NM_008649 // RefSeq // Mus musculus major urinary protein 5	7.5E-4	1.213
10369890	*Cisd1*	XR_032286 // RefSeq // PREDICTED: Mus musculus similar to phosphoribosylaminoimine	0.038	1.204
10461391	*Pcna*	NM_011045 // RefSeq // Mus musculus proliferating cell nuclear antigen	0.049	-1.391
10403658	*Gng4*	NM_010317 // RefSeq // Mus musculus guanine nucleotide binding protein	0.032	-1.344
10438064	*Vpreb1*	NM_016982 // RefSeq // Mus musculus pre-B lymphocyte gene 1	0.023	-1.329
10494643	*Hmgcs2*	NM_008256 // RefSeq // Mus musculus 3-hydroxy-3-methylglutaryl-Coenzyme A synthase	0.007	-1.323
10426875	*Atf1*	NM_007497 // RefSeq // Mus musculus activating transcription factor 1	0.012	-1.319
10472994	*Mtx2*	NM_016804 // RefSeq // Mus musculus metaxin 2, nuclear gene encoding	0.026	-1.316
10595805	*Rasa2*	NM_053268 // RefSeq // Mus musculus RAS p21 protein activator 2	0.045	-1.285
10421972	*Rpl36a*	NM_019865 // RefSeq // Mus musculus ribosomal protein L36A	0.003	-1.280
10577444	*Defb11*	NM_139221 // RefSeq // Mus musculus defensin beta 11	0.026	-1.277

10360460	*Chml*	NM_021350 // RefSeq // Mus musculus choroideremia-like	0.002	-1.268
10361651	*Nup43*	NM_145706 // RefSeq // Mus musculus nucleoporin 43	0.049	-1.264
10587633	*Mrap2*	NM_001177731 // RefSeq // Mus musculus melanocortin 2 receptor accessory protein	0.035	-1.263
10406777	*Gcnt4*	NM_001166065 // RefSeq // Mus musculus glucosaminyl (N-acetyl) transferase 4	0.0383	-1.263
10570029	*Myo16*	NM_001081397 // RefSeq // Mus musculus myosin XVI	0.039	-1.257
10469571	*Otud1*	NM_027715 // RefSeq // Mus musculus OTU domain containing 1	0.049	-1.251
10412719	*Synpr*	NM_028052 // RefSeq // Mus musculus synaptoporin	0.039	-1.250
10410115	*1110018J18Rik*	NM_025370 // RefSeq // Mus musculus RIKEN cDNA 1110018J18 gene	0.005	-1.249
10412100	*Map3k1*	NM_011945 // RefSeq // Mus musculus mitogen-activated protein kinase kinase kinase 1	0.043	-1.247
10449971	*Zfp763*	NM_028543 // RefSeq // Mus musculus zinc finger protein 763	0.026	-1.244
10466423	*Cep78*	NM_198019 // RefSeq // Mus musculus centrosomal protein 78	0.010	-1.244
10572085	*Nat1*	NM_008673 // RefSeq // Mus musculus N-acetyl transferase 1	0.024	-1.240
10588582	*6430571L13Rik*	BC116708 // GenBank // Mus musculus RIKEN cDNA 6430571L13 gene, mRNA (cDNA clone)	0.023	-1.240
10520355	*Htr5a*	NM_008314 // RefSeq // Mus musculus 5-hydroxytryptamine (serotonin) receptor 5A	0.022	-1.238
10566237	*Olfr624*	NM_001011865 // RefSeq // Mus musculus olfactory receptor 624	0.003	-1.237
10351277	*Nme7*	NM_138314 // RefSeq // Mus musculus non-metastatic cells 7	0.014	-1.236
10475946	*Zc3h6*	NM_178404 // RefSeq // Mus musculus zinc finger CCCH type containing 6	0.004	-1.232
10400143	*Stxbp6*	NM_144552 // RefSeq // Mus musculus syntaxin binding protein 6 (amisyn)	0.028	-1.225
10594044	*Islr*	NM_012043 // RefSeq // Mus musculus immunoglobulin superfamily containing leucine-rich repeat	0.030	-1.224
10368495	*Rspo3*	NM_028351 // RefSeq // Mus musculus R-spondin 3 homolog (Xenopus laevis)	0.047	-1.219
10450682	*H2-T23*	NM_010398 // RefSeq // Mus musculus	0.003	-1.217

		histocompatibility 2, T region locus 23		
10588083	*Faim*	NM_001122851 // RefSeq // Mus musculus Fas apoptotic inhibitory molecule	0.007	-1.217
10379028	*Mir451*	NR_029971 // RefSeq // Mus musculus microRNA 451, microRNA	0.024	-1.215
10547088	*Mbd4*	NM_010774 // RefSeq // Mus musculus methyl-CpG binding domain protein 4	0.013	-1.213
10567299	*Itpripl2*	NM_001033380 // RefSeq // Mus musculus inositol 1,4,5-triphosphate receptor	0.036	-1.211
10561008	*Ceacam1*	NM_001039185 // RefSeq // Mus musculus carcinoembryonic antigen-related cell adhesion	0.038	-1.209
10546430	*Adamts9*	NM_175314 // RefSeq // Mus musculus a disintegrin-like and metallopeptidase	0.006	-1.208
10469108	*Gm10857*	NR_033470 // RefSeq // Mus musculus predicted gene 10857	0.002	-1.206
10347106	*Rpe*	NM_025683 // RefSeq // Mus musculus ribulose-5-phosphate-3-epimerase	0.047	-1.206
10462346	*Rcl1*	NM_021525 // RefSeq // Mus musculus RNA terminal phosphate cyclase-like 1	0.017	-1.206
10589994	*Eomes*	NM_010136 // RefSeq // Mus musculus eomesodermin homolog (Xenopus laevis)	0.039	-1.204
10420596	*Tnfrsf19*	NM_013869 // RefSeq // Mus musculus tumor necrosis factor receptor superfamily	0.024	-1.203
10589587	*Setd2*	NM_001081340 // RefSeq // Mus musculus SET domain containing 2	0.005	-1.202
10484457	*Clp1*	ENSMUST00000028475 // ENSEMBL // Polyribonucleotide 5'-hydroxyl-kinase	0.023	-1.202
10380210	*Sfrs1*	NM_173374 // RefSeq // Mus musculus splicing factor, arginine/serine-rich 1	0.028	-1.202
10492757	*Plrg1*	NM_016784 // RefSeq // Mus musculus pleiotropic regulator 1, PRL1 homolog (Arabidopsis)	0.029	-1.200

[a]List of DEGs generated using Partek Genomics Suite Software with a ± 1.2-fold change cut off and $p < 0.05$.
[b]DEGs are listed from highest to lowest fold change.

Appendix D. Differentially expressed genes (DEGs) in the adult brain following prenatal ethanol exposure during the second trimester equivalent (T2-L).

Transcript ID	Gene Symbol[a]	mrna_assignment	*p*-value	Fold-Change[b]
10469320	*Gm9875*	ENSMUST00000064229 // ENSEMBL // Putative uncharacterized protein gene	0.044	1.337
10557229	*LOC100134980*	BC016578 // GenBank // Mus musculus hypothetical LOC100134980, mRNA	0.033	1.304
10461152	*Snhg1*	AK051045 // GenBank HTC // Mus musculus 9 days embryo whole body cDNA, RIKEN	0.010	1.265
10436200	*Gm8824*	XR_034572 // RefSeq // PREDICTED: Mus musculus hypothetical protein LOC100048225	0.049	1.260
10491060	*Spin3*	XR_031023 // RefSeq // PREDICTED: Mus musculus similar to spindlin (LOC675593)	0.012	1.254
10552570	*Klk1b11*	NM_010640 // RefSeq // Mus musculus kallikrein 1-related peptidase b11	0.049	1.254
10579915	*Smarca5*	NM_053124 // RefSeq // Mus musculus SWI/SNF related, matrix associated, actin	0.047	1.243
10418604	*Phf7*	NM_027949 // RefSeq // Mus musculus PHD finger protein 7	0.038	1.242
10473125	*Itga4*	NM_010576 // RefSeq // Mus musculus integrin alpha 4	0.029	1.235
10593095	*Cep164*	NM_001081373 // RefSeq // Mus musculus centrosomal protein 164	0.009	1.235
10398286	*Mir342*	NR_029771 // RefSeq // Mus musculus microRNA 342, microRNA	0.041	1.232
10544106	*Zc3hav1*	ENSMUST00000121946 // ENSEMBL // cdna:pseudogene chromosome:NCBIM37:6:38492303:3	0.049	1.231
10567450	*Dnahc3*	BC051401 // GenBank // Mus musculus dynein, axonemal, heavy chain 3	0.029	1.229
10474335	*Immp1l*	NM_028260 // RefSeq // Mus musculus IMP1 inner mitochondrial membrane peptidase-like (S. cerevisiae)	0.023	1.229
10358621	*Hmcn1*	NM_001024720 // RefSeq // Mus musculus hemicentin 1	0.036	1.225
10513920	*Gm11488*	ENSMUST00000117277 // ENSEMBL // cdna:pseudogene chromosome:NCBIM37:4:73158649:7	0.045	1.225
10603005	*Gm15204*	ENSMUST00000119454 // ENSEMBL // cdna:pseudogene	0.008	1.224

		chromosome:NCBIM37:X:158789528		
10584582	*Gm10694*	ENSMUST00000098870 // ENSEMBL // Putative uncharacterized protein gene	0.006	1.223
10491877	*D3Ertd751e*	NM_028667 // RefSeq // Mus musculus DNA segment, Chr 3, ERATO Doi 751, expressed	0.038	1.22
10399314	*Mfsd2b*	NM_001033488 // RefSeq // Mus musculus major facilitator superfamily domain containing 2B	0.045	1.216
10365098	*Tbxa2r*	NM_009325 // RefSeq // Mus musculus thromboxane A2 receptor	0.033	1.209
10371842	*Uhrf1bp1l*	NM_029166 // RefSeq // Mus musculus UHRF1 (ICBP90) binding protein 1-like	0.041	1.205
10362937	*Gm6983*	XR_033422 // RefSeq // PREDICTED: Mus musculus similar to ribosomal protein S8	0.019	1.204
10474915	*Gchfr*	NM_177157 // RefSeq // Mus musculus GTP cyclohydrolase I feedback regulator	0.012	1.203
10545079	*A530053G22Rik*	NR_015565 // RefSeq // Mus musculus RIKEN cDNA A530053G22 gene	0.049	1.202
10413596	*Sfmbt1*	NM_001166532 // RefSeq // Mus musculus Scm-like with four mbt domains 1	0.015	1.201
10423733	*Vps13b*	GENSCAN00000007934 // ENSEMBL // cdna:Genscan chromosome:NCBIM37:15:35501834:356	0.044	1.201
10438098	*Sdf2l1*	NM_022324 // RefSeq // Mus musculus stromal cell-derived factor 2-like 1	0.009	-1.783
10403943	*Hist1h2bm*	NM_178200 // RefSeq // Mus musculus histone cluster 1, H2bm	0.023	-1.467
10394735	*Pdia6*	NM_027959 // RefSeq // Mus musculus protein disulfide isomerase associated 6	0.014	-1.465
10443463	*Cdkn1a*	NM_007669 // RefSeq // Mus musculus cyclin-dependent kinase inhibitor 1A (P21)	0.021	-1.425
10544525	*Pdia4*	NM_009787 // RefSeq // Mus musculus protein disulfide isomerase associated 4	0.012	-1.414
10374035	*Xbp1*	NM_013842 // RefSeq // Mus musculus X-box binding protein 1	0.028	-1.367
10471586	*Hspa5*	NM_022310 // RefSeq // Mus musculus heat shock protein 5	0.005	-1.365
10596575	*Manf*	NM_029103 // RefSeq // Mus musculus mesencephalic astrocyte-derived	0.009	-1.349

		neurotrophic		
10374464	*Spred2*	BC040462 // GenBank // Mus musculus sprouty-related, EVH1 domain containing 2	0.031	-1.336
10397966	*Otub2*	NM_001177841 // RefSeq // Mus musculus OTU domain, ubiquitin aldehyde binding 2	0.047	-1.314
10408202	*Hist1h3f*	NM_013548 // RefSeq // Mus musculus histone cluster 1, H3f	0.023	-1.307
10408083	*Hist1h3g*	NM_145073 // RefSeq // Mus musculus histone cluster 1, H3g	0.030	-1.303
10404049	*Hist1h3d*	NM_178204 // RefSeq // Mus musculus histone cluster 1, H3d	0.041	-1.292
10404065	*Hist2h3b*	NM_178215 // RefSeq // Mus musculus histone cluster 2, H3b	0.029	-1.283
10520862	*Fosl2*	NM_008037 // RefSeq // Mus musculus fos-like antigen 2	0.040	-1.281
10403073	*Ighg*	X70423 // GenBank // M.musculus mRNA for monoclonal antibody heavy chain gamma 2	0.022	-1.280
10361250	*Camk1g*	NM_144817 // RefSeq // Mus musculus calcium/calmodulin-dependent protein kinase 1G	0.023	-1.266
10434675	*Dnajb11*	NM_026400 // RefSeq // Mus musculus DnaJ (Hsp40) homolog, subfamily B, member 11	0.003	-1.254
10363845	*Ccdc6*	NM_001111121 // RefSeq // Mus musculus coiled-coil domain containing 6	0.019	-1.254
10408246	*Hist1h3a*	NM_013550 // RefSeq // Mus musculus histone cluster 1, H3a	0.026	-1.245
10468980	*Fam107b*	BC021353 // GenBank // Mus musculus family with sequence similarity 107, member b	0.040	-1.245
10413726	*Tnnc1*	NM_009393 // RefSeq // Mus musculus troponin C, cardiac/slow skeletal	0.021	-1.245
10507328	*Prdx1*	NM_011034 // RefSeq // Mus musculus peroxiredoxin 1	0.049	-1.230
10535369	*Gm15770*	ENSMUST00000117498 // ENSEMBL // cdna:pseudogene chromosome:NCBIM37:5:143614295:	0.017	-1.230
10578984	*Tufm*	NM_172745 // RefSeq // Mus musculus Tu translation elongation factor, mitochondrial	0.048	-1.225
10447594	*Dynlt1a*	NM_001166629 // RefSeq // Mus musculus dynein light chain Tctex-type	0.005	-1.223

		1A		
10424213	*Zhx2*	NM_199449 // RefSeq // Mus musculus zinc fingers and homeoboxes 2	0.012	-1.221
10516765	*Serinc2*	NM_172702 // RefSeq // Mus musculus serine incorporator 2	0.016	-1.221
10419525	*A930018M24Rik*	BC144873 // GenBank // Mus musculus cDNA clone MGC:178429 IMAGE:9053421	0.042	-1.217
10524234	*Galnt9*	NM_198306 // RefSeq // Mus musculus UDP-N-acetyl-alpha-D-galactosamine:polypeptidase	0.015	-1.217
10494978	*Ptpn22*	NM_008979 // RefSeq // Mus musculus protein tyrosine phosphatase, non-receptor type 22 (lymphoid)	0.033	-1.216
10490946	*Hsp90aa1*	NM_010480 // RefSeq // Mus musculus heat shock protein 90, alpha (cytosolic)	0.041	-1.215
10465553	*Fkbp2*	NM_008020 // RefSeq // Mus musculus FK506 binding protein 2	0.042	-1.214
10578771	*Galnt7*	NM_144731 // RefSeq // Mus musculus UDP-N-acetyl-alpha-D-galactosamine: polypeptidase	0.019	-1.212
10448676	*Slc9a3r2*	NM_023055 // RefSeq // Mus musculus solute carrier family 9 (sodium/hydrogen exchange), isoform 3 regulator 2	0.006	-1.211
10548785	*Dynlt1c*	NM_001166630 // RefSeq // Mus musculus dynein light chain Tctex-type 1C	0.039	-1.208
10396237	*2700049A03Rik*	NM_001163378 // RefSeq // Mus musculus RIKEN cDNA 2700049A03 gene	0.007	-1.205
10416251	*Egr3*	NM_018781 // RefSeq // Mus musculus early growth response 3	0.040	-1.205
10363350	*P4ha1*	NM_011030 // RefSeq // Mus musculus procollagen-proline, 2-oxoglutarate 4-dioxygenase subunit alpha-1	0.003	-1.205
10406626	*Homer1*	NM_147176 // RefSeq // Mus musculus homer homolog 1 (Drosophila)	0.021	-1.203
10582429	*Cbfa2t3*	NM_009824 // RefSeq // Mus musculus core-binding factor, runt domain, alpha subunit	0.043	-1.203

[a]List of DEGs generated using Partek Genomics Suite Software with a ± 1.2-fold change cut off and $p < 0.05$.
[b]DEGs are listed from highest to lowest fold change.

Appendix E. Journal copyright approval form.

To whom it may concern:

Regarding the following paper published in the Journal of Behavioral and Brain Sciences:

Neurodevelopmenntal Timing of Ethanol Exposure May Contribute to Observed Heterogeneity of Behavioral Deficits in a Mouse Model of Fetal Alcohol Spectrum Disorder (FASD)

Katarzyna Mantha, Morgan Kleiber, Shiva Singh

PP. 85-999, Pub. Date: February 27, 2013

DOI: 100.4236/jbbs..2013.31009

The coauthor Katarzyna Mantha from University of Western Ontario is thereby allowed to include the above paper into her doctoral thesis "Neurodevelopmmental consequences of prenatal alcohol exposure: Behavioural and transcriptomic altterations in a mouse model", all the contents cited from the mentioned paper should be footnoted as references. Use of this paper for other purpose should be submitted to the JBBS editorial board office for permission.

Best Wishes

Karen Zhang

Editorial Assistant of JBBS

http://wwww.scirp.org/journal/jbbs/

Appendix F. Ingenuity Pathway Analysis network legend for relationship types, molecular shapes, and relationships.

Relationship types		Molecular shapes		Relationships	
A	Activation		Cytokine/Growth factor	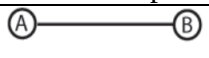	Binding
B	Binding		Enzyme	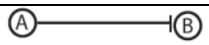	Inhibition
C	Causes/Leads to		G-protein coupled receptor	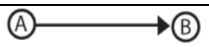	Acts on
CC	Chemical-chemical interaction		Ion channel		Inhibits and acts on
CP	Chemical-protein interaction		Kinase		Leads to
E	Expression (includes metabolism/synthesis for chemicals)		Ligand-dependent nuclear receptor	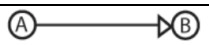	Translocates to
EC	Enzyme Catalysis		Peptidase	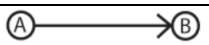	Reaction
I	Inhibition		Phosphatase		Direct interaction
L	Proteolysis (includes degradation for Chemicals)		Transcription regulator		Indirect interaction
LO	Localization		Translation regulator		
M	Biochemical Modification		Transmembrane receptor		
MB	Group/complex Membership		Transporter		
P	Phosphorylation/Dephosphorylation		microRNA		
PD	Protein-DNA binding		Complex/Group		
PP	Protein-Protein binding		Other		
PR	Protein-RNA binding				
RB	Regulation of binding				
RE	Reaction				
RR	RNA-RNA Binding				
T	Transcription				
TR	Translocation				

Curriculum Vitae

Katarzyna Mantha

---

1. Educational and Professional Experience

Sept 2009-Aug 2013	Doctoral Candidate, School of Graduate and Postdoctoral Studies, University of Western Ontario (*Supervisor: Dr. Shiva Singh*)
Sept 2009-Apr 2013	Teaching Assistant, Department of Biology, University of Western Ontario
Sept 2005-Apr 2009	Honors Bachelor of Science, Specialization in Genetics, Department of Biology, University of Western Ontario, *conferred June 13TH, 2009*

2. Conference Presentations

Oct 2012 — Mantha, K., Kleiber, M., and Singh, S.M.
Heterogeneous behavioural manifestations in a mouse model of Fetal Alcohol Spectrum Disorders: Assessing the effect of gestational time and gene expression
Poster presentation at the World Congress of Psychiatric Genetics in Hamburg, Germany

Oct 2011 — Janus, K., Kleiber, M., Chokroborty-Hoque, A., Laufer, B., Diehl, E., Wright, E., and Singh, S.
Mapping diagnostic heterogeneity in an animal model of Fetal Alcohol Spectrum Disorders (FASD)
Poster presentation at the 12th International Congress of Human Genetics/61st Annual Meeting of the American Society of Human Genetics at the Montreal Convention Centre, Montreal, Canada

Oct 2011 — Janus, K., Kleiber, M.L., Diehl, E.J., Chokroborty-Hoque, A., Laufer, B.I., Wright, E., and Singh, S.M.
Mapping diagnostic heterogeneity in an animal model of Fetal Alcohol Spectrum Disorders (FASD) Poster presentation at the 2ND Annual Biology Graduate Research Forum, University of Western Ontario

Nov 2010 — Janus, K., Wright, E., Kleiber, M., and Singh, S.
Genetical Genomics of a Mouse Model of Fetal Alcohol Spectrum Disorders (FASD)
Poster presentation at the 1ST Annual Biology Graduate Research Forum, University of Western Ontario

June 2010 Janus, K., Wright, E., Kleiber, M., and Singh, S.
Genetical Genomics of a Mouse Model of Fetal Alcohol Spectrum Disorders (FASD)
Poster presentation at the 53RD Annual Meeting of the Genetics Society of Canada at McMaster University, Hamilton, Ontario, Canada

3. Awards and Accomplishments

Apr 2013 People's Choice for Stellar Talk: Cell and Molecular, Society of Biology Graduate Students, University of Western Ontario

Oct 2012 Poster Award Finalist, International Society of Psychiatric Genetics, Hamburg, Germany

July 2012 National Institute on Alcohol Abuse and Alcoholism Travel Award, International Society of Psychiatric Genetics, Hamburg, Germany, *$2000*

May 2011 Graduate Teaching Assistantship Award, University of Western Ontario, *Nomination*

Oct 2010 3RD place poster award, 1ST Annual Biology Graduate Research Forum, University of Western Ontario

May 2010 Graduate Teaching Assistantship Award, University of Western Ontario, *Nomination*

4. Publications

Peer review Mantha, K., Laufer, B.I., and Singh, S.M. (2013) Prenatal alcohol exposure during the second trimester leads to long-term alterations in genes and molecular pathways in C57BL/6J offspring [*in preparation*].

Peer Review Mantha, K., Laufer, B.I., and Singh, S.M. (2013) Molecular changes during neurodevelopment following second-trimester binge ethanol exposure in a mouse model of fetal alcohol spectrum disorder: from short-term effects to long-term adaptation. *J Neurosci*. [*under review*].

Peer Review Laufer, B.I., Mantha, K., Kleiber, M.L., Diehl, E.J., Addison, S.M. and Singh, S.M. (2013) Long-lasting alterations to DNA methylation and ncRNAs could underlie the effects of fetal alcohol exposure in mice. *Dis. Model. Mech.* 6, pp. 1-16. doi: 10.1242/dmm.010975.

Peer Review Mantha, K., Kleiber, M.L. and Singh, S.M. (2013) Neurodevelopmental timing of ethanol exposure may contribute to observed heterogeneity of behavioural deficits in a mouse model of Fetal Alcohol Spectrum Disorders (FASD). *J. Beh. Brain Sci.* 3:1, pp.85-99. doi: 10.4236/jbbs.2013.31009.

Peer Review	Kleiber, M.L., Mantha, K., Stringer, R.L. and Singh, S.M. (2013) Neurodevelopmental alcohol exposure elicits long-term changes to gene expression that alters distinct molecular pathways depending on timing of exposure. *J. Neurodev. Disord.* 5:6, pp. 1-19. doi:10.1186/1866-1955-5-6.
Conference Proceedings	Anderson-Schmidt, H. *et al*. (2013) Selected rapporteur summaries from the XX world congress of psychiatric genetics, Hamburg, Germany, October 14-18, 2012. *Am. J. Med. Genet. B Neuropsychiatr Genet.* doi: 10.1002/ajmg.b.32132.

5. Teaching

Sept 2012-Apr 2013	Teaching Assistant	Investigative Techniques in Genetics, *4^{TH} year undergraduate*
Oct 2012-Jan 2013	Co-op Supervisor	University of Western Ontario and St. Thomas Valley District School Board, *high school student*
Sept 2011-Apr 2012	Teaching Assistant	Investigative Techniques in Genetics, *4^{TH} year undergraduate*
Sept 2010-Apr 2011	Teaching Assistant	(i) Scientific Methods in Biology, *2^{ND} year undergraduate* (ii) Genetics, *2^{ND} year undergraduate*
Sept 2009-Apr 2010	Teaching Assistant	(i) Scientific Methods in Biology, *2^{ND} year undergraduate* (ii) Genetics, *2^{ND} year undergraduate*

6. Committees and Affiliations

Sept 2012-Aug 2013	Graduate Student Bursary Committee member *Society of Graduate Student, University of Western Ontario*
July 2012-July 2013	International Society of Psychiatric Genetics
Sept 2012-May 2013	Chairperson of the Graduate Student Teaching Awards Committee *Society of Graduate Students, University of Western Ontario*
Nov 2011-May 2012	Graduate Student Teaching Awards Committee member *Society of Graduate Students, University of Western Ontario*
Mar 2011-Dec 2012	Genetics Society of America
Jan 2011-Dec 2012	American Society of Human Genetics
May 2010-Dec 2010	Genetics Society of Canada